

MEASUREMENT AND ANALYSIS OF THE RESOLVED RESONANCE
CROSS SECTIONS OF THE NATURAL HAFNIUM ISOTOPES

by

TIMOTHY CHRISTOPHER WARE

A thesis submitted to
The University of Birmingham
for the degree of
DOCTOR OF PHILOSOPHY

School of Physics and Astronomy
College of Engineering and Physical Sciences
The University of Birmingham
June 2010

UNIVERSITY OF
BIRMINGHAM

University of Birmingham Research Archive

e-theses repository

This unpublished thesis/dissertation is copyright of the author and/or third parties. The intellectual property rights of the author or third parties in respect of this work are as defined by The Copyright Designs and Patents Act 1988 or as modified by any successor legislation.

Any use made of information contained in this thesis/dissertation must be in accordance with that legislation and must be properly acknowledged. Further distribution or reproduction in any format is prohibited without the permission of the copyright holder.

ABSTRACT

Hafnium is a ductile metallic element with a large neutron absorption cross section. It can be used in reactor control rods to regulate the fission process. The NEA High Priority Request List for nuclear data presents a need for improved characterisation of the hafnium cross section in the resolved resonance region. This thesis presents new resonance cross section parameters for the six natural hafnium isotopes.

Cross section measurements, supported by the NUDAME and EUFRAT projects, were performed at the IRMM Geel GELINA time-of-flight facility. Capture experiments were conducted on the 12 m, 28 m and 58 m flight paths using C_6D_6 detectors and transmission experiments were performed at flight paths of 26 m and 49 m using a 6Li glass detector. The samples used were metallic natural hafnium discs of various thicknesses and hafnium oxide powders, with differing isotopic enrichments.

Data analysis was performed using the least square fitting REFIT code, which was updated during this work. The use of isotopically-enriched samples enabled previously unrecorded resonances to be allocated to the correct isotope. The resulting evaluated data files extend the upper energy limits of the resolved resonance regions for the ^{174}Hf , ^{176}Hf , ^{177}Hf , ^{178}Hf , ^{179}Hf and ^{180}Hf isotopes, relative to the current European recommended evaluation (JEFF3.1), to 250 eV, 3 keV, 1 keV, 3 keV, 1 keV and 3 keV respectively.

The natural hafnium resonance integral calculated from the new resonance parameters is 1.2% lower than the integral corresponding to the JEFF3.1 evaluated hafnium data. Comparison of calculated to experimental k-effective values for appropriate zero-power reactor assemblies show improvement over the JEFF3.1 data.

“An experiment is a question which science poses to Nature
and a measurement is the recording of Nature’s answer.”
- Max Planck (1858-1947)

In loving memory of my Grandad,
who showed pride in my every achievement
in a way only a grandfather can.

ACKNOWLEDGMENTS

Throughout my PhD research, I have received important contributions, as well as help in many small ways, from many people, for which I express my deepest gratitude.

Firstly, I thank my industry supervisor, Christopher Dean; not least for conceiving and laying the foundations of my project, but for imparting his expert knowledge of the nuclear data field, for sharing my learning experience and for his continuing advice, often into the later hours, be it in the office on a cold Winfrith evening or over a cold beer on a balmy Provence night.

Thank you to Mick Moxon, for freely giving me his time and (many years worth of) advice that have allowed me to develop my understanding of resonance analysis. He has also given me the privileged opportunity to co-author his REFIT code.

Many thanks to all at Serco, including Richard Hiles, Dave Hanlon, Glynn Hosking, John Lillington, Chris Maidment, Ray Perry, Paul Smith, the IT team and all those that provided the diverse conversations in the tea room. Thanks are also due to Ian Giles for his support of my work.

I am grateful to my University supervisor, David Weaver for academic guidance, as well as fielding numerous emails and expenses claims. Together with Paul Norman, I thank David for accepting me onto the PTNR MSc course and bringing me into the world of nuclear physics.

Thank you to Peter Schillebeeckx, Alessandro Borella, Stefan Kopecky, André Moens, Arjan Plompen, Peter Rullhusen, Peter Siegler and Ruud Wynants for supporting, preparing and undertaking the hafnium measurements and instructing me in time-of-flight techniques and

data reduction. I thank all the staff at the Neutron Physics Unit for making me most welcome during my visits.

The measurements were supported by the European Commission within the Sixth Framework Programme through NUDAME (EURATOM contract no. FP6-516487) and the Seventh Framework Programme through EUFRAT (EURATOM contract no. FP7-211499).

I thank Natalia Janeva and her colleagues of the Institute of Nuclear Research and Nuclear Energy, Sofia, Bulgaria for kindly loaning the enriched hafnium samples, without which many of the measurements used in my analysis would not have taken place.

Thank you to Gilles Noguère and his colleagues at CEA Cadarache for providing the results of their average parameter studies of hafnium. Thanks to Yaron Danon and Mike Trbovich of RPI and Jack Harvey of ORNL for kindly supplying data. Thank you to the NEA Databank staff for the distributing the REFIT code and scanning the Harwell measurement printouts.

From the School of Physics, I thank Norma Simpson and Anna Jenkin for answering all manner of questions, Andrew Davis and Louise Evans for sharing the PhD experience and Stuart Wilson, for his MSc thesis detailing the modification of application data libraries.

Some special mentions: to my Mum, my Dad, David and Julie for their unconditional support throughout, plus the free board-and-lodge whilst I was writing up; to the growing number I can call my family for always talking an interest; and to my many friends for giving me a life outside work and the distractions of archery, DIY and occasional pint or two.

Finally, a special thank you to my fiancée and best friend, Mel; for her love, her counsel and her unwavering support, throughout her MChem, teaching training and all that the last five years have brought us.

TABLE OF CONTENTS

1. INTRODUCTION	1
1.1. Motivations for This Work	1
1.1.1. Properties and Uses of Hafnium	1
1.1.2. Present Status of Hafnium Cross Section Data	2
1.2. Structure of This Thesis	4
1.3. Statement of the Author's Contribution	5
2. NEUTRON CROSS SECTIONS	6
2.1. General Description of Cross Sections	6
2.2 Representation of Cross Sections by Resonance Parameters	9
2.3 Storage of Resonance Parameters	14
2.4 Specifics of Hafnium Cross Sections	16
3. HAFNIUM CROSS SECTIONS MEASUREMENTS	20
3.1 Principles of Neutron Time-of-Flight Measurements	20
3.1.1 Neutron Transmission Measurements	21
3.1.2 Neutron Capture Measurements	22
3.2 Experimental Considerations	23
3.2.1 Background Correction	23
3.2.2 Dead Time Correction	24
3.3 High Resolution Cross Section Measurements at GELINA	25
3.3.1 The GELINA Time-of-Flight Facility	25
3.3.2 Capture Measurement Set-up	28
3.3.3 Natural and Isotopically-Enriched Hafnium Capture Measurements	30
3.3.4 Data Reduction	33
3.4 Natural Hafnium Transmission Measurement	37
3.5 Previous Measurements Used In This Work	39
3.5.1 ORNL 1963 Transmission Measurements	39
3.5.2 Harwell 1973 Capture Measurements	40
3.5.3 ORNL 1982 Capture Measurements	41
3.5.4 Geel 2001 Transmission Measurements	42
3.5.5 RPI 2003 Transmission and Capture Measurements	43

4. THE REFIT CODE	44
4.1 Neutron Resonance Analysis Using REFIT	44
4.2 Development of the REFIT code	48
4.2.1 REFIT-2007	48
4.2.2 REFIT-2009	49
4.2.3 Further Developments	51
4.3 The RESCON Code	53
5. ANALYSIS OF MEASUREMENT DATA	54
5.1 Assignment of Resonances to Isotopes	54
5.2 Experimental Considerations and Assumptions	57
5.2.1 Experimental Parameters	57
5.2.2 Abundance of Hafnium Isotopes and Impurities in Samples	63
5.2.3 Average Capture Widths	66
5.3 Analysis of 0.5 eV to 1 keV Neutron Energy Range	68
5.4 Analysis of 1 keV to 3 keV Neutron Energy Range	71
5.5 Resonance Parameters of the Hafnium Isotopes	74
6. DISCUSSION OF RESULTS	113
6.1 Construction of New Evaluated Files	113
6.2 Observations from New Resolved Parameters	114
6.3 Testing	121
6.4 Suggestions for Further Work	124
7. CONCLUSIONS	127
REFERENCES	129
APPENDIX A – SUBSIDUARY DATA ANALYSIS	134
A.1 Calculation of the Debye Temperature of Hafnium Samples	134
A.2 Transmission and Capture Yield Data	135
APPENDIX B – SUPPORTING DOCUMENTATION	151
B.1 High Priority Request List Entry for Hafnium Measurements	152
B.2 Application for Support from NUDAME Project	154
B.3 Application for Support from EUFRAT Project	160
B.4 Contribution to IRMM Neutron Physics Unit Scientific Report 2008	164

INDEX OF FIGURES

Figure 2.1 – Capture Cross Sections of the Natural Hafnium Isotopes.....	7
Figure 2.2 – Example of the ENDF6 Data Format.....	14
Figure 2.3 – Values contained in ENDF6 Format Resonance Parameter File	14
Figure 2.4 – Cumulative Number of ^{177}Hf and ^{179}Hf Resonances	19
Figure 2.5 – Cumulative $g_J \Gamma_n^0$ Values for ^{177}Hf and ^{179}Hf Resonances	19
Figure 3.1 – GELINA Moderated Neutron Spectrum	26
Figure 3.2 – Schematic of GELINA Accelerator and Target Hall	27
Figure 3.3 – Schematic of Flight Path Set-up for Capture Measurements	28
Figure 3.4 – Misalignment Observed Between Capture and Flux Spectra	37
Figure 3.5 – Schematic of Flight Path Set-up for Transmission Measurements	37
Figure 3.6 – Gap in Resolved Resonance Data for ^{176}Hf	41
Figure 5.1 – Comparison of Measured Capture Yields of Hafnium Samples at 28 m with the JEFF3.1 and New Resonance Allocations	56
Figure 6.1 – Cumulative Number of Resonances and $g_J \Gamma_n^0$ Values for ^{174}Hf	118
Figure 6.2 – Cumulative Number of Resonances and $g_J \Gamma_n^0$ Values for ^{176}Hf	118
Figure 6.3 – Cumulative Number of Resonances and $g_J \Gamma_n^0$ Values for ^{177}Hf	118
Figure 6.4 – Cumulative Number of Resonances and $g_J \Gamma_n^0$ Values for ^{178}Hf	118
Figure 6.5 – Cumulative Number of Resonances and $g_J \Gamma_n^0$ Values for ^{179}Hf	119
Figure 6.6 – Cumulative Number of Resonances and $g_J \Gamma_n^0$ Values for ^{180}Hf	119
Figure A.1 – Hafnium Transmission Data and Calculations (0.5 – 20 eV)	136
Figure A.2 – Hafnium Capture Data and Calculations (0.5 – 20 eV)	136
Figure A.3 – Hafnium Transmission Data and Calculations (20 – 50 eV)	137
Figure A.4 – Hafnium Capture Data and Calculations (20 – 50 eV)	137

Figure A.5 – Hafnium Transmission Data and Calculations (50 – 100 eV)	138
Figure A.6 – Hafnium Capture Data and Calculations (50 – 100 eV)	138
Figure A.7 – Hafnium Transmission Data and Calculations (100 – 150 eV)	139
Figure A.8 – Hafnium Capture Data and Calculations (100 – 150 eV)	139
Figure A.9 – Hafnium Transmission Data and Calculations (150 – 200 eV)	140
Figure A.10 – Hafnium Capture Data and Calculations (150 – 200 eV)	140
Figure A.11 – Hafnium Transmission Data and Calculations (200 – 250 eV)	141
Figure A.12 – Hafnium Capture Data and Calculations (200 – 250 eV)	141
Figure A.13 – Hafnium Transmission Data and Calculations (250 – 300 eV)	142
Figure A.14 – Hafnium Capture Data and Calculations (250 – 300 eV)	142
Figure A.15 – Hafnium Transmission Data and Calculations (300 – 350 eV)	143
Figure A.16 – Hafnium Capture Data and Calculations (300 – 350 eV)	143
Figure A.17 – Hafnium Transmission Data and Calculations (350 – 400 eV)	144
Figure A.18 – Hafnium Capture Data and Calculations (350 – 400 eV)	144
Figure A.19 – Hafnium Transmission Data and Calculations (400 – 500 eV)	145
Figure A.20 – Hafnium Capture Data and Calculations (400 – 500 eV)	145
Figure A.21 – Hafnium Transmission Data and Calculations (500 – 600 eV)	146
Figure A.22 – Hafnium Capture Data and Calculations (500 – 600 eV)	146
Figure A.23 – Hafnium Transmission Data and Calculations (600 – 700 eV)	147
Figure A.24 – Hafnium Capture Data and Calculations (600 – 700 eV)	147
Figure A.25 – Hafnium Transmission Data and Calculations (700 – 800 eV)	148
Figure A.26 – Hafnium Capture Data and Calculations (700 – 800 eV)	148
Figure A.27 – Hafnium Transmission Data and Calculations (800 – 900 eV)	149
Figure A.28 – Hafnium Capture Data and Calculations (800 – 900 eV)	149
Figure A.29 – Hafnium Transmission Data and Calculations (900 – 1000 eV)	150
Figure A.30 – Hafnium Capture Data and Calculations (900 – 1000 eV)	150

INDEX OF TABLES

Table 2.1 – Hafnium Average Resonance Spacings and Neutron Strength Functions	18
Table 3.1 – Details of Capture Measurement Set-ups	29
Table 3.2 – Isotopic Enrichments of Hafnium Oxide (HfO ₂) Samples	30
Table 3.3 – Details of Isotopically Enriched Hafnium Oxide (HfO ₂) Samples	31
Table 3.4 – Details of Natural Hafnium Metallic Samples	31
Table 3.5 – Capture Measurements Performed on Hafnium Samples	32
Table 3.6 – Details of Hafnium Samples used in Harwell 1973 Measurements	40
Table 3.7 – Details of Hafnium Samples used in Geel 2001 Measurements	42
Table 3.8 – RPI Data Sets Supplied	43
Table 5.1 – Binding Energies and Capture Detection Efficiencies	59
Table 5.2 – Experimental Parameters Input to REFIT	60
Table 5.3 – Flight Path Lengths Used for Analysis of Hafnium Sample Measurements	62
Table 5.4 – Abundance of Nuclides in Hafnium Oxide (HfO ₂) Samples Input to REFIT	66
Table 5.5 – Average Capture Widths of Hafnium Isotopes Used in Analysis	67
Table 5.6 – Hafnium Data Fitted Regions	70
Table 5.7 – Resonance Parameters for ¹⁷⁴ Hf	75
Table 5.8 – Resonance Parameters for ¹⁷⁶ Hf	76
Table 5.9 – Resonance Parameters for ¹⁷⁷ Hf	80
Table 5.10 – Resonance Parameters for ¹⁷⁸ Hf	97
Table 5.11 – Resonance Parameters for ¹⁷⁹ Hf	100
Table 5.12 – Resonance Parameters for ¹⁸⁰ Hf	111
Table 6.1 - JEFF3.1 Resolved Resonance Regions for Hafnium Isotopes	117
Table 6.2 - New Resolved Resonance Regions for Hafnium Isotopes	117
Table 6.3 - Hafnium Resonance Integrals	121

Table 6.4 – Calculated k-effectives for Test Cores	122
Table A.1 – Measurements of Debye Temperature for a Mono-Atomic Hafnium Crystal....	134
Table A.2 – Averages of Debye Temperatures of Hafnium.....	134

LIST OF ABBREVIATIONS

ADC	Analogue-to-Digital Converter
AGL	Analysis of Geel List-mode code
AGS	Analysis of Geel Spectra code
CEA	Commissariat à l'Énergie Atomique (French Atomic Energy Commission)
ENDF6	Evaluated Nuclear Data Format “6”, the international standard format for nuclear data library files
ENDF/B	Evaluated Nuclear Data File “B” library (US-based project)
EUFRAT	EUropean Facility for innovative Reactor And Transmutation data project
GELINA	GEel LINear Accelerator, a facility of the Neutron Physics Unit of IRMM
INRNE	Institute for Nuclear Research and Nuclear Energy, Sofia, Bulgaria
IRMM	Institute for Reference Materials and Measurements, Geel, Belgium
JANIS	JAvA-based Nuclear Information Software
JEF	Joint Evaluated File nuclear data library (the predecessor to JEFF)
JEFF	Joint Evaluated Fission and Fusion nuclear data library (European-based project)
JENDL	Japanese Evaluated Nuclear Data File library
MCNP	Monte Carlo N-Particle code
MLBW	Multi-Level Breit-Wigner
MONK	MONte carlo K-effective code
NEA	Nuclear Energy Agency, Paris, France
NUDAME	NUclear DATA MEasurement project
ORNL	Oak Ridge National Laboratory, Oak Ridge, Tennessee, USA
PENDF	Point-wise Evaluated Nuclear Data Format
REFIT	REsonance FITting code
RESCON	RESonance file format CONversion code
RPI	Rensselaer Polytechnic Institute, Troy, New York State, USA
RRR	Resolved Resonance Region
SLBW	Single Level Breit-Wigner
TOF	Time-Of-Flight
URR	Unresolved Resonance Region
WIMS	Winfrith Improved Multigroup Scheme code

1. INTRODUCTION

Nuclear data are used in the computational modelling of nuclear reactors, radiation shielding, and nuclear medicine. The accuracy of this modelling is dependent on the quality of the nuclear data provided. Neutron cross sections form one major set of nuclear data and this thesis reports on work to improve the characterisation of the cross sections of the six naturally occurring isotopes of the element hafnium (Hf).

1.1. Motivations for This Work

1.1.1. Properties and Uses of Hafnium

Hafnium is a ductile metallic element (atomic number, $Z = 72$) with six naturally occurring isotopes ^{174}Hf , ^{176}Hf , ^{177}Hf , ^{178}Hf , ^{179}Hf and ^{180}Hf , with relative natural abundances of 0.16%, 5.26%, 18.60%, 27.28%, 13.62% and 35.08% respectively. In nature, hafnium is found combined with zirconium. Whilst ^{174}Hf , the only radioactive isotope of the six (half life = 2×10^{15} years), is considered the least important for reactor applications, ^{177}Hf is considered the most important as it has the largest contribution to the neutron capture cross section of the natural metal.

The large absorption cross section of natural hafnium at thermal and epithermal neutron energies, together with favourable mechanical properties, make it a candidate for use in reactor control rods to regulate the fission process. As it is a resonance absorber it is particularly favoured for use in thermal fission reactors which have a harder (more energetic) neutron spectra, such as those using mixed-oxide (MOX) fuel, and is currently used in some light water reactor (LWR) systems [1]. Hence, it is important to understand the hafnium cross section in the resolved resonance energy region.

There have been a number of studies in the potential use of hafnium-based materials in future reactor design including;

- a) The use of hafnium hydrides (HfH_x) in the control rods of fast reactors [2], where the hydrogen in the compound moderates fast neutrons down to the resonance energy region of hafnium.
- b) The use of hafnium nitride (HfN) as an inert fuel matrix for waste transmutation, in particular that of transuranic nuclides in accelerator-driven systems (ADS) [3]. The compound provides a physically stable, high-temperature fuel matrix whilst the hafnium acts as a poison, due to its high absorption cross section, thus flattening the change in reactivity with respect to time. This results in higher burn-up as well as neutronic stability, leading to improved reactor safety and lower radiation damage to the system.
- c) The use of carbides such as $(\text{U,Zr,Hf})\text{C}$ as fuel materials in advanced innovative nuclear energy systems. These have high melting points ($>3500\text{ K}$) and are considered in the Generation IV roadmap [4].

1.1.2. Present Status of Hafnium Cross Section Data

Few studies have focussed on the neutron-induced total, capture and scattering cross sections in hafnium. Experimental data, which can be used for an evaluation of natural hafnium neutron-induced reactions in the thermal and resolved resonance region, are rather scarce and the evaluated data files are primarily based on the results of previous studies [5-11]. Recently capture and transmission measurements were performed using the Gaerttner Linear Accelerator Laboratory at Rensselaer Polytechnic Institute (RPI) [12, 13].

The Joint Evaluated Fission and Fusion (JEFF) nuclear data project [14], which is the main source of evaluated nuclear data in Europe, released the “JEFF3.1” evaluated nuclear data library in 2005. This is the most recent evaluated data file for hafnium, with the parameters of resonances below 200 eV updated via the results of the RPI work. The resultant JEFF3.1 files for the two odd mass number isotopes ^{177}Hf and ^{179}Hf (which have the most complex resonance structures) define resolved resonance regions below 250 eV, with unresolved resonance data defining the region 250 eV to 50 keV. The JEFF3.1 files for the abundant even mass number isotopes ^{176}Hf , ^{178}Hf and ^{180}Hf define resolved resonance regions below 700, 1500 and 2500 eV, respectively, with unresolved resonance data defining the remainder up to 50 keV. It should be noted that these files also contain older resolved resonance data from previous evaluations for energies above the defined RRR limits. These resonances are only used to influence the level of the cross section within the RRR. The JEFF3.1 file for ^{174}Hf contains only 12 resonances that are all below the RRR limit of 220 eV.

Validation of the JEFF3.1 library’s hafnium data [15] has shown that the new data give little improvement over its predecessor “JEF2.2” for benchmark integral cross section calculations. These comparisons between theoretical calculations based on the data libraries and experimental integral cross sections at the “EOLE” and “AZUR” zero-power reactors at the Commissariat à l’Énergie Atomique (CEA) facility at Cadarache, France [16, 17] concluded that the calculations underestimated the reactivity of the system with the hafnium control rods present. This was interpreted as an overestimation of the natural hafnium capture cross section in the epithermal energy range [18]. As a result of these studies, hafnium cross section measurements were placed on the international NEA High Priority Request List for nuclear data [19] (see Appendix B.1).

Furthermore, recent testing of the JEFF3.1 libraries [20] show that it is important to model energy regions containing resolvable resonances with true resolved resonance parameters, rather than statistically-based unresolved resonance parameters. This is due to the approximations used in unresolved resonance treatments in reactor physics codes. Whilst the approximations produce sufficiently accurate results, it is undesirable to use these models outside their validated range.

These circumstances highlighted the need for new cross section measurements of the hafnium isotopes in order to identify and accurately determine the parameters of previously unrecorded resonances, and to confirm or adjust, as appropriate, the parameters of known resonances. In doing this, the resolved resonance regions have been extended to higher neutron energies, thereby removing the need for the reactor physics codes' unresolved resonance treatments outside the energy range for which they have been validated.

The resolved resonance parameters produced during this work will form part of new evaluations for the naturally occurring hafnium isotopes in the next JEFF nuclear data library, expected to be released in 2010, which will succeed the JEFF3.1 library.

1.2. Structure of This Thesis

Chapter Two discusses neutron cross sections, particularly those in the “Resolved Resonance” neutron energy Region (RRR). These cross sections are most efficiently characterised by a set of neutron energy-dependent parameters, rather than point-wise data, which are derived from neutron resonance theory.

Chapter Three presents the cross section measurements that have been performed for this work using the Geel Linear Accelerator (GELINA) facility at the Institute for Reference

Measurements and Materials (IRMM), which is part of the European Commission Joint Research Centre, in Geel, Belgium. The chapter also reviews previous hafnium cross section measurements and how they feature in this work.

The analysis of the measurement data, from which the cross section parameters have been extracted, has been performed using the REFIT least-square fitting resonance analysis code [21]. The methods used in the code and the improvements that have been made to it as part of this work are discussed in Chapter Four. The techniques of the analysis and the resulting parameters are presented in Chapter Five.

Chapter Six discusses the findings of this project. These include the general features of the new evaluation hafnium data, testing of the new data via resonance integrals and benchmark calculations, and suggested further work based on issues arising during this work.

Overall conclusions are presented in Chapter Seven.

The Appendices present; a) subsidiary data analysis, including figures showing a small selection of measured data, and b) documentation justifying the need for new hafnium measurements and applications for the new measurements to be performed.

1.3. Statement of the Author's Contribution

The author was present at IRMM Geel whilst some of the new hafnium measurements were being performed, by the IRMM staff, to discuss the nature of the measurements and receive instruction on the data reduction process. The data reduction, resonance allocation and resonance analysis were conducted by the author with advice from several sources. The REFIT code was developed jointly by the author and M. Moxon.

2. NEUTRON CROSS SECTIONS

2.1. General Description of Cross Sections

A nuclear cross section is a representation of the probability of the nuclide in question undergoing a particular process induced by a beam of incident particles and is defined as [22]:

$$\frac{\text{number of events of the given kind per unit time per nucleus}}{\text{number of incident particles passing through unit area perpendicular to the beam direction per unit time}}$$

Each distinct process has an associated partial cross section and the total cross section is defined as the sum of all these partial cross sections. In this work, only neutron-induced processes are considered and for the natural hafnium isotopes and the incident neutron energies of interest, the only viable processes are radiative neutron capture (σ_γ) and elastic neutron scatter (σ_n). The total cross section (σ_{tot}) is therefore the sum of these two partial cross sections.

Neutron cross sections can be roughly divided into three energy regions according to the variation of the cross section with respect to incident neutron energy:

- the thermal region (below ~ 1 eV), where the capture cross section varies smoothly
- the resonance region (the focus of this work)
- the high energy region, where the capture cross section varies smoothly but other threshold reactions tend to dominate.

Figure 2.1 shows the capture cross sections at 300 K of the six natural hafnium isotopes for neutron energies between 0.1 eV and 10 keV. The changes in the structure, from the smooth

thermal cross section to the rapidly fluctuating resolved resonance region, followed by the smoother unresolved resonance and high energy regions are visible. These cross sections have been reconstructed from the parameters in the JEFF3.1 nuclear data library using the NJOY code [23] and displayed using the JANIS nuclear data visualisation software [24].

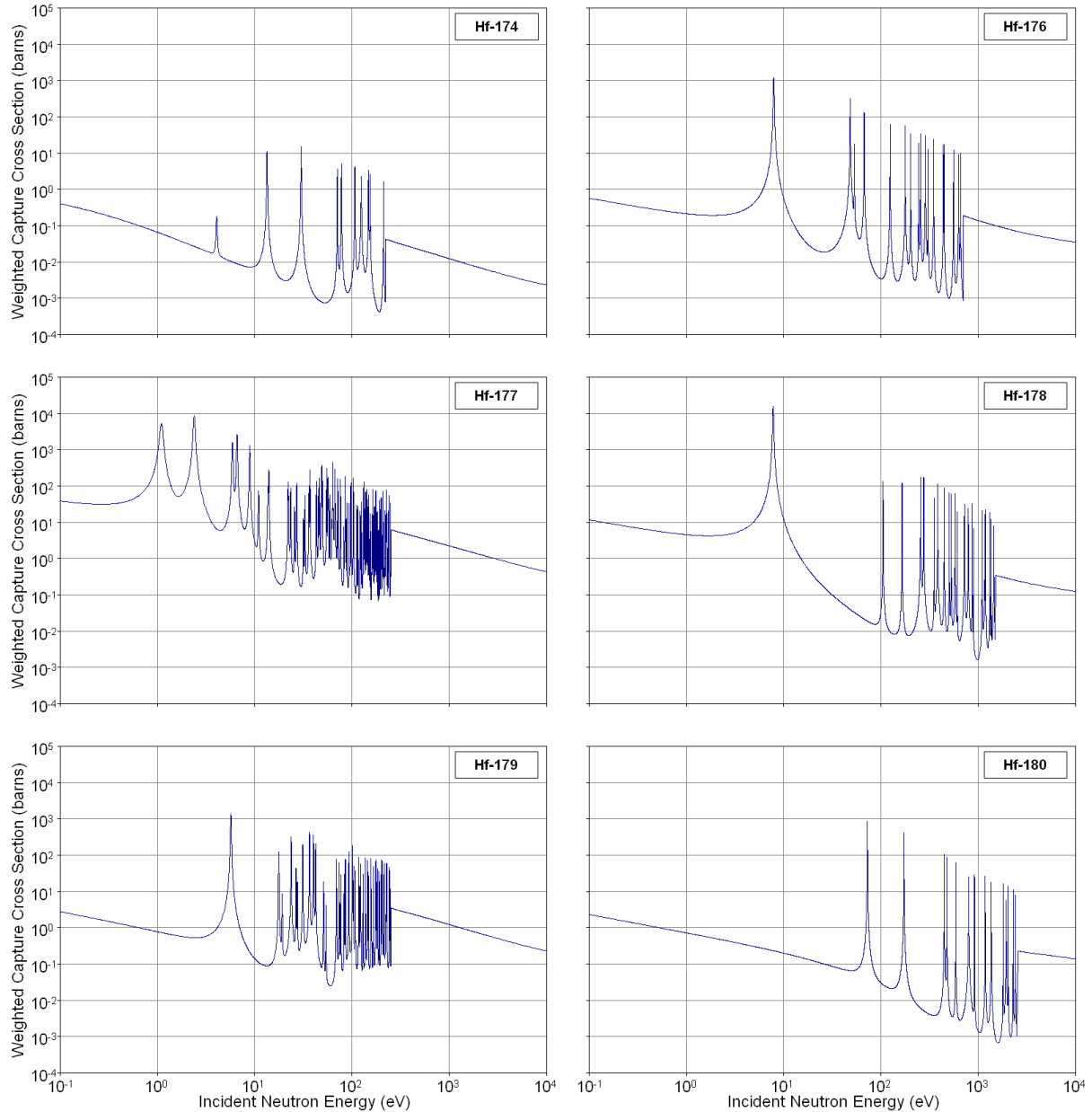


Figure 2.1 – Capture Cross Sections of the Natural Hafnium Isotopes Weighted Against Natural Abundance (JEFF3.1 data)

Accurate modelling of the resonance region is important for many isotopes in nuclear reactors, including hafnium. However, this energy range is also the most difficult to measure and to characterise due to the rapid fluctuations in the cross section. A large number of data points would be required to describe this resonance structure over the entire range. The exact resonance structure is also temperature dependent due to Doppler broadening resulting from the thermal motion of the nuclei. For these reasons, the Resolved Resonance Region (RRR) is described in evaluations using resonance parameters, defining the energy, size and shape of each of the resonances. On the other hand, in the Unresolved Resonance Region (URR), where the resonances become inseparable, i.e. the energy resolution of available experimental data is comparable to or broader than the spacing between the resonances, the structure must be described by average parameters based on the statistics of the set of resolved resonances rather than individual resonances.

The various computer codes that reconstruct cross sections will only use URR parameters above the defined RRR energy limit, i.e. the URR description will “override” any resolved resonances defined above the RRR limit. Therefore, the tails of any such resonances will contribute to the between resonance background cross section of the RRR but the peaks of these resonances will not feature in the reconstructed cross section. The REFIT code (see Chapter 4) is an exception to this rule; the code does not handle URR parameters and all resolved resonances defined in the file (within the energy limits defined by the user) will be used to reconstruct the cross sections.

2.2 Representation of Cross Sections by Resonance Parameters

An individual resolved resonance is characterised by the resonance energy (E_0), the partial reaction widths (e.g. the neutron width Γ_n , the capture width Γ_γ), the total angular momentum of the level and the orbital momentum of the incoming neutron.

Several formalisms have been developed to reconstruct the cross section structure from these parameters. One of the earliest and simplest is the Single Level Breit-Wigner formalism (SLBW) [25]. SLBW may be seen as a simplification of the more complex R-matrix formalism, by considering only one level. For isolated resonances, which are not affected by multi-level interference, accurate results can be obtained with the SLBW model. Where resonances are not well isolated, the Multi-Level Breit-Wigner (MLBW) formalism may be used. MLBW is an extension of SLBW in that it uses the same equations with an additional term to take account of the interference effect between resonances.

For more complex cases, with many overlapping resonances, the R-matrix formalism is preferred [22, 26]. However, for the R-matrix to be solved, some simplifications are required. One such simplification is the Reich-Moore approximation [27]. This method is used within the REFIT code.

The principle of the R-matrix formalism consists of assuming that both the incident particles (the neutron and nucleus) and the emerging reaction products to be ingoing and outgoing wave functions. Each allowable reaction is treated as a “channel” which is specified by the set of quantum numbers that defines it uniquely: the orbital angular momentum ℓ , the channel spin s and the total angular momentum J ($|\ell-s| \leq J \leq |\ell+s|$).

Since the nuclear forces are short-ranged, the region containing the nucleus is divided into an external and an internal region separated by an imaginary closed surface, of radius a_c , known as the channel radius. In the external region, the nuclear forces are negligible, so the wave function may be known analytically. However, in the internal region the nuclear forces dominate. The neutron (mass = 1) and the nucleus (mass = A) are merged together to form a system of A+1 nucleons which increases the complexity of the wave function so the internal region must be treated in terms of a so-called collision matrix $U_{cc'}$. For a given ingoing wave in channel c , leading to an outgoing wave in channel c' , the partial neutron cross section $\sigma_{cc'}$ may be expressed as:

$$\sigma_{cc'} = \pi \tilde{\lambda}^2 g_J |\delta_{cc'} - U_{cc'}|^2 \quad (2.1)$$

where: $\pi = 3.142\dots$

$$\tilde{\lambda} = \frac{\hbar}{\sqrt{2m_n E_n}} \text{ is the reduced de Broglie wavelength for a neutron of energy } E_n \quad (2.2)$$

$$g_J = \frac{2J+1}{2(2I+1)} \quad (2.3)$$

$$\delta_{cc'} = \delta_{\alpha\alpha'} \delta_{ll'} \delta_{ss'} \quad (2.4)$$

$$U_{cc'} = U_{\alpha l s, \alpha' l' s'}^J \quad (2.5)$$

g_J is spin weighting factor, i.e. the number of substates for the compound system $(2J+1)$ over the number of substates of the initial system consisting of a free neutron (2), and the target nucleus, $(2I+1)$, where I is the spin of the target nucleus. $\delta_{cc'}$ occurs because the ingoing and the outgoing particles cannot be distinguished if $c = c'$. $|U_{cc'}|^2$ is the probability of a transition

from channel c to channel c' . For the total cross section, there is only the incoming neutron, n , so the total cross section is expressed as a linear function of $U_{cc'}$:

$$\sigma_n = 2\pi\lambda^2 \sum_J g_J \sum_{l,s} (1 - \text{Re}(U_{cc'})) \quad (2.6)$$

where $\text{Re}(U_{cc'})$ is the real component of the collision matrix. For the elastic scattering cross section, the channels are the same incoming and outgoing neutron ($c = c' = n$). The elastic cross section is therefore expressed as:

$$\sigma_{nn} = \pi\lambda^2 \sum_J g_J \sum_{l,s} |1 - U_{cc'}|^2 \quad (2.7)$$

R-matrix theory expresses the collision matrix $U_{cc'}$, required to derive the above cross sections, in terms of the matrix R as follows [28]:

$$U_{cc'} = \exp(-i(\varphi_c + \varphi_{c'})) (\delta_{cc'} + 2i\sqrt{P_c} [(1 - RL^o)^{-1} R]_{cc'} \sqrt{P_c}) \quad (2.8)$$

$$R_{cc'} = \sum_r \frac{\gamma_{rc} \gamma_{rc'}}{E_r - E} \quad (2.9)$$

$$L_{cc'}^o = (S_c + iP_c - B_c) \delta_{cc'} \quad (2.10)$$

where:

– $R_{cc'}$ is the R-matrix element;

– φ_c is the hard-sphere potential scattering phase shift;

– S_c is the shift factor (real part of the logarithmic derivative of the outgoing wave function at the channel radius a_c);

– P_c is the penetration factor (imaginary part of the logarithmic derivative of the outgoing wave function at the channel radius a_c);

– B_c is boundary conditions at the channel radius a_c .

As only neutron induced reactions are being considered, B_c can be approximated as $-\ell$, [28] and at lower energies, the total angular momentum can be treated as zero ($\ell = 0$), i.e. only s-wave resonances are being considered, so the appropriate expressions for the other factors may be used;

$$\varphi_n = \rho,$$

$$S_n = 0,$$

$$P_n = \rho,$$

$$\rho = ka_c, \quad \text{where } k \text{ is the wave number}$$

Several non-trivial matrix inversions are still required to calculate the collision matrix. Therefore, the Reich-Moore approximation is now used, as this method neglects the off-diagonal contribution of photon channels (i.e. for $c' = \gamma$). This is a valid approximation as there are many channels, which have a decay amplitude of similar magnitude and random sign, so their contribution to the sum over the channels ($c \in \gamma$) tends to cancel for $c \neq c'$ [29];

$$\sum_{\substack{c, c' \in \gamma \\ c \neq c'}} \gamma_{rc} \gamma_{rc'} \equiv 0 \tag{2.11}$$

Therefore, the R-matrix becomes the reduced R-matrix, in that $R_{cc'}$ is only defined over the non-photonic channels and the photon channel is explicitly taken into account through the total radiation width Γ_{γ} ;

$$R_{cc} = \sum_r \frac{\gamma_{rc} \gamma_{rc'}}{E_r - E - i\Gamma_{r\gamma}/2} \quad (c, c' \notin \gamma) \quad (2.12)$$

$$\Gamma_{r\gamma} = \sum_{c \in \gamma} \Gamma_{rc} \quad (2.13)$$

For non-fissile nuclei, the only energetically allowed processes are elastic scattering ($c' = n$) and radiative capture ($c' = \gamma$) so the one-channel Reich-Moore expression may be used. Consequently, the reduced R-matrix becomes an R-function expressed as follows [27];

$$R_{nn} = \sum_r \frac{\gamma_{rn}^2}{E_r - E - i\Gamma_{r\gamma}/2} \quad (2.14)$$

From this reduced R-matrix, we get a reduced collision matrix that is a function of the R-function;

$$U_{nn} = \exp(-i(\varphi_n + \varphi_n)) \left(1 + 2i\sqrt{\rho} \left[(1 - R_{nn} i\rho)^{-1} R_{nn} \right] \sqrt{\rho} \right) = e^{-2i\varphi_n} \frac{1 + ik a_n R_{nn}}{1 - ik a_n R_{nn}} \quad (2.15)$$

The total (σ_{tot}) and elastic (σ_n) cross sections can then be obtained computationally, by substituting Equation 2.15 into Equations 2.6 and 2.7 respectively, and the capture cross section (σ_γ) can be obtained by the difference;

$$\sigma_\gamma = \sigma_{tot} - \sigma_n \quad (2.16)$$

The values of E_r , Γ_γ , and Γ_n for each resonance and a_c for each nuclide can be derived using resonance analysis codes, such as REFIT [21]. The analysis method used in REFIT is discussed in Section 4.1.

2.3 Storage of Resonance Parameters

The resonance parameters derived from resonance analysis are stored in evaluated nuclear data files such as those of the JEFF project. Within the JEFF nuclear data library, there are several sub-libraries including the incident neutron data library. This library is divided into files and “File 2” contains the neutron cross section resonance parameters.

All modern evaluated data libraries utilise the “ENDF6” standard data format [30]. The format for resolved resonance parameters is summarised in the following example from the

¹⁷⁷Hf JEFF3.1 file;

7.217700+4	1.754200+2	0	0	1	07234	2151	1
7.217700+4	1.000000+0	0	0	2	07234	2151	2
1.000000-5	2.500000+2	1	3	0	17234	2151	3
3.500000+0	8.000000-1	0	0	1	47234	2151	4
1.754200+2	8.000000-1	0	0	1080	1807234	2151	5
1.100100+0-3.000000+0	2.225000-3	6.523000-2	0.000000+0	0.000000+0	07234	2151	6
2.386800+0-4.000000+0	8.040000-3	6.070000-2	0.000000+0	0.000000+0	07234	2151	7
5.900200+0-3.000000+0	5.320000-3	6.200000-2	0.000000+0	0.000000+0	07234	2151	8

Figure 2.2 – Example of the ENDF6 Data Format

For example, line 7 of Figure 2.2 describes the resonance at 2.3868 eV has a spin of -4, neutron width of 8.04 meV and gamma width of 60.7 meV. Figure 2.3 presents the values contained in the resonance parameter file, where commas have been added for additional clarity; these do not exist in the real file as shown in Figure 2.2. The definitions of these values follow Figure 2.3;

ZA,	AWR,	0,	0,	NIS,	0,MAT,2,151,K
ZAI,	ABN,	0,	LFW,	NER,	0,MAT,2,151,K
EL,	EH,	LRU,	LRF,	NRO,	NAPS,MAT,2,151,K
SPI,	AP,	LAD,	0,	NLS,	NLSC,MAT,2,151,K
AWRI,	APL,	L,	0,	6*NRS,	NRS,MAT,2,151,K
ER1,	AJ1,	GN1,	GG1,	GFA1,	GFB1,MAT,2,151,K
ER2,	AJ2,	GN2,	GG2,	GFA2,	GFB2,MAT,2,151,K
ERn,	AJn,	GNn,	GGn,	GFA n,	GFBn,MAT,2,151,K

Figure 2.3 – Values contained in ENDF6 Format Resonance Parameter File

Starting with the right hand end of each record:

MAT	Material identifier
2,151,K	File number, section number, line number

Then in the body of the record:

ZA	Designation for the material (= 1000*Z + A)
AWR	Ratio of the mass of the material to that of a neutron
NIS	Number of isotopes in the material (=1)
ZAI	Designation for isotope (= 1000*Z + A)
ABN	Abundance of an isotope in the material (=1 in an isotopic file)
LFW	Flag for average fission widths in URR (=0, no average fission widths given)
NER	Number of resonance energy ranges (=2, RRR and URR)
EL	Lower limit for energy range
EH	Upper limit for energy range
LRU	Flag for resolved/unresolved resonance parameters (=1, resolved parameters)
LRF	Flag for parameter representation used (=3, Reich-Moore R-matrix)
NRO	Flag for energy dependence of scattering radius (=0, energy independent)
NAPS	Flag controlling the use of the scattering radius (=1 use the given value AP rather than calculating it from the isotopic mass)
SPI	Spin, I , of the target nucleus
AP	Scattering radius (units = 10^{-12} cm)
LAD	Flag for use of these parameters for angular distributions (=0 do not use)
NLS	Number of ℓ -values (neutron orbital angular momentum) in the energy region
NLSC	Number of ℓ -values used for calculation of elastic angular distributions
AWRI	Ratio of the mass of the isotope to that of a neutron
APL	ℓ -dependent scattering radius (units = 10^{-12} cm)
L	Value of ℓ
NRS	Number of resolved resonances for a given ℓ -value
ER	Resonance energy (in the laboratory system)
AJ	Spin, J , of the resonance
GN	Neutron width, Γ_n
GG	Radiation width, Γ_γ
GFA	First partial fission width (= 0.0 for hafnium isotopes)
GFB	Second partial fission width (= 0.0 for hafnium isotopes)

2.4 Specifics of Hafnium Cross Sections

The placement of hafnium cross section measurements on the NEA High Priority Request List [19] is justified by discrepancies in nuclear reactor core experiments and calculations [16, 17] as discussed in Section 1.1.2. However, further justification can be gained inspection of the actual resolved resonance data, opposed to the “application” library data.

The JEFF3.1 hafnium evaluation, used as a starting point for this work, was formed from new parameters derived from the RPI measurements [12, 13] for resolved resonances below 200 eV and parameters from the ENDF/B-VI.8 nuclear data library [31] for resolved resonances above 200 eV. The JEFF3.1 hafnium evaluation also contains unresolved resonance data defined up to 50 keV and taken from the JENDL3.3 nuclear data library. The ENDF/B-VI.8 library is primarily based on the results of previous studies [5-11], the most recent being published in 1984. The parameters in the ENDF/B-VI.8 files are defined for use with the MLBW formalism. However, the same values are present in the JEFF3.1 files, which require the use of the Reich-Moore formalism to reconstruct the cross sections. It is also noted that there are many resonances defined in the JEFF3.1 evaluation (imported from the ENDF/B-VI.8 evaluation) at energies above the defined upper energy limit of the RRR (see Table 6.1).

The make-up of the JEFF3.1 hafnium evaluation demonstrates a common occurrence in cross section evaluations that several different evaluations, which generally will overlap, have been joined together. In theory, the overlap should be exact but in reality the agreement between evaluations in the overlap varies and depends on the measurement set-ups and the evaluation tools. Therefore, a consistent set of resonance parameters describing the whole of the RRR of hafnium using the same cross section formalism (i.e. Reich-Moore) is desirable.

Further inspection of the hafnium resolved resonances in the JEFF3.1 files reveal that the number of “missing” resonances increases with neutron energy. Aside from visible “gaps” in the resonance structure, resonance statistics can be used to estimate the “completeness” of the evaluated data, as described below.

The spacing between individual resonances in any given nuclide can vary greatly, however the average spacing over several resonances and indeed larger energy ranges is consistent. In the case of the hafnium isotopes, the values for the average s-wave resonance spacing (D_0) have been subject to change due to an increased number of resolved resonances being identified over the last few decades. Values recently published by the IAEA [32] are given in Table 2.1.

The average compound nucleus cross section is directly related to the neutron strength function. The s-wave neutron strength function S_0 (a dimensionless quantity) is defined as:

$$S_0 = \frac{\langle g_J \Gamma_n^0 \rangle}{D_0} \quad (2.17)$$

where D_0 is the average s-wave resonance spacing, g_J spin weighting factor, (Equation 2.3) and Γ_n^0 is the reduced neutron width, which is defined for each s-wave resonance as:

$$\Gamma_n^0 = \frac{\Gamma_n}{\sqrt{E_R}} \quad (2.18)$$

where E_R is the resonance energy above the neutron threshold. Values of S_0 for hafnium were also published by the IAEA [32] and are given in Table 2.1.

Table 2.1 – Hafnium Average Resonance Spacings and Neutron Strength Functions [32]

Isotope	D_0 (eV)	S_0 (10^{-4})
^{174}Hf	18.0 ± 5.0	2.6 ± 0.6
^{176}Hf	30.0 ± 7.0	1.7 ± 0.4
^{177}Hf	2.4 ± 0.3	2.6 ± 0.3
^{178}Hf	57.0 ± 6.0	2.1 ± 0.3
^{179}Hf	4.6 ± 0.3	2.5 ± 0.4
^{180}Hf	94.0 ± 15.0	1.9 ± 0.6

It is noted that this work only considers s-wave resonances as p-wave resonances are not observed at the relatively low energies associated with the resolved resonance regions of the hafnium isotopes. Few p-wave hafnium resonances have been identified, all but one being in ^{180}Hf above 3 keV.

The average resonance spacings and the neutron strength functions are important input parameters for the statistical models used to parameterise the cross sections in the unresolved resonance region. These parameters result from a statistical analysis of the resolved resonance parameters. Therefore, the parameters of the resolved resonances at the upper end of the RRR should be consistent with the average parameters in order to preserve the average cross section. This ensures that the unresolved resonance parameterisation is consistent with the upper end of the RRR, so preventing a large step change in the average cross section at the RRR-URR boundary. For this reason, the analysis of the hafnium URR soon to be finalised at CEA Cadarache will include the resolved resonance parameters derived from this work.

The consistency between the resolved resonance parameters and the average spacing and strength function can be checked using the cumulative number of observed resonances and cumulative reduced neutron widths as a function of neutron energy. This method also gives an estimate of how many unidentified resonances there may be. Figure 2.4 presents the cumulative number of observed and theoretical resonances for ^{177}Hf and ^{179}Hf . Figure 2.5

presents the cumulative observed and theoretical $g_J \Gamma_n^0$ for ^{177}Hf and ^{179}Hf resonances. The theoretical values are derived from the values presented in Table 2.1, whilst the observed data is taken from the JEFF3.1 hafnium evaluation. Similar comparisons are made with the results of this work, for all the natural hafnium isotopes, in Section 6.2.

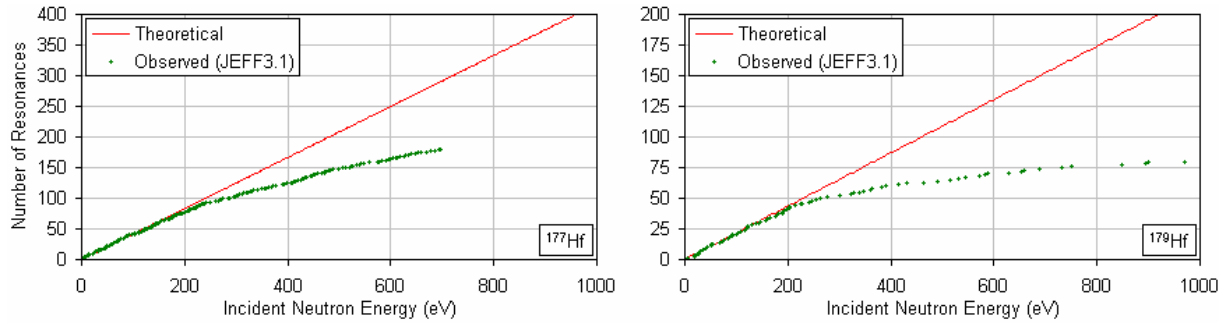


Figure 2.4 – Cumulative Number of ^{177}Hf and ^{179}Hf Resonances

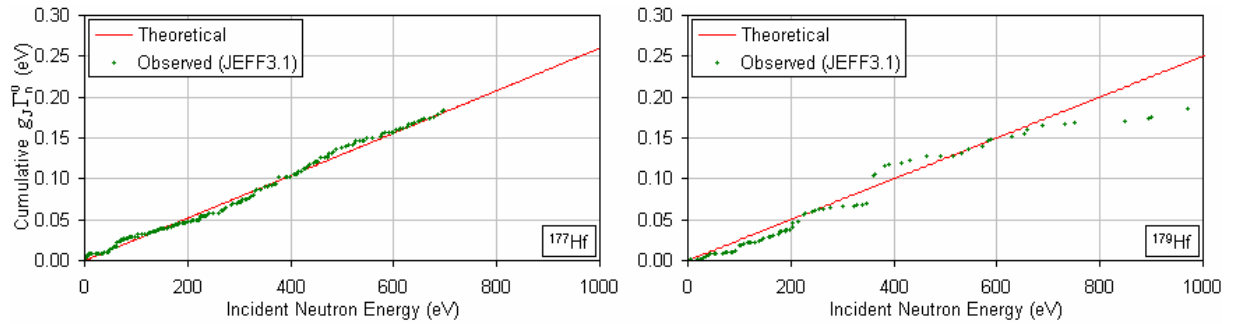


Figure 2.5 – Cumulative $g_J \Gamma_n^0$ Values for ^{177}Hf and ^{179}Hf Resonances

As these figures show, the frequency of observed resonances decreases with increasing neutron energy. The number of observable ^{177}Hf and ^{179}Hf resonances in previous hafnium measurements is limited due to the experimental resolution at higher energies being too low to resolve the tightly spaced resonances. Therefore, high-resolution measurements of isotopically-enriched hafnium samples are required to identify previously unrecorded resonances and allocate them to the correct isotope. In doing so, consistency between the resolved and unresolved resonance cross sections for the hafnium isotopes can be improved.

3. HAFNIUM CROSS SECTIONS MEASUREMENTS

3.1 Principles of Neutron Time-of-Flight Measurements

Time-of-flight (TOF) techniques are commonly used to perform cross section measurements. The principle of time-of-flight measurements is that the energy of a neutron can be determined from its time of flight across a known distance. In general, a short burst of neutrons is produced from a source and the time T_n recorded when a neutron interacts in a detector at distance L from the source. Then the non-relativistic neutron energy E_n is defined as;

$$E_n = \frac{1}{2} m_n \left(\frac{L}{T_n} \right)^2 \quad (3.1)$$

where m_n is the neutron mass. Provided that E_n is defined in electron-Volts, distance in metres and time in micro-seconds (all common units in nuclear data measurement), a “working” equation is defined as;

$$E_n(t) = \left(\frac{72.298 L}{T_n} \right)^2 \quad (3.2)$$

Time-of-flight facilities perform different types of measurement in order to determine cross sections as a function of the neutron energy. (The derivation of the cross sections from the measurements is detailed in Section 4.1.) The type of detector and set up used is dependent on the measurement being performed. Two of the most common types of measurement are neutron transmission and neutron capture.

3.1.1 Neutron Transmission Measurements

In neutron transmission measurements, neutrons that have not interacted with the material of the sample are recorded. This is accomplished by placing a neutron detector some distance behind the sample. A series of shields and collimators are positioned in front and behind the sample to prevent neutrons that do not pass through the sample, or that are scattered within the sample, from reaching the detector (see Figure 3.5). The interaction of a neutron within the detector, via the ${}^6\text{Li}(n,\alpha){}^3\text{He}$ reaction, for example, produces an electronic signal that can be used to record the time of arrival T_n of the neutron at the detector.

The ratio of the count rate with the sample in the neutron beam $C_{in}(T_n)$ and that of the sample out of the beam $C_{out}(T_n)$ is used to determine the measured transmission $T_{exp}(T_n)$;

$$T_{exp}(T_n) = N_T \frac{C_{in}(T_n) - B_{in}(T_n)}{C_{out}(T_n) - B_{out}(T_n)} \quad (3.3)$$

The normalisation constant N_T accounts for the ratio of the integrated intensities of the incident neutron beam during the “sample in” and “sample out” cycles. At GELINA, the counts from the BF_3 proportional detectors in the target hall (see Section 3.3.1) for each cycle were used to deduce N_T . $C_{in}(T_n)$ and $C_{out}(T_n)$ include a correction for dead time effects in the detector and associated electronics (see Section 3.2.2). $B_{in}(T_n)$ and $B_{out}(T_n)$ are background terms, explained in Section 3.2.1.

3.1.2 Neutron Capture Measurements

At resolved resonance neutron energies, the only viable reaction resulting in the emission of γ -rays for hafnium (being non-fissile) is radiative neutron capture. Therefore, neutron capture can be measured by detecting the γ -rays emitted from the sample when a compound nucleus de-excites to the ground state following absorption of a neutron. As such, the γ -ray detectors are positioned around the sample, ideally covering all angles, outside the path of the incident neutron beam. The γ -ray detectors should have a neutron capture detection efficiency independent of the composition of the γ -ray cascade, a fast timing response and a low efficiency for detecting the scattered neutrons. A γ -ray detector made from a C_6D_6 organic scintillator [33] meets these requirements.

Similarly to the transmission measurement, the measured capture yield $Y_{\text{exp}}(T_n)$ is obtained from the ratio of the observed γ -rays from the sample $C_S(T_n)$ to those observed $C_\phi(T_n)$ from a detector (usually a ^{10}B -ion chamber) measuring the incident neutron flux (see Figure 3.3);

$$Y_{\text{exp}}(T_n) = N_C \frac{C_S(T_n) - B_S(T_n)}{C_\phi(T_n) - B_\phi(T_n)} F_\phi(T_n) Y_\phi(T_n) \quad (3.4)$$

The normalization factor N_C is used as, in most cases, the geometry of the detection systems is not well-defined and it is hard to determine the absolute neutron flux together with the solid angles and absolute detection efficiencies. The factor F_ϕ corrects for the attenuation of the neutron beam through the exit window of the ionisation chamber and the attenuation due to the air between ionisation chamber and the sample. Y_ϕ is the theoretical capture yield of the ^{10}B layer in the ionisation chamber, defined by Equation 4.2 and calculated using the $^{10}\text{B}(n,\alpha)$ and ^{10}B total cross sections. As with transmission measurements, the observed counts, $C_S(T_n)$ and $C_\phi(T_n)$, should be corrected for dead time effects and background. Corrections for the

sensitivity of the γ -ray detectors to neutrons and for γ -ray attenuation in the sample are made during the resonance analysis stage of the work and are discussed in Section 4.1.

3.2 Experimental Considerations

3.2.1 Background Correction

The background counts subtracted in both Equations 3.3 and 3.4 can be attributed to various sources. Some are independent of the time of flight, such as natural sources, cosmic background and long-lived neutron activation of experimental apparatus. Others are time dependent, such as decay of the neutron source, scattering of neutrons into the sample from apparatus and “overlap” neutrons (see below). This background is measured by placing “black filters” [34] in the neutron beam, i.e. a material that has resonances with very large peak cross sections. These should attenuate all neutrons at energies across the peaks creating large dips in the spectrum. Any counts appearing in these regions can be attributed to the background. A time-dependent function can be fitted to the background count rate in the minima of these dips in the spectrum so a background can be defined for the entire measured region.

The measurement of a single neutron pulse may be affected by slow neutrons from the previous pulses, in particular whilst operating at long flight paths at high accelerator pulse frequencies, where the slower neutrons are overtaken by fast neutrons from the following pulse. These “overlap” neutrons therefore appear as a time-dependent background in the measured spectra. It is possible to reduce the number of overlap neutrons by absorbing them with an “anti-overlap” beam filter; either boron-10, which has a absorption cross section inversely proportional to neutron velocity ($\propto 1/v$), or cadmium, with a large absorption resonance at ~ 0.17 eV (peak capture cross section ~ 7700 b), that “blacks out” below ~ 0.7 eV.

3.2.2 Dead Time Correction

Dead time is the period after a neutron/ γ -ray is incident in the detector in which any further interactions will not be registered. The minimum dead time is that taken for the amplitude of the resultant pulse to fall back below the bias level of the electronics. In general, the user will set a longer time that allows the effects of the interaction to subside. The electronics do not register any other interactions during this period. The true detector counts C' can be estimated from the observed detector counts C and the dead time τ :

$$C'(T_n) = \frac{C(T_n)}{1 - \int_{T_n - \tau}^{T_n} C(t) dt} \quad (3.5)$$

At GELINA, the dead time of the capture and flux detectors are monitored continuously by registering the distribution of the TOF differences between consecutive events. The dead time for the Geel capture measurements described in Section 3.3 is 2.8 μ s. The dead time correction for the measurements at the 12 m station was less than 6% and for the 30 m and 60 m measurements, it was less than 1%.

3.3 High Resolution Cross Section Measurements at GELINA

The new measurements for this work were performed at the GELINA time-of-flight facility, part of the Institute for Reference Measurements and Materials (IRMM), near Geel, Belgium.

These measurements were made possible by applications to the NUClear DATA MEasurements project (NUDAME) [35-37] (see Appendix B.2) and the EUropean Facility for innovative Reactor And Transmutation neutron data (EUF RAT) project [38, 39] (see Appendix B.3). The endorsement of the proposed measurements allowed access to beam time and necessary equipment and expertise at Geel as well as supporting visits to Geel. The isotopic hafnium samples were kindly loaned by the Institute of Nuclear Research and Nuclear Energy (INRNE), Sofia, Bulgaria.

The NUDAME project was a Specific Support Action funded under the Sixth Framework Programme of the European Atomic Energy Community which concluded in March 2008. The EUFRAT project succeeds NUDAME and runs until October 2012 under the Seventh Framework Programme.

3.3.1 The GELINA Time-of-Flight Facility

The GEel LINear Accelerator (GELINA) [40] is used to achieve very short neutron pulses for time-of-flight measurements. The pulsed electron accelerator, operating at frequencies of between 50 and 800 Hz, produces electron pulses with a maximum energy of 150 MeV. These pulses are then compressed to ~1 ns in width by a post-acceleration compression magnet [41] before striking a rotating uranium target. The scattering of electrons in the target produces Bremsstrahlung radiation leading to production of neutrons mainly by (γ, n) and (γ, f) reactions in the uranium [42]. The result is a fission-like neutron spectrum; the majority of neutrons having energies of ~2 MeV. This neutron spectrum is moderated by two water-filled

beryllium containers adjacent to the target, in order to give a higher proportion of neutrons in the resolved resonance energy region, with an overall neutron energy range between ~ 1 meV and ~ 20 MeV [43]. The measured neutron spectrum is shown in Figure 3.1. These moderated neutron pulses are collimated into beams down the 12 flight paths arranged around the target as in Figure 3.2.

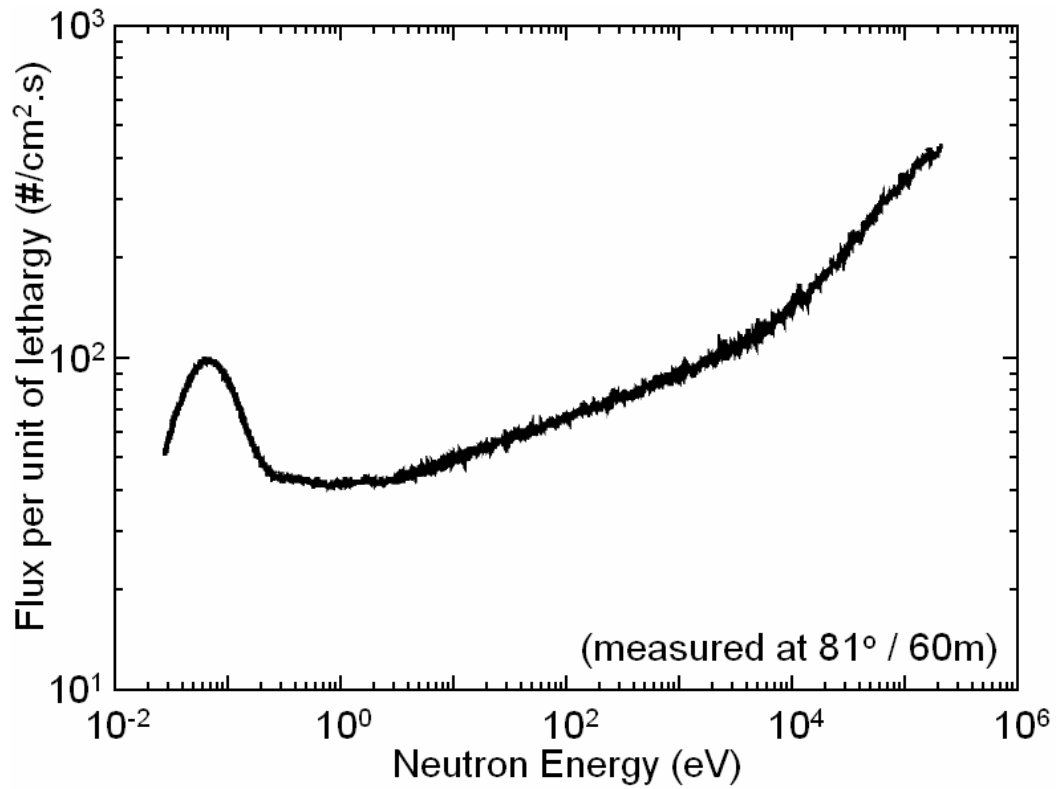


Figure 3.1 – GELINA Moderated Neutron Spectrum [40]

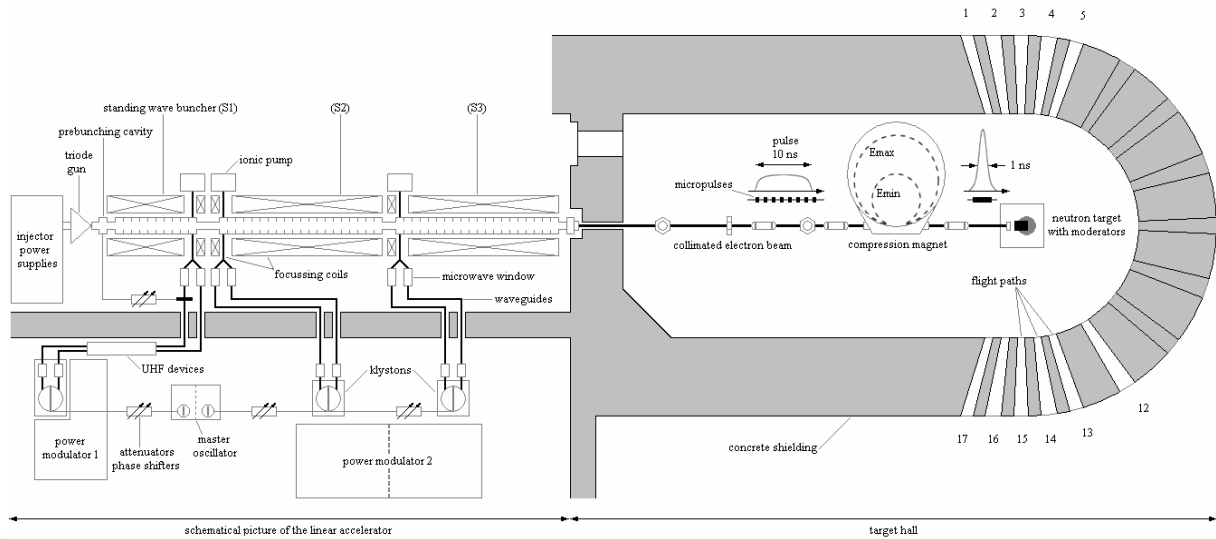


Figure 3.2 – Schematic of GELINA Accelerator and Target Hall [44]

Measurement stations are positioned along each flight path, ranging from 8 m to 400 m from the source. In capture measurements, the sample is positioned in the neutron beam with γ -ray detectors facing the sample. In transmission measurements, the neutron detector is placed in the neutron beam and the sample is placed about half way between the detector and source and covers the whole of the neutron beam.

Two BF_3 proportional counters are positioned on the ceiling above the target and are used to monitor the stability of the accelerator and to normalise the spectra to the same total neutron intensity.

The timing of the neutrons' flight is initiated by the trigger signal used to fire the LINAC. When a signal is received from the neutron/ γ -ray detector, the time is recorded. The timing is recorded with the IRMM Fast Time Coder with a 0.5 ns resolution [45].

3.3.2 Capture Measurement Set-up

The capture measurements for this project were performed at the three capture stations at GELINA. The set-up of these stations follow the general scheme shown in Figure 3.3. The key distinctions between the measurement stations are the flight path length and angle to the moderator, and the number of capture and flux detectors. These details are given in Table 3.1.

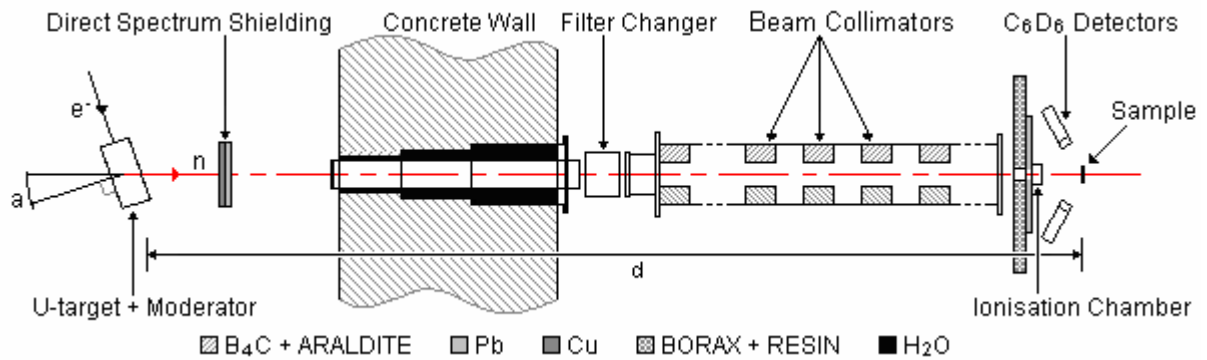


Figure 3.3 – Schematic of Flight Path Set-up for Capture Measurements [43]

Neutrons exiting the moderator enter the evacuated flight tube (the flight tube is shielded from the “direct spectrum”; neutrons emitted directly from the uranium target) which passes through the 3 m concrete wall of the target hall to the filter changer. This holds the anti-overlap filters (^{10}B or $^{\text{nat}}\text{Cd}$) and background filters (Ag, Bi, Co, Na, S, and W). The evacuated flight tube between the filter changer and measurement station contains collimators composed of copper and lead. The resulting moderated neutron beam is about 75 mm in diameter at the sample position. The shielding construction between the flight tube and sample reduces the background from scattered neutrons.

The γ -rays originating from the capture reaction in the sample were detected with C_6D_6 -based liquid scintillators [33] of 10 cm diameter and 7.5 cm height. The measurements were carried out with the detectors positioned at angles of 125° with respect to the neutron flux direction. Each scintillator is coupled to a photo-multiplier (PM) tube through a quartz window. For

each detector, the anode signal from the PM tube is used to determine the time of arrival of the neutron and the signal of the 9th dynode is used to provide information about the energy of the detected γ -ray. The gamma flash from the target is used as a reference for measuring the actual timing of the electron burst and the overall time resolution of the detection chain (i.e. the detectors, cabling and electronics), which is about 2.5 ns [43].

The energy dependence of the neutron flux below 150 keV was continuously measured with a (Frisch-gridded) ^{10}B ionisation chamber, with three back-to-back layers of ^{10}B evaporated on an aluminium backing, with a diameter of 84 mm [43]. The chamber operates with a continuous flow of a mixture of argon (90%) and methane (10%) at atmospheric pressure as detector gas [43].

Table 3.1 – Details of Capture Measurement Set-ups

Flight Path Number	Nominal flight path length (d)	Angle to moderator (a)	Number of C_6D_6 detectors	Number of ^{10}B detectors
5	12 m	18°	2*	2
15	28 m	0°	2	2
14	58 m	9°	4	1

*Four detectors were used for the April 2007 $^{\text{nat}}\text{Hf}$ measurements (see Table 3.5)

For each detected event in the C_6D_6 or ^{10}B -ion detector, the time and the pulse height (i.e. energy of incident γ -ray or $^7\text{Li}/\alpha$) of the event are recorded sequentially using the DAC2000 data acquisition system developed at Geel [46]. Operating in this so-called “list mode” allows rapid unformatted storage of the data. Processing of these data is then performed off-line. The simultaneous flux and capture measurements use separate electronic and data acquisition systems to reduce dead time effects.

3.3.3 Natural and Isotopically-Enriched Hafnium Capture Measurements

Capture measurements were performed on two types of sample; metallic hafnium discs containing the hafnium isotopes at their natural abundances, and hafnium oxide samples enriched in specific isotopes. The overlapping resonance structure of the hafnium isotopes mean that measurements of natural hafnium sample alone cannot distinguish between the different isotopes. Isotopically-enriched samples are therefore required to attribute resonances to particular isotopes as well as to resolve the structure of peaks in the natural cross section which are the result of resonances in the different isotopes occurring at very similar neutron energies. For these reasons, samples were sought via application to the NUDAME project [36] (Appendix B.2) and kindly loaned from INRNE Sofia. The enrichments of these oxide samples are given, with uncertainties where known, in Table 3.2 [47]. Whilst no uncertainties are given for most of the values, the simultaneous analysis of the different samples with REFIT gave confidence in (most of) these values (see Section 5.2.2).

Table 3.2 – Isotopic Enrichments of Hafnium Oxide (HfO₂) Samples

Major isotope	Abundance (%)					
	¹⁷⁴ Hf	¹⁷⁶ Hf	¹⁷⁷ Hf	¹⁷⁸ Hf	¹⁷⁹ Hf	¹⁸⁰ Hf
¹⁷⁶ Hf	<0.05	65.0	22.9	6.3	1.8	4.0
¹⁷⁷ Hf	<0.05	1.0	85.4	11.3	0.9	1.4
¹⁷⁸ Hf	<0.05	0.8	1.9	92.4 ± 0.2	3.3	1.6
¹⁷⁹ Hf	<0.05	0.2	1.3	4.1	72.1 ± 0.4	22.3
cf. natural	0.16	5.26	18.60	27.28	13.62	35.08
[48]	± 0.01	± 0.07	± 0.09	± 0.07	± 0.02	± 0.16

Five aluminium cans of compressed hafnium oxide were prepared from these samples at Geel. The specifications [49] of these measurement-ready samples are given in Table 3.3.

Table 3.3 – Details of Isotopically Enriched Hafnium Oxide (HfO₂) Samples

Sample	Mass of oxide (g)	Thickness of oxide (mm)	Internal can diameter (mm)	Atomic mass [50]	Thickness (atoms/barn)
¹⁷⁶ Hf	5.3424 ± 0.0001	2.0620 ± 0.0379	30.1300 ± 0.0387	207.93123	2.17×10 ⁻³ ± 5.57×10 ⁻⁶
¹⁷⁷ Hf	4.7070 ± 0.0001	3.2230 ± 0.0498	30.0900 ± 0.0082	208.93305	1.91×10 ⁻³ ± 1.04×10 ⁻⁶
¹⁷⁸ Hf-1	4.4570 ± 0.0001	2.5020 ± 0.1125	30.0600 ± 0.0141	209.93353	1.80×10 ⁻³ ± 1.69×10 ⁻⁶
¹⁷⁸ Hf-2	0.9006 ± 0.0001	1.0520 ± 0.0097	20.0300 ± 0.005	209.93353	0.82×10 ⁻³ ± 0.42×10 ⁻⁶
¹⁷⁹ Hf	5.3175 ± 0.0001	2.4520 ± 0.0558	30.0600 ± 0.0238	210.93565	2.14×10 ⁻³ ± 3.39×10 ⁻⁶

Several natural hafnium metallic samples of were provided by Geel for measurement. The specifications for these were verified [49] and are detailed in Table 3.4. The atoms/barn values stated have been calculated assuming the natural samples are 97.0% pure, with the remainder being zirconium [51].

Table 3.4 – Details of Natural Hafnium Metallic Samples

Nominal thickness	Mass (g)	Thickness (mm)	Diameter (mm)	Atomic mass [50]	Thickness (atoms/barn)
1 mm	33.3600 ± 0.0001	1.0810 ± 0.0018	54.995 ± 0.040	178.4849	4.6053×10 ⁻³ ± 6.75×10 ⁻⁶
0.26 mm	16.1961 ± 0.0001	0.2566 ± 0.0092	80.04 ± 0.01	178.4849	1.0532×10 ⁻³ ± 2.63×10 ⁻⁷
0.079 mm	5.0697 ± 0.0001	0.079 ± 0.0009	80.04 ± 0.02	178.4849	3.2969×10 ⁻⁴ ± 1.65×10 ⁻⁷
0.024 mm	1.4849 ± 0.0001	0.0244 ± 0.0010	80.04 ± 0.02	178.4849	9.6565×10 ⁻⁵ ± 4.83×10 ⁻⁸

Capture measurements were performed using the samples described above. These included measurements with black resonance filters in the beam as well as only the carbon fibre sample holder and aluminium can (in the case of the oxide samples). These measurements were used

to derive background spectra for both the capture and flux measurements. The measurements that were prepared for resonance analysis are detailed in Table 3.5. The flight path lengths presented here are nominal lengths; the effective flight path lengths, as calculated with the REFIT code are presented in Section 5.2.1.

Table 3.5 – Capture Measurements Performed on Hafnium Samples

Sample	Flight Path Length (m)	LINAC Frequency (Hz)	Overlap filter	Total beam time (hours)
^{nat} Hf 0.26 mm	12.89	50	-	8
^{nat} Hf 0.079 mm	12.89	50	-	11
^{nat} Hf 0.024 mm	12.89	50	-	24
^{nat} Hf 1 mm	58.586	800	¹⁰ B	257
¹⁷⁷ Hf	12.95	800	¹⁰ B	94
¹⁷⁸ Hf -1	12.95	800	¹⁰ B	96
¹⁷⁸ Hf -2	12.95	800	¹⁰ B	42
¹⁷⁹ Hf	12.95	800	¹⁰ B	144
^{nat} Hf 1 mm	12.95	800	¹⁰ B	23
¹⁷⁶ Hf	28.82	800	¹⁰ B	95
¹⁷⁷ Hf	28.82	800	¹⁰ B	41
¹⁷⁸ Hf -1	28.82	800	¹⁰ B	109
¹⁷⁹ Hf	28.82	800	¹⁰ B	148
^{nat} Hf 1 mm	28.82	800	¹⁰ B	37
¹⁷⁶ Hf	28.82	50	^{nat} Cd	192
¹⁷⁹ Hf	28.82	50	^{nat} Cd	39

3.3.4 Data Reduction

The Analysis of Geel List-mode (AGL) code package [52] was used to convert the raw measurement data into counts binned into 30720 time-of-flight channels. The channel widths increase in discrete steps with increasing time-of-flight in order that resonances throughout the energy region of interest are mapped with a sufficient number of points.

The stability of the detection systems and the accelerator operating conditions (i.e. frequency, current and neutron output) were checked. The inclusion (or rejection) of each one-hour cycle of the measurement run was determined from the ratios of various observed counts, including the total counts output from each ADC (Analogue-to-Digital Converter) and those from the central neutron monitor. The data from cycles with ratios lying outside a defined deviation from the average ratio were rejected from the analysis. The ratios were calculated and rejects suggested by the AGL_rej code and the results manually checked before cycles were rejected from further processing. Particular attention was paid to measurements with few total counts such as those of the sample holders where poorer statistics resulted in a higher number of suggested rejects by AGL_rej.

The alignment of the calibrations of each ADCs was verified by “binning” the γ -ray energies into 1024 channels using the AGL_amp code. A multiplication factor was applied where necessary. Typically this was less than 3% and not worse than 10%. A bias window was defined to reduce background noise by excluding outlying counts. For the C_6D_6 ADCs this was 185 keV, the threshold of the detectors, to above 7626 keV, the highest neutron binding energy in hafnium (^{177}Hf). For the ^{10}B ion chamber ADC(s), this was 840 keV and 2800 keV, the deposition energy limits of the $^{10}\text{B}(n,\alpha)^7\text{Li}$ reaction products.

The C₆D₆ detectors' calibration (channel verses γ -ray energy) was verified based upon measurements of the 2.6 MeV γ -ray from the ²³²Th decay chain, before and after the hafnium measurements. [53] This calibration allowed the pulse-height weighting to be applied effectively.

The Geel C₆D₆ detectors utilise the so-called total energy detection principle, [33] which relies on the use of a low efficiency detector. For such a detector, where the γ -ray detection efficiency is very small, essentially only one γ -ray from the entire γ -ray cascade is registered, the capture detection efficiency can be approximated by [33];

$$\varepsilon_C = 1 - \prod_i (1 - \varepsilon_{\gamma_i}) \approx 1 - (1 - \varepsilon_{\gamma})^n \approx \sum_i \varepsilon_{\gamma_i} \quad \text{for } \varepsilon_{\gamma} \ll 1 \quad (3.6)$$

If the efficiency of detecting a γ -ray detection is proportional to the incident γ -ray energy, then the efficiency of detecting a capture event becomes proportional to the sum of the energies of the γ -rays emitted in the capture event, i.e. the total excitation energy (the neutron binding energy plus the neutron kinetic energy, in the centre-of-mass frame) and so is independent of the γ -ray cascade path. The so-called Pulse Height Weighting Technique [33] applies a weighting to the response function of the detection system to achieve this required proportionality between the capture event detection efficiency and the incident γ -ray energy.

The weighting function $W(E_d)$ is defined as;

$$\int_0^\infty R_d(E_d, E_\gamma) W(E_d) dE_d = E_\gamma \quad (3.7)$$

where $R_d(E_d, E_\gamma)$ is the detector response function, i.e. the probability that a γ -ray with an energy E_γ results in an observed deposited energy E_d . The integral of $R_d(E_d, E_\gamma)$ corresponds to the overall efficiency $\varepsilon(E_\gamma)$ for detecting a γ -ray;

$$\int_0^{\infty} R_d(E_d, E_\gamma) dE_d = \varepsilon(E_\gamma) \quad (3.8)$$

Reliable weighting functions require an accurate description of the response of the detection system to γ -rays and this response is dependent on the photon transport in both the sample and the detector assembly. Consequently, a weighting function is required for each detector and sample configuration. Photon transport calculations were performed by A. Borella with the Monte-Carlo N-Particle (MCNP) code [54] to simulate the detector response function for each configuration. Borella then derived each weighting functions to satisfy Equation 3.7 using a least squares fit approach. The resultant weighting functions for each sample were then provided in the form of eight-term polynomial functions.

The above information together with the list-mode data files were then processed with the AGL_fast code to produce spectra suitable for further processing with the AGS code package.

The Analysis of Geel Spectra (AGS) code package [55, 56] was first used to perform a dead time correction for each detector. The counts for the capture detectors were summed together to form a single spectrum. This operation was repeated for the flux detectors. During these processes, AGS generates uncertainties due to counting statistics and propagates these through subsequent operations to provide uncertainties on the resultant capture yields.

Using the black resonances in the ancillary measurements, a background was manually fitted for both the capture and flux measurements. For capture spectra, the background is of the form;

$$B(t) = a_1 \exp(-b_1 t) + a_2 \exp(-b_2 t) + c \quad (3.9)$$

and for flux spectra, the background is of the form;

$$B(t) = at^b + k \quad (3.10)$$

where t is the time-of-flight and c and k are time-independent constants. These equations were provided in the AGS input together with their coefficients. AGS then generates spectra from these equations and subtracts them from the appropriate measured spectrum.

The capture spectrum is then divided by the flux spectrum and multiplied by the correction factor (cf. Equation 3.4). The correction factor arises from the difference in the flux spectrum entering the flux detector and that entering the sample which is a result of neutron absorption in the thin layer of ^{10}B in the flux detector and the attenuation of the beam by the exit window of the detector and the ~ 1 m of air between the detector and sample face. The dominant feature of this correction factor is the $1/v$ absorption calculated in AGS from the ^{10}B cross section.

The resultant yields were normalised using the saturated, low energy ^{177}Hf resonances. An appropriate normalisation constant was then applied within AGS. These normalisations were later checked using the REFIT code.

The high energy “black” resonances of the background filters, including the 100 keV sulphur resonance are visible in the capture yields. The position of these resonances in the spectra, revealed that the capture and flux measurements were not aligned in energy when the given flight path length and initial delay values were used (Figure 3.4). The initial delay of the flux measurements was therefore artificially adjusted to align these high energy resonances in the flux spectra with those of the capture spectra. This misalignment only had a noticeable effect at neutron energies well above the hafnium resolved resonance region.

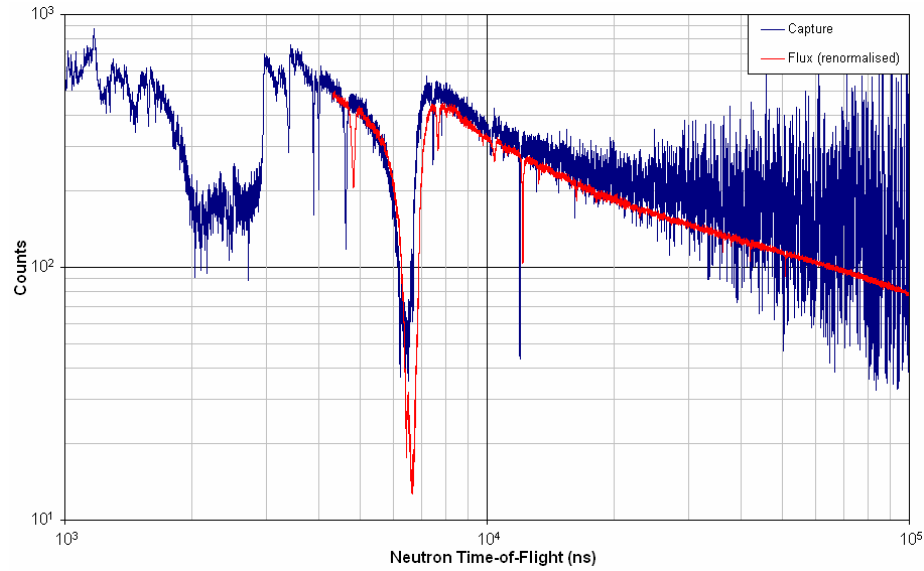


Figure 3.4 – Misalignment Observed Between Capture and Flux Spectra

3.4 Natural Hafnium Transmission Measurement

A transmission measurement was performed on a thick metallic, naturally enriched, hafnium sample at the Geel 50 m transmission station on Flight Path 4. The transmission set up is presented in Figure 3.5. A similar set up was used for previous hafnium measurements conducted by Siegler at the 26 m station on Flight Path 2, which are described further in Section 3.5.4. The beam line of both flight paths is at 9° to the normal of the moderator face.

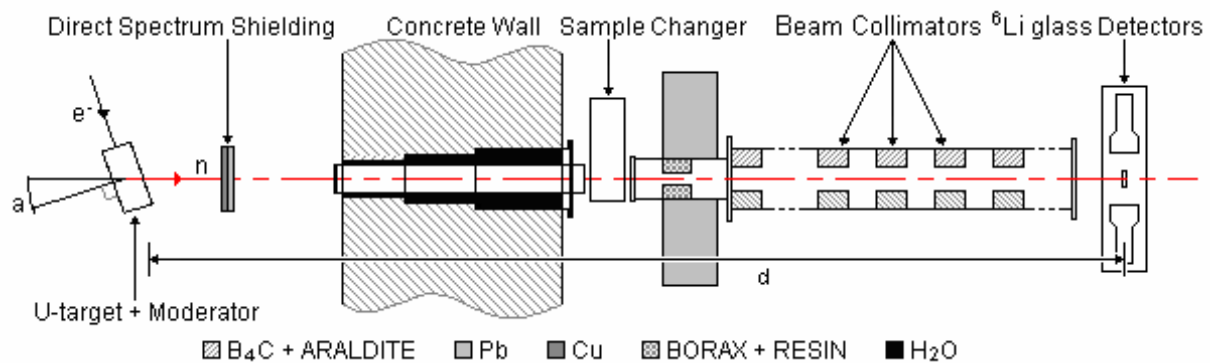


Figure 3.5 – Schematic of Flight Path Set-up for Transmission Measurements [43]

The hafnium sample used for this measurement was comprised of 15 metallic discs, with a nominal combined thickness of 16 mm. The discs had a measured diameter of 55.0 ± 0.05 mm and a combined mass of 498.97 ± 0.13 g. A purity of 97.0% was once again assumed [51], giving $6.893 \times 10^{-2} \pm 3.797 \times 10^{-5}$ atoms/barn of hafnium.

The data reduction of the measurement was performed using the AGS code in a similar manner to the capture measurements, with a background being derived from the black resonances of Co (132 eV) and Na (2.85 keV). Credit is due to S. Kopecky for the sample analysis and data reduction, as well as conducting this measurement.

It is noted that the application to the EUFRAT project, which supported this measurement, proposed the measurement of a ~50 mm natural hafnium sample. However, such a measurement was not possible in the scheduled measurement period as: a) additional sample material was not available at Geel; b) the relatively low neutron flux intensity at the 50 m measurement station combined with such a thick sample would have resulted in very few neutrons reaching the detector and; c) the 26 m station, which offers a higher neutron flux, was unavailable due to the upgrading of the Flight Path 2 components.

3.5 Previous Measurements Used In This Work

The new hafnium measurements described above offer improved information on the resonance cross sections of the natural hafnium isotopes, as few previous measurements have produced data for isotopically-enriched samples in the 200 – 2500 eV neutron energy range, none of which benefited from the improved experimental resolution of modern measurement apparatus. However, there are specific aspects of some previous works which justify their inclusion in the resonance analysis to complement the new measurements.

3.5.1 ORNL 1963 Transmission Measurements

Transmission measurements were conducted at Oak Ridge National Laboratory (ORNL) in 1963 on isotopically-enriched samples of hafnium oxide [6]. The raw counts, experimental parameters, calculated transmission yields and calculated cross sections for a total of 22 measurements covering different isotopic enrichments and neutron energy ranges were kindly provided as copies of the original computer printouts by J. Harvey. These were electronically scanned and processed with character recognition software by the author. Using the raw counts and background and dead time corrections parameters provided by J. Harvey, the calculated values were then recomputed. There now exist exact electronic copies of the print outs of these data.

Prior to the availability of the enriched isotopic sample measurements described in Section 3.3.3, these measurements were to be used in the resonance analysis performed with the REFIT code. However, due to the limit on data sets allowed in a REFIT problem and the superior resolution of the new Geel measurements, these measurements have instead been used for verifying the existence of resonances in the neutron energy range below 50 eV.

3.5.2 Harwell 1973 Capture Measurements

Capture measurements were performed at the Harwell LINAC for two samples of natural hafnium and three isotopically-enriched samples (^{176}Hf , ^{178}Hf , ^{180}Hf) in 1973 [8]. The details of these samples are given in Table 3.6. The print outs of these data, including capture yields and associated uncertainties, were provided by M. Moxon. These were electronically scanned by the NEA Databank and reconstructed into formatted data files by the author, which were then checked for accuracy against the original print outs.

Table 3.6 – Details of Hafnium Samples used in Harwell 1973 Measurements

Sample	Main Isotope	Abundance (%)						Thickness (atoms/barn)
		^{174}Hf	^{176}Hf	^{177}Hf	^{178}Hf	^{179}Hf	^{180}Hf	
Natural metallic	-	0.16	5.26	18.60	27.28	13.62	35.08	8.5048×10^{-5}
	^{176}Hf							0.6985×10^{-3}
Enriched oxide	^{176}Hf	0.1	68.7	14.9	8.68	2.73	4.99	1.4490×10^{-3}
	^{178}Hf	<0.05	0.52	4.36	89.14	2.90	3.07	1.2232×10^{-3}
	^{180}Hf	<0.05	0.23	1.00	2.22	2.66	93.89	1.7170×10^{-3}

In a similar situation to the 1963 ORNL measurements, these data were the best capture measurements of isotopically-enriched hafnium samples prior to the recent Geel measurements. The resolution of the data is comparable to that of the Geel data in the 5 – 400 eV energy region. However, at higher energies the resolution of the Geel data is superior.

In addition, the recent Geel measurements have included measurements of ^{176}Hf -, ^{178}Hf - and naturally-enriched samples similar those used in the Harwell measurements. Therefore, it is only the ^{180}Hf -enriched sample measurement that has been included in the resonance analysis performed using REFIT.

3.5.3 ORNL 1982 Capture Measurements

The JEFF3.1 ^{180}Hf file contains resolved resonance parameters up to 10 keV. However, the RRR-URR boundary is set at 2.5 keV, resulting in the defined resonance structure at higher energies being replaced by the unresolved treatment in the majority of processing codes. These resolved parameters were originally derived from capture measurements performed at Oak Ridge National Laboratory by Beer and Macklin [10, 11] and (more recently) have been “resolved” into s- and p-wave resonances. From the relevant references it can be seen that new parameters were derived for the isotopes; ^{176}Hf (for resonances in the range 2.7 – 5.2 keV), ^{177}Hf (2.6 – 2.7 keV), ^{178}Hf (2.6 – 8.9 keV), ^{179}Hf (2.6 – 3.1 keV) and ^{180}Hf (2.7 – 9.9 keV).

It is clear that, as the previously existing resolved resonance parameters only extend to ~2.5 keV for ^{180}Hf , only the ^{180}Hf parameters were placed in the evaluated files, as there cannot be an energy gap within the resolved resonance region data in the ENDF6 format file, which would be the case if the Beer and Macklin data for ^{176}Hf and ^{178}Hf were included, as demonstrated in Figure 3.6.

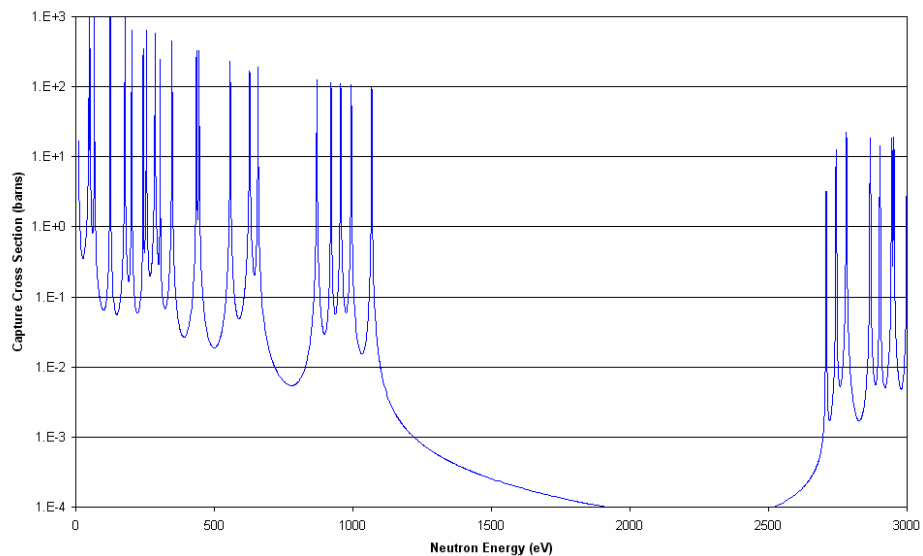


Figure 3.6 – Gap in Resolved Resonance Data for ^{176}Hf

Therefore, it was proposed that the analysis extend the resolved resonance region to ~2.5 keV for ^{176}Hf and ^{178}Hf in order that the Beer-Macklin parameters be inserted into the evaluated file, so extending the resolved resonance region for the even-mass isotopes well into the keV range. This is further discussed in Section 5.4. This has not been done for the odd-mass isotopes, as the new Geel measurements do not have sufficient resolution above ~1 keV to define the resonances of these isotopes up to ~2.6 keV. Furthermore, if the experimental resolution did allow extension to ~2.6 keV, there would be little to gain from the addition of the Beer-Macklin parameters for these isotopes.

3.5.4 Geel 2001 Transmission Measurements

Transmission measurements of natural hafnium samples were performed at Geel in 2001 [57]. Metallic hafnium discs were stacked to create three samples, of nominal thicknesses 1, 2 and 15 mm and measured at 300 K and, with the use of a cryostat, at 77 K, at the 26 m measurement station. The raw data was processed in a similar manner as described in Section 3.4. The resultant transmissions were submitted to EXFOR and retrieved for this work.

The thicknesses of these samples were recalculated and are given in Table 3.7. The purity of hafnium was again assumed to be 97.0% with 3% zirconium [51]. The change in atoms/barn values (<0.3%) due to the cooling to 77 K was neglected as the coefficient of linear expansion is not well known ($\sim 6 \times 10^{-6} \text{ K}^{-1}$).

Table 3.7 – Details of Hafnium Samples used in Geel 2001 Measurements

Nominal Thickness (mm)	Thickness (atoms/barn)
1	4.5953×10^{-3}
2	9.1906×10^{-3}
15	6.4334×10^{-2}

3.5.5 RPI 2003 Transmission and Capture Measurements

The JEFF3.1 evaluation for hafnium below 200 eV is based on the analysis conducted at Rensselaer Polytechnic Institute (RPI) [12]. On request, 29 sets of measurement data were supplied by RPI staff. Table 3.8 presents the 17 hafnium samples that were used in the 29 different measurements (marked “×” and “*”).

Table 3.8 – RPI Data Sets Supplied

Sample Name	Sample type	Thickness of Hf (atoms/barn)	Thermal Trans.	Thermal Capture	Epi-Thermal Trans.	Epi-Thermal Capture
0.5 mil	Natural Hf metal	4.621×10^{-5}				×
1 mil	Natural Hf metal	9.984×10^{-5}	*			
2 mil	Natural Hf metal	2.369×10^{-4}	*	×		×
4 mil	Natural Hf metal	4.537×10^{-4}	*	×		
10 mil	Natural Hf metal	1.139×10^{-3}	*	×	×	×
20 mil	Natural Hf metal	2.303×10^{-3}	*		×	
50 mil	Natural Hf metal	5.755×10^{-3}	*		×	×
100 mil	Natural Hf metal	1.154×10^{-2}			×	
Cell 1-1	^{176}Hf enriched solution	3.888×10^{-5}			×	×
Cell 1-4	^{178}Hf enriched solution	2.017×10^{-5}			×	
Cell 1-5	^{178}Hf enriched solution	1.048×10^{-5}			×	×
Cell 1-6	^{178}Hf enriched solution	2.467×10^{-6}			×	×
Cell 1-7	Natural Hf solution	2.923×10^{-5}			×	
Cell 2-3	^{176}Hf enriched solution	2.183×10^{-5}			×	
Cell 2-4	^{176}Hf enriched solution	6.949×10^{-6}				×
Cell 2-6	^{178}Hf enriched solution	1.367×10^{-6}				×
Cell 2-7	^{178}Hf enriched solution	6.868×10^{-7}				×

The six “thermal” transmission measurements of natural hafnium (marked “*”) were used along with new Geel data for analysis of the 0.5 – 20 eV region by the author (Section 5.3). The other data supplied by RPI were used in the reanalysis of the 8 eV doublet by M. Moxon (Section 5.3).

4. THE REFIT CODE

The REFIT (REsonance FITting) code is used to derive resolved resonance parameters from the analysis of neutron transmission and capture yield data. The latter part of this chapter outlines the origins of the code and discusses the developments made during this project. The methods used in within the code for resonance analysis are discussed below.

4.1 Neutron Resonance Analysis Using REFIT

REFIT uses a least square fitting method to fit theoretical transmission/capture yield values to measured values by adjustment of nuclear and experiment parameters. The fit can be performed for several measured data sets simultaneously. The initial values of the nuclear and experiment parameters, the measurements and nuclides under consideration, the measured and nuclear data filenames, the neutron energy ranges under investigation and the parameters to be adjusted in the fit are input to the code via the “control” file.

The code uses the Reich-Moore approximation to R-matrix theory (described in Section 2.2) to calculate nuclear cross sections from the resonance parameters supplied by the user, i.e. it calculates the components of the collision matrix (Equation 2.15) in order to calculate the total, elastic and capture cross sections (Equations 2.6, 2.7 and 2.16) for each of the nuclides specified in the problem.

These cross sections are then Doppler broadened according to the appropriate effective temperature of each nuclide. The product of the nuclides’ abundance and cross sections are then summed over all nuclides in each sample to give the “sample” cross sections for all the measured data sets in the problem.

The sample cross sections are then used to calculate the theoretical transmission or capture yield required for each measurement, as defined in Equations 4.1 and 4.2 respectively:

$$T(E_n) = \exp(-n\sigma_T(E_n)) \quad (4.1)$$

$$Y(E_n) = (1 - \exp(-n\sigma_T(E_n))) \frac{\sigma_C(E_n)}{\sigma_T(E_n)} \quad (4.2)$$

where σ_T is the total cross section, σ_C is the capture cross section and n is the thickness (atoms/barn) of the sample. E_n is the neutron energy corresponding to the time-of-flight, T_n (Equation 3.2). The transmission/yield is then resolution broadened (which takes account of factors such as the electron pulse width and the spread in time of neutrons leaving the source for the particular experimental conditions). Detector efficiency must also be considered; for transmission measurements, the properties of the neutron detector must be provided, for capture measurements, the binding energy of the compound nuclei must be known (see Sections 3.3.4 and 5.2.1) and γ -ray absorption within the sample should be considered (see Section 5.2.1). In addition, a correction is added to the capture yield to account for the scattering of neutrons within the sample. This correction allows for: a) neutrons that have been initially scattered within the sample then captured on a subsequent interaction (hence the scattered neutron's energy does not correspond to its the time-of-flight) and; b) neutrons that have been scattered out of the sample into the detector and triggered a detector response (a function of the detectors' sensitivity to neutrons, see Section 5.2.1).

Having constructed a theoretical transmission/yield, which takes account of experimental conditions, a residual for every data point to be used in determining the resonance parameters, is then defined as;

$$residual = \frac{measured\ value - calculated\ value}{uncertainty\ on\ measured\ value} \quad (4.3)$$

The range of each measured data set to be “fitted” is defined by either neutron energy or time-of-flight. Several data ranges can be defined for each data set. If a range is to be used to derive resonance parameters, then a residual is calculated for each data point in that range. A least square fit is then performed to minimise the value χ^2 , where;

$$\chi^2 = \sum_{i=1}^M r_i^2 \quad (4.4)$$

$$\text{and } r_i = f(x_1, x_2, \dots, x_N) \quad (4.5)$$

where M is the number of data points to be fitted and N is the number of parameters (x_1, x_2, \dots, x_N) to be adjusted in the fit. The preset limit within the REFIT code for M is 100,000 and for N, 185. The least square fitting method in REFIT is a compromise between three different algorithms: Newton-Raphson, Steepest Descent and Marquardt. The method is implemented by routines created by M. Powell [58] and developed by M. Moxon for use in REFIT. In order to minimise the sum of the squares of the residuals, numerous nuclear and experiment parameters may be adjusted, including:

- resonance energy, radiation width, neutron width, fission width or spin (affects the nuclear cross sections)
- nuclide abundance, areal density (i.e. atoms/barn) or effective temperature of the sample (affects the sample cross sections)
- flight path length or the time-of-flight of the first data channel (affects the calculation of the neutron energy corresponding to each measured data channel)

- properties of the neutron source (affects the resolution function)
- neutron/ γ -ray detector properties (affects the resolution function and detector efficiency)
- background or normalisation correction parameters (corrects errors in the data reduction).

Whilst it is possible to adjust any combination of these parameters in a single fit, it is common practice to fix those parameters that can be well defined by other means such as a chemical/physical analysis of the sample, calibration of the flight path, use of detectors with well-defined properties. Knowledge of these details is key if REFIT is to be used for analysis of a resonance structure where the resonance parameters are considered to be poorly known.

After each iteration, the residuals are recalculated using the updated parameter values from the previous iteration. If nuclear parameters have been changed, then the nuclear cross sections, sample cross sections and theoretical transmissions/yields will all be recalculated. The program will continue until the variation in parameter values between iterations is less than the desired accuracy of the parameters specified by the user, or the maximum number of iterations (as set by the user) is reached.

A measure of the quality of the fit of the calculation to the measured data is defined as;

$$\chi^2/dof = \frac{\chi^2}{\text{degrees of freedom}} = \frac{\chi^2}{(M - N)} \quad (4.6)$$

A χ^2/dof value of unity indicates an optimum fit to the data, i.e. the calculation agrees with the measured data to within the uncertainties on the measured data points. χ^2/dof should not be much less than unity as this indicates that the uncertainties assigned to the measured data are too large.

4.2 Development of the REFIT code

The REFIT code was developed by M. Moxon for resonance analysis of cross section measurements performed at the UKAEA Harwell LINAC from the 1970s onwards. Whilst the code had been periodically submitted to the Nuclear Energy Agency (NEA) Databank for international release, the most recent submission prior to the current work was in 1997. Despite REFIT still being in use at Geel, code developments were sporadic, with no formal releases, several operating system dependent versions in existence and no recent supporting documentation [59]. Therefore, an updated version of REFIT was desired for analysis of the hafnium cross section measurements in this project.

4.2.1 REFIT-2007

An initial update to REFIT was undertaken by M. Moxon, C. Dean and the author, in preparation for a new submission of the code to the Nuclear Energy Agency (NEA) Databank for international release.

New subroutines were added to the source code to allow resonance parameters to be supplied in the international standard ENDF6 data format [30] as well as the existing “REFIT” format. The code was also made to output fitted resonance parameters in ENDF6 format. This feature has improved the overall usability of the code.

Many smaller modifications were also made to the source code to improve portability, including the separation of 8-bit real and 4-bit integer variables in common blocks to resolve problems with misalignment in common storage and the extension of filename character strings from 64 to 128 characters to allow for complex file directory structures. In addition, several coding errors were identified and corrected.

Test cases for the submission were created for uranium, copper and “resium” (a fictitious element, with properties designed to test the code’s capabilities). The REFIT control files, the data files used and the REFIT outputs were included. A users’ guide, containing code theory and input description was developed from a previous paper on REFIT, was included in the package.

The complete package was submitted to the NEA Data Bank where it was tested on various computer platforms and made available for distribution on by request. The REFIT-2007 [60] code package (NEA-0914/07) can be viewed at the NEA Data Bank Computer Programs website [61].

4.2.2 REFIT-2009

The hafnium data analysis, in this thesis, was performed using “REFIT-2009”. This code version was developed from the REFIT-2007 version by M. Moxon and the author.

Modifications included the correction of several coding errors that were identified including the ENDF6 format data reading subroutine. The output from the code was improved by inclusion of subroutines to output tabulated data files, compatible with common data graphing software packages, directly from the main program. This removed the need for an external routine to produce such files and greatly improves the speed with which the results can be plotted. Additionally, the clarity with which information is displayed in the main REFIT output file has been improved.

In recent years previous to this project, the majority of REFIT code developments were performed on a single operating system and code compiler software. This gave rise to the presence of several non-standard FORTRAN statements and a reliance on compiler-specific default compilation options for correct operation. The use of different operating systems and

code compiler software, as well as investigation of compiler options, identified such issues. Modifications have been implemented to resolve these issues and improve code portability between computer systems.

Various stages in the iteration process within REFIT are terminated when specific internal variables equal specific limits. However, the routines containing the relevant decision statements were written for and originally used with single-precision real variables. However, as REFIT now operates using double-precision real variables, a time penalty is incurred with additional iterations required in order that two double-precision real values be equal to the sixteenth significant figure. Therefore, a further modification has been implemented such that iteration stages cease when the relevant variables are within 1×10^{-7} of the target values.

REFIT is able to determine the abundance of an isotope in a sample. Modifications developed by M. Moxon enable the abundance of an element (i.e. all isotopes with the same atomic number) in a sample to be determined. These modifications, together with routines developed at Geel by A. Brusegan and S. Kopecky [62] to input resolution functions as tabular values and to model the shape and porosity of samples have also been included.

The complete REFIT-2009 package has been submitted to the NEA Data Bank for testing prior to distribution via the NEA Data Bank Computer Programs website [61].

4.2.3 Further Developments

Several further improvements have been developed for the REFIT code by the author and limited testing performed. However, these were not included in the REFIT-2009 code version, as they were not essential to the hafnium measurement analysis and could not be incorporated into the code within the constrained timetable for the production of the hafnium results.

The REFIT source code includes around 30 separate files. The bulk of the coding is contained within a single file, with the remainder containing the declarations for common variable blocks. The modern FORTRAN “module” feature has been used to declare all common variables individually within the main source file. This removes the need for these numerous externally-declared common statements. This improves the clarity with which data are passed throughout the program, allows for easier implementation of dynamic array allocation, improves the portability of the code, and allows for easier fault tracing and further development as all the source code is contained within a single file.

The volume of data generated by REFIT is far greater than the capacity of computer memory that was available in the 1970s when the code was first developed. To this end, REFIT writes temporary files to disk in order to store this data during the calculation. As the memory available in modern computing now far exceeds the size of the REFIT temporary files, it is preferable to use memory storage rather than disk storage, particularly due to the time required for read/write operations. Therefore, code modifications have been written to store these temporary data in multi-dimensional arrays. These replace the original subroutine, which organised the data into the direct-access scratch files and recovered and reconstructed the data when required.

To ensure the continued use of REFIT in the wider cross section evaluation community, improvements to the user interface are desirable; this was a conclusion of the Neutron Resonance Analysis Summer School 2008 [63]. An update to the format of the various REFIT input files was developed based on feedback from the summer school. The changes include free-format input, arrangement of input parameters into more logical groups, removal of redundant control flags and parameters and the creation of additional “control blocks”. The “EXPERT” control block contains several parameters that are present in the standard control file format that are rarely changed and should only be so by an expert user. Therefore, the revised program sets default values for these parameters unless the “EXPERT” keyword is present, in which case the values following the keyword are adopted. The “PRINT” control block contains several flags in the standard control file format that invoke the print out of information that is more relevant to a code developer than a user. Therefore, the revised program will default to “no print” unless the “PRINT” keyword is present, in which case the flags specified after the keyword are used. This new interface is made back-compatible with the REFIT-2007/REFIT-2009 control file format; if older format control files are used, an internal conversion routine will generate a new format control file, from the older file supplied by the user, prior to executing the main program.

These further code developments, as well as the developments for REFIT-2009, REFIT-2007 and other older code versions (prior to this project) have resulted in some subroutines being superseded by more modern FORTRAN features. These redundant routines have been removed from the source code. Additionally, some control parameters are now redundant and some program output is no longer relevant. These inputs and outputs have also been removed.

4.3 The RESCON Code

The RESCON (RESONance file format CONversion) code was written to convert ENDF6 format resonance parameters into a REFIT format resonance parameter files. However, previous code versions required data to be manually extracted from ENDF6 file into an input file prior to running the code. The source code has been updated and tested by the author to produce the RESCON-2009 version, which handles ENDF6 format files directly with a brief, interactive user interface. The routine has been used in test cases to ensure consistency between the handling of the REFIT and ENDF6 data formats by the REFIT code and is included in the REFIT-2009 code package.

5. ANALYSIS OF MEASUREMENT DATA

The resonance analysis of the measured hafnium capture yields and transmissions was performed in several stages. For the neutron resonance theory to be correctly applied, it was necessary to assign each resonance peak to its relevant hafnium isotope. The REFIT code was then used to adjust the resonance parameters in order to fit the calculation to the measurement. The primary analysis covered the 0.5 eV to 1 keV neutron energy range, with an additional analysis of the 1 keV to 3 keV neutron energy range for the isotopes ^{176}Hf , ^{178}Hf and ^{180}Hf only.

5.1 Assignment of Resonances to Isotopes

The allocation of resonances was primarily performed by overlaying plots of the capture yields from the 30 m measurements of the enriched oxide and natural 1 mm foil hafnium samples. The Moxon enriched sample measurements [8] were also used for verifying the resonance allocation, particularly for ^{180}Hf , as there is no new ^{180}Hf -enriched sample measurement available.

The change in the structure of each yield curve relative to the others enabled resonances to be allocated. Some resonances are only visible and their isotope identifiable using the enriched samples due to the overlap in the resonance structures of the six natural isotopes. Small resonances or those in minor isotopes are commonly hidden by large or major isotope resonances. Such resonances may only be visible in samples enriched in the relevant isotope.

The starting point for the resonance identification was the resonances listed in the JEFF3.1 evaluated hafnium files. This included the resonances below 200 eV recently analysed in the work at RPI [12]. Above 200 eV, the resonance information comes from the ENDF/B-VI.8

evaluation [31]; resonances are identified up to 211 eV for ^{174}Hf , 1068 eV for ^{176}Hf , 697 eV for ^{177}Hf , 2090 eV for ^{178}Hf , 689 eV for ^{179}Hf and 11,350 eV for ^{180}Hf . It was noted that the RPI analysis produced new parameters for the resonances defined in the ENDF/B-VI.8 evaluation and did not change the isotope or spin allocation of any resonances (although four more ^{179}Hf resonances were introduced).

This list of resonances was modified and added to such that resonances were identified to up to 250 eV for ^{174}Hf , 1 keV for $^{177,179}\text{Hf}$ and 3 keV for $^{176,178,180}\text{Hf}$ (the ^{180}Hf resonances above 3 keV could not be verified using the new Geel data, as discussed in Section 5.4). The modifications included correction of the energy and/or isotope assignment of known resonances and the splitting of known single resonance peaks into doublet or even triplet peaks. For new resonances, crude average neutrons widths were assigned as starting values. The gamma widths initially assigned were the averages given in the JEFF3.1 files. The determination of the final gamma width values is described in section 5.2.3.

For the isotopes ^{177}Hf and ^{179}Hf , where there are two possible s-wave resonance spins for each isotope, the spin value was arbitrary assigned such that the distribution between the two spin values was approximately equal. This method of assignment was necessary as experimental data to determine the spins of resonances is scarce for resonances below ~ 300 eV and non-existent for the numerous “new” resonances above 300 eV. As the spin weighting function is a component of the R-matrix formulism (Equation 2.1), the shape of the resonance as calculated by REFIT does have a dependence on the spin assignment. However, there is a strong correlation between the resonance spin and width values. Therefore, to determine the spin allocation of resonances by REFIT analysis of capture yields and transmissions alone, would require the resonance widths for each resonance to be fitted twice (once for each spin

value), with the better fit indicating the most likely spin value. This method was not feasible within the timescales of this work. However, it was found that whilst analysing some doublet resonance peaks in ^{177}Hf , with the resonance pair assigned different spins, REFIT swapped the resonances around, i.e. the fitted energy and neutron width values of one resonance was similar to the starting values of the other, so these resonance were effectively assigned the spin values which gave the best fit to the measured data.

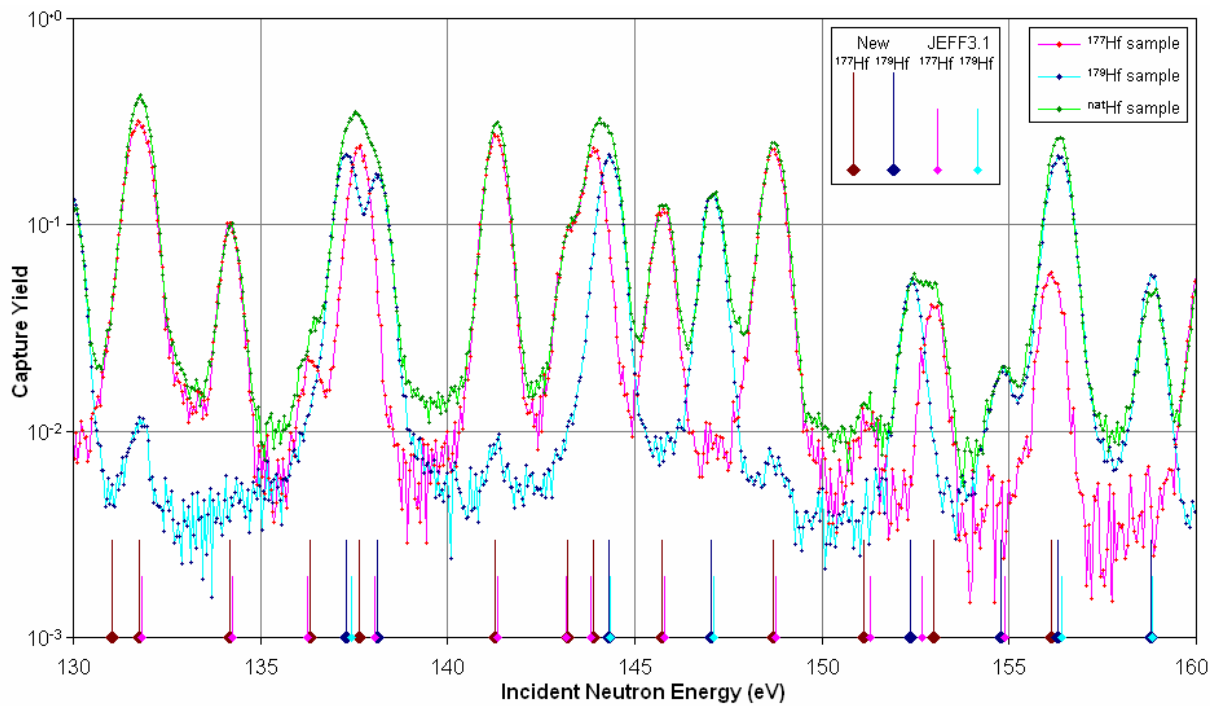


Figure 5.1 – Comparison of Measured Capture Yields of Hafnium Samples at 28 m with the JEFF3.1 and New Resonance Allocations

Figure 5.1 demonstrates the process of allocating resonances to isotopes. The 130 – 160 eV energy region shown in the figure can be regarded as a typical hafnium resonance structure. Natural hafnium has a relatively simple cross section structure in this specific region as the only resonances present are associated with the ^{177}Hf and ^{179}Hf isotopes. The overlaying of the capture yields of ^{177}Hf , ^{179}Hf and naturally enriched hafnium samples reveals the resonance-isotope association. The figure also compares the allocation of resonances in the

JEFF3.1 evaluation (short vertical markers) and this work (longer markers). Differences between the resonance allocations occur at 137 eV, 153 eV and 156 eV.

Overall, this process of assigning resonances has revealed around one dozen resonances below 200 eV which were previously unidentified or assigned to the wrong isotope. This commonly occurred where the new capture measurements showed a doublet peak, previously designated a singlet. Above 200 eV, there was found to be an increasing number of unidentified resonances, with identified resonances occasionally being misassigned. Above 700 eV, the majority of resonances were previously unidentified, chiefly due to a complete absence of ^{177}Hf resonances and only seven ^{179}Hf resonances in previous evaluations. Section 5.5 presents the resonances and their parameters produced from this work and compares them with those from previous evaluations.

5.2 Experimental Considerations and Assumptions

Whilst it is possible to allow the REFIT code to adjust any experimental or nuclear parameter associated with the measured data or nuclear data used in an analysis, it is not desirable as the code may adjust the “wrong” parameter in order to obtain a good fit to the data due to the strong correlation between some parameters. Therefore, it is preferable to determine some parameters by other means (discussed in Section 4.1) and input them to REFIT as fixed values. This is particularly the case for hafnium where resonance parameters, especially those at higher neutron energies, are poorly known.

5.2.1 Experimental Parameters

The physical dimensions and mass of the samples are required to determine the respective areal densities (atoms/barn). These parameters were determined by physical analysis of the samples and are given in Tables 3.3 and 3.4.

The classical ideal gas model [64, 65] was used in the analysis of all samples to calculate the Doppler broadening of resonances. The model assumes that the nuclei in the solid have the same velocity distribution as an ideal gas at an effective temperature, T_{eff} . The effective temperature for each nuclide is a REFIT input parameter and was calculated from the sample temperature, T_S , the Debye temperature, T_D , of the material and Boltzmann's constant, k_B , using Equation 5.1 [22];

$$T_{\text{eff}} = \frac{3}{8} T_D k_B \coth\left(\frac{\frac{3}{8} T_D}{T_S}\right) \quad (5.1)$$

For the recent Geel measurements, a sample temperature of 293 K (which is equivalent to 25.252 meV) was assumed. A Debye temperature for hafnium of 252 K was derived from a recent survey of Debye temperature measurements by G. Noguère [66], as detailed in Appendix A.1. Using these values and Equation 5.1, an effective temperature for all nuclei in the Geel measurements in this analysis was defined as 302.9 K (26.10 meV).

The efficiency of capture event detection is proportional to the total energy of the γ -ray cascade resulting from neutron capture and therefore the binding energy of the nuclei in the samples, as the Pulse Height Weighting Technique has been applied during the data reduction (Section 3.3.4). The binding energies [67] of all nuclei in all samples (including impurities, see Section 5.2.2) were normalised to that of ^{177}Hf (having the highest binding energy of the six natural hafnium isotopes). The resultant ratios were used as the nuclei-dependent capture detection efficiencies. These are presented together with the binding energies in Table 5.1.

For the total energy of the γ -ray cascade to be equal to the nuclide's binding energy, it is assumed that the excited compound nucleus decays to its ground state following neutron capture. For the majority of nuclei considered in this analysis, this assumption is well-

founded. However, it was noted that for thermal neutron capture in ^{178}Hf , the ($^{178}\text{Hf}+n$) compound nuclei is more likely to decay to the ^{179m}Hf isomer state than the ^{179}Hf ground state, with a branching ratio of 0.63 ± 0.08 [68, 69]. This isomer state subsequently decays to the ground state with a half-life of 18.67 ± 0.04 seconds. Therefore, the total energy of the initial γ -ray cascade is the binding energy (6098.99 keV) less the energy level of the isomer (375.037 keV), [48] so equals 5723.95 keV. The ^{178}Hf capture detection efficiency was recalculated as 0.7688 ± 0.0038 , which assumed a branching ratio to the isomer of 0.63 $((5723.95 \times 0.63 + 6098.99 \times 0.37) / 7625.96)$. In addition, a preliminary REFIT run was performed using the Geel capture data and allowing the ^{178}Hf capture detection efficiency to vary. This run produced a value of 0.7560 ± 0.0002 , thereby showing good agreement with the theoretical value. A value of 0.7600 was input to REFIT instead of that given in Table 5.1.

Table 5.1 – Binding Energies and Capture Detection Efficiencies

Nuclide	Binding Energy (keV) [S_n]	Capture Detection Efficiency [$S_n / S_n(^{177}\text{Hf})$]
^{174}Hf	6708.50 ± 0.40	0.8797
^{176}Hf	6383.40 ± 0.70	0.8371
^{177}Hf	7625.96 ± 0.18	1.0000
^{178}Hf	6098.99 ± 0.08	0.7998 (see above)
^{179}Hf	7387.78 ± 0.15	0.9688
^{180}Hf	5694.80 ± 0.07	0.7468
^{16}O	4144.13 ± 0.11	0.5434
^{55}Mn	7270.45 ± 0.13	0.9534
^{79}Br	7892.35 ± 0.11	1.0349
^{81}Br	7593.04 ± 0.11	0.9957

The likelihood of a capture event being detected is also dependent on the γ -rays resulting from the capture event escaping the sample. In the case of physically thick or dense samples, it is possible for γ -ray to be absorbed by other atoms in the sample. The REFIT code can account for this effect via input of data based upon Monte Carlo calculations of γ -ray absorption in the

sample concerned. Such calculations must be specific to each sample/detector configurations and were not available for the experimental setups used in this work. However, the hafnium samples used are relatively thin and any γ -ray absorption effects are minimal.

Whilst the C_6D_6 detectors used for neutron capture measurements at Geel have a very low sensitivity to those neutrons that have been scattered from the sample and apparatus into the detector, a study of this sensitivity has been performed by M. Moxon [70] using various capture measurement data from Geel. From this, a neutron energy dependent neutron detection efficiency, ε_n , has been derived and has been used in this work;

$$\varepsilon_n = 0.0053434 E_n^{-0.5} + 0.0002914 \quad (5.2)$$

The REFIT code reconstructs the resolution function of the measurement set-up using several physically-meaningful parameters. These parameters have been established through previous work to determine the properties of the electron pulse and the uranium target at Geel [53, 70]. The values of these parameters are given in Table 5.2. It is noted that uncertainties for these values were not available [53].

Table 5.2 – Experimental Parameters Input to REFIT

Parameter	Value
Thickness of the moderator (metres)	0.040
Number density of hydrogen in the moderator (atoms/barn)	0.2409
Effective mean diameter of the moderator (metres)	0.120
Neutron source decay time (microseconds)	0.0035
Mean width of electron pulse (microseconds)	0.0010
Ratio of top to bottom of trapezium shaped neutron pulse	0.70
Effective diameter of neutron beam at face of moderator (metres)	0.120
Effective mean free path of a 1 eV neutron in moderator (metres)	0.005983
Angle of neutron beam to normal of the moderator face (radians)	See Table 3.1
Gaussian spread in neutron pulse	None
Amplitude of secondary neutron pulse relative to primary pulse	0.016727
Delay of secondary neutron pulse	0.0
Decay of secondary neutron pulse = $\exp[-\ln(2).t / (a.E^b)]$	2.5433, -0.5633

In order that the peak energies of the resolved resonances are correctly determined and that all measurement data sets are aligned on the same neutron energy scale, the effective flight path length of each data set, defined in the REFIT code as the distance from emitting face of neutron source to incident face of detector/sample, is adjusted by the code. (The adjusted value will be that which gives the best fit to the data, so is not necessarily equal to physical length.) In order to do this, a REFIT run was performed over the 80 – 150 eV energy region with only the data set having the longest flight path (58.586 m). The flight path length was given as a fixed parameter with the variables being the resonance energies of the 48 resonances in the region. A second REFIT run was then performed over the same energy region incorporating the remaining data sets. The resonance energies were fixed at the values produced by the first run and the variables were the flight path lengths of the data sets. Table 5.3 presents the resulting values of the flight path lengths, which were fixed for the remainder of the analysis.

Due to the format in which REFIT prints out the values, the flight paths are given to six figures, i.e. to ± 0.1 mm. Most of the associated uncertainties quoted by REFIT are less than ± 0.1 mm. Table 5.3 quotes the actual values and uncertainties produced by REFIT and the precision of the uncertainties have not been made consistent with the precision of the actual value.

Table 5.3 – Flight Path Lengths Used for Analysis of Hafnium Sample Measurements

Measurement	Flight Path Length (m) Quoted (Table 3.5)	Flight Path Length (m) Fitted and Used
Geel Capture 60m 800Hz ^{nat} Hf 1mm	58.586	58.586 (fixed)
Geel Capture 10m 50Hz ^{nat} Hf 0.26mm	12.89	12.8909 ± 0.00007
Geel Capture 10m 50Hz ^{nat} Hf 0.079mm	12.89	12.8905 ± 0.00011
Geel Capture 10m 50Hz ^{nat} Hf 0.024mm	12.89	12.8903 ± 0.00018
Geel Capture 10m 800Hz ¹⁷⁷ Hf	12.95	12.9479 ± 0.00002
Geel Capture 10m 800Hz ¹⁷⁸ Hf-1	12.95	12.9484 ± 0.00005
Geel Capture 10m 800Hz ¹⁷⁸ Hf-2	12.95	12.9482 ± 0.00015
Geel Capture 10m 800Hz ¹⁷⁹ Hf	12.95	12.9470 ± 0.00002
Geel Capture 10m 800Hz ^{nat} Hf 1mm	12.95	12.9514 ± 0.00002
Geel Capture 30m 800Hz ¹⁷⁶ Hf	28.82	28.8216 ± 0.00008
Geel Capture 30m 800Hz ¹⁷⁷ Hf	28.82	28.8225 ± 0.00007
Geel Capture 30m 800Hz ¹⁷⁸ Hf-1	28.82	28.8198 ± 0.00014
Geel Capture 30m 800Hz ¹⁷⁹ Hf	28.82	28.8202 ± 0.00005
Geel Capture 30m 800Hz ^{nat} Hf 1mm	28.82	28.8265 ± 0.00004
Geel Capture 30m 50Hz ¹⁷⁶ Hf	28.82	28.8220 ± 0.00015
Geel Capture 30m 50Hz ¹⁷⁹ Hf	28.82	28.8206 ± 0.00041
Geel Transmission 30m ^{nat} Hf 15mm 300K	$\left. \begin{array}{l} \\ \\ \\ \\ \\ \end{array} \right\} \begin{array}{l} 26.443 \\ \pm 0.002 \\ [57] \end{array}$	26.4596 ± 0.00005
Geel Transmission 30m ^{nat} Hf 15mm 77K		26.4596 ± 0.00004
Geel Transmission 30m ^{nat} Hf 2mm 300K		26.4512 ± 0.00004
Geel Transmission 30m ^{nat} Hf 2mm 77K		26.4512 ± 0.00003
Geel Transmission 30m ^{nat} Hf 1mm 300K		26.4508 ± 0.00005
Geel Transmission 30m ^{nat} Hf 1mm 77K		26.4508 ± 0.00004
Geel Transmission 50m ^{nat} Hf 16mm	49.3445 [62]	49.3557 ± 0.00009
Harwell Capture 32m ¹⁸⁰ Hf	32.6 [8]	32.6209 ± 0.00069

It is noted that the neutron energy is dependent on the “initial delay”; the time between the first timing channel and the arrival of the neutron pulse. For the Geel measurements, the initial delay is -40 – 6000 ns and measured to ~1 ns. For a ~12 m flight path, the time-of-flight of a 300eV neutron (the limit of the “good” resolution data) is ~50 μs. For a ~26 m flight path, the time-of-flight of a 1 keV neutron (the limit of full resonance analysis) is ~60 μs. These minimum time-of-flights corresponding to useful measurement data are one to

three orders of magnitude greater than the initial delay times. Therefore, for the majority of neutron energies of interest to this project, the time-of-flight is insensitive to adjustments in the initial delay time.

5.2.2 Abundance of Hafnium Isotopes and Impurities in Samples

For resonance analysis, the isotopic compositions of the measured samples need to be known so that the cross section of the sample can be correctly determined. This composition must include both the nuclides to be analysed and impurities present in the sample. In the specific case of the measurements under this project, there were several known sources of “impurity” which include “true” impurities in the sample but also the materials that make up the measurement apparatus, which have noticeable interactions with the incident neutron beam. REFIT can account for the presence of these nuclides by inclusion of the relevant nuclear data files together with relative abundances of these nuclides.

The analysis of natural hafnium samples assumes the hafnium isotopes are present in their natural abundances (Table 3.2) and that 97.0% by weight of the sample is hafnium. The remaining 3.0% is mainly zirconium (~2.8%) with traces (<100 ppm) of other metals [51]. Assuming that the zirconium isotopes are present in their natural abundances, and that 3.0% of the sample is zirconium, it contributes an essentially constant ~0.2 barns to the total sample cross section across the range 0.5 eV to 1 keV. Notable exceptions are peaks at 182 eV (0.6 barns), 293 eV (9.4 barns), 301 eV (1.9 barns) and 682 eV (5.5 barns). Therefore, given the natural hafnium capture cross section between resonances, across the same range, is 5 – 10 barns, it was assumed that the zirconium is not visible in the capture yields or transmissions except at 293 eV. Therefore, the zirconium was accounted for by reducing the density (atoms/barn) of the sample to correspond to 97.0% by weight hafnium and by

excluding all the natural hafnium data in the 291 - 294 eV region from the REFIT calculation (therefore using only the enriched hafnium samples to determine the 292.5 eV ^{179}Hf resonance).

For the isotopically-enriched hafnium oxide samples, the samples were assumed to be one part hafnium to two parts oxygen (i.e. only HfO_2). The oxygen was assumed to be 100% ^{16}O and nuclear data for ^{16}O was included in the REFIT input. (Natural oxygen is 99.762% ^{16}O , 0.038% ^{17}O , 0.200% ^{18}O ; the ^{17}O cross sections are very similar to those of ^{16}O , there is no cross section data available for ^{18}O .) Therefore, the abundance of oxygen was input to REFIT as 2.0 with the sum of the hafnium isotopes being 1.0, as when setting up the calculation, REFIT renormalizes the fractions of all nuclides to 1.0. The isotopic abundances for the hafnium isotopes were initially input as the values given in Table 3.2. However, it was found during analysis that the given abundances of some of the minor isotopes were inaccurate, as the fits to the resonances of these isotopes were good for some measurements but less so for others. Therefore, these abundances were adjusted by the program to achieve a better fit to the measured data. The corrected values as used in the final analysis are given in Table 5.4 (in bold). Whilst the change in abundance of these minor isotopes is large relative to the quoted abundance (for which uncertainties were not given) (Table 3.2), the implied change in abundance of the remaining nuclides in the samples is insignificant.

The hafnium oxide samples are contained in aluminium cans. The total cross section of aluminium (100% ^{27}Al) is a flat ~ 1.4 barns across the hafnium resonance range, though the ~ 103 barn resonance at 5.9 keV is visible in the measured capture yields (though the resolution is poor). As this is the only visible feature of ^{27}Al and it is outside the hafnium resolved resonance region, any neutron capture in aluminium “seen” by the C_6D_6 detectors

was not accounted for. However, it was realised that manganese (100% ^{55}Mn) is present as an impurity in the aluminium cans. ^{55}Mn has a broad 3280 barn resonance at 337 eV (within the hafnium resolved resonance region). This resonance is just visible in the capture yields as a rise in the between-resonance cross section level. Therefore, the ^{55}Mn can be assigned a pseudo-abundance in order to reproduce this rise in the cross section. This abundance was adjusted by REFIT during the analysis of the 300 – 350 eV region. The fitted values of the ^{55}Mn pseudo-abundance are given in Table 5.4.

In addition to “known” impurities, bromine was identified as a contaminant in the carbon-fibre sample holders used with some of enriched hafnium oxide samples. The natural bromine isotopes, ^{79}Br and ^{81}Br (with abundances 50.69% and 49.31% respectively [48]), have resolved resonance structures which overlap with those of the hafnium isotopes. These resonances are observable in the affected capture yields. Therefore, pseudo-abundances were determined by REFIT for the bromine isotopes via inclusion of the ENDF/B-VII.0 nuclear data library files for ^{79}Br and ^{81}Br (the most recent evaluation for these isotopes). These pseudo-abundances are given in Table 5.4.

As the bromine and the manganese are not contained in the sample itself, it should be noted that the corresponding pseudo-abundances: a) should not be considered as a fraction of the actual sample but as a number of atoms relative to that in the sample; b) are not necessarily the number of bromine/manganese atoms present but the number required to reproduce the observed capture yield; c) vary between measurements but not necessarily between samples as different sample holders may have been used for different measurements of the same sample.

Table 5.4 – Abundance of Nuclides in Hafnium Oxide (HfO₂) Samples Input to REFIT

Measurement	Abundance (%)								
	¹⁷⁴ Hf	¹⁷⁶ Hf	¹⁷⁷ Hf	¹⁷⁸ Hf	¹⁷⁹ Hf	¹⁸⁰ Hf	⁷⁹ Br	⁸¹ Br	⁵⁵ Mn
¹⁷⁷ Hf (10m 800Hz)	0.02	1.0	85.4	11.3	0.9	1.4	2.18	2.12	1.00
¹⁷⁸ Hf-1 10m 800Hz)	0.02	0.12	1.9	92.4	3.3	1.6	2.20	2.20	1.00
¹⁷⁸ Hf-2 (10m 800Hz)	0.02	0.12	1.9	92.4	3.3	1.6	10.00	10.00	1.00
¹⁷⁹ Hf (10m 800Hz)	0.02	0.2	0.88	4.1	72.1	22.3	0.00	0.00	1.00
¹⁷⁶ Hf (30m 800Hz)	0.032	65.0	22.9	6.3	1.8	4.0	0.01	0.01	2.42
¹⁷⁷ Hf (30m 800Hz)	0.02	1.0	85.4	11.3	0.9	1.4	0.00	0.00	1.44
¹⁷⁸ Hf-1 (30m 800Hz)	0.02	0.12	1.9	92.4	3.3	1.6	1.89	1.89	3.14
¹⁷⁹ Hf (30m 800Hz)	0.02	0.2	0.88	4.1	72.1	22.3	0.00	0.00	2.23
¹⁷⁶ Hf (30m 50Hz)	0.032	65.0	22.9	6.3	1.8	4.0	1.72	1.67	2.42
¹⁷⁹ Hf (30m 50Hz)	0.02	0.2	0.88	4.1	72.1	22.3	0.0	0.0	2.14

5.2.3 Average Capture Widths

For capture measurements on thin samples, the area, A_γ , of the resonance is defined by the neutron width, Γ_n , the capture width, Γ_γ , sample thickness, n , the reduced neutron wavelength, $\tilde{\lambda}$, and the spin weighting factor, g :

$$A_\gamma = 2n\pi^2 \tilde{\lambda}^2 g \frac{\Gamma_n \Gamma_\gamma}{\Gamma_n + \Gamma_\gamma} \quad (5.3)$$

If one of the resonance widths is much greater than the other, the resonance area becomes dependent on the “minor” width, i.e.:

$$\begin{aligned} A_\gamma (\Gamma_n \ll \Gamma_\gamma) &\approx ng\Gamma_n \\ A_\gamma (\Gamma_n \gg \Gamma_\gamma) &\approx ng\Gamma_\gamma \end{aligned} \quad (5.4)$$

Therefore, the resonance widths cannot be simultaneously determined from a capture measurement alone and it must be assumed that one width (Γ_γ) dominates and is therefore fixed whilst Γ_n is adjusted. If the overall fit was not greatly affected by the value of an individual resonance's Γ_γ , the “fitted” value would be different with each run of REFIT without converging to any one value. Furthermore, the value could become unrealistically high with a high uncertainty associated with it. This problem was most apparent for ^{174}Hf resonances, where the very low abundance of the isotope resulted in “fitted” values being very different to the starting (JEFF3.1) values due to the measurements being insensitive to such resonances. An average capture width was used for all ^{177}Hf and ^{179}Hf resonances above 50 eV and for resonances below 50 eV where the resonance area was deemed insensitive to Γ_γ . For resonances in the even-mass isotopes, average capture widths were also used where Γ_n was much less than Γ_γ .

Average capture widths for each isotope were determined from a weighted average of fitted capture widths for that isotope. The relatively high uncertainty quoted for the average Γ_γ values is due to the low number of resonances where individual Γ_γ values could be determined in that isotope, and in some cases the wide distribution of individual Γ_γ values for those resonances.

Table 5.5 – Average Capture Widths of Hafnium Isotopes Used in Analysis

Isotope	Average Capture Width, Γ_γ (meV)	Standard Deviation (meV)
^{174}Hf	60.0	9.6
^{176}Hf	51.0	9.8
^{177}Hf	63.6	7.8
^{178}Hf	54.8	12.3
^{179}Hf	54.5	7.7
^{180}Hf	57.5	3.2

5.3 Analysis of 0.5 eV to 1 keV Neutron Energy Range

Hafnium resonance parameters for the 0.5 eV to 1 keV neutron energy range were derived by the simultaneous analysis of several measurement data sets using the REFIT code in ~50 eV energy segments (see Table 5.6).

Resonance parameters for the 0.5 – 20 eV neutron energy range were derived using the Geel 12 m capture measurement data for the ^{177}Hf , ^{178}Hf -1, ^{178}Hf -2, ^{179}Hf enriched and 1, 0.26, 0.079 and 0.024 mm natural hafnium samples, together with the RPI transmission measurements of 0.001, 0.002, 0.004, 0.010, 0.020 and 0.050 inch natural hafnium metallic samples. The exception to this was the parameters of the 7.8 eV ^{178}Hf / ^{176}Hf doublet. A separate reanalysis of the RPI solution samples measurements was performed by M. Moxon [71] to derive the 7.8 eV doublet parameters. This work was performed independently, but in parallel to the main analysis, partly due to the time required, particularly as the most complex (and time consuming) multiple scattering correction in REFIT was required in order to accurately model the large amount of neutron scattering. These isotopically-enriched solution samples were manufactured specifically for analysis of the 7.8 eV doublet and have a low density of hafnium (Table 3.8), so the doublet peak in the capture measurements does not saturate, unlike the thicker isotopically-enriched oxide samples (Table 3.3) measured at Geel, where the calculation of the saturated capture peak is insensitive to (small) changes in the resonance parameters.

The resonance parameters of the 20 – 1000 eV neutron energy range were derived using all the Geel capture yield data as stated in Table 3.5, together with the transmission measurements of Kopecky (Section 3.4) and Siegler (Section 3.5.4). The Geel 12 m capture data was not used above 250 eV due to poor experimental resolution.

During the REFIT analysis, it was found that the quality of the fit in some energy regions was poor. In these cases, inspection of the REFIT graphical output showed differences in the shape of the calculated and measured capture peaks. These differences were attributed to resonances that were not identified during the initial resonance allocation (Section 5.1). The majority of these additional resonances were the result of overlapping resonances, often resonance doublets in the ^{177}Hf isotope. As the initial resonance allocation had only used the measured capture yield data, without the comparison of the calculated yield, some single ^{177}Hf resonance peaks identified at this initial stage were later “split” into ^{177}Hf doublets in order to obtain a better fit to the measured data. The addition of the additional resonances to the nuclear data files was verified by an improved quality of fit in subsequent REFIT calculations.

As newly identified resonances were initially assigned an arbitrary average neutron width it was necessary in most cases to manually adjust individual neutron widths to obtain a better starting value in order to speed up the fitting process. This was achieved by comparing an initial REFIT calculation with the measured data. As the peak height of a resonance is proportional to the resonance area, which is proportional to the neutron width, a more accurate neutron width was obtained by multiplying the current neutron width by the ratio of the measured peak height to the calculated peak height. This procedure was also used occasionally throughout the analysis to accelerate the fitting of the resonance parameters.

Fits were performed for each energy segment in an iterative fashion. The graphical and numerical outputs of each REFIT run were assessed to determine which parameters required further adjustment in subsequent runs. The quality of the fit for a segment was assessed by visual inspection of the fitted curve relative to the experimental data, using REFIT’s graphical output, the χ^2 (see Equation 4.2) values for individual data sets and the overall χ^2 value for

run. When the fit to the data for a segment was considered sufficiently good and the change in χ^2 values and resonance parameters were negligible relative to the previous iteration, the parameters were deemed final. Table 5.6 gives the final χ^2/dof (see Equation 4.6) for each fitted segment together with the number of hafnium resonances contained with the segment and the number of measured data sets used to analyse it, which gives an indication of the complexity of the fitting task.

Table 5.6 – Hafnium Data Fitted Regions

Lower Limit of Section (eV)	Upper Limit of Section (eV)	Number of Resonances	Number of Data Sets	Number of Fitted Data Points	Number of Variables	Final χ^2/dof
0.5	20.0	14	14	39968	54	1.1336
20.0	80.0	52	24	72108	165	2.5272
80.0	150.0	53	24	31181	143	3.2770
150.0	196.0	37	24	14614	109	2.7354
196.0	250.5	42	24	12042	118	3.3944
250.5	297.0	40	16	4716	107	6.5097
297.0	353.0	33	16	4787	99	2.9674
353.0	402.5	29	16	3366	84	3.3015
402.5	440.0	26	16	2139	76	4.7369
440.0	495.5	31	15	3177	89	5.4180
495.5	552.5	34	15	3575	94	3.3778
552.5	603.0	32	16	2748	92	2.8196
603.0	650.0	20	15	2454	64	5.1894
650.0	699.0	25	15	2271	73	5.4059
699.0	796.0	54	15	3848	137	4.8000
796.0	901.0	57	15	3465	141	5.2047
901.0	1000.5	50	15	2760	129	6.4553

5.4 Analysis of 1 keV to 3 keV Neutron Energy Range

At neutron energies around 1 keV the experimental resolution of the Geel 30 m capture measurements of the isotopically-enriched hafnium samples becomes too low to resolve the tightly-spaced ^{177}Hf and ^{179}Hf resonances. Therefore, allocation of resonances to isotopes becomes difficult, particularly for the numerous narrow and closely spaced ^{177}Hf and ^{179}Hf resonances, to the point where the resonances become unresolvable using these data. For this reason, the analysis of ^{177}Hf and ^{179}Hf resonances is limited to neutron energies below 1 keV.

In contrast, the greater spacing and generally wider resonances of ^{176}Hf , ^{178}Hf and ^{180}Hf are still resolvable to around 3 keV. To analyse resonances to this neutron energy provides an overlap with the analysis of Beer and Macklin [10, 11] (see Section 3.5.3). As previous “low” energy studies for ^{176}Hf and ^{178}Hf only extend to 1 keV and 2 keV respectively, the Beer and Macklin results for these isotopes, which begin at 2.7 keV, could not be included in any evaluated data files due to the energy gap between the results. The analysis of the Geel data to 3 keV enables the Beer and Macklin results for these isotopes to be included in the evaluated files, thereby extending the resolved resonance regions to ~5 keV for ^{176}Hf , ~9 keV for ^{178}Hf and ~10 keV for ^{180}Hf .

However, when compared with the Geel isotopically-enriched sample data, together with the (very low resolution) Harwell ^{180}Hf sample data, some of the Beer and Macklin resonance energies, particularly those of smaller resonances, did not agree with the observed resonance peaks. It is possible that the “extra” resonances presented by Beer and Macklin are actually doublets in the odd-mass isotopes. Furthermore, the average resonance spacings of these resonances are much tighter than those of the sub-keV resonances. Therefore, as higher resolution measurements in this energy range, or indeed Beer and Macklin’s original neutron

capture data, are not available to verify the existence of these resonances, the Beer and Macklin resonance parameters above 3 keV have not been inserted in the evaluated files produced in this project. Consequently, the resolved resonance regions for the abundant even-mass isotopes in this evaluation have upper limits of 3 keV.

The resonance energies of the ^{176}Hf , ^{178}Hf and ^{180}Hf isotopes in this neutron energy region were identified by visual inspection of the available data sets and then fitted using REFIT. The average capture widths, as listed in Table 5.5, were used for all resonances in the three isotopes. The method of determining resonances parameters for each of the isotopes in this energy range was dependent on the measurement data available for each isotope.

Whilst the recent Geel measurements include 30 m capture data for the ^{176}Hf -enriched sample, the enrichment of ^{176}Hf is relatively low (65.0%) compared to the major isotope in other samples (Table 3.2), with relatively high ^{177}Hf content (22.9%). Consequently, the majority of the resonance structures in the ^{176}Hf sample capture yield are due to ^{177}Hf . To identify the ^{176}Hf resonances, the ^{176}Hf sample capture yield was overlaid on the ^{177}Hf sample capture yield so the ^{177}Hf resonance structure could be visually “subtracted”, thereby highlighting the ^{176}Hf resonances. It was not possible to determine neutron widths for the ^{176}Hf resonances using REFIT due to the ^{177}Hf resonance structure, for which no resonances are identified in REFIT’s nuclear data input. Therefore, the ^{176}Hf neutron widths were determined by calculating the reduced neutron widths, Γ_n^0 , of sub-keV resonances (Equation 5.5) and then averaging to get the average reduced neutron width based on the sub-keV resonances

$$\langle \Gamma_n^0 \rangle = \left\langle \Gamma_n E^{-\frac{1}{2}} \right\rangle \text{ from resonances with } E < 1 \text{ keV} \quad (5.5)$$

This average reduced neutron width was then used to calculate the “average” neutron widths for the 1 - 3 keV resonances (Equation 5.6).

$$\Gamma_n = \langle \Gamma_n^0 \rangle E^{\frac{1}{2}} \text{ for resonances with } E > 1 \text{ keV} \quad (5.6)$$

In contrast to the ^{176}Hf sample, the ^{178}Hf sample measured at Geel has a high ^{178}Hf enrichment (92.4%) with no other isotopes greater than 3.5% in abundance (Table 3.2). Therefore, the ^{178}Hf resonances dominate the resonance structure of the capture yield data. Thus, the neutron widths for the ^{178}Hf resonances in the 1 -3 keV range were individually derived using REFIT and the Geel 30 m capture data for the ^{178}Hf enriched sample. To account for the ^{177}Hf and ^{179}Hf present in the sample, and their contribution to the capture yield, an additional constant background value was allowed to vary during the fit, as a substitute for the absence of nuclear data for the two isotopes in this neutron energy region.

The analysis of the ^{180}Hf resonances in the 1 – 3 keV energy region suffers the same difficulties as the ^{176}Hf analysis. The “best” Geel measurements for the analysis are the 30 m capture data for the ^{179}Hf -enriched sample (22.3% ^{180}Hf) and the 30 m and 60 m capture data for 1 mm natural hafnium (35.08% ^{180}Hf) disc (Tables 3.3 – 3.5). Consequently, the ^{180}Hf are well-masked by the resonance structure of at least one other isotope. Therefore, the Harwell ^{180}Hf -enriched sample capture data (Section 3.5.2) were used to verify the existence of the resonances. However, the resolution of the Harwell data at these energies is too poor to extract neutron widths and so the resonances were assigned the existing values given in the JEFF3.1 ^{180}Hf evaluated file.

5.5 Resonance Parameters of the Hafnium Isotopes

The tables in this section present the final set of resonance parameters derived in this analysis for each of the natural hafnium isotopes: ^{174}Hf (Table 5.7, page 75), ^{176}Hf (Table 5.8, pages 76-79), ^{177}Hf (Table 5.9, pages 80-96), ^{178}Hf (Table 5.10, pages 97-99), ^{179}Hf (Table 5.11, pages 100-110), and ^{180}Hf (Table 5.12, pages 111-112). The parameter value is followed by the uncertainty, in parentheses “()”, as determined by REFIT (which is based only on the statistical accuracy of the measured data and does not include uncertainties on sample dimensions etc.). Average radiation widths are presented with standard deviations, in square brackets “[]”. Each table is followed by notes relevant to values in the table.

The new resonance parameters (labelled as “Ware”) are compared with the parameters present in the JEFF3.1 (presented with uncertainties and standard deviations from Trbovich [12]) and JEF2.2 hafnium files: the current and previous European “standard”. The JEFF3.1 parameters were used as a starting point for this work and during the resonance allocation, it was noted that some “new” resonances were present in the JEF2.2 files but not the JEFF3.1. It should be noted that whilst the new parameters and those of JEFF3.1 below 200 eV were derived using the Reich-Moore formalism, the parameters in JEF2.2 and JEFF3.1 above 200 eV were derived using the Multi-Level Breit-Wigner formalism. The new evaluation is also compared with the JEFF3.1 evaluation in the figures presenting selected transmission and capture yield data in Appendix A.2.

Table 5.7 – Resonance Parameters for ^{174}Hf

E _R (eV)			Γ _γ (meV)			Γ _n (meV)			Spin
Ware	JEFF3.1	JEF2.2	Ware	JEFF3.1	JEF2.2	Ware	JEFF3.1	JEF2.2	
4.289 (0.003)	4.06 (0.04)	-	60 [9.6]	52 (5)	-	0.179 (0.007)	0.015 (0.001)	-	0.5
13.378 (0.002)	13.373 (0.004)	13.381	60 [9.6]	65 [29]	59.94	3.950 (0.061)	5.7 (0.2)	3.657	0.5
29.985 (0.001)	29.985 (0.003)	30.072	53.517 (0.895)	65 [29]	59.94	31.551 (0.126)	36.3 (0.8)	28.27	0.5
70.504 (0.008)	70.66 (0.02)	70.5	876	65 [29]	54.58	54.997 (1.263)	24 (2)	12	0.5
77.808 (0.002)	77.85 (0.01)	77.9	64.822 (2.038)	51 (4)	54.58	80.507 (1.061)	83 (4)	65	0.5
106.95 (0.01)	106.95 (0.02)	107.1	72.602 (2.850)	65 [29]	54.58	106.330 (0.945)	177 (10)	122	0.5
124.36 (0.03)	124.36 (0.03)	124.6	65 [29]	65 [29]	54.58	680 (27)	680 (27)	50	0.5
147.61 (0.01)	147.63 (0.04)	147.6	304.86 (11.02)	102 (10)	54.58	242.980 (3.012)	358 (24)	120	0.5
152.74 (0.02)	153.40 (0.04)	153.5	60 [9.6]	65 [29]	54.58	108.210 (4.690)	219 (17)	85	0.5
-	-	172.7	-	-	54.58	-	-	13	0.5
195.86 (0.14)	-	191.8	60 [9.6]	-	54.58	82	-	3.5	0.5
211.50 (0.01)	211	211	60 [9.6]	60	54.58	141.148 (2.483)	180	180	0.5
233.77 (0.22)	-	231	60 [9.6]	-	54.58	19.100 (5.071)	-	85	0.5
261	-	250	60 [9.6]	-	54.58	36	-	89	0.5
-	-	270	-	-	54.58	-	-	92	0.5

It is noted that the parameters of the 124 eV resonance (Table 5.7) have been assigned the JEFF3.1 values as reliable values could not be determined. Uncertainties are not given on the 196 eV and 261 eV neutron widths as fully converged values could not be obtained with REFIT. The value obtained for the capture width of the 70.5 eV resonance is unrealistically large. This is due to the calculated capture yields being insensitive to this parameter. This is discussed further in Section 6.2.

Table 5.8 – Resonance Parameters for ^{176}Hf

Ware	E_R (eV)		Ware	Γ_γ (meV)		Ware	Γ_n (meV)		Spin
	JEFF3.1	JEF2.2		JEFF3.1	JEF2.2		JEFF3.1	JEF2.2	
7.9034 (0.0009)	7.8891 (0.0003)	7.8858	44.728 (1.067)	61.8 (0.6)	52.8	9.388 (0.059)	10.15 (0.04)	8.51	0.5
48.239 (0.0002)	48.2540 (0.0009)	48.26	58.055 (0.141)	49 (1)	60	112.94 (0.116)	107 (2)	104.5	0.5
53.270 (0.0007)	53.282 (0.004)	53.321	70.732 (1.624)	55 [9]	60	1.499 (0.006)	1.69 (0.03)	1.326	0.5
67.256 (0.0013)	67.218 (0.002)	67.237	62.808 (0.894)	55 [9]	60	16.491 (0.203)	26.0 (0.6)	19.3	0.5
124.04 (0.001)	124.079 (0.008)	123.9	60.917 (0.757)	55 [9]	60	43.521 (0.126)	32 (2)	62	0.5
177.80 (0.002)	177.15 (0.01)	179.13	68.229 (1.275)	55 [9]	60	44.053 (0.350)	86 (4)	57.8	0.5
201.71 (0.002)	201.6	203.36	56.361 (0.639)	51	60	39.553 (0.321)	39	47.5	0.5
243.55 (0.002)	243.2	243.2	58.241 (1.227)	51	52.8	16.987 (0.120)	22	22	0.5
255.18 (0.006)	255	257.76	53.036 (1.985)	51	60	102.16 (2.732)	95	84.6	0.5
286.74 (0.007)	286	289	60.493 (3.425)	51	60	210.74 (6.774)	285	260	0.5
304.56 (0.002)	304.5	304.5	51.761 (1.297)	51	52.8	20.094 (0.174)	21	21	0.5
347.2 (0.002)	347.2	349.7	55.488 (0.486)	51	60	171.92 (1.112)	173	160	0.5
396.27 (0.034)	-	394.3	51 [9.8]	-	52.8	0.498 (0.047)	-	10	0.5
423.97 (0.041)	-	-	51 [9.8]	-	-	1.0593 (0.065)	-	-	0.5
435.14 (0.008)	435.6	438.87	51 [9.8]	51	60	134.77 (5.356)	167	167	0.5
444.18 (0.005)	444.8	448.8	53.548 (0.688)	51	60	155.39 (2.404)	173	173	0.5
475.94 (0.009)	-	498.4	179.43 (18.247)	-	52.8	18.761 (0.299)	-	11	0.5
533.68 (0.007)	-	-	43.684 (1.498)	-	-	32.465 (0.769)	-	-	0.5
546.95 (0.004)	-	548	50.818 (0.749)	-	52.8	76.619 (0.696)	-	12	0.5
577.17 (0.010)	557.1	577.1	351.67 (24.85)	51	52.8	34.341 (0.472)	335	335	0.5
-	-	602.3	-	-	52.8	-	-	12	0.5

Ware	E _R (eV)		Ware	Γ_γ (meV)		Ware	Γ_n (meV)		Spin
	JEFF3.1	JEF2.2		JEFF3.1	JEF2.2		JEFF3.1	JEF2.2	
626.16 (0.007)	627.5	627.5	65.937 (0.747)	51	52.8	726.87 (6.083)	640	640	0.5
655.87 (0.011)	657.5	657.5	55.255 (0.820)	51	52.8	176.63 (6.447)	270	270	0.5
-	-	692.9	-	-	52.8	-	-	26	0.5
730.85 (0.010)	-	728.3	76.489 (3.010)	-	52.8	38.621 (1.070)	-	27	0.5
749.39 (0.010)	-	763.8	47.13 (0.878)	-	52.8	101.74 (2.614)	-	28	0.5
780.72 (0.022)	-	-	20.998 (28.479)	-	-	47.804 (36.02)	-	-	0.5
791.95 (0.012)	-	799.2	63.629 (2.258)	-	52.8	166.09 (9.453)	-	28	0.5
-	-	834.6	-	-	52.8	-	-	29	0.5
869.67 (0.007)	870	870	66.947 (0.908)	51	52.8	1296.8 (7.282)	280	280	0.5
-	-	895.5	-	-	52.8	-	-	30	0.5
921.31 (0.074)	921	921	53.1 (1.169)	51	52.8	148.55 (55.731)	145	145	0.5
931.59 (0.022)	-	-	55.745 (14.386)	-	-	45.018 (8.719)	-	-	0.5
955.59 (0.038)	956	956	57.158 (4.621)	51	52.8	246.39 (7.563)	300	300	0.5
978.91 (1.516)	-	-	29	-	-	11	-	-	0.5
994.06 (0.013)	994	994	44.88 (1.887)	51	52.8	217.92 (9.113)	270	270	0.5
1030.3 (0.013)	-	1030.5	51 [9.8]	-	52.8	157.98 (20.75)	-	32	0.5
1067.34 (0.012)	1068	1068	51 [9.8]	51	52.8	160.79 (21.12)	250	250	0.5
-	-	1101	-	-	52.8	-	-	210	0.5
1135.95 (0.016)	-	1134	51 [9.8]	-	52.8	165.88 (21.79)	-	210	0.5
1180 (0.016)	-	1168	51 [9.8]	-	52.8	169.07 (22.21)	-	220	0.5
-	-	1201	-	-	52.8	-	-	220	0.5
-	-	1234	-	-	52.8	-	-	220	0.5

E _R (eV)			Γ_γ (meV)			Γ_n (meV)			Spin
Ware	JEFF3.1	JEF2.2	Ware	JEFF3.1	JEF2.2	Ware	JEFF3.1	JEF2.2	
1264 (0.014)	-	1267	51 [9.8]	-	52.8	174.98 (22.98)	-	230	0.5
1282.6 (0.016)	-	1300	51 [9.8]	-	52.8	176.27 (23.15)	-	230	0.5
1371.3 (0.020)	-	-	51 [9.8]	-	-	182.26 (23.94)	-	-	0.5
1446.1 (0.028)	-	-	51 [9.8]	-	-	187.16 (24.58)	-	-	0.5
1501.6 (0.022)	-	-	51 [9.8]	-	-	190.72 (25.05)	-	-	0.5
1531 (0.023)	-	-	51 [9.8]	-	-	192.58 (25.29)	-	-	0.5
1597.5 (0.026)	-	-	51 [9.8]	-	-	196.72 (25.84)	-	-	0.5
1622.9 (0.027)	-	-	51 [9.8]	-	-	198.27 (26.04)	-	-	0.5
1679.4 (0.032)	-	-	51 [9.8]	-	-	201.7 (26.49)	-	-	0.5
1737.9 (0.032)	-	-	51 [9.8]	-	-	205.18 (26.95)	-	-	0.5
1788.4 (0.038)	-	-	51 [9.8]	-	-	208.14 (27.34)	-	-	0.5
1813.6 (0.048)	-	-	51 [9.8]	-	-	209.6 (27.53)	-	-	0.5
1842.1 (0.033)	-	-	51 [9.8]	-	-	211.24 (27.75)	-	-	0.5
1966.1 (0.040)	-	-	51 [9.8]	-	-	218.23 (28.66)	-	-	0.5
1991 (0.046)	-	-	51 [9.8]	-	-	219.61 (28.85)	-	-	0.5
2011.4 (0.041)	-	-	51 [9.8]	-	-	220.74 (28.99)	-	-	0.5
2116.4 (0.047)	-	-	51 [9.8]	-	-	226.42 (29.74)	-	-	0.5
2139.7 (0.055)	-	-	51 [9.8]	-	-	227.66 (29.9)	-	-	0.5
2169.6 (0.047)	-	-	51 [9.8]	-	-	229.25 (30.11)	-	-	0.5
2194.2 (0.054)	-	-	51 [9.8]	-	-	230.55 (30.28)	-	-	0.5
2277.1 (0.055)	-	-	51 [9.8]	-	-	234.86 (30.85)	-	-	0.5
2300.8 (0.049)	-	-	51 [9.8]	-	-	236.08 (31.01)	-	-	0.5

E _R (eV)			Γ _γ (meV)			Γ _n (meV)			Spin
Ware	JEFF3.1	JEF2.2	Ware	JEFF3.1	JEF2.2	Ware	JEFF3.1	JEF2.2	
2323 (0.058)	-	-	51 [9.8]	-	-	237.22 (31.16)	-	-	0.5
2333.9 (0.064)	-	-	51 [9.8]	-	-	237.77 (31.23)	-	-	0.5
2429.5 (0.071)	-	-	51 [9.8]	-	-	242.59 (31.86)	-	-	0.5
2463.2 (0.064)	-	-	51 [9.8]	-	-	244.27 (32.08)	-	-	0.5
2522.5 (0.069)	-	-	51 [9.8]	-	-	247.19 (32.47)	-	-	0.5
2544.2 (0.098)	-	-	51 [9.8]	-	-	248.25 (32.61)	-	-	0.5
2560.7 (0.082)	-	-	51 [9.8]	-	-	249.06 (32.71)	-	-	0.5
2608.2 (0.072)	-	-	51 [9.8]	-	-	251.36 (33.02)	-	-	0.5
2638.7 (0.076)	-	-	51 [9.8]	-	-	252.82 (33.21)	-	-	0.5
2785.1 (0.143)	-	-	51 [9.8]	-	-	259.74 (34.12)	-	-	0.5
2871.2 (0.142)	-	-	51 [9.8]	-	-	263.72 (34.64)	-	-	0.5
2899.8 (0.105)	-	-	51 [9.8]	-	-	265.04 (34.81)	-	-	0.5
2947.1 (0.124)	-	-	51 [9.8]	-	-	267.19 (35.1)	-	-	0.5
3000.4 (0.125)	-	-	51 [9.8]	-	-	269.59 (35.41)	-	-	0.5

The uncertainties quoted on the neutron widths for ¹⁷⁶Hf resonances above 1 keV (Table 5.8) are propagated from the uncertainties on the neutron widths for the resonances below 1 keV, used to derive the average reduced neutron width and the estimate neutron widths above 1 keV (see Section 5.4). No uncertainties are given on the 979 eV resonance parameters, as fully converged values could not be obtained with REFIT.

Table 5.9 – Resonance Parameters for ^{177}Hf

E _R (eV)			Γ _γ (meV)			Γ _n (meV)			Spin
Ware	JEFF3.1	JEF2.2	Ware	JEFF3.1	JEF2.2	Ware	JEFF3.1	JEF2.2	
1.1007 (0.0001)	1.1001 (0.0001)	1.0964	64.852 (0.103)	65.23 (0.08)	62.83	2.239 (0.003)	2.225 (0.002)	2.219	-3
2.3879 (0.0001)	2.3868 (0.0001)	2.3837	61.606 (0.095)	60.7 (0.2)	61	7.821 (0.010)	8.04 (0.02)	8	-4
5.9028 (0.0001)	5.9002 (0.0002)	5.8937	62.773 (0.161)	62 (2)	65.47	5.384 (0.008)	5.32 (0.05)	5.348	-3
6.5802 (0.0001)	6.5780 (0.0002)	6.5691	58.424 (0.161)	55.6 (0.8)	64.96	7.870 (0.015)	8.21 (0.06)	8.0488	-4
8.8775 (0.0001)	8.8766 (0.0002)	8.8588	60.258 (0.287)	57.3 (0.4)	64.97	5.783 (0.015)	5.89 (0.03)	5.705	-4
10.958 (0.0002)	10.9607 (0.0007)	10.941	63.6 [7.8]	57 [13]	75.52	0.505 (0.002)	0.490 (0.003)	0.497	-3
13.677 (0.0003)	13.6810 (0.0008)	13.687	63.6 [7.8]	57 [13]	64.82	0.581 (0.002)	0.603 (0.004)	0.5434	-4
13.967 (0.0002)	13.9696 (0.0003)	13.971	63.6 [7.8]	57 [13]	74.56	2.957 (0.005)	2.71 (0.01)	3.064	-3
21.985 (0.0001)	21.9844 (0.0007)	22.005	63.6 [7.8]	57 [13]	67.34	1.790 (0.002)	1.7633 (0.009)	1.565	-4
22.288 (0.0002)	22.298 (0.002)	22.312	63.6 [7.8]	57 [13]	66.5	0.797 (0.002)	0.840 (0.009)	0.7593	-3
23.436 (0.0001)	23.426 (0.002)	23.521	63.6 [7.8]	57 [13]	61.3	1.289 (0.002)	1.32 (0.03)	1.588	-4
25.643 (0.0002)	25.641 (0.002)	25.665	63.6 [7.8]	57 [13]	63.3	0.528 (0.001)	0.545 (0.008)	0.473	-3
27.033 (0.0001)	27.0364 (0.0008)	27.063	63.6 [7.8]	57 [13]	63.3	2.922 (0.005)	2.84 (0.02)	2.696	-3
31.604 (0.0024)	31.608 (0.005)	31.627	63.6 [7.8]	57 [13]	63.3	0.248 (0.002)	0.36 (0.01)	0.34	-4*
32.835 (0.0002)	32.841 (0.001)	32.853	63.6 [7.8]	57 [13]	63.3	1.288 (0.002)	1.30 (0.01)	1.1305	-4
36.1 (0.0002)	36.095 (0.001)	36.111	63.6 [7.8]	57 [13]	63.3	3.465 (0.006)	3.53 (0.03)	2.457	-3
36.965 (0.0001)	36.9805 (0.0008)	36.978	58.5 (0.220)	57 [13]	63.3	9.272 (0.011)	8.92 (0.06)	9.4368	-4
-	-	42.6	-	-	66.5	-	-	0.39	-3
43.066 (0.0001)	43.082 (0.001)	43.241	69.378 (0.331)	57 [13]	63.3	5.036 (0.007)	5.13 (0.03)	4.716	-4
45.157 (0.0002)	45.165 (0.001)	45.301	63.6 [7.8]	57 [13]	63.3	3.083 (0.007)	3.37 (0.02)	2.61	-4
46.237 (0.0001)	46.256 (0.001)	46.419	80.681 (0.337)	57 [13]	63.3	7.065 (0.009)	7.00 (0.07)	5.16	-4

E _R (eV)			Γ_γ (meV)			Γ_n (meV)			Spin
Ware	JEFF3.1	JEF2.2	Ware	JEFF3.1	JEF2.2	Ware	JEFF3.1	JEF2.2	
48.835 (0.0001)	48.861 (0.001)	49.038	63.6 [7.8]	57 (5)	63.3	38.538 (0.064)	36 (1)	35.79	-3
49.607 (0.0002)	49.627 (0.001)	49.787	73.165 (0.512)	57 [13]	63.3	6.128 (0.010)	5.92 (0.08)	4.93	-4
54.785 (0.0001)	54.815 (0.001)	54.73	63.6 [7.8]	57 [13]	61.3	16.899 (0.025)	20.6 (0.2)	16.1	-4
56.376 (0.0001)	56.402 (0.001)	56.32	63.6 [7.8]	57 [13]	66.5	14.313 (0.020)	14.2 (0.1)	14.68	-3
57.06 (0.0002)	57.082 (0.002)	57.01	63.6 [7.8]	57 [13]	61.3	4.237 (0.008)	4.23 (0.04)	3.88	-4
59.305 (0.0003)	59.323 (0.002)	59.24	63.6 [7.8]	57 [13]	66.5	4.256 (0.008)	4.2535 (0.04)	4.11	-3
62.216 (0.0006)	62.228 (0.004)	62.16	63.6 [7.8]	57 [13]	66.5	1.415 (0.005)	1.63 (0.03)	1.55	-3
63.515 (0.0001)	63.552 (0.001)	63.643	63.6 [7.8]	54.3 (0.7)	55.13	80.794 (0.017)	70.2 (0.7)	64.7	-4
66.673 (0.0006)	66.773 (0.007)	66.71	63.6 [7.8]	119 (2)	66.5	29.913 (0.117)	41.6 (0.5)	24	-3
66.952 (0.0012)	-	66.73	63.6 [7.8]	-	61.3	13.058 (0.111)	-	17.5	-4
70.049 (0.0019)	70.098 (0.009)	69.98	63.6 [7.8]	57 [13]	61.3	0.415 (0.004)	0.68 (0.03)	0.48	-4
71.407 (0.0002)	71.44 (0.001)	71.32	63.6 [7.8]	57 [13]	61.3	14.292 (0.024)	14.08 (0.1)	14.4	-4
72.21 (0.0016)	72.05 (0.02)	72.24	63.6 [7.8]	72 (7)	66.5	1.977 (0.013)	2.2011 (0.03)	1.92	-3
75.703 (0.0011)	75.672 (0.007)	75.51	63.6 [7.8]	57 [13]	66.5	2.996 (0.019)	2.9 (0.2)	2.05	-3
76.105 (0.0003)	76.135 (0.002)	76.01	63.6 [7.8]	57 [13]	61.3	15.574 (0.030)	15.0 (0.3)	16.4	-4
-	-	80.4	-	-	66.5	-	-	0.11	-3
82.402 (0.0019)	82.35 (0.01)	82.35	63.6 [7.8]	57 [13]	61.3	0.478 (0.003)	0.64 (0.02)	0.548	-4
84.713 (0.0007)	-	-	63.6 [7.8]	-	-	31.780 (0.377)	-	-	-3
84.764 (0.0013)	84.762 (0.002)	84.57	63.6 [7.8]	57 [13]	61.3	1.347 (0.106)	23.5 (0.3)	25.61	-4
85.348 (0.0011)	85.31 (0.08)	85.27	63.6 [7.8]	57 [13]	66.5	6.457 (0.042)	0.38 (0.07)	4.2	-3
86.823 (0.0012)	86.861 (0.007)	86.75	63.6 [7.8]	57 [13]	61.3	0.946 (0.005)	1.14 (0.03)	0.922	-4
88.614 (0.0005)	88.639 (0.003)	88.52	63.6 [7.8]	57 [13]	66.5	4.300 (0.017)	4.58 (0.06)	4.62	-3

E _R (eV)			Γ_γ (meV)			Γ_n (meV)			Spin
Ware	JEFF3.1	JEF2.2	Ware	JEFF3.1	JEF2.2	Ware	JEFF3.1	JEF2.2	
93.248 (0.0006)	93.312 (0.006)	93.15	63.6 [7.8]	57 [13]	66.5	5.000 (0.016)	4.7 (0.1)	4.97	-3
97.155 (0.0003)	97.208 (0.002)	97.05	63.6 [7.8]	98 (13)	61.3	19.395 (0.035)	17.4 (0.3)	18.92	-4
-	-	98.1	-	-	66.5	-	-	0.12	-3
99.09 (0.002)	102.5 (0.1)	99	63.6 [7.8]	57 [13]	61.3	0.999 (0.006)	0.019 (0.002)	0.878	-3*
103.175 (0.0003)	103.258 (0.002)	103.08	63.6 [7.8]	57 [13]	62.68	57.399 (0.102)	59 (1)	58.25	-3
104.24 (0.004)	-	104.1	63.6 [7.8]	-	61.3	0.628 (0.007)	-	1.14	-4
-	-	108	-	-	61.3	-	-	0.29	-4
111.59 (0.002)	111.56 (0.01)	111.45	63.6 [7.8]	57 [13]	66.5	2.415 (0.024)	2.3 (0.1)	2.56	-3
111.99 (0.001)	112.03 (0.007)	111.92	63.6 [7.8]	57 [13]	61.3	3.792 (0.022)	4.1 (0.1)	4.01	-4
114.65 (0.007)	-	114.44	63.6 [7.8]	-	66.5	0.314 (0.008)	-	0.298	-4*
115.21 (0.001)	115.243 (0.005)	115.07	63.6 [7.8]	57 [13]	66.5	3.597 (0.014)	4.05 (0.06)	4.98	-4*
-	-	117.3	-	-	61.3	-	-	0.62	-4
121.36 (0.001)	121.34 (0.01)	121.22	63.6 [7.8]	57 [13]	66.5	4.252 (0.018)	4.2 (0.2)	5.07	-3
-	122.1 (0.1)	-	-	57 [13]	-	-	2.5 (0.2)	-	-3
122.86 (0.005)	122.18 (0.02)	122.67	63.6 [7.8]	57 [13]	61.3	0.880 (0.019)	0.54 (0.05)	0.97	-4*
123.83 (0.001)	123.88 (0.01)	123.71	63.6 [7.8]	57 [13]	66.5	10.214 (0.047)	8 (1)	10.8	-3
126.29 (0.007)	126.36 (0.02)	126.15	63.6 [7.8]	57 [13]	61.3	0.609 (0.022)	0.82 (0.03)	0.7	-4
131.04 (0.018)	131.843 (0.002)	130.1	63.6 [7.8]	67 (2)	61.3	0.247 (0.016)	59 (2)	0.18	-3*
131.75 (0.001)	-	131.42	63.6 [7.8]	-	66.72	48.766 (0.111)	-	61.9	-4*
134.18 (0.001)	134.245 (0.006)	134.06	63.6 [7.8]	57 [13]	61.3	3.818 (0.012)	4.21 (0.08)	3.76	-4
136.33 (0.004)	136.27 (0.02)	136.2	63.6 [7.8]	57 [13]	66.5	0.922 (0.011)	1.7 (0.2)	0.74	-3
137.64 (0.001)	138.061 (0.005)	137.48	63.6 [7.8]	57 [13]	61.3	18.988 (0.097)	16.2 (0.6)	12.3	-3*

E _R (eV)			Γ_γ (meV)			Γ_n (meV)			Spin
Ware	JEFF3.1	JEF2.2	Ware	JEFF3.1	JEF2.2	Ware	JEFF3.1	JEF2.2	
141.28 (0.001)	141.351 (0.003)	141.15	63.6 [7.8]	57 [13]	61.3	21.767 (0.049)	21.1 (0.2)	21.8	-4
143.22 (0.002)	143.16 (0.02)	143.17	63.6 [7.8]	57 [13]	66.5	4.594 (0.036)	3.7 (0.2)	5	-3
143.90 (0.001)	143.84 (0.01)	143.76	63.6 [7.8]	57 [13]	61.3	14.533 (0.057)	9.5 (0.6)	11.1	-4
145.73 (0.001)	145.793 (0.006)	145.58	63.6 [7.8]	57 [13]	66.5	7.821 (0.068)	7.6 (0.1)	7.54	-3
148.69 (0.001)	148.765 (0.004)	148.55	63.6 [7.8]	57 [13]	66.5	22.305 (0.064)	21 (0.5)	21.04	-3
151.13 (0.026)	151.3 (0.03)	151.08	63.6 [7.8]	57 [13]	61.3	0.314 (0.012)	0.67 (0.05)	0.44	-4
152.99 (0.003)	152.67 (0.01)	152.86	63.6 [7.8]	57 [13]	61.3	1.701 (0.018)	3.82 (0.09)	1.85	-4
156.12 (0.003)	154.88 (0.02)	156.01	63.6 [7.8]	57 [13]	66.5	3.254 (0.024)	1.53 (0.07)	3.17	-3
160.17 (0.001)	160.229 (0.008)	160.02	63.6 [7.8]	57 [13]	61.3	3.331 (0.013)	3.91 (0.08)	3.47	-4
163.19 (0.001)	-	163	63.6 [7.8]	-	66.5	43.779 (0.139)	-	21.3	-3
164.99 (0.003)	163.284 (0.003)	163.02	63.6 [7.8]	57 [13]	61.3	3.369 (0.031)	45.8 (0.6)	15.8	-4*
-	-	167.1	-	-	61.3	-	-	0.27	-4
167.53 (0.001)	167.596 (0.007)	167.33	63.6 [7.8]	57 [13]	66.5	8.425 (0.028)	9.346 (0.2)	8.36	-3
171.22 (0.001)	171.06 (0.01)	171.08	63.6 [7.8]	57 [13]	66.5	11.596 (0.058)	10 (1)	13.6	-3
174.48 (0.002)	174.326 (0.007)	174.27	63.6 [7.8]	57 [13]	61.3	11.649 (0.059)	27 (3)	12.71	-4
176.26 (0.001)	176.325 (0.008)	176.13	63.6 [7.8]	57 [13]	66.5	59.724 (0.213)	45 (6)	54.9	-3
177.05 (0.001)	176.88 (0.03)	176.81	63.6 [7.8]	57 [13]	61.3	44.034 (0.171)	9 (1)	43.9	-4
179.19 (0.105)	179.31 (0.06)	178.89	63.6 [7.8]	57 [13]	66.5	0.343 (0.055)	0.46 (0.04)	0.86	-3*
181.26 (0.002)	181.35 (0.01)	181.06	63.6 [7.8]	57 [13]	61.3	4.813 (0.025)	5.6 (0.1)	5.26	-4
-	-	183.5	-	-	66.5	-	-	0.4	-3
184.76 (0.004)	184.90 (0.02)	184.62	63.6 [7.8]	57 [13]	61.3	1.574 (0.014)	1.66 (0.07)	1.26	-4
187.06 (0.025)	188.48 (0.03)	188	63.6 [7.8]	57 [13]	61.3	0.198 (0.009)	1.8 (0.2)	0.29	-4

Ware	E _R (eV)		Ware	Γ_γ (meV)		Ware	Γ_n (meV)		Spin
	JEFF3.1	JEF2.2		JEFF3.1	JEF2.2		JEFF3.1	JEF2.2	
-	-	188.02	-	-	66.5	-	-	0.38	-3
192.89 (0.002)	193.012 (0.006)	192.7	63.6 [7.8]	57 [13]	61.3	6.955 (0.034)	15.0 (0.3)	7.08	-4
194.3 (0.002)	194.400 (0.009)	194.09	63.6 [7.8]	57 [13]	66.5	8.744 (0.053)	9.8 (0.2)	8.69	-3
-	-	195.9	-	-	61.3	-	-	1.7	-4
199.37 (0.001)	199.488 (0.006)	199.18	63.6 [7.8]	57 [13]	61.3	20.501 (0.061)	21.0 (0.4)	21.25	-4
202.03 (0.002)	201.8	201.84	63.6 [7.8]	65	66.5	17.637 (0.119)	19.2	19.8	-3
202.96 (0.008)	205.7	-	63.6 [7.8]	65	-	1.969 (0.048)	1.378	-	-3*
204.38 (0.001)	-	205.64	63.6 [7.8]	-	61.3	0.646 (0.022)	-	0.69	-3*
206.71 (0.018)	-	205.66	63.6 [7.8]	-	66.5	0.425 (0.014)	-	0.89	-4*
208.84 (0.001)	208.6	208.67	63.6 [7.8]	54	61.3	52.499 (0.18)	44.44	41.15	-3*
210.30 (0.003)	210	210.06	63.6 [7.8]	65	66.5	4.938 (0.03)	4.343	4.37	-3
212.21 (0.007)	212.1	212.1	63.6 [7.8]	65	66.5	1.346 (0.031)	2.057	2.06	-3
212.41 (0.165)	217	212.9	63.6 [7.8]	65	61.3	0.201 (0.031)	6.222	0.4	-4
217.35 (0.002)	-	217.1	63.6 [7.8]	-	61.3	5.83 (0.024)	-	6.16	-4
219.82 (0.001)	219.5	219.6	63.6 [7.8]	65	66.5	8.412 (0.03)	11.43	11.7	-4*
222.43 (0.004)	222.3	222.33	63.6 [7.8]	65	66.5	3.036 (0.027)	3.143	3.55	-3
223.52 (0.003)	223.3	223.33	63.6 [7.8]	65	61.3	5.795 (0.049)	5.956	5.88	-4
224.94 (0.002)	224.7	224.7	63.6 [7.8]	65	66.5	103.98 (0.779)	131.43	136	-3
226.87 (0.002)	226.6	226.68	63.6 [7.8]	65	61.3	9.316 (0.102)	11.11	10.69	-4
229.37 (0.003)	229.1	229.15	63.6 [7.8]	65	66.5	8.858 (0.072)	7.429	7.54	-3
229.73 (0.019)	-	-	63.6 [7.8]	-	-	0.276 (0.058)	-	-	-3
232.65 (0.019)	232.2	232.54	63.6 [7.8]	65	61.3	0.681 (0.023)	0.711	0.8	-4

Ware	E _R (eV)		Ware	Γ_γ (meV)		Ware	Γ_n (meV)		Spin
	JEFF3.1	JEF2.2		JEFF3.1	JEF2.2		JEFF3.1	JEF2.2	
236.50 (0.002)	236.2	236.26	63.6 [7.8]	65	66.5	11.913 (0.047)	12.23	12.2	-3
-	-	236.7	-	-	61.3	-	-	2.4	-4
238.88 (0.001)	238.6	238.69	63.6 [7.8]	65	66.5	90.813 (0.238)	58.29	59.6	-3
241.05 (0.002)	240.7	240.81	63.6 [7.8]	58	61.3	18.561 (0.190)	19.56	18.9	-4
-	-	244.6	-	-	61.3	-	-	4.7	-4
249.06 (0.002)	248.7	248.4	63.6 [7.8]	65	61.3	16.68 (0.16)	27.429	4.7	-4*
249.61 (0.011)	-	248.85	63.6 [7.8]	-	66.5	3.610 (0.127)	-	27.6	-3
-	-	252.1	-	-	61.3	-	-	0.44	-4
253.41 (0.185)	-	252.8	63.6 [7.8]	-	66.5	0.107 (0.283)	-	0.52	-3
-	-	255.9	-	-	61.3	-	-	0.45	-4
256.19 (0.017)	-	256.7	63.6 [7.8]	-	66.5	2.331 (0.109)	-	0.52	-4*
259.82 (0.008)	259.7	259.66	63.6 [7.8]	65	61.3	1.940 (0.223)	1.778	1.78	-4
-	-	260.6	-	-	66.5	-	-	0.52	-3
263.10 (1.403)	-	263.7	63.6 [7.8]	-	61.3	0.161 (0.286)	-	0.45	-4
264.81 (0.006)	264.5	264.56	63.6 [7.8]	66	66.5	85.814 (2.055)	82.286	85.3	-3
267.94 (0.002)	267.6	267.65	63.6 [7.8]	65	61.3	37.386 (1.565)	38.133	36.1	-4
272.50 (0.003)	272.2	272.29	63.6 [7.8]	65	61.3	38.989 (0.464)	44.444	45.3	-4
273.53 (0.005)	273.2	273.24	63.6 [7.8]	65	66.5	24.672 (0.566)	19.2	19.4	-3
275.44 (0.115)	-	277.1	63.6 [7.8]	-	66.5	1.281 (1.169)	-	2.1	-4*
276.59 (0.031)	-	277.5	63.6 [7.8]	-	61.3	1.032 (0.151)	-	3.8	-3*
280.62 (0.119)	-	280.9	63.6 [7.8]	-	66.5	0.164 (0.237)	-	2.1	-3
283.45 (0.141)	-	282.8	63.6 [7.8]	-	61.3	0.999 (0.153)	-	3.8	-4

Ware	E _R (eV)		Ware	Γ_γ (meV)		Ware	Γ_n (meV)		Spin
	JEFF3.1	JEF2.2		JEFF3.1	JEF2.2		JEFF3.1	JEF2.2	
284.91 (0.421)	-	284.79	63.6 [7.8]	-	66.5	8.804 (6.992)	-	180	-4*
285.07 (0.024)	284.7	284.8	63.6 [7.8]	80	61.3	173.73 (0.892)	182.85	5.3	-3*
288.28 (0.975)	287.9	287.99	63.6 [7.8]	65	61.3	0.107 (0.747)	9.333	9.14	-4
288.33 (0.019)	-	289.5	63.6 [7.8]	-	66.5	12.798 (1.608)	-	1.1	-3
-	-	293.3	-	-	61.3	-	-	0.93	-4
294.76 (0.074)	294.2	294.29	63.6 [7.8]	65	66.5	5.690 (0.259)	4.8	4.77	-3
298.81 (0.003)	298.5	298.58	63.6 [7.8]	65	61.3	45.621 (0.444)	64.889	67.4	-4
299.59 (0.003)	299.7	299.74	63.6 [7.8]	65	66.5	25.701 (0.203)	10.629	10.75	-3
302.74 (0.004)	302.4	302.37	63.6 [7.8]	65	61.3	6.361 (0.065)	3.543	2.78	-3*
-	-	304.4	-	-	66.5	-	-	0.89	-3
307.35 (0.001)	307	306.96	63.6 [7.8]	70	61.3	106.05 (0.553)	103.11	96.9	-4
-	-	308.7	-	-	66.5	-	-	1.9	-3
309.36 (0.012)	-	309	63.6 [7.8]	-	66.5	2.075 (0.048)	-	2.4	-3
311.4 (0.004)	311	310.92	63.6 [7.8]	65	61.3	7.33 (0.086)	7.556	7.52	-4
314 (0.004)	313.6	313.6	63.6 [7.8]	65	66.5	9.945 (0.101)	18.286	18.2	-3
-	-	315.4	-	-	61.3	-	-	2.8	-4
-	-	318.6	-	-	66.5	-	-	3.2	-3
320.26 (0.002)	319.9	319.85	63.6 [7.8]	77	61.3	26.884 (0.183)	26.667	26.2	-4
323.13 (0.011)	323.6	323.6	63.6 [7.8]	65	66.5	8.402 (0.188)	38.222	50.5	-3*
324.02 (0.003)	-	-	63.6 [7.8]	-	-	44.013 (0.382)	-	-	-4
325.43 (0.004)	-	325.1	63.6 [7.8]	-	61.3	9.964 (0.122)	-	2.8	-3*
327.59 (0.010)	327.5	327.46	63.6 [7.8]	65	66.5	19.259 (0.742)	132.57	115	-3

Ware	E _R (eV)		Ware	Γ_γ (meV)		Ware	Γ_n (meV)		Spin
	JEFF3.1	JEF2.2		JEFF3.1	JEF2.2		JEFF3.1	JEF2.2	
327.87 (0.004)	-	-	63.6 [7.8]	-	-	61.854 (0.841)	-	-	-4
330.69 (0.001)	330.4	330.38	63.6 [7.8]	65	61.3	144.900 (0.623)	138.67	134	-4
333.64 (0.006)	333.4	333.4	63.6 [7.8]	60	66.5	25.555 (0.443)	50.286	36.1	-3
334.33 (0.008)	-	-	63.6 [7.8]	-	-	10.900 (0.266)	-	-	-4
338.81 (0.061)	-	-	63.6 [7.8]	-	-	0.508 (0.072)	-	-	-4
340.94 (0.004)	341.8	341.79	63.6 [7.8]	60	61.3	8.000 (0.075)	32	32.4	-3*
342.32 (0.002)	-	-	63.6 [7.8]	-	-	26.303 (0.146)	-	-	-4
345.23 (0.008)	-	-	63.6 [7.8]	-	-	4.194 (0.065)	-	-	-4
348.86 (0.004)	348.7	348.74	63.6 [7.8]	65	66.5	59.354 (0.756)	106.29	102	-3
349.70 (0.006)	-	-	63.6 [7.8]	-	-	23.432 (0.388)	-	-	-4
355.29 (0.003)	354.7	354.74	63.6 [7.8]	65	61.3	13.848 (0.11)	11.022	11	-4
357.58 (0.002)	357.1	357.08	63.6 [7.8]	65	66.5	57.914 (0.344)	51.429	50.5	-3
362.85 (0.002)	362.3	362.33	63.6 [7.8]	65	61.3	14.384 (0.107)	11.556	12.8	-4
367.84 (0.003)	367.5	367.45	63.6 [7.8]	75	61.3	44.493 (0.414)	54.222	56.3	-4
368.71 (0.011)	-	-	63.6 [7.8]	-	-	7.886 (0.202)	-	-	-3
370.83 (0.003)	370.7	370.67	63.6 [7.8]	65	66.5	30.199 (0.274)	38.8571	38.7	-3
371.93 (0.006)	-	-	63.6 [7.8]	-	-	12.152 (0.179)	-	-	-4
375.24 (0.004)	-	375.53	63.6 [7.8]	-	61.3	72.365 (1.001)	-	133	-4
376.19 (0.006)	375.6	375.57	63.6 [7.8]	65	66.5	118.05 (1.214)	340.57	172	-4*
377.06 (0.006)	-	-	63.6 [7.8]	-	-	66.549 (1.343)	-	-	-3
384.12 (0.009)	-	-	63.6 [7.8]	-	-	8.077 (0.149)	-	-	-4
390.29 (0.006)	389.8	389.84	63.6 [7.8]	65	66.5	28.381 (0.433)	24.889	32	-3*

Ware	E _R (eV)		Ware	Γ_γ (meV)		Ware	Γ_n (meV)		Spin
	JEFF3.1	JEF2.2		JEFF3.1	JEF2.2		JEFF3.1	JEF2.2	
394.18 (0.006)	393.6	393.63	63.6 [7.8]	65	61.3	7.412 (0.092)	6.044	6	-4
399.54 (0.004)	398.8	398.82	63.6 [7.8]	65	66.5	15.807 (0.144)	12.571	12.3	-3
401.96 (0.020)	-	-	63.6 [7.8]	-	-	1.796 (0.062)	-	-	-4
406.68 (0.002)	406.2	406.15	63.6 [7.8]	61	61.3	55.271 (0.449)	72	64.4	-4
409.49 (0.004)	408.8	408.8	63.6 [7.8]	65	66.5	22.062 (0.181)	17.143	17.1	-3
413.34 (0.003)	412.9	412.88	63.6 [7.8]	65	66.5	47.759 (0.381)	30.222	39	-4*
415.43 (0.006)	414.9	414.9	63.6 [7.8]	65	61.3	68.651 (1.618)	125.71	93.3	-3*
415.7 (0.008)	-	-	63.6 [7.8]	-	-	21.669 (0.754)	-	-	-4
419.41 (0.003)	418.8	418.8	63.6 [7.8]	65	66.5	25.647 (0.174)	24.889	31.8	-4*
421.64 (0.010)	-	-	63.6 [7.8]	-	-	5.480 (0.124)	-	-	-3
425.37 (0.004)	-	-	63.6 [7.8]	-	-	43.510 (0.329)	-	-	-3
426.73 (0.003)	426.1	426.09	63.6 [7.8]	65	61.3	53.982 (0.42)	80.889	82.6	-4
429.73 (0.005)	429.2	429.18	63.6 [7.8]	65	66.5	38.630 (0.575)	46.857	47.4	-3
432.43 (0.004)	431.7	431.7	63.6 [7.8]	65	61.3	38.527 (0.38)	35.556	35.5	-4
434.01 (0.006)	433.6	433.56	63.6 [7.8]	65	66.5	79.312 (1.41)	66.286	72	-3
435.77 (0.011)	434.9	434.92	63.6 [7.8]	65	61.3	92.263 (5.403)	51.556	51.9	-4
436.74 (0.010)	435.9	435.91	63.6 [7.8]	65	66.5	76.318 (3.782)	72	84.7	-3
443.78 (0.006)	443.4	443.4	63.6 [7.8]	65	61.3	31.351 (0.572)	45.333	42.9	-4
447.32 (0.008)	446.6	446.57	63.6 [7.8]	65	66.5	37.76 (0.902)	77.714	73.6	-3
450.03 (0.004)	449.4	449.43	63.6 [7.8]	65	61.3	19.059 (0.198)	24.889	24.9	-4
454.59 (0.010)	453.8	453.81	63.6 [7.8]	65	61.3	6.141 (0.105)	6.857	5.3	-3*
-	-	457.34	-	-	61.3	-	-	73.3	-4

Ware	E _R (eV)		Ware	Γ_{γ} (meV)		Ware	Γ_n (meV)		Spin
	JEFF3.1	JEF2.2		JEFF3.1	JEF2.2		JEFF3.1	JEF2.2	
457.94 (0.002)	457.4	457.38	63.6 [7.8]	58	66.5	99.904 (0.760)	151.111	94.2	-4*
462.59 (0.006)	-	-	63.6 [7.8]	-	-	15.499 (0.171)	-	-	-3
467.31 (0.007)	466.6	466.58	63.6 [7.8]	65	66.5	7.653 (0.096)	7.289	9.38	-4*
470.90 (0.004)	470.8	470.77	63.6 [7.8]	65	61.3	45.856 (0.427)	43.429	37.9	-3*
472.49 (0.004)	472.2	472.17	63.6 [7.8]	65	66.5	39.957 (0.312)	57.778	74.5	-4*
475.51 (0.007)	475	474.99	63.6 [7.8]	65	61.3	137.61 (3.007)	114.29	87.8	-3*
479.37 (0.004)	478.7	478.7	63.6 [7.8]	65	61.3	40.995 (0.190)	58.667	62.6	-4
481.09 (0.063)	481.6	481.58	63.6 [7.8]	65	66.5	2.311 (0.321)	17.143	16.6	-4*
482.18 (0.014)	-	-	63.6 [7.8]	-	-	19.574 (0.618)	-	-	-3
483.65 (0.032)	-	488.58	63.6 [7.8]	-	61.3	2.167 (0.117)	-	82	-3*
489.18 (0.004)	488.6	488.62	63.6 [7.8]	68	66.5	124.67 (1.343)	186.67	106	-4*
498.06 (0.013)	498.5	498.51	63.6 [7.8]	65	61.3	10.504 (0.219)	66.286	54.9	-3*
499.25 (0.005)	-	-	63.6 [7.8]	-	-	101.15 (0.937)	-	-	-3
500.62 (0.013)	-	-	63.6 [7.8]	-	-	9.993 (0.218)	-	-	-4
503.30 (0.006)	-	-	63.6 [7.8]	-	-	25.965 (0.306)	-	-	-3
505.54 (0.025)	-	-	63.6 [7.8]	-	-	2.590 (0.093)	-	-	-4
507.70 (0.006)	507.2	507.15	63.6 [7.8]	65	61.3	46.641 (0.716)	64	59.8	-4
508.64 (0.013)	-	-	63.6 [7.8]	-	-	12.136 (0.356)	-	-	-4
512.54 (0.006)	512.2	512.19	63.6 [7.8]	65	61.3	47.293 (0.507)	77.714	56.1	-3*
513.88 (0.006)	-	-	63.6 [7.8]	-	-	23.724 (0.257)	-	-	-4
518.22 (0.023)	-	-	63.6 [7.8]	-	-	2.801 (0.100)	-	-	-3
521.14 (0.005)	520.7	520.71	63.6 [7.8]	65	61.3	17.161 (0.162)	24.889	24.7	-4

Ware	E _R (eV)		Ware	Γ _γ (meV)		Ware	Γ _n (meV)		Spin
	JEFF3.1	JEF2.2		JEFF3.1	JEF2.2		JEFF3.1	JEF2.2	
523.38 (0.004)	523	523.02	63.6 [7.8]	65	66.5	34.776 (0.269)	56.889	73.2	-4*
525.74 (0.007)	525.5	525.46	63.6 [7.8]	65	61.3	167.22 (4.315)	162.29	116	-3*
527.56 (0.012)	-	-	63.6 [7.8]	-	-	17.074 (0.502)	-	-	-4
534.28 (0.008)	533.2	533.2	63.6 [7.8]	65	66.5	22.19 (0.401)	11.556	14.3	-3*
536.87 (0.016)	-	-	63.6 [7.8]	-	-	3.692 (0.091)	-	-	-4
539.77 (0.007)	539.1	539.1	63.6 [7.8]	65	66.5	14.75 (0.186)	11.429	11.7	-3
542.33 (0.013)	541.3	541.3	63.6 [7.8]	65	61.3	12.351 (0.275)	6.222	6.2	-4
549.12 (0.004)	548.6	548.63	63.6 [7.8]	60	66.5	120.46 (1.118)	124.44	147	-4*
550.38 (0.022)	-	-	63.6 [7.8]	-	-	8.466 (0.308)	-	-	-3
555.27 (0.016)	-	-	63.6 [7.8]	-	-	7.074 (0.18)	-	-	-3
556.94 (0.016)	557.2	557.22	63.6 [7.8]	65	66.5	5.263 (0.201)	16	15.6	-4*
558.58 (0.008)	-	-	63.6 [7.8]	-	-	16.773 (0.414)	-	-	-3
560.77 (0.014)	-	-	63.6 [7.8]	-	-	5.569 (0.137)	-	-	-4
563.79 (0.014)	-	-	63.6 [7.8]	-	-	5.433 (0.129)	-	-	-3
569.65 (0.011)	-	-	63.6 [7.8]	-	-	8.401 (0.157)	-	-	-4
572.59 (0.014)	-	-	63.6 [7.8]	-	-	10.015 (0.184)	-	-	-4
574.16 (0.008)	573.7	573.74	63.6 [7.8]	65	61.3	50.357 (0.727)	55.111	55.4	-3*
575.64 (0.010)	-	-	63.6 [7.8]	-	-	39.387 (0.907)	-	-	-3
578.34 (0.017)	577.4	577.4	63.6 [7.8]	65	61.3	28.757 (1.466)	176	124	-4*
580.22 (0.040)	-	-	63.6 [7.8]	-	-	4.637 (0.417)	-	-	-3
582.47 (0.009)	581.9	581.92	63.6 [7.8]	65	66.5	45.069 (1.884)	60.571	60.7	-4*
584.18 (0.019)	-	-	63.6 [7.8]	-	-	20.657 (1.037)	-	-	-3

Ware	E _R (eV)		Ware	Γ_γ (meV)		Ware	Γ_n (meV)		Spin
	JEFF3.1	JEF2.2		JEFF3.1	JEF2.2		JEFF3.1	JEF2.2	
588.05 (0.012)	-	-	63.6 [7.8]	-	-	6.798 (0.136)	-	-	-4
592.26 (0.006)	591.1	591.1	63.6 [7.8]	65	66.5	27.702 (0.272)	16	20.6	-4*
597.48 (0.006)	596.9	596.92	63.6 [7.8]	65	61.3	25.299 (0.300)	17.829	13.9	-3*
599.96 (0.010)	599.1	598.97	63.6 [7.8]	65	66.5	13.610 (0.321)	10.489	13.4	-4*
605.28 (0.007)	604.7	604.66	63.6 [7.8]	54	66.5	58.234 (1.348)	104.89	135	-4*
611.36 (0.006)	610.4	610.4	63.6 [7.8]	65	61.3	64.156 (0.841)	41.143	32.1	-3*
613.28 (0.006)	612.5	612.52	63.6 [7.8]	65	61.3	48.084 (0.738)	48.889	53.9	-4
616.97 (0.021)	-	-	63.6 [7.8]	-	-	5.798 (0.166)	-	-	-3
619.81 (0.006)	618.9	618.92	63.6 [7.8]	65	61.3	29.299 (0.302)	23.111	23	-4
626.07 (0.025)	625.5	625.54	63.6 [7.8]	65	61.3	11.944 (0.465)	68.571	53.4	-3*
629.23 (0.004)	628.7	628.7	63.6 [7.8]	65	66.5	113.43 (1.211)	152	173	-4*
634.32 (0.011)	633.2	633.16	63.6 [7.8]	65	66.5	14.206 (0.232)	7.429	7.48	-3
639.86 (0.024)	640.6	640.59	63.6 [7.8]	65	61.3	9.890 (0.272)	76.444	76.5	-3*
641.42 (0.005)	-	-	63.6 [7.8]	-	-	64.128 (0.721)	-	-	-4
646.71 (0.008)	646.4	646.4	63.6 [7.8]	65	66.5	110.20 (3.138)	162.29	147	-4*
647.55 (0.028)	-	-	63.6 [7.8]	-	-	27.087 (1.232)	-	-	-3
654.72 (0.010)	653.9	653.89	63.6 [7.8]	65	61.3	47.337 (1.566)	72.889	72.7	-4
656.68 (0.016)	-	-	63.6 [7.8]	-	-	27.660 (0.824)	-	-	-3
658.31 (0.015)	657.8	657.8	63.6 [7.8]	65	66.5	15.847 (0.380)	57.143	56.9	-4*
659.75 (0.009)	-	-	63.6 [7.8]	-	-	33.264 (0.606)	-	-	-3
665.82 (0.043)	-	-	63.6 [7.8]	-	-	2.386 (0.128)	-	-	-4
669.83 (0.006)	669.2	669.15	63.6 [7.8]	65	61.3	48.428 (0.532)	40.889	40.9	-3*

Ware	E _R (eV)		Ware	Γ_{γ} (meV)		Ware	Γ_n (meV)		Spin
	JEFF3.1	JEF2.2		JEFF3.1	JEF2.2		JEFF3.1	JEF2.2	
672.05 (0.010)	-	-	63.6 [7.8]	-	-	14.387 (0.275)	-	-	-4
676.50 (0.011)	676.5	676.47	63.6 [7.8]	65	66.5	21.297 (0.383)	83.429	83.2	-4*
678.07 (0.008)	-	-	63.6 [7.8]	-	-	41.078 (0.667)	-	-	-3
684.93 (0.005)	684.7	684.7	63.6 [7.8]	65	66.5	227.63 (3.126)	151.11	163	-3*
687.10 (0.008)	-	-	63.6 [7.8]	-	-	30.263 (0.756)	-	-	-4
690.95 (0.092)	-	-	63.6 [7.8]	-	-	2.004 (0.159)	-	-	-3
693.46 (0.011)	693.1	693.11	63.6 [7.8]	65	61.3	118.59 (3.561)	171.43	131	-4*
693.82 (0.012)	-	-	63.6 [7.8]	-	-	40.689 (2.140)	-	-	-3
697.39 (0.004)	696.6	696.63	63.6 [7.8]	65	61.3	135.18 (1.167)	124.44	97	-4
702.54 (0.013)	-	-	63.6 [7.8]	-	-	15.376 (0.306)	-	-	-3
706.16 (0.027)	-	-	63.6 [7.8]	-	-	6.730 (0.252)	-	-	-4
708.89 (0.031)	-	-	63.6 [7.8]	-	-	4.422 (0.169)	-	-	-3
712.23 (0.012)	-	-	63.6 [7.8]	-	-	170.09 (4.289)	-	-	-4
713.45 (0.067)	-	-	63.6 [7.8]	-	-	16.967 (8.042)	-	-	-3
713.96 (0.063)	-	714	63.6 [7.8]	-	66.5	24.451 (7.543)	-	135	-4*
722.48 (0.012)	-	727	63.6 [7.8]	-	66.5	119.89 (3.388)	-	114	-3
727.54 (0.027)	-	-	63.6 [7.8]	-	-	187.18 (12.666)	-	-	-4
728.11 (0.033)	-	-	63.6 [7.8]	-	-	99.393 (14.791)	-	-	-3
731.65 (0.041)	-	-	63.6 [7.8]	-	-	6.445 (0.304)	-	-	-4
733.33 (0.014)	-	-	63.6 [7.8]	-	-	30.673 (0.699)	-	-	-3
737.13 (0.009)	-	-	63.6 [7.8]	-	-	31.838 (0.425)	-	-	-4
739.81 (0.008)	-	-	63.6 [7.8]	-	-	62.262 (1.678)	-	-	-3

Ware	E _R (eV)		Ware	Γ_{γ} (meV)		Ware	Γ_n (meV)		Spin
	JEFF3.1	JEF2.2		JEFF3.1	JEF2.2		JEFF3.1	JEF2.2	
744.57 (0.030)	-	-	63.6 [7.8]	-	-	24.555 (0.687)	-	-	-4
749.95 (0.011)	-	-	63.6 [7.8]	-	-	48.943 (1.291)	-	-	-3
752.77 (0.016)	-	-	63.6 [7.8]	-	-	20.545 (2.117)	-	-	-4
755.63 (0.013)	-	-	63.6 [7.8]	-	-	31.688 (2.490)	-	-	-4
756.73 (0.047)	-	-	63.6 [7.8]	-	-	16.776 (2.921)	-	-	-3
760.99 (0.012)	-	-	63.6 [7.8]	-	-	91.968 (2.736)	-	-	-3
761.62 (0.016)	-	-	63.6 [7.8]	-	-	47.929 (1.749)	-	-	-4
767.10 (0.020)	-	-	63.6 [7.8]	-	-	13.723 (0.343)	-	-	-4
769.84 (0.011)	-	-	63.6 [7.8]	-	-	29.495 (1.060)	-	-	-3
774.33 (0.009)	-	-	63.6 [7.8]	-	-	120.61 (3.252)	-	-	-4
775.07 (0.015)	-	-	63.6 [7.8]	-	-	89.622 (3.144)	-	-	-3
781.70 (0.065)	-	-	63.6 [7.8]	-	-	15.354 (0.982)	-	-	-3
785.47 (0.020)	-	-	63.6 [7.8]	-	-	58.003 (3.594)	-	-	-3
787.59 (0.021)	-	-	63.6 [7.8]	-	-	50.865 (5.944)	-	-	-4
792.83 (0.047)	-	-	63.6 [7.8]	-	-	49.904 (3.209)	-	-	-3
794.75 (0.052)	-	-	63.6 [7.8]	-	-	17.515 (4.983)	-	-	-4
799.18 (0.012)	-	-	63.6 [7.8]	-	-	80.942 (1.975)	-	-	-3
802.97 (0.041)	-	-	63.6 [7.8]	-	-	6.649 (0.311)	-	-	-4
807.70 (0.012)	-	808.9	63.6 [7.8]	-	66.5	147.56 (2.713)	-	200	-3
809.04 (0.013)	-	809.1	63.6 [7.8]	-	61.3	135.04 (3.029)	-	156	-4
811.68 (0.007)	-	-	63.6 [7.8]	-	-	86.699 (1.116)	-	-	-4
815.78 (0.020)	-	-	63.6 [7.8]	-	-	21.336 (0.615)	-	-	-3

Ware	E _R (eV)		Ware	Γ_{γ} (meV)		Ware	Γ_n (meV)		Spin
	JEFF3.1	JEF2.2		JEFF3.1	JEF2.2		JEFF3.1	JEF2.2	
819.35 (0.027)	-	-	63.6 [7.8]	-	-	8.028 (0.238)	-	-	-4
823.53 (0.018)	-	-	63.6 [7.8]	-	-	33.878 (0.928)	-	-	-3
828.28 (0.007)	-	-	63.6 [7.8]	-	-	82.284 (0.798)	-	-	-4
834.53 (0.011)	-	-	63.6 [7.8]	-	-	63.167 (0.934)	-	-	-3
836.63 (0.014)	-	-	63.6 [7.8]	-	-	21.324 (0.765)	-	-	-4
841.76 (0.014)	-	-	63.6 [7.8]	-	-	47.916 (0.929)	-	-	-3
844.33 (0.011)	-	844	63.6 [7.8]	-	61.3	93.916 (2.192)	-	71	-4
851.23 (0.014)	-	-	63.6 [7.8]	-	-	35.140 (0.917)	-	-	-3
859.38 (0.036)	-	-	63.6 [7.8]	-	-	28.646 (2.076)	-	-	-3
861.04 (0.024)	-	-	63.6 [7.8]	-	-	54.183 (3.366)	-	-	-4
869.52 (0.028)	-	-	63.6 [7.8]	-	-	80.227 (6.991)	-	-	-3
870.48 (0.174)	-	-	63.6 [7.8]	-	-	5.167 (1.458)	-	-	-3
872.89 (0.022)	-	-	63.6 [7.8]	-	-	28.525 (1.015)	-	-	-4
874.61 (0.043)	-	-	63.6 [7.8]	-	-	10.006 (0.723)	-	-	-4
883.05 (0.043)	-	-	63.6 [7.8]	-	-	7.820 (0.444)	-	-	-4
886.04 (0.040)	-	887	63.6 [7.8]	-	61.3	14.765 (0.527)	-	157	-4
888.29 (0.013)	-	-	63.6 [7.8]	-	-	105.08 (2.759)	-	-	-3
891.22 (0.018)	-	-	63.6 [7.8]	-	-	18.177 (0.221)	-	-	-4
894.30 (0.013)	-	894.9	63.6 [7.8]	-	61.3	199.42 (5.168)	-	146	-3*
897.61 (0.007)	-	895.1	63.6 [7.8]	-	66.5	109.03 (1.473)	-	188	-4*
904.17 (0.016)	-	-	63.6 [7.8]	-	-	50.028 (1.241)	-	-	-4
906.01 (0.023)	-	-	63.6 [7.8]	-	-	83.784 (20.014)	-	-	-3

Ware	E _R (eV)		Ware	Γ_γ (meV)		Ware	Γ_n (meV)		Spin
	JEFF3.1	JEF2.2		JEFF3.1	JEF2.2		JEFF3.1	JEF2.2	
913.70 (0.031)	-	-	63.6 [7.8]	-	-	12.718 (0.689)	-	-	-4
916.14 (0.019)	-	-	63.6 [7.8]	-	-	68.587 (19.329)	-	-	-3
922.59 (0.032)	-	-	63.6 [7.8]	-	-	19.876 (1.924)	-	-	-4
927.37 (0.019)	-	928	63.6 [7.8]	-	66.5	142.94 (11.177)	-	185	-3
929.05 (0.02)	-	-	63.6 [7.8]	-	-	66.646 (5.267)	-	-	-4
931.84 (0.073)	-	-	63.6 [7.8]	-	-	28.986 (14.233)	-	-	-4
937.59 (0.015)	-	-	63.6 [7.8]	-	-	73.732 (2.303)	-	-	-3
941.05 (0.048)	-	-	63.6 [7.8]	-	-	29.923 (2.225)	-	-	-3
947.72 (0.044)	-	-	63.6 [7.8]	-	-	10.143 (0.749)	-	-	-4
950.74 (0.035)	-	-	63.6 [7.8]	-	-	19.102 (1.582)	-	-	-3
953.68 (0.022)	-	-	63.6 [7.8]	-	-	98.664 (25.316)	-	-	-4
957.40 (0.027)	-	-	63.6 [7.8]	-	-	73.533 (25.32)	-	-	-3
962.56 (0.057)	-	-	63.6 [7.8]	-	-	10.364 (0.979)	-	-	-4
968.44 (1.199)	-	-	63.6 [7.8]	-	-	22.609 (97.657)	-	-	-3
969.72 (0.677)	-	-	63.6 [7.8]	-	-	44	-	-	-4
975.07 (0.818)	-	-	63.6 [7.8]	-	-	24.472 (17.565)	-	-	-4
976.48 (0.122)	-	-	63.6 [7.8]	-	-	41.037 (31.248)	-	-	-4
980.69 (1.352)	-	-	63.6 [7.8]	-	-	5.293 (2.622)	-	-	-3
989.34 (0.106)	-	-	63.6 [7.8]	-	-	11.547 (1.675)	-	-	-3
990.89 (0.115)	-	1018.5	63.6 [7.8]	-	61.3	8.810 (1.586)	-	111	-4
998.91 (0.072)	-	1019.5	63.6 [7.8]	-	66.5	22.557 (7.038)	-	143	-3

The spin values in Table 5.9 marked “*” indicate that the spin value assigned to the corresponding resonance in the new evaluation is different to either the value in JEFF3.1, JEF2.2 or both. As the initial values of the resonance parameters were taken from the JEFF3.1 evaluation, the spin assignments of the new evaluation are in better agreement with the JEFF3.1 assignments than the JEF2.2 assignments. No uncertainties are given on the 969 eV resonance parameters, as fully converged values could not be obtained with REFIT.

Table 5.10 – Resonance Parameters for ^{178}Hf

E _R (eV)			Γ_γ (meV)			Γ_n (meV)			Spin
Ware	JEFF3.1	JEF2.2	Ware	JEFF3.1	JEF2.2	Ware	JEFF3.1	JEF2.2	
7.7835 (0.0008)	7.7865 (0.0001)	7.7718	48.311 (0.182)	53 (0.2)	58.262	54.431 (0.059)	53.83 (0.08)	51.542	0.5
28.771 (0.007)	-	28.672	51.0 (12.3)	-	51	0.0065 (0.0003)	-	0.0062	0.5 ^p
104.85 (0.001)	104.904 (0.002)	104.76	50.884 (0.559)	53	51	8.121 (0.016)	7.16 (0.08)	7.54	0.5
164.57 (0.001)	164.707 (0.003)	164.59	75.582 (1.940)	53	51	13.145 (0.091)	13.5 (0.1)	8.7	0.5
255.3 (0.003)	255.2	255.17	58.549 (0.996)	45	45.6	232.92 (1.101)	220	241	0.5
275.05 (0.004)	274.8	274.75	64.895 (2.902)	52	50.4	223.57 (1.316)	230	221	0.5
-	-	287.2	-	-	70	-	-	45	0.5
351.81 (0.002)	351.5	351.49	51.105 (3.728)	51	57	9.856 (0.069)	16	16.1	0.5
382.50 (0.002)	382.1	382.05	78.030 (0.444)	59	59.4	385.30 (1.446)	425	420	0.5
445.80 (0.003)	446.5	446.47	50.660 (0.434)	51	51	155.02 (1.208)	160	146	0.5
502.02 (0.003)	502.3	502.33	64.584 (1.076)	51	51	53.697 (0.553)	85	35	0.5
526.37 (0.004)	527.3	527.28	55.579 (0.510)	44	44	133.09 (1.911)	130	134	0.5
577.85 (0.006)	577.5	577.52	79.094 (0.604)	54	54.2	392.43 (3.941)	360	410	0.5
593.51 (0.024)	-	-	54.8 [12.3]	-	-	1.930 (0.168)	-	-	0.5
604.81 (0.005)	608.5	608.51	57.968 (1.451)	51	51	38.531 (0.832)	15	15	0.5
-	-	664	-	-	51	-	-	15	0.5
719.83 (0.004)	719.3	719.32	65.518 (0.470)	51	51.1	988.18 (2.386)	1050	1049	0.5
780.63 (0.005)	789.5	789.5	51.927 (0.451)	49	49	910.45 (3.059)	1300	1300	0.5
815.17 (0.016)	-	-	54.8 [12.3]	-	-	7.431 (0.198)	-	-	0.5
860.25 (0.010)	866	866	52.256 (0.796)	46	46	109.03 (1.974)	190	187	0.5
873.27 (0.051)	-	-	54.8 [12.3]	-	-	2.893 (0.207)	-	-	0.5

Ware	E _R (eV)		Ware	Γ_γ (meV)		Ware	Γ_n (meV)		Spin
	JEFF3.1	JEF2.2		JEFF3.1	JEF2.2		JEFF3.1	JEF2.2	
883.81 (0.010)	892	892	42.914 (1.070)	50	50	44.220 (0.988)	8	8	0.5
-	-	943	-	-	51	-	-	38	0.5
987.78 (0.013)	-	994.5	44.558 (1.956)	-	51	32.561 (1.950)	-	39	0.5
1017.5 (0.018)	-	-	54.8 [12.3]	-	-	13.768 (2.754)	-	-	0.5
1030.2 (0.013)	-	1046	54.8 [12.3]	-	51	31.041 (6.208)	-	40	0.5
1090.2 (0.012)	1097	1097	54.8 [12.3]	47	47	72.650 (3.776)	550	550	0.5
1156 (0.019)	1167	1167	54.8 [12.3]	51	51	77.553 (3.433)	1160	1160	0.5
1180.7 (0.016)	1190	1190	54.8 [12.3]	51	51	81.590 (4.473)	190	190	0.5
1244.4 (0.016)	-	-	54.8 [12.3]	-	-	85.010 (17.000)	-	-	0.5
1255.5 (0.029)	-	1251.5	54.8 [12.3]	-	51	14.160 (2.832)	-	106	0.5
1301.4 (0.021)	1313	1313	54.8 [12.3]	51	51	94.343 (19.604)	540	540	0.5
1348.5 (0.020)	1359	1359	54.8 [12.3]	51	51	102.33 (7.179)	45	45	0.5
-	-	1402.5	-	-	51	-	-	112	0.5
1436.7 (0.021)	1446	1446	54.8 [12.3]	51	51	468 (233)	2550	2550	0.5
1487.1 (0.023)	-	1494	54.8 [12.3]	-	51	89.906 (5.768)	-	116	0.5
1554.0 (0.025)	-	1542	54.8 [12.3]	-	51	88.978 (17.796)	-	118	0.5
1584.9 (0.028)	-	1590	54.8 [12.3]	-	51	113.51 (37.837)	-	120	0.5
-	-	1638	-	-	51	-	-	121	0.5
1698.0 (0.030)	-	1686	54.8 [12.3]	-	51	102.0 (7.638)	-	123	0.5
-	-	1734	-	-	51	-	-	125	0.5
1808.4 (0.040)	-	1782	54.8 [12.3]	-	51	57.984 (3.258)	-	127	0.5
1831.4 (0.036)	1830	1830	54.8 [12.3]	51	51	90.150 (6.907)	2120	2120	0.5

E _R (eV)			Γ _γ (meV)			Γ _n (meV)			Spin
Ware	JEFF3.1	JEF2.2	Ware	JEFF3.1	JEF2.2	Ware	JEFF3.1	JEF2.2	
-	-	1882	-	-	51	-	-	130	0.5
-	-	1934	-	-	51	-	-	132	0.5
-	-	1986	-	-	51	-	-	134	0.5
2024.3 (0.043)	-	2038	54.8 [12.3]	-	51	106.9 (9.962)	-	135	0.5
2061.4 (0.048)	-	-	54.8 [12.3]	-	-	136.5 (68.3)	-	-	0.5
2084.0 (0.046)	2090	2090	54.8 [12.3]	51	51	101.19 (9.455)	1060	1060	0.5
-	-	2140.5	-	-	51	-	-	497	0.5
2188.4 (0.048)	-	2191	54.8 [12.3]	-	51	109.5 (11.25)	-	503	0.5
-	-	2242	-	-	51	-	-	509	0.5
-	-	2292	-	-	51	-	-	514	0.5
2313.1 (0.059)	-	2343	54.8 [12.3]	-	51	105.12 (16.777)	-	520	0.5
2363.1 (0.053)	-	2393	54.8 [12.3]	-	51	101.18 (9.799)	-	525	0.5
2459 (0.061)	-	2444	54.8 [12.3]	-	51	94.116 (14.928)	-	1062	0.5
2491.8 (0.065)	-	-	54.8 [12.3]	-	-	116.39 (16.256)	-	-	0.5
2586.8 (0.066)	-	-	54.8 [12.3]	-	-	120.69 (15.226)	-	-	0.5
2603.8 (0.070)	-	-	54.8 [12.3]	-	-	87.127 (9.730)	-	-	0.5
2658.5 (0.071)	-	-	54.8 [12.3]	-	-	91.76 (18.352)	-	-	0.5
2741.6 (0.081)	-	-	54.8 [12.3]	-	-	104.32 (11.872)	-	-	0.5
2771.3 (0.079)	-	-	54.8 [12.3]	-	-	95.750 (21.589)	-	-	0.5
2835.4 (0.081)	-	-	54.8 [12.3]	-	-	105.79 (15.308)	-	-	0.5
2893.6 (0.089)	-	-	54.8 [12.3]	-	-	90.340 (18.068)	-	-	0.5
2961.9 (0.090)	-	-	54.8 [12.3]	-	-	93.812 (18.763)	-	-	0.5

The 28.8 eV resonance in Table 5.11 (marked “p”) was designated a p-wave resonance in the JEF2.2 evaluated file.

Table 5.11 – Resonance Parameters for ^{179}Hf

E _R (eV)			Γ _γ (meV)			Γ _n (meV)			Spin
Ware	JEFF3.1	JEF2.2	Ware	JEFF3.1	JEF2.2	Ware	JEFF3.1	JEF2.2	
5.6925 (0.0001)	5.6885 (0.0002)	5.6862	53.286 (0.134)	47 (2)	62.64	4.261 (0.008)	4.27 (0.04)	4.64	5
6.6674 (0.0003)	-	-	54.5 [7.7]	-		0.212 (0.001)	-		4
17.648 (0.0002)	17.6533 (0.0006)	17.658	54.5 [7.7]	52	64.13	2.193 (0.005)	2.09 (0.01)	2.065	4
19.123 (0.0016)	19.131 (0.004)	19.136	54.5 [7.7]	52	62.8	0.104 (0.001)	0.124 (0.004)	0.107	5
23.651 (0.0001)	23.6577 (0.0006)	23.666	52.854 (0.129)	52	64.1	8.381 (0.008)	7.47 (0.09)	7.681	5
26.540 (0.0002)	26.540 (0.002)	26.535	54.5 [7.7]	52	64.1	1.253 (0.002)	1.27 (0.01)	1.14	4
27.405 (0.0005)	27.418 (0.004)	27.405	54.5 [7.7]	52	63.7	0.422 (0.001)	0.433 (0.009)	0.4152	5
31.150 (0.0001)	31.156 (0.006)	31.153	57.298 (0.178)	52	64.1	8.530 (0.009)	8.1447 (0.06)	7.72	4
36.511 (0.0001)	36.520 (0.007)	36.552	60.171 (0.135)	52	62.8	28.721 (0.035)	26.00 (0.04)	29.753	5
40.120 (0.0001)	40.1350 (0.0005)	40.28	59.146 (0.128)	61 (3)	62.8	25.006 (0.027)	23.5 (0.4)	23.4	5
-	-	42.277	-	-	62.8	-	-	0.367	5
42.314 (0.0001)	42.3270 (0.0007)	42.487	63.231 (0.192)	52	64.1	15.307 (0.018)	15.3 (0.2)	12.63	4
-	-	47.723	-	-	64.1	-	-	0.4363	4
50.782 (0.0006)	50.785 (0.005)	50.77	54.5 [7.7]	52	64.1	1.153 (0.004)	1.11 (0.03)	1.007	5*
51.137 (0.0012)	51.149 (0.009)	51.11	54.5 [7.7]	52	62.8	0.644 (0.004)	0.71 (0.03)	0.466	4*
-	-	52.8	-	-	62.8	-	-	0.51	5
54.803 (0.0004)	54.08 (0.01)	54.77	54.5 [7.7]	52	64.1	6.085 (0.019)	0.33 (0.03)	5.25	4
69.055 (0.0003)	69.089 (0.002)	69.03	54.5 [7.7]	52	64.1	10.760 (0.021)	10.6 (0.1)	10.28	4
73.561 (0.0004)	73.589 (0.002)	73.53	54.5 [7.7]	52	64.1	9.689 (0.023)	9.2 (0.4)	8.54	4

E _R (eV)			Γ_γ (meV)			Γ_n (meV)			Spin
Ware	JEFF3.1	JEF2.2	Ware	JEFF3.1	JEF2.2	Ware	JEFF3.1	JEF2.2	
76.668 (0.0006)	76.702 (0.005)	76.63	54.5 [7.7]	52	62.8	3.095 (0.009)	3.26 (0.06)	2.85	5
82.983 (0.0005)	83.013 (0.004)	82.94	54.5 [7.7]	52	62.8	4.433 (0.011)	4.69 (0.07)	4.85	4*
85.444 (0.0007)	85.433 (0.003)	85.42	54.5 [7.7]	52	64.1	4.787 (0.017)	11.8 (0.4)	7	5*
92.099 (0.0006)	92.125 (0.004)	92.07	54.5 [7.7]	52	64.1	12.235 (0.039)	11.7 (0.2)	1	4
92.723 (0.0004)	92.7852 (0.003)	92.67	54.5 [7.7]	52	62.8	28.382 (0.066)	27 (0.6)	37.2	5
101.30 (0.001)	101.382 (0.001)	101.2	54.5 [7.7]	52	62.8	121.72 (0.167)	113.8 (1)	99	5
103.72 (0.001)	103.821 (0.006)	103.7	54.5 [7.7]	52	64.1	9.527 (0.036)	9.8 (0.2)	8.81	5*
107.81 (0.001)	107.858 (0.004)	107.8	54.5 [7.7]	52	62.8	9.962 (0.025)	9.5 (0.1)	9.6	4*
117.2 (0.001)	117.278 (0.002)	117.2	54.5 [7.7]	44 (2)	62.8	32.175 (0.094)	31 (1)	33.4	5
120.14 (0.002)	120.165 (0.008)	120.1	54.5 [7.7]	52	64.1	2.498 (0.012)	3.46 (0.08)	2.4	4
121.95 (0.001)	121.86 (0.03)	121.9	54.5 [7.7]	52	64.1	7.504 (0.031)	3.7 (0.3)	1	4
122.61 (0.001)	122.689 (0.005)	122.6	54.5 [7.7]	52	62.8	15.6 (0.054)	15.8 (0.4)	22.4	5
129.97 (0.001)	130.024 (0.005)	129.9	54.5 [7.7]	52	64.1	9.562 (0.027)	10.2 (0.2)	10.9	4
137.28 (0.001)	137.426 (0.004)	137.2	54.5 [7.7]	52	62.8	25.546 (0.115)	36.6 (0.7)	23	5
138.13 (0.001)	-	138.1	54.5 [7.7]	-	64.1	16.058 (0.083)	-	27.8	4
144.30 (0.001)	144.341 (0.006)	144.2	54.5 [7.7]	52	62.8	24.050 (0.082)	32 (2)	24.9	5
147.05 (0.001)	147.103 (0.006)	147	54.5 [7.7]	52	64.1	13.280 (0.055)	12.2 (0.3)	11.7	4
152.38 (0.002)	-	150.2	54.5 [7.7]	-	62.8	2.959 (0.016)	-	0.74	5
154.79 (0.005)	-	152.3	54.5 [7.7]	-	64.1	1.160 (0.013)	-	1	4
156.31 (0.001)	156.393 (0.003)	156.3	54.5 [7.7]	58 (2)	62.8	41.412 (0.219)	45 (1)	38.4	5
158.79 (0.002)	158.835 (0.008)	158.6	54.5 [7.7]	52	64.1	4.070 (0.019)	4.7 (0.1)	1	4
165.73 (0.001)	165.807 (0.005)	165.7	54.5 [7.7]	52	62.8	22.145 (0.074)	23.7 (0.6)	19.9	5

Ware	E_R (eV)		Ware	Γ_γ (meV)		Ware	Γ_n (meV)		Spin
	JEFF3.1	JEF2.2		JEFF3.1	JEF2.2		JEFF3.1	JEF2.2	
174.29 (0.001)	-	174.2	54.5 [7.7]	-	62.8	75.942 (0.346)	-	60	4*
174.96 (0.001)	174.904 (0.008)	174.9	54.5 [7.7]	52	64.1	34.092 (0.224)	77 (9)	73.3	4
177.97 (0.001)	177.996 (0.006)	177.9	54.5 [7.7]	52	62.8	27.052 (0.149)	66 (6)	24.1	5
182.67 (0.001)	182.790 (0.005)	182.6	54.5 [7.7]	52	64.1	32.209 (0.102)	32.8 (0.6)	53.3	4
188.61 (0.002)	188.75 (0.02)	188.5	54.5 [7.7]	52	62.8	9.037 (0.039)	6.1 (0.4)	29	4*
189.85 (0.001)	189.953 (0.007)	189.8	54.5 [7.7]	52	64.1	28.078 (0.109)	20.2 (0.5)	1	4*
192.94 (0.002)	191.25 (0.06)	192.9	54.5 [7.7]	52	64.1	11.303 (0.053)	0.91 (0.08)	5.6	4
197.97 (0.001)	198.052 (0.008)	197.9	54.5 [7.7]	52	62.8	14.240 (0.074)	16.1 (0.3)	18	5
202.63 (0.001)	202.6	202.6	54.5 [7.7]	66	62.8	58.166 (0.256)	81.818	85.9	5
204.24 (0.002)	204.1	204.1	54.5 [7.7]	66	64.1	6.337 (0.050)	148.89	146	4
205.89 (0.001)	-	-	54.5 [7.7]	-	-	93.397 (0.217)	-	-	5
210.27 (0.021)	-	-	54.5 [7.7]	-	-	0.478 (0.018)	-	-	4
213.13 (0.001)	-	213.1	54.5 [7.7]	-	62.8	46.185 (0.316)	-	56	4*
213.33 (0.003)	213.1	214	54.5 [7.7]	66	64.1	14.173 (0.127)	56.364	0.88	5*
223.83 (0.006)	-	224	54.5 [7.7]	-	64.1	8.727 (0.122)	-	0.91	4
224.59 (0.002)	224.5	224.5	54.5 [7.7]	66	62.8	200.62 (0.881)	255.56	209	5*
227.82 (0.001)	227.7	227.7	54.5 [7.7]	66	64.1	78.184 (0.318)	60.909	74.4	4*
229.75 (0.007)	-	233.7	54.5 [7.7]	-	62.8	1.453 (0.033)	-	13	5
238.75 (0.011)	-	-	54.5 [7.7]	-	-	1.050 (0.020)	-	-	5
241.72 (0.001)	241.6	241.6	54.5 [7.7]	66	64.1	58.712 (0.374)	74.444	74.4	4
243.04 (0.003)	-	242.9	54.5 [7.7]	-	62.8	5.947 (0.068)	-	13	4*
245.36 (0.001)	245.3	245.3	54.5 [7.7]	66	64.1	35.482 (0.160)	51.111	51	5*

Ware	E _R (eV)		Ware	Γ_γ (meV)		Ware	Γ_n (meV)		Spin
	JEFF3.1	JEF2.2		JEFF3.1	JEF2.2		JEFF3.1	JEF2.2	
-	-	248.5	-	-	62.8	-	-	13	5
251.94 (0.003)	-	251.8	54.5 [7.7]	-	64.1	5.625 (0.075)	-	0.95	5*
253.39 (0.002)	254.2	254.2	54.5 [7.7]	66	62.8	32.783 (0.452)	55.455	55.5	5
255.51 (0.024)	-	-	54.5 [7.7]	-	-	1.056 (0.069)	-	-	5
256.60 (0.012)	-	-	54.5 [7.7]	-	-	2.101 (0.114)	-	-	4
258.52 (0.038)	-	263.9	54.5 [7.7]	-	64.1	0.328 (0.034)	-	10	5*
263.00 (0.003)	263.9	264	54.5 [7.7]	66	62.8	5.930 (0.127)	10	14	5*
270.15 (0.005)	-	270	54.5 [7.7]	-	64.1	3.831 (0.052)	-	5.8	4
273.62 (0.006)	-	273.5	54.5 [7.7]	-	62.8	4.941 (0.072)	-	14	5
275.19 (0.021)	-	-	54.5 [7.7]	-	-	2.830 (0.513)	-	-	4
276.41 (0.003)	276.3	276.3	54.5 [7.7]	66	62.8	38.682 (1.764)	45.455	45.5	5
279.57 (0.060)	-	-	54.5 [7.7]	-	-	0.212 (0.037)	-	-	5
284.68 (0.162)	-	284.7	54.5 [7.7]	-	64.1	5.890 (5.677)	-	5.9	5*
288.82 (0.021)	-	288.7	54.5 [7.7]	-	64.1	0.767 (0.038)	-	5.9	5*
292.59 (0.020)	-	292.4	54.5 [7.7]	-	62.8	17.775 (6.479)	-	14	4*
295.33 (0.170)	-	299.5	54.5 [7.7]	-	62.8	0.134 (0.041)	-	15	4*
300.74 (0.002)	300.6	300.6	54.5 [7.7]	66	64.1	41.204 (0.264)	38.889	38.9	4
306.36 (0.003)	-	306.3	54.5 [7.7]	-	64.1	9.058 (0.085)	-	6.1	5*
-	-	306.6	-	-	62.8	-	-	15	5
313.63 (0.006)	-	313.6	54.5 [7.7]	-	62.8	4.397 (0.067)	-	15	5
-	-	314.4	-	-	64.1	-	-	6.2	4
-	-	320.3	-	-	62.8	-	-	15	5

Ware	E _R (eV)		Ware	Γ_γ (meV)		Ware	Γ_n (meV)		Spin
	JEFF3.1	JEF2.2		JEFF3.1	JEF2.2		JEFF3.1	JEF2.2	
322.59 (0.003)	322.5	322.5	54.5 [7.7]	66	64.1	24.929 (0.231)	8.889	8.9	4
327.14 (0.002)	327	327	54.5 [7.7]	66	62.8	40.86 (0.466)	30.909	31	5
333.06 (0.004)	-	332.9	54.5 [7.7]	-	64.1	13.510 (0.164)	-	6.4	4
338.35 (0.002)	338.2	338.2	54.5 [7.7]	66	62.8	65.497 (0.440)	54.545	54.5	5
-	-	340.6	-	-	64.1	-	-	6.5	4
346.20 (0.003)	346.1	346.1	54.5 [7.7]	66	62.8	49.951 (0.420)	59.091	59	5
349.70 (0.005)	-	348.4	54.5 [7.7]	-	64.1	15.244 (0.224)	-	6.5	4
356.24 (0.008)	-	356.1	54.5 [7.7]	-	64.1	6.125 (0.094)	-	6.6	4
360.81 (0.002)	360.7	360.7	54.5 [7.7]	47.8	62.8	14.219 (0.119)	1172.7	16	5
362.87 (0.369)	-	364.4	54.5 [7.7]	-	62.8	1.100 (0.181)	-	63.6	4*
364.59 (0.002)	364.4	365.7	54.5 [7.7]	66	64.1	54.667 (0.603)	63.636	6.7	5*
372.26 (0.004)	-	372.1	54.5 [7.7]	-	62.8	29.278 (0.300)	-	16	4*
375.32 (0.006)	-	375.2	54.5 [7.7]	-	64.1	14.008 (0.201)	-	6.8	5*
-	-	378.8	-	-	62.8	-	-	16	5
381.81 (0.004)	381.7	381.7	54.5 [7.7]	66	64.1	401.5 (4.058)	383.33	383	4
385.83 (0.005)	-	385.6	54.5 [7.7]	-	62.8	12.718 (0.137)	-	16	5
389.23 (0.003)	-	389	54.5 [7.7]	-	64.1	61.074 (0.883)	-	6.9	4
390.85 (0.004)	390.6	390.6	54.5 [7.7]	66	62.8	48.272 (0.815)	90.909	91	5
395.33 (0.012)	-	395.3	54.5 [7.7]	-	64.1	4.052 (0.088)	-	7	4
401.32 (0.008)	-	401.1	54.5 [7.7]	-	62.8	5.670 (0.088)	-	17	5
403.99 (0.028)	-	403.8	54.5 [7.7]	-	64.1	1.449 (0.067)	-	7	4
408.92 (0.025)	-	408.8	54.5 [7.7]	-	62.8	1.589 (0.069)	-	17	5

Ware	E _R (eV)		Ware	Γ_γ (meV)		Ware	Γ_n (meV)		Spin
	JEFF3.1	JEF2.2		JEFF3.1	JEF2.2		JEFF3.1	JEF2.2	
411.58 (0.003)	-	411.4	54.5 [7.7]	-	64.1	28.098 (0.220)	-	7.1	4
413.71 (0.017)	413.6	413.6	54.5 [7.7]	66	64.1	2.919 (0.087)	23.636	28.8	5*
421.17 (0.036)	-	-	54.5 [7.7]	-	-	1.262 (0.071)	-	-	5
423.55 (0.003)	-	423.5	54.5 [7.7]	-	62.8	43.271 (0.355)	-	17	4*
429.05 (0.003)	-	428.9	54.5 [7.7]	-	62.8	174.92 (1.819)	-	17	4*
430.89 (0.012)	-	-	54.5 [7.7]	-	-	13.880 (0.720)	-	-	5
431.19 (0.008)	431.9	431.9	54.5 [7.7]	66	64.1	44.060 (1.287)	205.56	206	4
436.38 (0.021)	-	-	54.5 [7.7]	-	-	2.795 (0.095)	-	-	5
442.91 (0.043)	-	-	54.5 [7.7]	-	-	1.233 (0.084)	-	-	4
452.51 (0.009)	-	-	54.5 [7.7]	-	-	5.692 (0.089)	-	-	5
459.91 (0.006)	-	-	54.5 [7.7]	-	-	27.299 (0.596)	-	-	5
460.84 (0.004)	462.8	462.8	54.5 [7.7]	66	62.8	146.80 (1.544)	233.33	191	4*
465.62 (0.016)	-	-	54.5 [7.7]	-	-	2.913 (0.072)	-	-	5
471.45 (0.009)	-	-	54.5 [7.7]	-	-	11.479 (0.201)	-	-	4
475.55 (0.014)	-	-	54.5 [7.7]	-	-	7.932 (0.261)	-	-	5
478.71 (0.006)	-	-	54.5 [7.7]	-	-	13.492 (0.193)	-	-	5
488.58 (0.004)	-	-	54.5 [7.7]	-	-	101.37 (1.967)	-	-	4
490.50 (0.008)	489.6	489.6	54.5 [7.7]	66	64.1	9.730 (0.163)	0.818	83	5*
494.66 (0.020)	-	-	54.5 [7.7]	-	-	3.024 (0.091)	-	-	4
502.07 (0.017)	-	-	54.5 [7.7]	-	-	4.997 (0.148)	-	-	5
506.47 (0.006)	-	-	54.5 [7.7]	-	-	27.841 (0.340)	-	-	4
511.60 (0.005)	-	-	54.5 [7.7]	-	-	21.190 (0.254)	-	-	5

E _R (eV)			Γ _γ (meV)			Γ _n (meV)			Spin
Ware	JEFF3.1	JEF2.2	Ware	JEFF3.1	JEF2.2	Ware	JEFF3.1	JEF2.2	
515.16 (0.018)	514	514	54.5 [7.7]	66	64.1	3.895 (0.111)	33.333	33	4
522.86 (0.024)	-	-	54.5 [7.7]	-	-	2.628 (0.098)	-	-	5
528.70 (0.004)	-	-	54.5 [7.7]	-	-	90.029 (1.172)	-	-	5
530.24 (0.009)	532	532	54.5 [7.7]	66	62.8	17.585 (0.462)	127.27	127	4*
542.45 (0.004)	-	-	54.5 [7.7]	-	-	214.87 (2.064)	-	-	5
543.70 (0.005)	546	546	54.5 [7.7]	66	64.1	60.570 (0.922)	288.89	289	5*
551.35 (0.010)	-	-	54.5 [7.7]	-	-	8.118 (0.147)	-	-	5
554.67 (0.015)	-	-	54.5 [7.7]	-	-	6.305 (0.165)	-	-	4
560.50 (0.012)	-	-	54.5 [7.7]	-	-	8.310 (0.165)	-	-	5
566.22 (0.011)	-	-	54.5 [7.7]	-	-	22.049 (0.435)	-	-	4
567.38 (0.014)	-	-	54.5 [7.7]	-	-	35.702 (0.571)	-	-	4
568.49 (0.007)	-	-	54.5 [7.7]	-	-	49.869 (0.803)	-	-	5
571.48 (0.007)	571	571	54.5 [7.7]	66	64.1	25.364 (0.334)	144.44	144	4
580.55 (0.006)	-	-	54.5 [7.7]	-	-	145.02 (4.286)	-	-	5
583.12 (0.01)	583	583	54.5 [7.7]	66	62.8	211.22 (8.703)	263.64	264	4*
585.50 (0.010)	587	587	54.5 [7.7]	66	64.1	20.115 (0.704)	100	122	5*
595.01 (0.005)	-	-	54.5 [7.7]	-	-	36.120 (0.415)	-	-	5
600.80 (0.005)	-	-	54.5 [7.7]	-	-	73.934 (0.976)	-	-	4
612.29 (0.008)	-	-	54.5 [7.7]	-	-	27.547 (0.448)	-	-	5
618.22 (0.015)	-	-	54.5 [7.7]	-	-	8.582 (0.187)	-	-	4
626.79 (0.006)	630	630	54.5 [7.7]	66	62.8	131.50 (4.608)	205.56	168	5*
638.54 (0.007)	-	-	54.5 [7.7]	-	-	42.492 (0.552)	-	-	4

Ware	E _R (eV)		Ware	Γ_{γ} (meV)		Ware	Γ_n (meV)		Spin
	JEFF3.1	JEF2.2		JEFF3.1	JEF2.2		JEFF3.1	JEF2.2	
645.82 (0.009)	-	-	54.5 [7.7]	-	-	21.407 (0.414)	-	-	5
648.32 (0.006)	-	-	54.5 [7.7]	-	-	184.05 (2.885)	-	-	4
654.11 (0.007)	652	652	54.5 [7.7]	66	64.1	238.32 (4.542)	190.91	233	5*
655.15 (0.012)	658	658	54.5 [7.7]	66	62.8	187.24 (9.261)	218.18	218	4*
664.72 (0.007)	-	-	54.5 [7.7]	-	-	31.440 (0.396)	-	-	5
672.62 (0.014)	-	-	54.5 [7.7]	-	-	13.384 (0.303)	-	-	4
677.03 (0.012)	-	-	54.5 [7.7]	-	-	18.904 (0.360)	-	-	5
681.53 (0.004)	-	-	54.5 [7.7]	-	-	107.05 (1.035)	-	-	4
685.50 (0.007)	-	-	54.5 [7.7]	-	-	78.028 (2.088)	-	-	5
689.13 (0.013)	689	689	54.5 [7.7]	66	62.8	15.669 (0.276)	300	245	4*
694.73 (0.033)	-	-	54.5 [7.7]	-	-	3.900 (0.165)	-	-	5
701.42 (0.044)	-	-	54.5 [7.7]	-	-	2.855 (0.155)	-	-	4
705.93 (0.008)	-	-	54.5 [7.7]	-	-	35.147 (0.534)	-	-	5
713.31 (0.028)	-	-	54.5 [7.7]	-	-	29.678 (2.504)	-	-	4
714.68 (0.020)	-	-	54.5 [7.7]	-	-	37.490 (2.100)	-	-	5
717.18 (0.038)	-	-	54.5 [7.7]	-	-	4.927 (0.215)	-	-	4
722.66 (0.042)	-	-	54.5 [7.7]	-	-	16.021 (0.985)	-	-	5
724.22 (0.057)	-	-	54.5 [7.7]	-	-	13.679 (1.604)	-	-	4
728.77 (0.008)	-	-	54.5 [7.7]	-	-	73.185 (1.909)	-	-	5
735.35 (0.010)	-	733	54.5 [7.7]	-	62.8	33.424 (0.539)	-	73	4*
741.24 (0.008)	-	-	54.5 [7.7]	-	-	40.341 (0.664)	-	-	5
745.05 (0.011)	-	-	54.5 [7.7]	-	-	93.542 (2.884)	-	-	4

Ware	E _R (eV)		Ware	Γ _γ (meV)		Ware	Γ _n (meV)		Spin
	JEFF3.1	JEF2.2		JEFF3.1	JEF2.2		JEFF3.1	JEF2.2	
752.54 (0.012)	-	751	54.5 [7.7]	-	64.1	30.273 (0.657)	-	89	5*
755.69 (0.055)	-	-	54.5 [7.7]	-	-	5.632 (0.263)	-	-	5
764.86 (0.009)	-	-	54.5 [7.7]	-	-	53.614 (0.703)	-	-	4
767.08 (0.014)	-	-	54.5 [7.7]	-	-	23.496 (0.705)	-	-	5
785.29 (0.015)	-	-	54.5 [7.7]	-	-	294.43 (14.193)	-	-	4
787.11 (0.036)	-	-	54.5 [7.7]	-	-	13.642 (0.825)	-	-	5
790.43 (0.022)	-	-	54.5 [7.7]	-	-	47.386 (4.806)	-	-	4
799.68 (0.010)	-	-	54.5 [7.7]	-	-	55.221 (1.700)	-	-	4
802.77 (0.010)	-	-	54.5 [7.7]	-	-	41.007 (1.275)	-	-	5
806.83 (0.019)	-	-	54.5 [7.7]	-	-	18.361 (0.559)	-	-	4
809.08 (0.013)	-	-	54.5 [7.7]	-	-	35.760 (1.213)	-	-	5
820.51 (0.035)	-	-	54.5 [7.7]	-	-	6.979 (0.270)	-	-	4
823.31 (0.009)	-	-	54.5 [7.7]	-	-	98.026 (2.161)	-	-	4
826.30 (0.035)	-	-	54.5 [7.7]	-	-	6.617 (0.229)	-	-	5
829.95 (0.027)	-	-	54.5 [7.7]	-	-	6.973 (0.243)	-	-	4
839.83 (0.007)	-	-	54.5 [7.7]	-	-	105.51 (1.424)	-	-	5
842.27 (0.027)	-	-	54.5 [7.7]	-	-	12.824 (1.103)	-	-	5
843.80 (0.013)	-	-	54.5 [7.7]	-	-	115.48 (4.289)	-	-	4
847.12 (0.010)	-	848	54.5 [7.7]	-	64.1	38.308 (0.610)	-	139	5*
851.93 (0.010)	-	-	54.5 [7.7]	-	-	90.941 (1.791)	-	-	5
853.93 (0.029)	-	-	54.5 [7.7]	-	-	8.711 (0.714)	-	-	4
858.18 (0.009)	-	-	54.5 [7.7]	-	-	67.577 (0.998)	-	-	5

Ware	E _R (eV)		Ware	Γ_{γ} (meV)		Ware	Γ_n (meV)		Spin
	JEFF3.1	JEF2.2		JEFF3.1	JEF2.2		JEFF3.1	JEF2.2	
861.43 (0.020)	-	-	54.5 [7.7]	-	-	49.001 (2.498)	-	-	4
863.09 (0.020)	-	-	54.5 [7.7]	-	-	21.239 (0.838)	-	-	5
867.02 (0.021)	-	-	54.5 [7.7]	-	-	14.135 (0.375)	-	-	4
870.18 (0.022)	-	-	54.5 [7.7]	-	-	13.522 (0.376)	-	-	5
873.90 (0.012)	-	-	54.5 [7.7]	-	-	60.551 (1.558)	-	-	4
878.04 (0.043)	-	-	54.5 [7.7]	-	-	3.981 (0.188)	-	-	5
884.90 (0.014)	-	-	54.5 [7.7]	-	-	93.990 (2.758)	-	-	4
887.40 (0.011)	-	-	54.5 [7.7]	-	-	101.98 (3.304)	-	-	5
890.30 (0.022)	-	-	54.5 [7.7]	-	-	19.169 (0.513)	-	-	4
893.86 (0.009)	-	893	54.5 [7.7]	-	62.8	102.43 (4.677)	-	136	5
901.01 (0.015)	-	900	54.5 [7.7]	-	62.8	22.649 (0.451)	-	91	5
907.26 (0.013)	-	-	54.5 [7.7]	-	-	88.658 (9.092)	-	-	5
917.36 (0.067)	-	-	54.5 [7.7]	-	-	57.920 (7.878)	-	-	4
919.67 (0.067)	-	-	54.5 [7.7]	-	-	246.39 (153.3)	-	-	5
930.12 (0.045)	-	927	54.5 [7.7]	-	62.8	15.873 (0.504)	-	155	4*
933.68 (0.030)	-	-	54.5 [7.7]	-	-	18.632 (0.536)	-	-	5
936.76 (0.019)	-	-	54.5 [7.7]	-	-	56.683 (2.848)	-	-	4
939.84 (0.020)	-	-	54.5 [7.7]	-	-	18.713 (1.021)	-	-	5
944.48 (0.223)	-	-	54.5 [7.7]	-	-	2.387 (1.506)	-	-	4
948.63 (0.011)	-	-	54.5 [7.7]	-	-	59.256 (2.249)	-	-	5
959.11 (0.240)	-	-	54.5 [7.7]	-	-	213.21 (32.404)	-	-	5
959.13 (0.502)	-	-	54.5 [7.7]	-	-	44.904 (26.128)	-	-	4

E _R (eV)			Γ _γ (meV)			Γ _n (meV)			Spin
Ware	JEFF3.1	JEF2.2	Ware	JEFF3.1	JEF2.2	Ware	JEFF3.1	JEF2.2	
964.38 (0.030)	-	-	54.5 [7.7]	-	-	308.60 (43.949)	-	-	4
965.12 (0.014)	-	-	54.5 [7.7]	-	-	102.40 (8.598)	-	-	5
968.59 (0.032)	-	-	54.5 [7.7]	-	-	196.26 (40.459)	-	-	4
972.28 (0.336)	-	971	54.5 [7.7]	-	64.1	12.760 (4.044)	-	700	5*
975.07 (0.500)	-	-	54.5 [7.7]	-	-	17	-	-	4
976.78 (0.107)	-	-	54.5 [7.7]	-	-	93.518 (34.498)	-	-	5
980.65 (0.082)	-	-	54.5 [7.7]	-	-	21.468 (0.593)	-	-	5
987.82 (0.630)	-	-	54.5 [7.7]	-	-	2.387 (1.500)	-	-	4
1000.15 (0.026)	-	1010	54.5 [7.7]	-	64.1	143.77 (53.570)	-	244	4

The spin values in Table 5.11 marked “*” indicate that the spin value assigned to the corresponding resonance in the new evaluation is different to either the value in JEFF3.1, JEF2.2 or both. As the initial values of the resonance parameters were taken from the JEFF3.1 evaluation, the spin assignments of the new evaluation are in better agreement with the JEFF3.1 assignments than the JEF2.2 assignments. No uncertainties are given on the 975 eV resonance parameters, as fully converged values could not be obtained with REFIT.

Table 5.12 – Resonance Parameters for ^{180}Hf

Ware	E_R (eV)		Ware	Γ_γ (meV)		Ware	Γ_n (meV)		Spin
	JEFF3.1	JEF2.2		JEFF3.1	JEF2.2		JEFF3.1	JEF2.2	
72.419 (0.0002)	72.4640 (0.0007)	72.33	45.778 (0.1274)	28.9 (0.2)	43.5	62.367 (0.070)	63.3 (0.2)	70	0.5
171.88 (0.001)	172.062 (0.003)	173.96	85.092 (0.249)	52 (2)	76	112.59 (0.203)	115 (2)	170	0.5
447.22 (0.003)	447	452.6	58.803 (0.604)	46	46	164.18 (1.156)	210	177	0.5
474.78 (0.004)	477	476	38.068 (0.635)	41	41	97.292 (1.161)	130	117	0.5
584.28 (0.007)	587	587	63.403 (1.406)	46	46	67.303 (1.590)	78	197	0.5
788.30 (0.006)	797	797	129.47 (1.483)	51	45	1626.3 (7.414)	1900	2000	0.5
909.40 (0.010)	913	913	51.556 (2.080)	42	42	56.118 (1.164)	65	124	0.5
-	-	1046	-	-	45	-	-	35	0.5
1178.9 (0.006)	1178	1178	57.5 [3.2]	51	54	680	680	680	0.5
1349.7 (0.012)	1359	1359	57.5 [3.2]	51	45	1150	1150	1150	0.5
1444.0 (0.008)	-	1505	57.5 [3.2]	-	45	99.965	-	42	0.5
-	-	1652	-	-	45	-	-	44	0.5
1799.4 (0.012)	1798	1798	57.5 [3.2]	51	45	273	273	273	0.5
1931.4 (0.012)	1931	1931	57.5 [3.2]	51	45	3700	3700	3700	0.5
2007.5 (0.016)	2025	2025	57.5 [3.2]	51	45	245	245	245	0.5
-	-	2152	-	-	45	-	-	140	0.5
2281.5 (0.022)	2280	2280	57.5 [3.2]	51	45	590	590	590	0.5
2404.4 (0.026)	2405	2405	57.5 [3.2]	51	45	1370	1370	1370	0.5
-	-	2539	-	-	45	-	-	150	0.5
2697.9 (0.032)	2700	2672	57.5 [3.2]	51	45	11.826	11.826	150	0.5
2731.5 (0.030)	2733	-	57.5 [3.2]	51	-	173.22	173.22	-	0.5

Ware	E _R (eV)		Ware	Γ _γ (meV)		Ware	Γ _n (meV)		Spin
	JEFF3.1	JEF2.2		JEFF3.1	JEF2.2		JEFF3.1	JEF2.2	
-	2782	-	-	51	-	-	1.545	-	1.5 ^p
2795.2 (0.038)	2794	2808	57.5 [3.2]	51	45	10.781	10.781	150	0.5
-	2851	-	-	51	-	-	4.282	-	1.5 ^p
2882.6 (0.035)	2884	-	57.5 [3.2]	51	-	153.80	153.80	-	0.5
-	2903	-	-	51	-	-	2.028	-	1.5 ^p
-	2981	2942	-	51	45	-	3.471	160	1.5 ^p
-	3042	-	-	51	-	-	2.082	-	1.5 ^p
3059	3059	3076	57.5 [3.2]	47.8	45	1290	1290	1270	0.5

The spin values in Table 5.12 marked “^p” indicate that the resonance was designated a p-wave resonance in the JEFF3.1 evaluated file. These p-wave resonances originate from the Beer and Macklin work [10, 11] and were not observable in the Geel measurement data, as discussed in Section 5.4.

6. DISCUSSION OF RESULTS

This chapter presents the findings of this project, including; general features of the new evaluated hafnium data, testing of the new data via resonance integrals and benchmark calculations, and suggested further work based on issues arising during the course of this work.

6.1 Construction of New Evaluated Files

Negative energy resonance parameters were also included in the provisional evaluated files. These parameters were derived by M. Moxon [70] from a survey of hafnium 2200 m/s (“thermal”) cross section measurements, and the contribution to the 2200 m/s cross section from the positive energy resonances, as described by the new parameters in Tables 5.7 - 5.12.

In order to conduct the testing and other work with the new hafnium resonance parameters, they were inserted, in ENDF6 format [30], into new, provisional, evaluated files. These files contained all elements of the JEFF3.1 hafnium evaluated files, with the exception of the header and resonance region information (Files 1 and 2). The new resolved resonance parameters replaced those of JEFF3.1 and the lower limit of the unresolved resonance region was raised accordingly. For the testing of the new resolved resonance data, the use of the JEFF3.1 unresolved resonance data was deemed valid, as the step-changes in the cross sections at the new RRR-URR boundaries were no more significant than the step-changes at the JEFF3.1 RRR-URR boundaries. The description of the URR for the hafnium isotopes is due to be revised by CEA Cadarache using the new resolved resonance parameters.

The complete evaluated files were passed through the ENDF Utility codes [72] to check for inconsistencies and formatting errors. Point-wise cross sections (PENDF) files were generated by R. Perry from the new resonance parameters using the NJOY processing code [23].

6.2 Observations from New Resolved Parameters

Capture yields calculated from the JEFF3.1 and new resonance parameters for the natural hafnium sample Geel measurements show a good agreement up to 200 eV (Figures A1 - A10), demonstrating that the RPI and Geel measurements are consistent. A notable exception to this is the identification of the small ^{179}Hf resonance at 6.67 eV, usually “hidden” by the larger 6.58 eV ^{177}Hf and revealed in the analysis of the ^{179}Hf -enriched sample. Above 200 eV (Figures A11 - A30), there is a noticeable systematic shift ($\sim 0.1\%$) in the energy scale of the two calculated capture yields. This arises from the JEFF3.1 files being constructed from the RPI parameters below 200 eV and the ENDF/B-VI.8 parameters above 200 eV. The neutron energy calibration of these two evaluations evidently differed slightly, thereby resulting in a step-change in the energy scale at 200 eV. The adjustment of the effective flight path lengths in this work (Section 5.2.1) resulted in the resonance energies being in good agreement with the RPI resonance energies.

Whilst the JEFF3.1 calculated capture yields for the natural hafnium samples generally agree with the new calculated yields (and the measured yields) to around 300 eV (allowing for the step-change in energy scale at 200 eV), there are greater differences in the calculated capture yields for the isotopically-enriched samples. As the RPI evaluation did not use any isotopically-enriched sample measurements above 10 eV, it is assumed that errors in the assignment of resonances to isotopes of the ENDF/B-VI.8 evaluation went undetected. As this work is the first to use measurements of samples enriched in different hafnium isotopes for

the 30 - 1000 eV for 35 years, the re-allocation of resonances below 200 eV (the limit of the RPI work) has shown around ten resonances to be associated with the wrong isotope (often a ^{179}Hf resonance assigned to ^{177}Hf) or completely absent from all previous evaluations. This trend of previously unassigned and incorrectly assigned resonances continued above 200 eV, increasing in frequency with increasing neutron energy.

The higher resolution of the new measurements above ~200 eV compared with previous experiments has allowed the tighter spaced resonances to be individually resolved. This is particularly the case for ^{177}Hf ; where many resonance peaks have now been treated as doublets (i.e. both resonances are in ^{177}Hf) in order to obtain a good fit to the measured data.

One effect of “missed” resonances, observed by Trbovich [12], is that the fit to the RPI data near 165 eV was not good due to the “complex set of three known resonances” and further commented that it was possible that there were one or more unidentified resonances in this region. The new isotopically-enriched sample measurements revealed a second ^{177}Hf resonance, which is masked by the ^{178}Hf resonance in natural hafnium sample measurements (see Figures A.9 and A.10). The addition of new resonances, such as the ^{177}Hf resonance at 165 eV, leads to changes in the parameters of nearby previously identified resonances.

Despite the “missed” resonances below 200 eV, the general agreement between the JEFF3.1 and current evaluations does provide some verification of the evaluation of the new measurements at Geel, as different evaluation routes have been used, one based on the REFIT code [21] and the other on the SAMMY code [73]. This agreement below 200 eV therefore helps to give confidence in the present evaluation of the RRR above 200 eV using the Geel measurements and REFIT code.

It is noted that some resonance parameters have large uncertainties associated with them or their values are significantly different to previous evaluations. This is a result of the calculated capture yields / transmissions being insensitive to the parameters of these resonances. This is particularly the case for some ^{174}Hf resonance parameters, where the resonances lie among resonances of the more abundant isotopes. The very low abundance of ^{174}Hf in the measured samples means that the structure of the measured data is governed by the resonances of the abundant isotopes and not the ^{174}Hf resonances. Hence, some of the new ^{174}Hf resonance parameter values are significantly different to the JEFF3.1 values.

It is noted that the values used for the nuclear radii of the six hafnium isotopes were those in the JEFF3.1 evaluation. The fit to the transmission measurement of the thick (16 mm) natural hafnium sample has shown that these values were acceptable.

Overall, the new evaluation extends the limits of the resolved resonance region for the six hafnium isotopes beyond those of the JEFF3.1 evaluation, and for all previous evaluations except in the case of the ^{180}Hf isotope. Tables 6.1 and 6.2 compare the energy limits and number of resonances in the resolved resonance region for each isotope in the JEFF3.1 and the new evaluations. The decision not to extend the resolved resonance energy limit of ^{180}Hf to that of the Beer and Macklin [10, 11] evaluation was discussed in Section 5.4. Hence, the total number of ^{180}Hf resonances in the new evaluation is fewer than that in the JEFF3.1 evaluation.

Table 6.1 - JEFF3.1 Resolved Resonance Regions for Hafnium Isotopes

Isotope	RRR lower (eV)	RRR upper (eV)	Highest resonance (eV)	URR upper (eV)	Negative energy resonances	Resonances in RRR	Resonances above RRR	Total resonances in file
¹⁷⁴ Hf	10 ⁻⁵	220	220	50000	2	10	0	12
¹⁷⁶ Hf	10 ⁻⁵	700	1000	50000	2	17	5	24
¹⁷⁷ Hf	10 ⁻⁵	250	700	50000	0	94	86	180
¹⁷⁸ Hf	10 ⁻⁵	1500	2090	50000	1	22	2	25
¹⁷⁹ Hf	10 ⁻⁵	250	1010	50000	2	48	33	83
¹⁸⁰ Hf	10 ⁻⁵	2500	11350	50000	2 (s)	14 (s)	74 (s)	90 (s)
					0 (p)	0 (p)	66 (p)	66 (p)
Total					9	205	200 (s) 66 (p)	414 (s) 66 (p)

Table 6.2 - New Resolved Resonance Regions for Hafnium Isotopes

Isotope	RRR lower (eV)	RRR upper (eV)	Highest resonance (eV)	URR upper (eV)	Negative energy resonances	Resonances in RRR	Resonances above RRR	Total resonances in file
¹⁷⁴ Hf	10 ⁻⁵	250	261	50000	2	12	1	15
¹⁷⁶ Hf	10 ⁻⁵	3000	3000	50000	2	72	0	74
¹⁷⁷ Hf	10 ⁻⁵	1000	999	50000	2	329	0	331
¹⁷⁸ Hf	10 ⁻⁵	3000	2962	50000	2	53	0	55
¹⁷⁹ Hf	10 ⁻⁵	1000	1000	50000	2	217	0	219
¹⁸⁰ Hf	10 ⁻⁵	3000	3059	50000	2 (s)	19 (s)	1 (s)	22 (s)
					12	702	2	716
Total					12	702	2	716

The new evaluation increases the number of identified resonances for all isotopes bar ¹⁸⁰Hf. In particular, the increase in the number of resonances and upper limit of the RRR for ¹⁷⁶Hf, ¹⁷⁷Hf and ¹⁷⁹Hf is significant. The numbers of observed resonances, in the JEFF3.1 and new evaluations, are compared to the theoretical number of resonances, based on published values of the average resonance spacing [32], in Figures 6.1 – 6.6. These figures also compare the observed reduced neutron widths (Γ_n^0) for both evaluations with the theoretical values, based on published strength function values and cumulative $g_I \Gamma_n^0$ values (see Section 2.4).

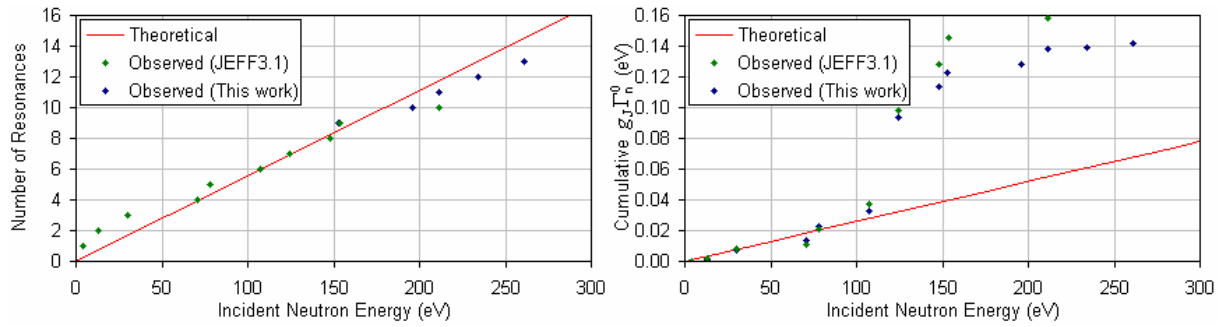


Figure 6.1 – Cumulative Number of Resonances and $g_J \Gamma_n^0$ Values for ^{174}Hf

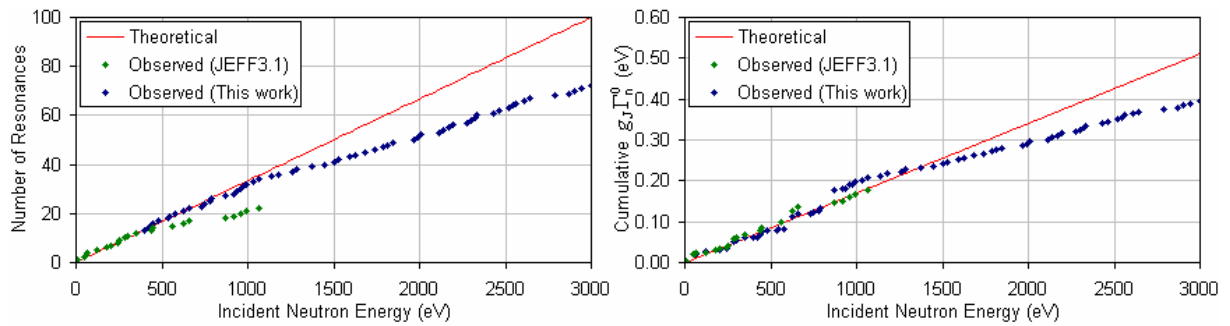


Figure 6.2 – Cumulative Number of Resonances and $g_J \Gamma_n^0$ Values for ^{176}Hf

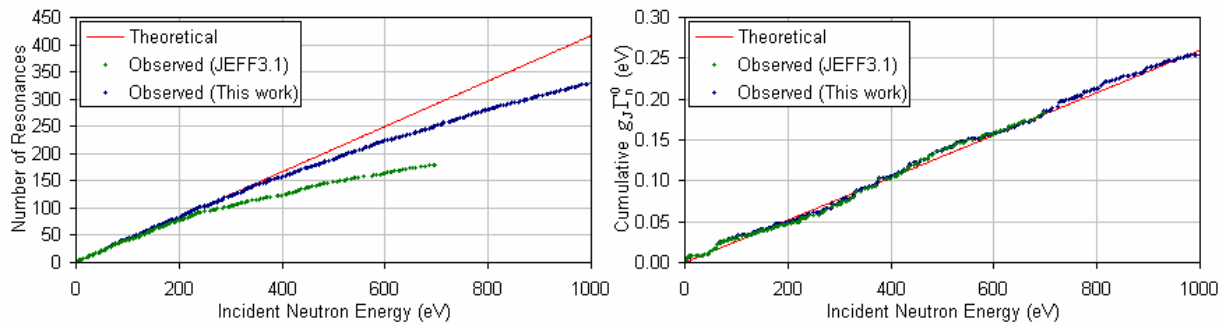


Figure 6.3 – Cumulative Number of Resonances and $g_J \Gamma_n^0$ Values for ^{177}Hf

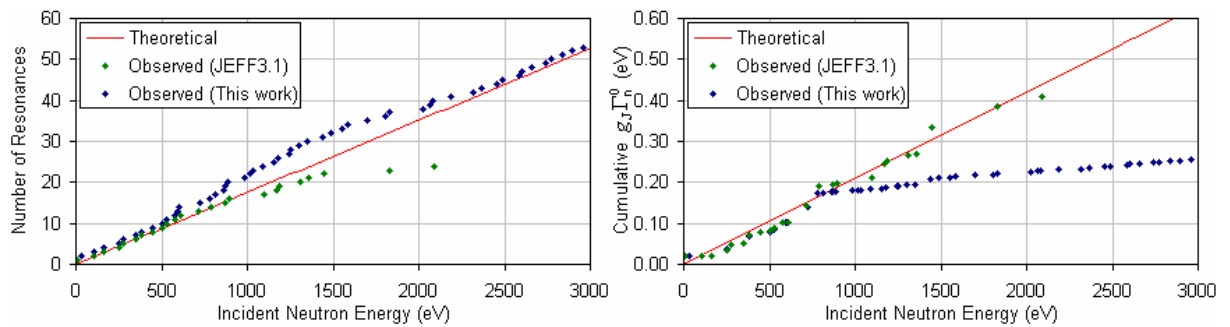


Figure 6.4 – Cumulative Number of Resonances and $g_J \Gamma_n^0$ Values for ^{178}Hf

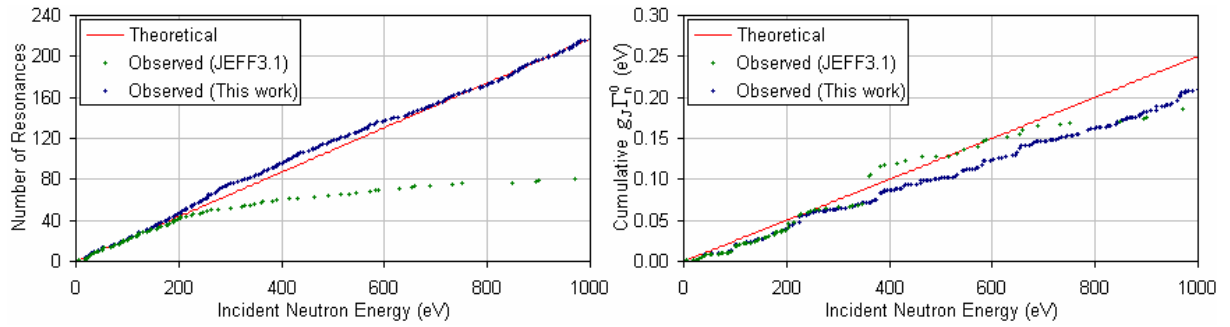


Figure 6.5 – Cumulative Number of Resonances and $g_J \Gamma_n^0$ Values for ^{179}Hf

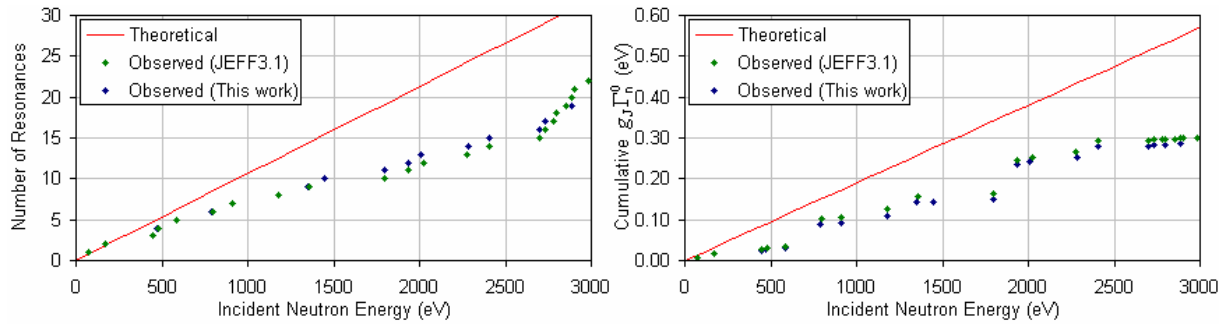


Figure 6.6 – Cumulative Number of Resonances and $g_J \Gamma_n^0$ Values for ^{180}Hf

Whilst the number of observed ^{174}Hf resonances is in good agreement with the theoretical, the fit to ^{174}Hf strength function deviates after the 107 eV resonance. This could be due to an over-wide Γ_n value for the 124 eV resonance. As this analysis could not determine reliable values for this resonance, the JEFF3.1 values were used. Using the JEF2.2 Γ_n value of 50 meV, rather than the JEFF3.1 Γ_n value of 680 meV, for this resonance would give better agreement between the theoretical and observed $g_J \Gamma_n^0$ cumulative value.

The number of ^{176}Hf resonances has been increased; however, the observed number drops away from the theoretical above ~1 keV. This may be due to smaller ^{176}Hf resonances being unobservable due to the relatively high concentration of ^{177}Hf in the ^{176}Hf -enriched sample. The ^{176}Hf Γ_n^0 values above 1 keV are consistent with one another but deviate from the theoretical. This could be due to the drop-off in observed resonance frequency or that the Γ_n^0

values were calculated from sub-keV observed Γ_n^0 values, rather than the published neutron strength function used to calculate the theoretical curve.

The number of observed ^{177}Hf has been greatly increased, though there still appears to be an increasing number of missing resonances at higher energies. This is due to the experimental resolution being insufficient to resolve ^{177}Hf resonance doublets at these energies.

The ^{178}Hf -enriched sample measurement enabled ^{178}Hf resonances to be identified up to 3 keV. However, accurate determination of the neutron widths for the resonances above 1 keV proved difficult due to the “noise” in the capture yield caused by unrecorded ^{177}Hf and ^{179}Hf resonances, as well as assuming a fixed average capture width for these resonances.

The number of observed ^{179}Hf resonances is much improved. This is partly due to reassigning ^{177}Hf resonances in the JEFF3.1 file to ^{179}Hf ; an outcome of using the isotopically-enriched samples. The ^{179}Hf Γ_n^0 values remain reasonably consistent.

Both the cumulative number of observed resonances and observed $g\Gamma_n^0$ values for ^{180}Hf are lower than the theoretical values defined by the average resonance spacing and neutron strength function given by Reference [32]. This is the case for both the JEFF3.1 and new evaluations. However, it is noted that the published average parameters for ^{180}Hf have large uncertainties associated with them.

The overall improved agreement between the new resolved resonance parameters and the published average parameters indicates that the consistency between the hafnium resolved and unresolved resonance cross sections will be improved. The analysis of the hafnium URR, soon to be finalised at CEA Cadarache, will consider the parameters derived from this work when adjusting the average parameters, to ensure the consistency between the two regions.

6.3 Testing

Resonance integrals (defined over the neutron energy range 0.5 eV to 100 keV) were calculated for the new evaluations for each isotope by C. Dean using the INTER code [72] and PENDF cross section files. The elemental resonance integral was calculated using the natural abundances of each isotope (Table 3.2). These resonance integrals are compared with those of previous evaluations in Table 6.3.

Table 6.3 - Hafnium Resonance Integrals

Evaluation	¹⁷⁴ Hf	¹⁷⁶ Hf	¹⁷⁷ Hf	¹⁷⁸ Hf	¹⁷⁹ Hf	¹⁸⁰ Hf	^{nat} Hf	Diff
This Work	451	633	7164	1798	530	37.2	1942	-
RPI	375±20	692±2	7196±8	1872±4	506±3	28.8±0.1	1965	1.2%
JEFF-3.1	441	694	7210	1871	508	29.6	1968	1.3%
ENDFB-VII.0	355	400	7214	1915	548	34.3	1973	1.6%
Mug 2005	307±15	708±15	7200±200	1882±20	620±30	33±1	1986	2.3%
JEF-2.2	320	613	7235	1923	543	35.4	1990	2.5%
JENDL-3.3	362	893	7209	1914	522	33.9	1993	2.6%
JEFF-3.0	362	893	7209	1914	522	33.9	1993	2.6%
Mug 1984	436±35	880±40	7173±200	1950±120	630±30	35±1	2011	3.6%

Testing by D. Hanlon, R. Hiles and R. Perry [74] used a simplified model of a theoretical reactor core, consisting of 17 “slabs” of material representing a hafnium control rod, enriched uranium fuel, light water moderator and boron-based poison in a zirconium matrix. This theoretical core model has similar characteristics to real-world reactor cores. Cases were run using the deterministic WIMS code [75] and the Monte-Carlo MONK code [76], using application libraries updated by R. Perry. The tests, designed to compare the JEFF3.1 and new evaluated hafnium files, re-enforce the conclusions by Perry [20], Wilson [77] and the author that using the unresolved resonance treatments in these codes, outside of their validated range, leads to a difference in the k-effective values produced by each code for the same 17-region slab model. Increasing the upper limit of the resolved resonance region to higher energies and

the corresponding addition of resolved resonances in the evaluated files (and therefore application libraries) leads to a convergence of the results gained from the WIMS and MONK methods.

Further testing of the new evaluated files by Hanlon, Hiles and Perry [74] compared experimental and MONK-calculated k-effective values for suitable real-world zero-power reactor core assemblies. The two assemblies consisted of hafnium blocks, of different size, surrounded by enriched uranium fuel. As these were critical assemblies, the measured k-effective values are 1.0000. The MONK-calculated k-effective values are given in Table 6.4.

Table 6.4 – Calculated k-effectives for Test Cores

Test Case	Calculated k-effective		Difference (pcm)
	JEFF3.1 Hf Data	New Hf Data	
“Core 1”	1.0011 ± 0.0002	1.0001 ± 0.0002	-100 ± 28
“Core 2”	1.0026 ± 0.0002	1.0010 ± 0.0002	-160 ± 28

Whilst the calculated k-effective values for both evaluations slightly overestimate the experimental values, there is improved agreement with measured values when using the new RRR data compared with the JEFF3.1 data. It is noted that the new evaluation gives lower k-effectives than the JEFF3.1 evaluation, indicating more neutron capture is modelled when using the new evaluation.

Furthermore, use of the new hafnium data for these models shows improved agreement between WIMS and MONK k-effective values and improved calculation to experiment ratios. The apparent increase in neutron capture appears to contradict the requirement based on CEA experimental results [16, 17] that the natural hafnium capture cross section should be decreased. It therefore appears that the relative change in the hafnium cross section between

evaluations is dependent on the reactor system modelled and the neutron spectra of the system. It is noted that the details of reactor configurations used in the CEA experiments are unknown.

The dependency of the neutron capture on the neutron spectra is reinforced by a) considering the resonance integrals and b) configuration changes in the 17-region slab model described above. Whilst the resonance integral, which in the case of hafnium has decreased by ~1.2% for the new evaluation relative to the JEFF3.1 evaluation, gives a theoretical indication of the total neutron capture in a given material, it is believed that this indicator is only reliable when the material in question is present in small quantities, i.e. it is an impurity or dilute poison. However, when the material is present in large quantities, such as hafnium (being the major component of a control rod), it is conceivable that the neutron spectrum “blacks out” at large resonances. Therefore, the total neutron capture is no longer proportional to the resonance integral. The effect of a change in neutron spectrum was demonstrated in the testing on the 17-region slab model by replacement of the boron-containing “poison” slab with zirconium [74]. The resulting difference in the k-effective of these two configurations was due to the boron absorbing a large amount of the lower energy neutrons, thereby making the k-effective value more sensitive to the hafnium cross section at higher energies.

6.4 Suggestions for Further Work

During the course of this work, several issues have emerged which merit further investigation that may lead to further improvements the evaluation of hafnium cross sections as well as resonance analysis methods and reactor physics methods in general.

The results of this work could be extended through further high resolution capture and transmission measurements of natural and isotopically-enriched hafnium samples, to include samples enriched in ^{180}Hf and, if possible, ^{174}Hf . These measurements would allow:

- confirmation of the new resonance allocation and identification of more ^{177}Hf resonances by resolving ^{177}Hf resonance doublets above ~ 400 eV
- improvement in the accuracy of all resonance width values in the 500 - 1000 eV range
- further extension of resolved resonance analysis above 1000 keV for ^{177}Hf and ^{179}Hf
- verification or dismissal of the Beer and Macklin resonance parameters
- determination of individual Γ_γ values for ^{177}Hf and ^{179}Hf resonances, which could provide evidence of a possible spin-dependence of the ^{177}Hf and ^{179}Hf average Γ_γ values
- accurate parameters to be determined for the ^{174}Hf resonances using a ^{174}Hf -enriched sample, which are difficult to achieve using natural hafnium samples.

However, the availability of facilities to perform measurements at these neutron energies and sufficient resolution may be a limiting factor as the longer neutron flight paths required for such resolution suffer from a loss of flux intensity. Therefore, a stronger neutron source may

be required to ensure a sufficiently high number of neutrons reach the sample/detector to enable good statistics on the measurements.

Further measurements of hafnium nuclear properties could include high-resolution γ -ray spectroscopy (using high-purity germanium detectors) up to 1 keV in order to determine the spins of resonances in ^{177}Hf and ^{179}Hf , through the identification of characteristic γ -rays from neutron capture to each spin state. Measurement of solid state effects with hafnium metal and hafnium oxide sample would enable phonon spectra (the vibration modes of the atomic lattice) to be produced, to be used for more accurate modelling of Doppler broadening effects (including improved measurements of hafnium Debye temperatures). Chemical analysis would enable an independent determination of the isotopic content of the samples to be used for the cross section measurements.

The effects of absorption of γ -rays (from capture events) within hafnium samples could be included in the analysis. This would require the modelling of each sample and detector configuration used in the measurements, using a Monte Carlo code such as MCNP [54].

Further evaluation of the hafnium resonances could also focus more on the sensitivity of the calculated capture yields, and therefore natural hafnium cross sections, to the parameters of minor isotopes and resonances. This study could include the sensitivity to “global” parameters including nuclear radii and average neutron capture widths of the isotopes.

There is a large scope for further developments to the REFIT code, including the inclusion of uncertainties on experimental parameters, such as flight path length, sample composition and neutron source properties, when calculating the uncertainties on resonance parameters. In addition to the propagation of uncertainties, the production of covariances in ENDF6 format could be developed. As REFIT has several models to account for the effects of Doppler

broadening and the multiple scattering of neutrons, a study of the accuracy of each model would enable the user to select a model based on desired accuracy and computation run time.

There are clear differences in the k-effective values produced by different reactor physics codes (namely WIMS and MONK) for the same reactor models and this difference is attributed to differences in the treatment of the unresolved resonance region, when applied to hafnium resonances below a few keV. Therefore, continuation of the investigation to understand the root cause of these differences may improve the treatment of the unresolved resonances of some other nuclides.

7. CONCLUSIONS

This thesis presents work that improves the neutron cross section data for the six natural hafnium isotopes, a need of the NEA High Priority Request List for nuclear data [19]. Cross section measurements were performed at the IRMM Geel GELINA time-of-flight facility. Capture experiments were conducted on the ~12 m, ~28 m and ~58 m flight paths using C_6D_6 detectors and transmission experiments were performed at flight paths of ~26 m and ~49 m using a 6Li glass detector. The samples used in these measurements were metallic natural hafnium foils and discs, of various thicknesses, and hafnium oxide powders, with differing isotopic enrichments, in aluminium cans.

As the resolved resonance regions of the six isotopes overlap, the measurements of the isotopically-enriched samples, containing higher than natural concentrations of ^{176}Hf , ^{177}Hf , ^{178}Hf or ^{179}Hf , were required to allocate each resonance to the correct isotope. Many (~350) resonances were identified that were not recorded in any previous hafnium cross section evaluation. Additionally, some previously recorded resonances were found not to have been allocated to the correct isotope in earlier evaluations.

The measurement data has been analysed using the R-matrix least square fitting code REFIT [21]. The parameters derived during the analysis describe the resolved resonances of the isotopes ^{174}Hf , ^{176}Hf , ^{177}Hf , ^{178}Hf , ^{179}Hf and ^{180}Hf and the upper energy limits of the resolved resonance regions for these isotopes have been increased (relative to the JEFF3.1 evaluation) to 250 eV, 3 keV, 1 keV, 3 keV, 1 keV and 3 keV respectively.

The resonance integral of natural hafnium, calculated from the new resonance parameters, is 1942 b, ~1.2% lower than the integral corresponding to the JEFF3.1 parameters. However,

calculated k-effectives for appropriate reactor core models are lower for the new hafnium data than the JEFF3.1 hafnium data, indicating that more neutron capture is modelled. The k-effective values calculated using the new data have better agreement with measured k-effectives for the zero-power reactor assemblies in the test cases used, compared with those obtained with JEFF3.1 data. The “conflict” between the lower resonance integral and higher neutron capture suggests that the neutron capture is not only dependent on the effective cross section but also on the neutron spectrum in the modelled reactor assembly.

REFERENCES

- [1] Westing House Nuclear; www.westinghousenuclear.com: retrieved 09/12/08
- [2] K. Kenji, I. Tomohiko, T. Takayuki, Y. Michio, K. Ken, I. Kunihiro, “Development of Advanced Control Rod of Hafnium Hydride for Fast Reactors”, Proc. ICAPP’06, 2006
- [3] K. Tuček, M. Jolkkonen, J. Wallenius, W. Gudowski, “Studies of an accelerator-driven transuranium burner with hafnium-based inert matrix fuel”, Nuclear technology, 157 (2007) 277-298
- [4] S. Anghaie, “Generation IV Roadmap: Description of Candidate Nonclassical Reactor Systems Report”, 2002, <http://gif.inel.gov>: retrieved 05/12/08
- [5] G. Rohr, H. Weigmann, “Short range energy dependence of the neutron widths of ^{177}Hf resonances”, Nuclear Physics, Section A, 264 (1976) 93-104
- [6] T. Fuketa, J.A. Harvey, “Level spacings and s-wave neutron strength functions of the isotopes of hafnium”, ORNL report ORNL-3778, 1965.
- [7] T. Fuketa, “Analysis of total neutron cross section data for the hafnium isotopes”, RPI report RPI-328-68, 1966
- [8] M.C. Moxon, D.A.J. Endacott, T.J. Haste, J.E. Jolly, J.E. Lynn, M.G. Sowerby, “Differential neutron cross-sections of natural hafnium and its isotopes for neutron energies up to 30 eV”, Harwell report AERE R7864, 1974
- [9] H.I. Liou, J. Rainwater, G. Hacken, U.N. Singh, “Neutron resonance spectroscopy: ^{177}Hf ”, Physical Review C, 11 (1975) 2022-2026
- [10] H. Beer, R.L. Macklin, “ $^{178,179,180}\text{Hf}$ and ^{180}Ta (n,g) cross sections and their contribution to stellar nucleosynthesis”, Physical Review C, 26 (1982) 1404-1416
- [11] H. Beer, G. Walter, R.L. Macklin, P.J. Patchett, “Neutron capture cross sections and solar abundances of $^{160,161}\text{Dy}$, $^{170,171}\text{Yb}$, $^{175,176}\text{Lu}$, and $^{176,177}\text{Hf}$ for the s-process analysis of the radionuclide ^{176}Lu ”, Physical Review C, 30 (1984) 464-478
- [12] M.J. Trbovich, “Hafnium neutron cross sections and resonance analysis”, PhD Thesis, RPI, 2003
- [13] M.J. Trbovich, “Hafnium resonance parameter analysis using neutron capture and transmission experiments”, Int. Conf. on Nuclear Data for Science and Technology, Santa Fe, New Mexico, 2004
- [14] The JEFF Nuclear Data Project: <http://www.nea.fr/html/dbdata/JEFF>
- [15] G. Noguère, A. Courcelle, J. Palau, P. Siegler, “Low neutron energy cross sections of the hafnium isotopes”, in, OECD/NEA JEF/DOC-1077, 2005
- [16] J.M. Palau, “Corrélations entre données nucléaires et expériences intégrales à plaques: le cas du hafnium”, CEA Report CEA-R-5843, 1999
- [17] A. Santamarina, “Rapport de qualification R1 du produit APOLLO2.5/CEA93.V6”, CEA Report CEA-SPRC/LEPh/02-003, 2002

- [18] G. Noguère, A. Courcelle, P. Siegler, J. Palau, O. Litaize, “Revision of the resolved resonance range of the hafnium isotopes for JEFF-3.1”, CEA/Cadarache Technical Note, NT-SPRC/LEPh-05/201, 2005
- [19] The NEA Nuclear Data High Priority Request List: <http://www.nea.fr/html/dbdata/hprl/index.html> retrieved 03/10/09
- [20] R.J. Perry, J.G. Hosking, C.J. Dean, R.P. Hiles, “Tested JEFF3.1 Nuclear Data Libraries”, SERCO/TAS/000334.04/001, 2008
- [21] M.C. Moxon, T.C. Ware, C.J. Dean, “REFIT-2009: Users' guide”, UKNSF(2010)P243, 2010
- [22] J.E. Lynn, “The theory of neutron resonance reactions”, Clarendon Press, 1968
- [23] R.E. MacFarlane, D.W. Muir, “The NJOY nuclear data processing system, version 91”, LA-12740, Los Alamos National Laboratory, 1994
- [24] A. Nouri, “JANIS: A New Java Based Nuclear Data Display Program”, Nuclear Energy Agency, 2001
- [25] G. Breit, E. Wigner, “Capture of slow neutrons”, Physical Review, 49 (1936) 519-531
- [26] A.M. Lane, R.G. Thomas, “R-matrix theory of nuclear reactions”, Reviews of Modern Physics, 30 (1958) 257-353
- [27] C.W. Reich, M.S. Moore, “Multilevel formula for the fission process”, Physical Review, 111 (1958) 929-933
- [28] F.H. Fröhner, “Evaluation and analysis of nuclear resonance data: JEFF Report 18”, Nuclear Energy Agency, 2000
- [29] C.E. Porter, R.G. Thomas, “Fluctuations of nuclear reaction widths”, Physical Review, 104 (1956) 483-491
- [30] M. Herman, A. Trkov, “ENDF-6 Formats Manual”, National Nuclear Data Centre, BNL, Upton, New York, 2005
- [31] ENDF/B Evaluated Nuclear Data Library: <http://www.nndc.bnl.gov/exfor/endl00.jsp>
- [32] T. Belgia, O. Bersillon, R. Capote Noy, T. Fukahori, G. Zhigang, S. Goriely, M. Herman, A.V. Ignatyuk, S. Kailas, A.J. Koning, P. Oblozinsky, V. Plujko, P.G. Young, “Handbook for calculations of nuclear reaction data, RIPL-2 (Reference Input Parameter Library-2)”, IAEA-TECDOC-1506, 2006
- [33] A. Borella, G. Aerts, F. Gunsing, M. Moxon, P. Schillebeeckx, R. Wynants, “The use of C₆D₆ detectors for neutron induced capture cross-section measurements in the resonance region”, Nuclear Inst. and Methods in Physics Research, A, 577 (2007) 626-640
- [34] D.B. Syme, Nucl. Instrum. Methods, 198 (1982) 357-364
- [35] The NUDAME Project: <http://irmm.jrc.ec.europa.eu/html/nudame/index.htm>
- [36] C. Dean, “Capture cross section measurements of isotopic enriched Hf samples”, NUDAME proposal PAC3/1, 2006
- [37] G. Noguère, “High-Resolution Capture and Transmission Measurements of the Natural Hafnium”, NUDAME proposal PAC1/1, 2005

- [38] The EUFRAT Project: <http://irmm.jrc.ec.europa.eu/html/activities/eufrat/index.htm>
- [39] T.C. Ware, "Total cross section measurements of natural hafnium samples", EUFRAT proposal PAC1/1, 2008
- [40] M. Flaska, A. Borella, D. Lathouwers, L.C. Mihailescu, W. Mondelaers, A.J.M. Plompen, H. van Dam, T.H.J.J. Hagen, "Modelling of the GELINA neutron target using coupled electron-photon-neutron transport with MCNP4C3 code", Nuc. Instr. and Methods A, 53 (2004)
- [41] D. Tronc, J.M. Salome, K.H. Böckhoff, "New pulse compression system for intense relativistic electron beams", Name: Nucl. Instrum. Methods Phys. Res., Sect. A, (1985)
- [42] J. Salome, "Neutron producing targets at GELINA", Nuclear Instruments and Methods, 179 (1981) 13-19
- [43] A. Borella, "Determination of the neutron resonance parameters for ^{206}Pb and of the thermal neutron capture cross section for ^{206}Pb and ^{209}Bi ", PhD Thesis, Univ. Gent, 2005
- [44] J. Heyse, W. Mondelaers, P. Schillebeeckx, "High Resolution Neutron Cross Section Measurements by Time-of-Flight", EC-JRC-IRMM, 2005
- [45] S. de Jonge, "Fast Time Digitizer Type 8514 A", IRMM Report GE/DE/R/24/87, 1987
- [46] J. Gonzalez, "Modular Multi-Parameter Multiplexer (MMPM) hardware description and user guide", IRMM Report GE/R/INF/06/97, 1997
- [47] N. Janeva, Private Communication, 2007
- [48] J.K. Tuli, "Nuclear Wallet Cards", Brookhaven National Laboratory, Upton, NY, 2005
- [49] A. Moens, Private Communication, 2008
- [50] A.H. Wapstra, G. Audi, C. Thibault, "The AME2003 atomic mass evaluation (I). Evaluation of input data, adjustment procedures", Nuclear Physics, Section A, 729 (2003) 129-336
- [51] Goodfellow Product Catalogue: www.goodfellow.com
- [52] A. Borella, "AGL2 - User manual", IRMM internal report, 2007
- [53] P. Schillebeeckx, Private Communication, 2008
- [54] J. Briesmeister, "MCNP – A General Monte Carlo N-Particle Transport Code – Version 4C2" Los Alamos National Laboratory, Los Alamos, NM, USA, 2000
- [55] C. Bastian, "AGS, a set of UNIX commands for neutron data reduction", Int. Conf. Neutrons in Research and Industry, Crete, Greece, 1996
- [56] C. Bastian, "AGS Commands", IRMM internal report, 2007
- [57] P. Siegler, K. Dietze, P. Ribon, "Testing of neutron data by comparison of measured and calculated average transmissions", Int. Conf. on Nuclear Data for Science and Technology, Tsukuba, Japan, 2001
- [58] "Harwell Subroutine Library", Harwell Report AERE-R-9185, 1985
- [59] M.C. Moxon, J.B. Brisland, "REFIT, A least square fitting program for resonance analysis of neutron transmission and capture data", Report AEA-InTec-0470, 1991

- [60] M.C. Moxon, T.C. Ware, C.J. Dean, "REFIT-2007: Users' guide", UKNSF(2007)P216, 2007
- [61] NEA Data Bank Computer Program Services: <http://www.nea.fr/dbprog/>
- [62] S. Kopecky, Private Communication, 2009
- [63] Neutron Resonance Analysis Summer School, IRMM Geel, 2008: http://irfu.cea.fr/Sphn/NRA_school_2008/
- [64] H.A. Bethe, Nuclear Physics B. Nuclear Dynamics, Theoretical, Rev. Mod. Phys. 9 (1937)
- [65] W.E. Lamb, "Capture of neutrons by atoms in a crystal", Phys Rev, 55 (1939).
- [66] G. Noguere, E. Rich, C. De Saint Jean, O. Litaize, P. Siegler, V. Avrigeanu, "Average neutron parameters for hafnium", Nuclear Physics, Section A, (2009)
- [67] S.F. Mughabghab, "Atlas of Neutron Resonances: Resonance Parameters and Thermal Cross Sections: Z= 1-100", Elsevier Science & Technology, 2006
- [68] S.A. Karamian, J.J. Carroll, J. Adam, E.N. Kulagin, E.P. Shabalin, "Production of long-lived hafnium isomers in reactor irradiations", High Energy Density Physics, 2 (2006) 48-56
- [69] S.F. Mughabghab, M. Divadeenam, N.E. Holden, "Neutron Resonance Parameters and Thermal Cross Sections: Z= 61-100", Academic Press, 1984
- [70] M.C. Moxon, Private Communication
- [71] M.C. Moxon, "Analysis of the 8eV Doublet in Hf", OECD/NEA JEF/DOC-1313, 2009
- [72] C.L. Dunford, "ENDF Utility Codes Release 7.01/02", Los Alamos National Laboratory, Los Alamos, NM, USA, 2005
- [73] N.M. Larson, "Updated Users Guide for SAMMY: Multilevel R-Matrix fits to Neutron Data Using Bayes' Equations", ORNL/TM-9179/R5, Oak Ridge National Laboratory, 2000.
- [74] R.P. Hiles, T.C. Ware, M.C. Moxon, C.J. Dean, "New Hf Nuclear data Evaluation for the Resolved Reference Range", Serco/TS/000334.12/002, 2010
- [75] T.D. Newton, "Developments within WIMS10", International Conference on the Physics of Reactors, Interlaken, Switzerland, 2008
- [76] M.J. Armishaw, A.J. Cooper, "Current Status and Future Direction of the MONK Software Package", Int. Conf. on Nuclear Criticality Safety, St. Petersburg, 2007
- [77] S.A. Wilson, "Investigation of Hafnium Nuclear Data in the MONK and ECCO Criticality Codes", MSc Thesis, University of Birmingham, 2008
- [78] N.M. Wolcott, Proceedings of the conference de physique des basses temperature, Paris, 1955, pp. 286
- [79] G.D. Kneip, J.O. Betterton, J.O. Scarbrough, "Low-Temperature Specific Heats of Titanium, Zirconium, and Hafnium", Physical Review, 130 (1963) 1687
- [80] J.O. Betterton, J.O. Scarbrough, "Low-Temperature Specific Heats of Zr-Ti, Zr-Hf, and Zr-Sc Alloys", Physical Review, 168 (1968) 715-725

- [81] H.X. Gao, L.M. Peng, “Parameterization of the temperature dependence of the Debye-Waller factors”, *Acta Crystallographica Section A: Foundations of Crystallography*, 55 (1999) 926-932
- [82] S.A. Ostanin, V.Y. Trubitsin, “Calculation of the P-T phase diagram of hafnium, *Computational Materials Science*”, 17 (2000) 174-177
- [83] I.D. Feranchuk, A.A. Minkevich, A.P. Ulyanenko, “About non-Gaussian behaviour of the Debye-Waller factor at large scattering vectors”, *Eur. Phys. J. Appl. Phys*, 24 (2003) 21-26

APPENDIX A – SUBSIDIARY DATA ANALYSIS

A.1 Calculation of the Debye Temperature of Hafnium Samples

A survey of hafnium Debye temperature measurements by G. Noguère [66] gave seven measurements from different sources, which are presented in Table A.1. Noguère gave a weighted average and standard deviation calculated from these measurements. The weighted average was recalculated and is given in Table A.2. Four measurements (marked “*”) did not quote an uncertainty. These were assigned an uncertainty of 1 K for purpose of the recalculation.

Table A.1 – Measurements of Debye Temperature for a Mono-Atomic Hafnium Crystal

Author	Year	Reference	Debye Temp. (K)	Uncertainty (K)
Wolcott*	1955	[78]	261	(1)
Kneip	1963	[79]	252.3	0.9
Betterton	1968	[80]	251.5	1.2
Gao*	1999	[81]	252	1
Ostanin*	2000	[82]	250	(1)
Feranchuk*	2002	[83]	215	(1)
			280	(1)

* Uncertainty not quoted; assumed to be 1 K

Table A.2 – Averages of Debye Temperatures of Hafnium

	All values	excl *
Unweighted Average	251.93	251.69
Weighted Average	252.01	251.71 [#]
Standard Deviation	0.48	19.31 [#]
Uncertainty	0.58	0.38

[#] Agrees with values calculated by Noguère [66]

Based on this survey, a value of 252 K was used as the Debye temperature for all hafnium samples in this work.

A.2 Transmission and Capture Yield Data

This section presents figures comparing measured transmissions and capture yields used in the resonance analysis with the transmissions and yields calculated from the parameters in the new evaluation and those in the JEFF3.1 evaluation.

Whilst several measurements were used to analyse each neutron energy region, only the most pertinent measurement data for each region are shown, for the purpose of clarity and brevity. The neutron capture yield/transmission axes use a linear scale, to emphasize the importance of the fit to the larger resonances and to suppress the appearance of experimental noise at low values; again for the purpose of clarity.

Above 200 eV, the JEFF3.1 parameters were taken from the ENDF/B-VI.8 library, which was derived using the MLBW formalism. However, all the cross sections for these plots have been reconstructed using REFIT, which uses the Reich Moore formalism (see Section 2.2). There is a systematic shift in the energy scale between the RPI parameters and the ENDF/B-VI.8 parameters. Therefore, all the “JEFF3.1” calculated curves have been scaled by a factor of 1.0009 in energy to realign the resonances. This also improves the clarity of the figures.

At the 8 eV resonance doublet (Figure A.2), it is noted that the calculation clearly does not reproduce the measurement. This is due to the large multiple scattering effects in this region that are not correctly model using the simpler (and faster) multiple scattering correction in REFIT, which was used to generate these plots. This discrepancy reinforces earlier discussion that the hafnium oxide samples used are too thick to resolve the doublet; the apparent double peak is a result of the multiple scattering, it is not a direct result of a resonance doublet in the cross section.

Figure A.1 – Hafnium Transmission Data and Calculations (0.5 – 20 eV)

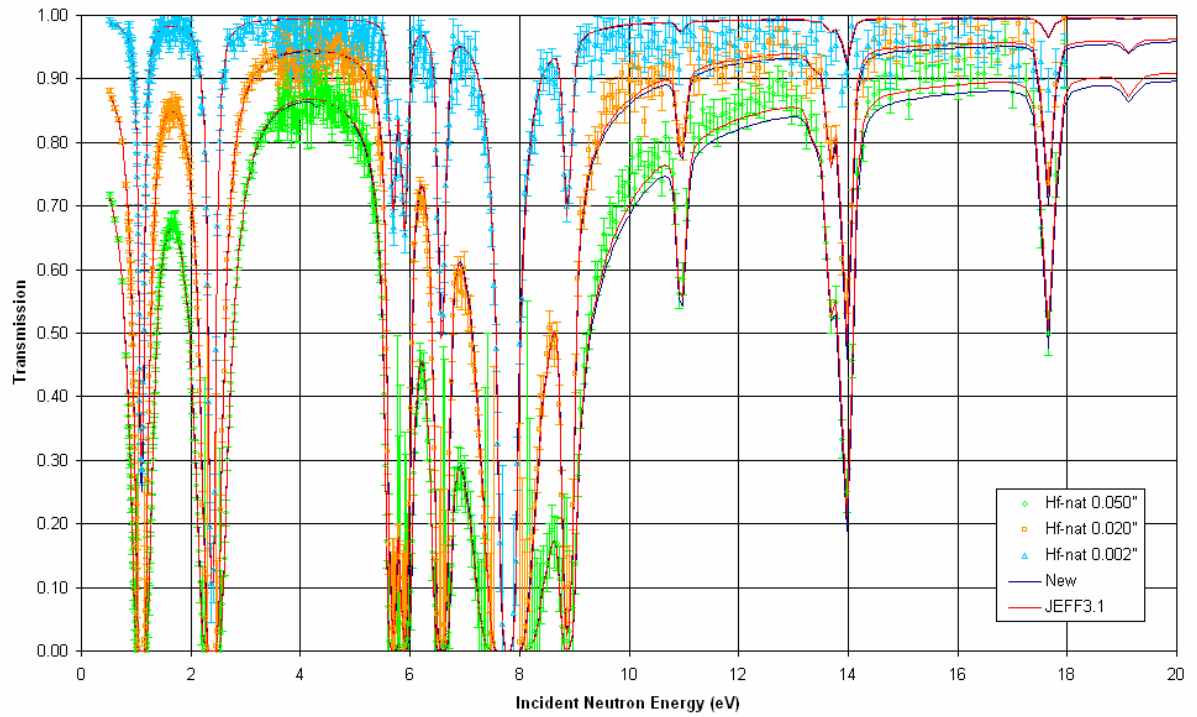


Figure A.2 – Hafnium Capture Data and Calculations (0.5 – 20 eV)

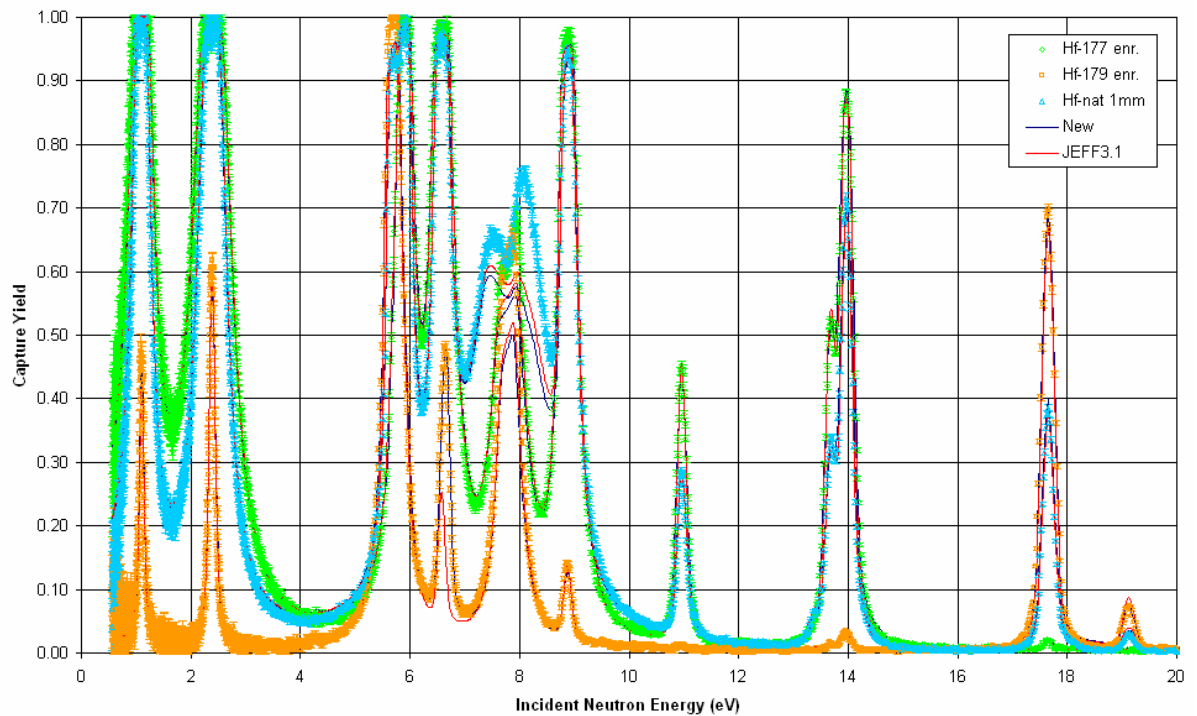


Figure A.3 – Hafnium Transmission Data and Calculations (20 – 50 eV)

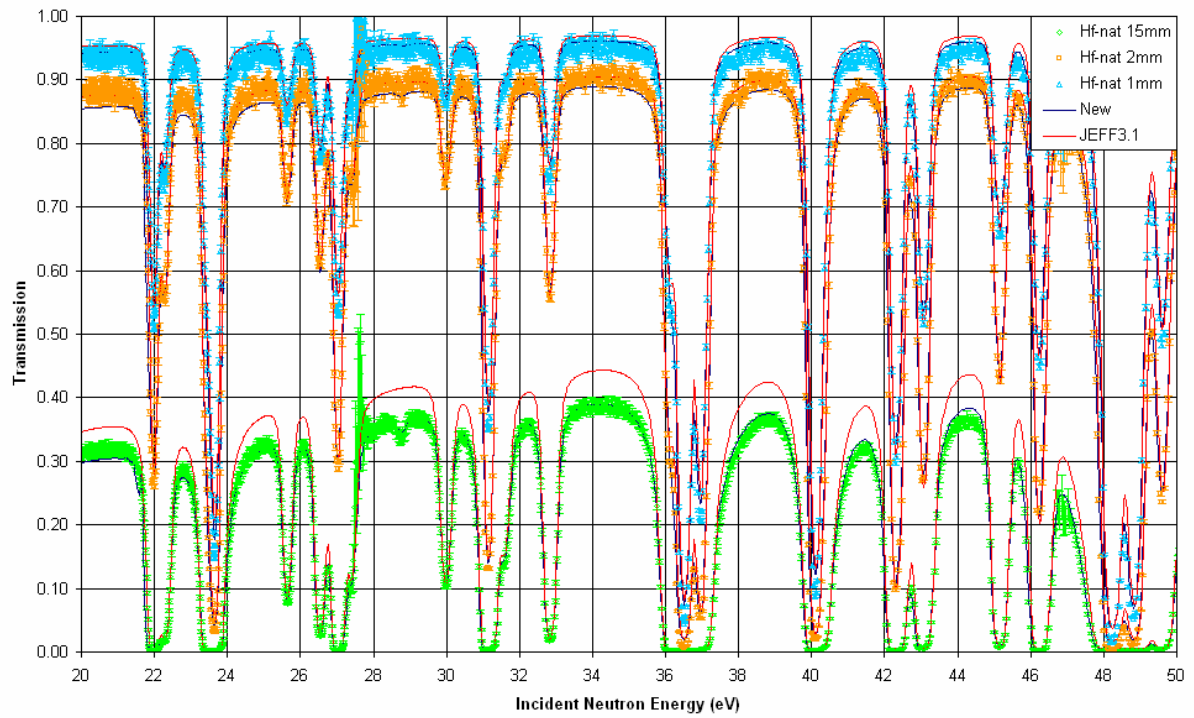


Figure A.4 – Hafnium Capture Data and Calculations (20 – 50 eV)

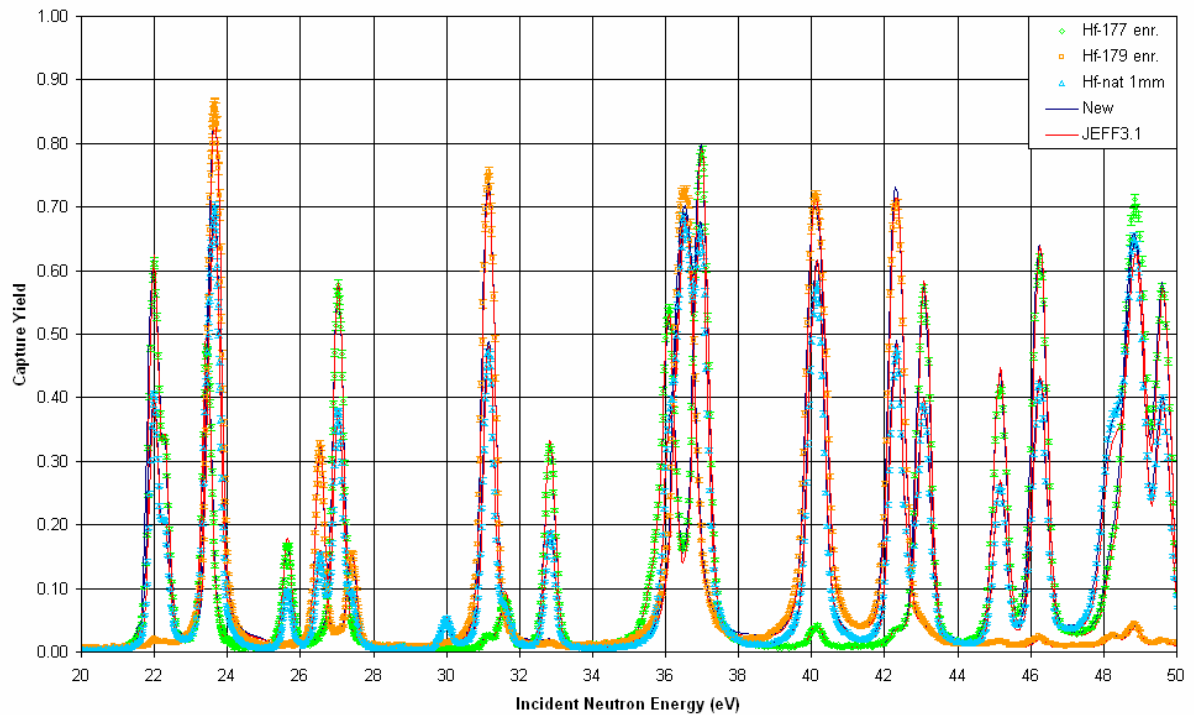


Figure A.5 – Hafnium Transmission Data and Calculations (50 – 100 eV)

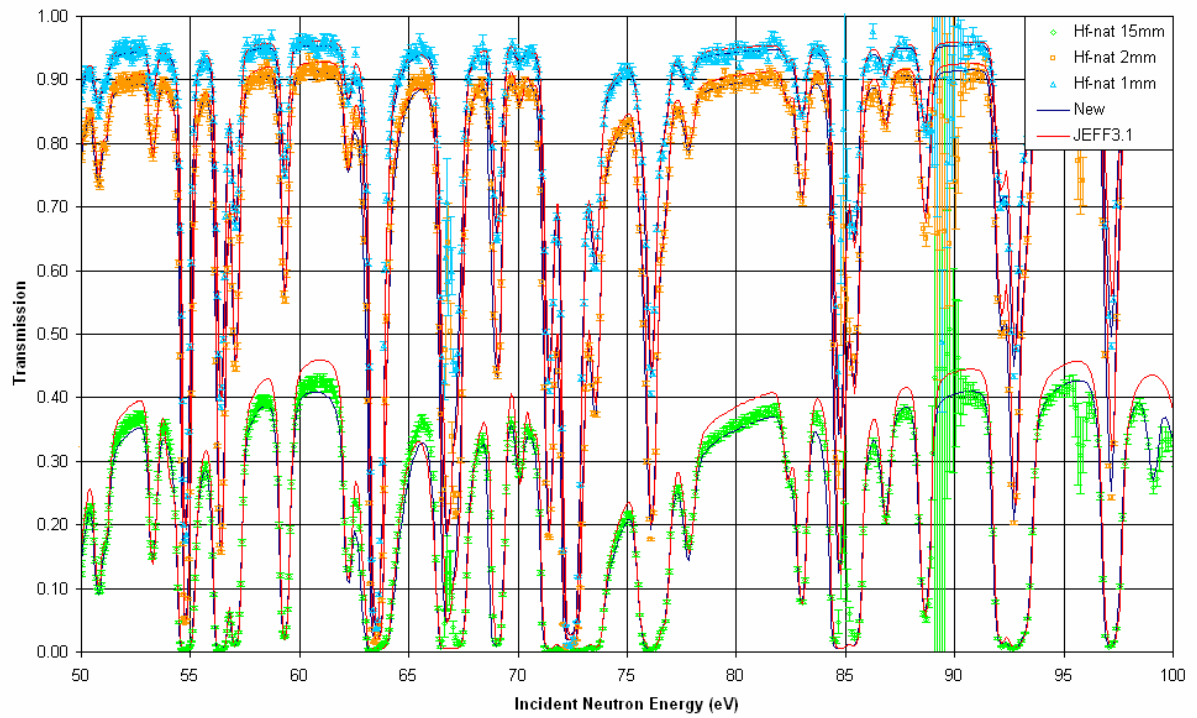


Figure A.6 – Hafnium Capture Data and Calculations (50 – 100 eV)

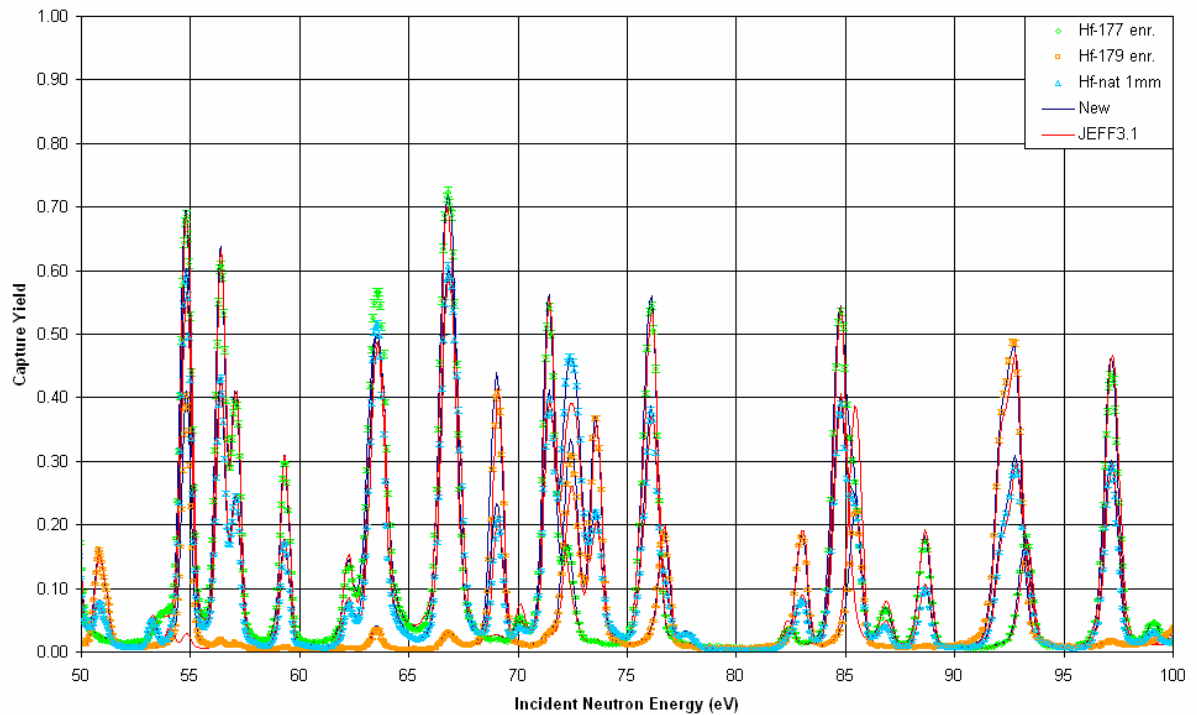


Figure A.7 – Hafnium Transmission Data and Calculations (100 – 150 eV)

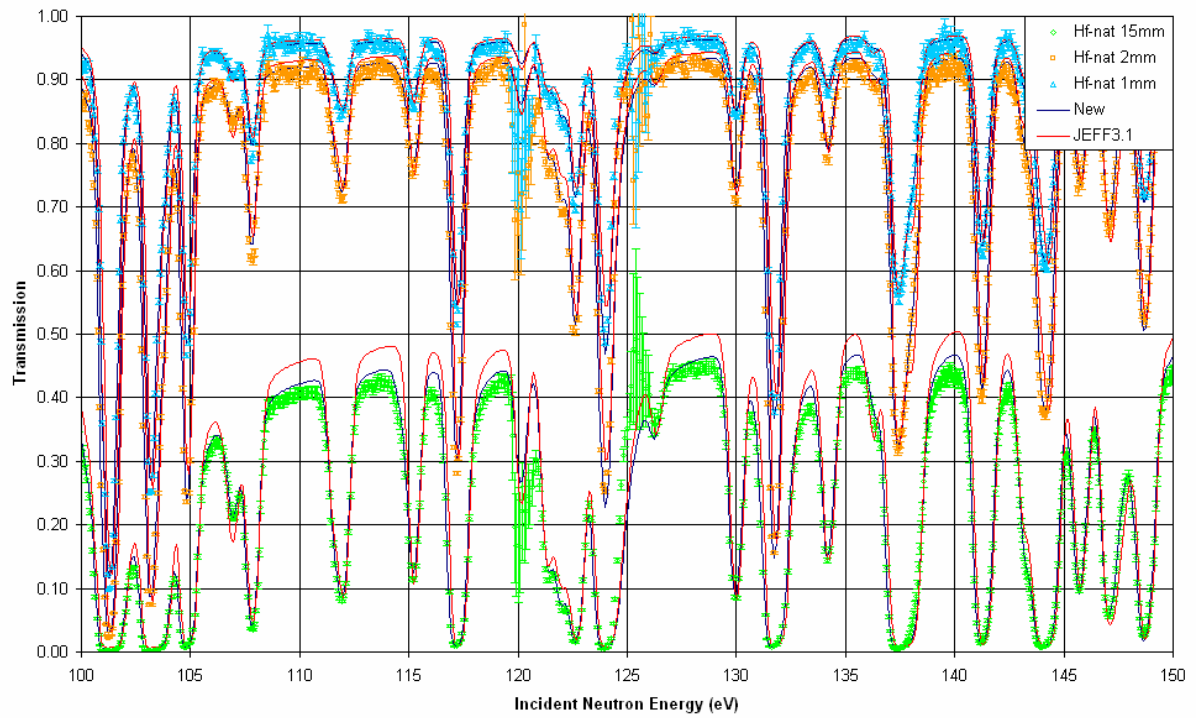


Figure A8 – Hafnium Capture Data and Calculations (100 – 150 eV)

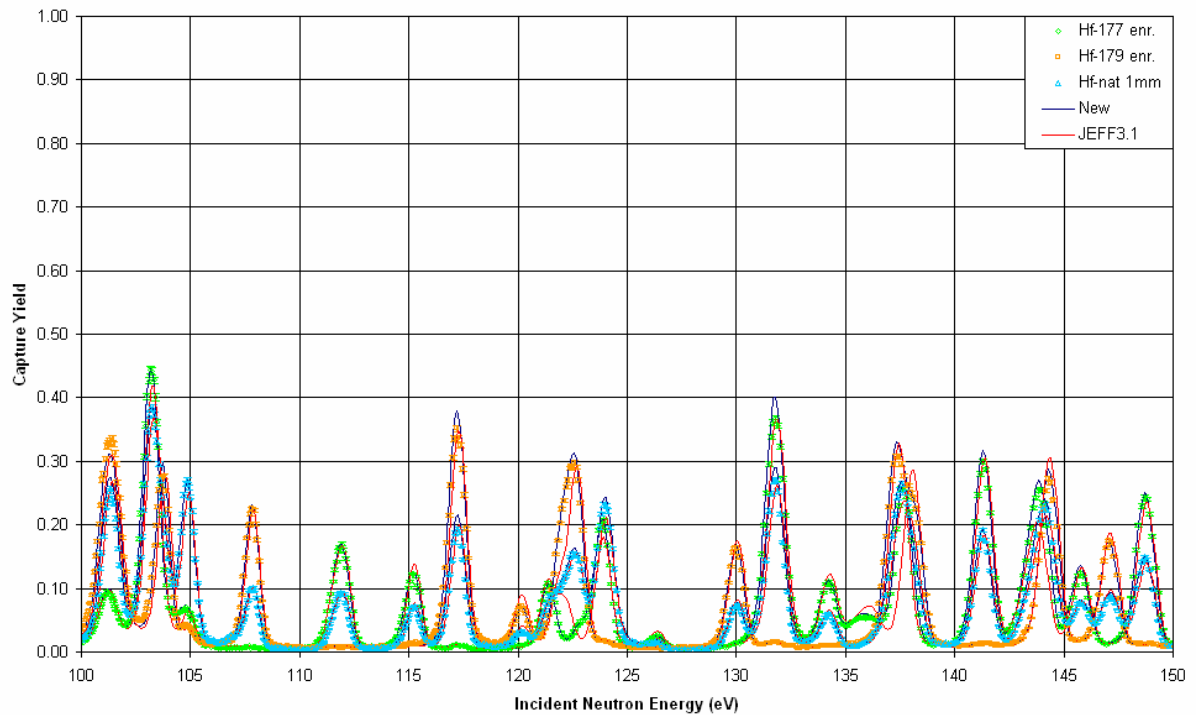


Figure A.9 – Hafnium Transmission Data and Calculations (150 – 200 eV)

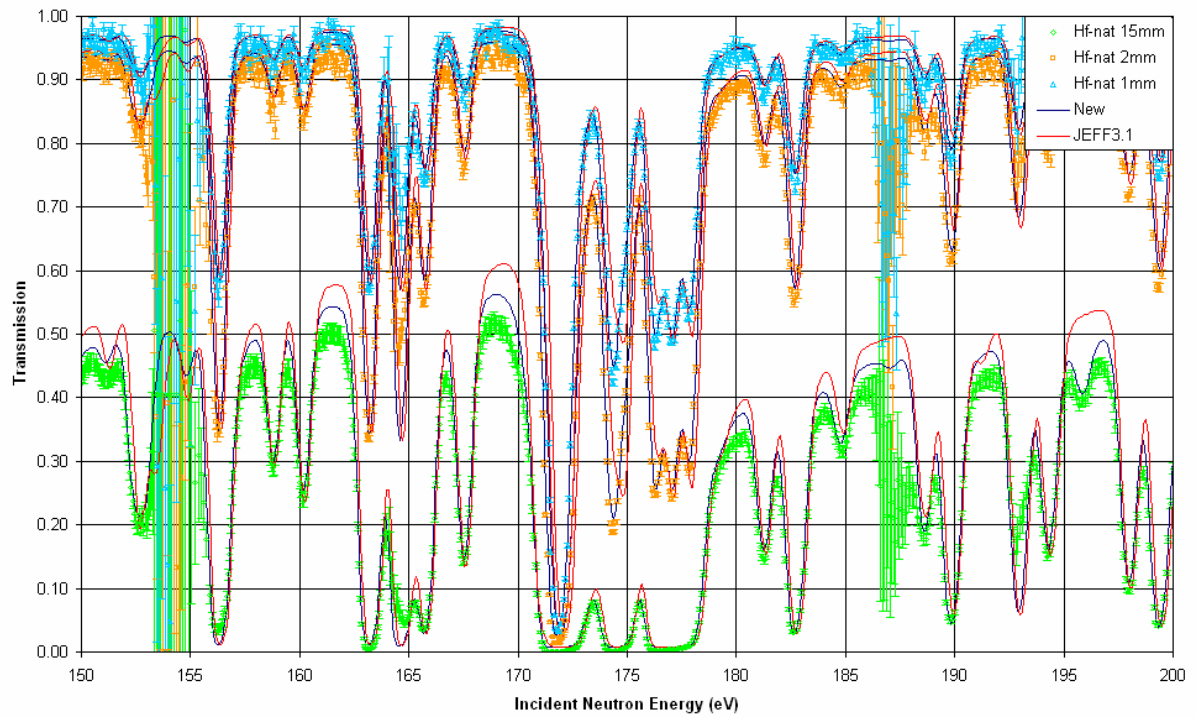


Figure A.10 – Hafnium Capture Data and Calculations (150 – 200 eV)

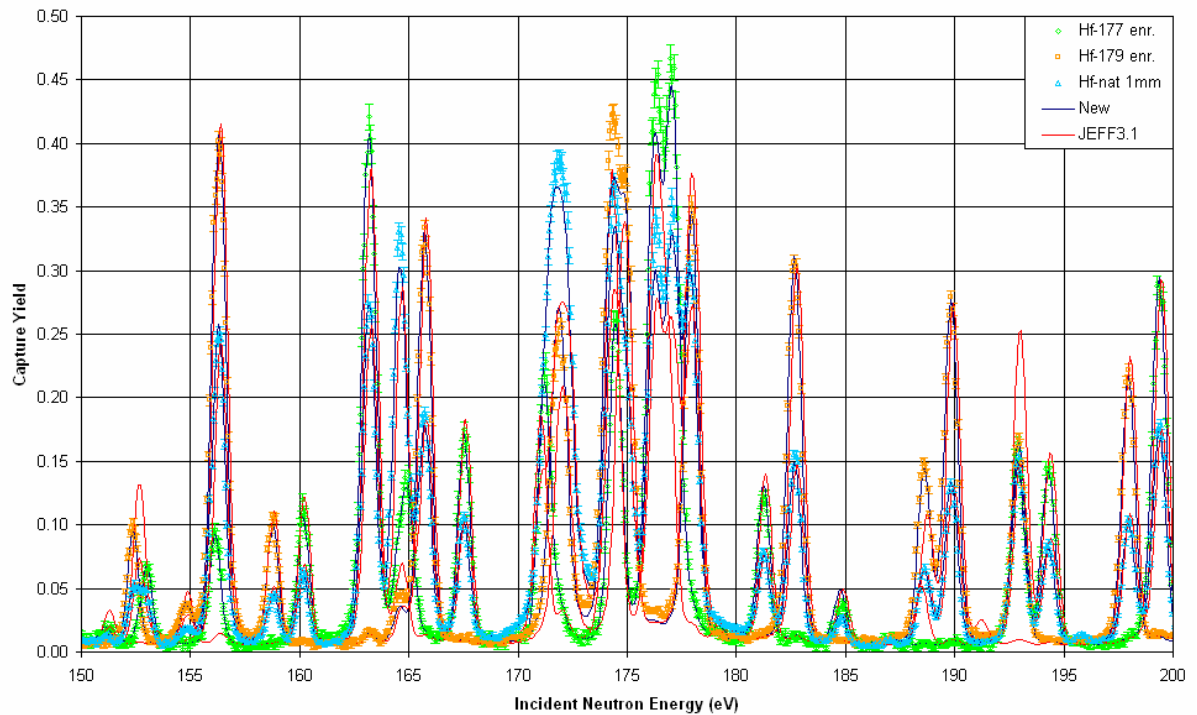


Figure A.11 – Hafnium Transmission Data and Calculations (200 – 250 eV)

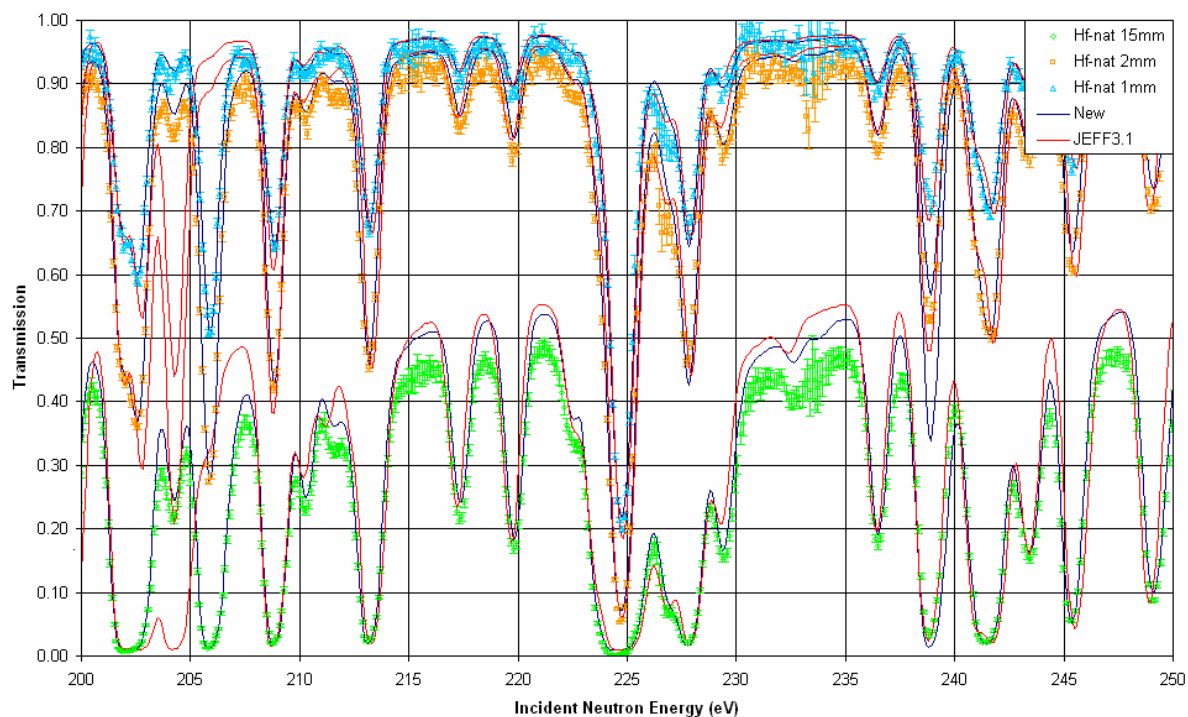


Figure A.12 – Hafnium Capture Data and Calculations (200 – 250 eV)

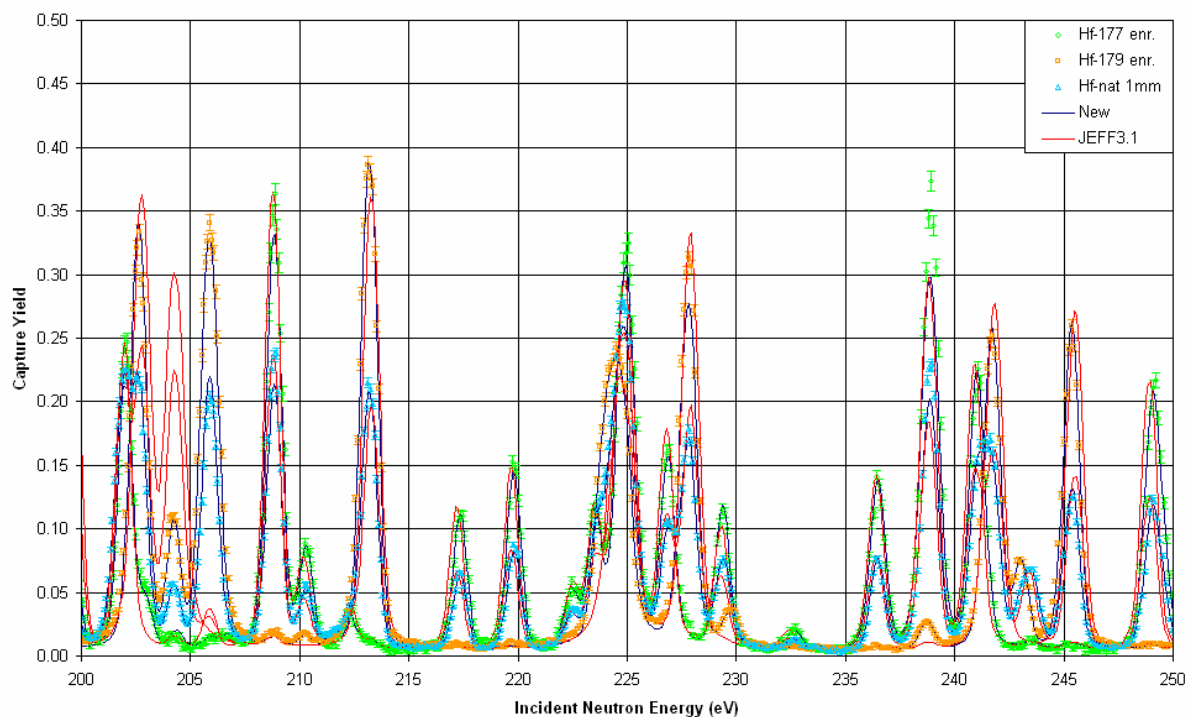


Figure A.13 – Hafnium Transmission Data and Calculations (250 – 300 eV)

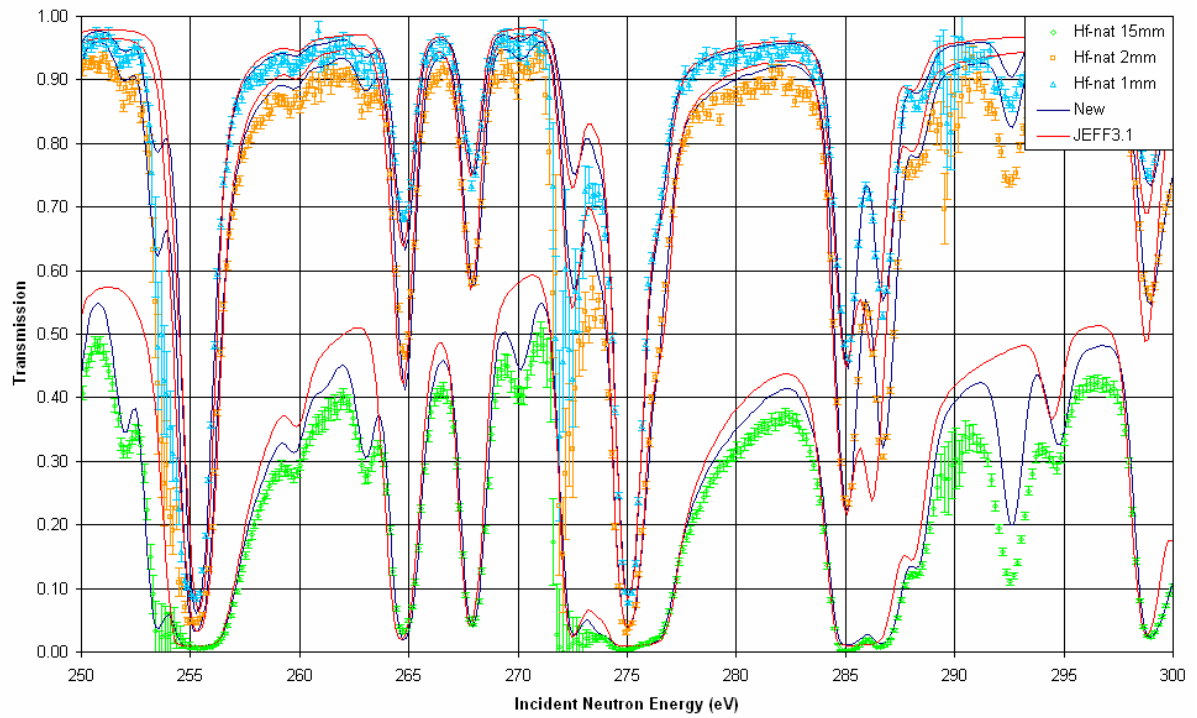


Figure A.14 – Hafnium Capture Data and Calculations (250 – 300 eV)

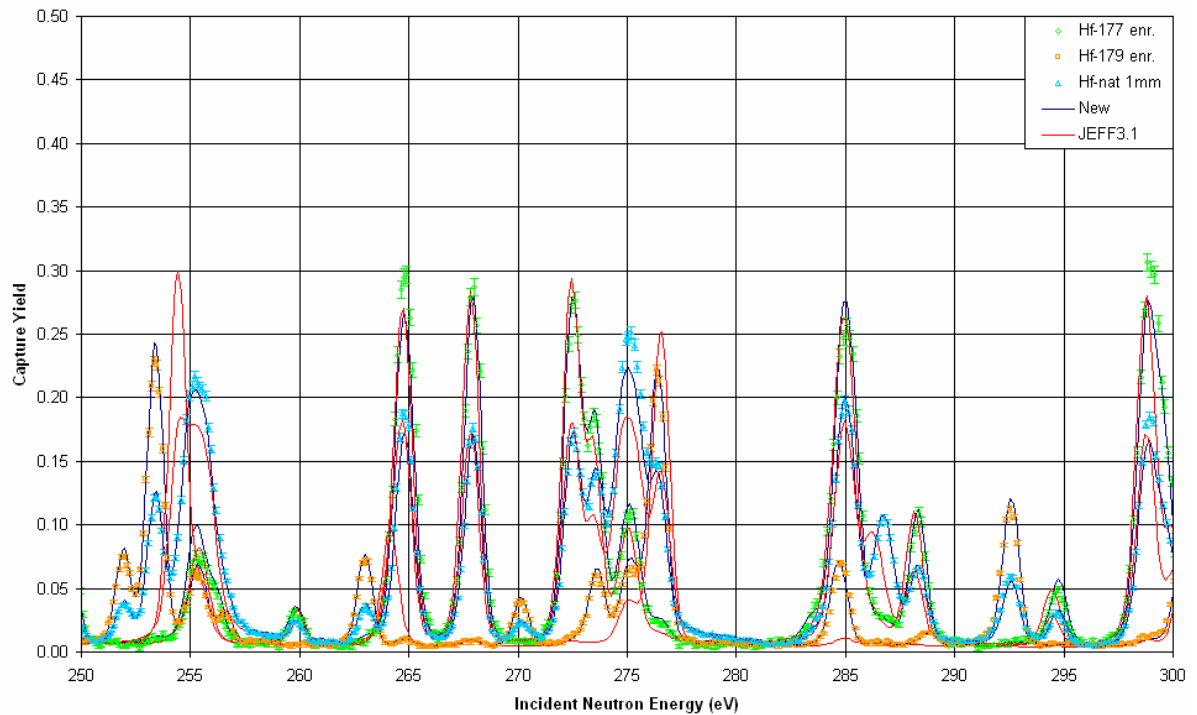


Figure A.15 – Hafnium Transmission Data and Calculations (300 – 350 eV)

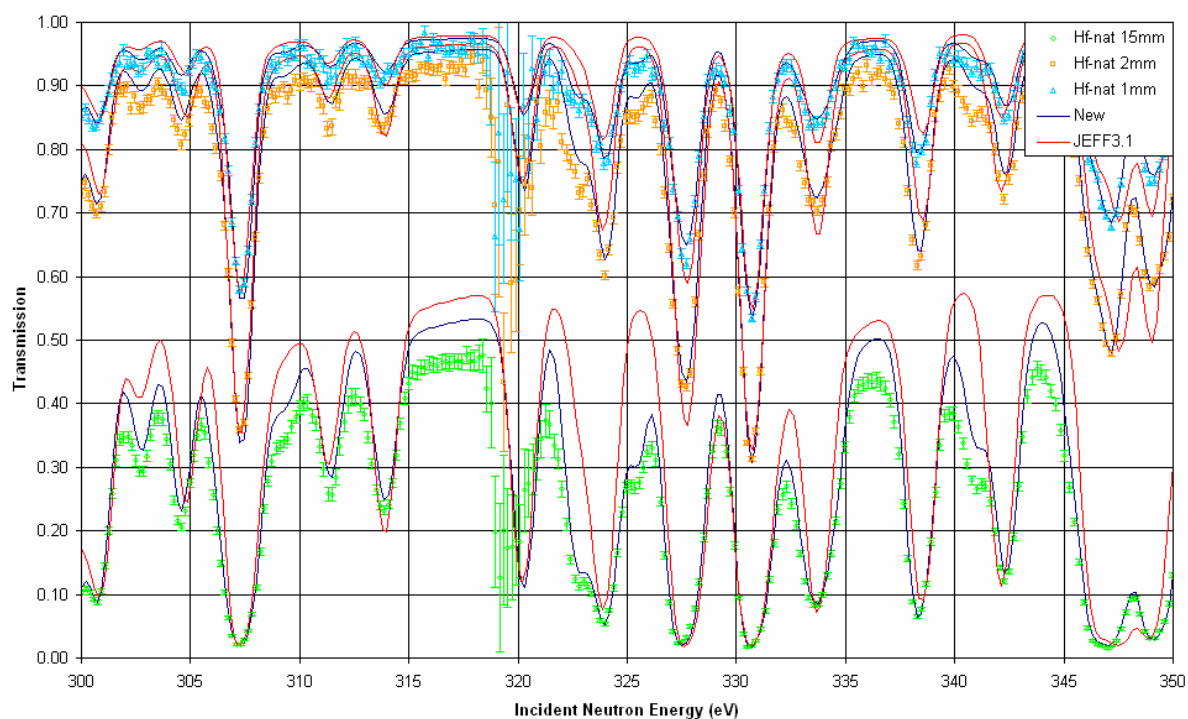


Figure A.16 – Hafnium Capture Data and Calculations (300 – 350 eV)

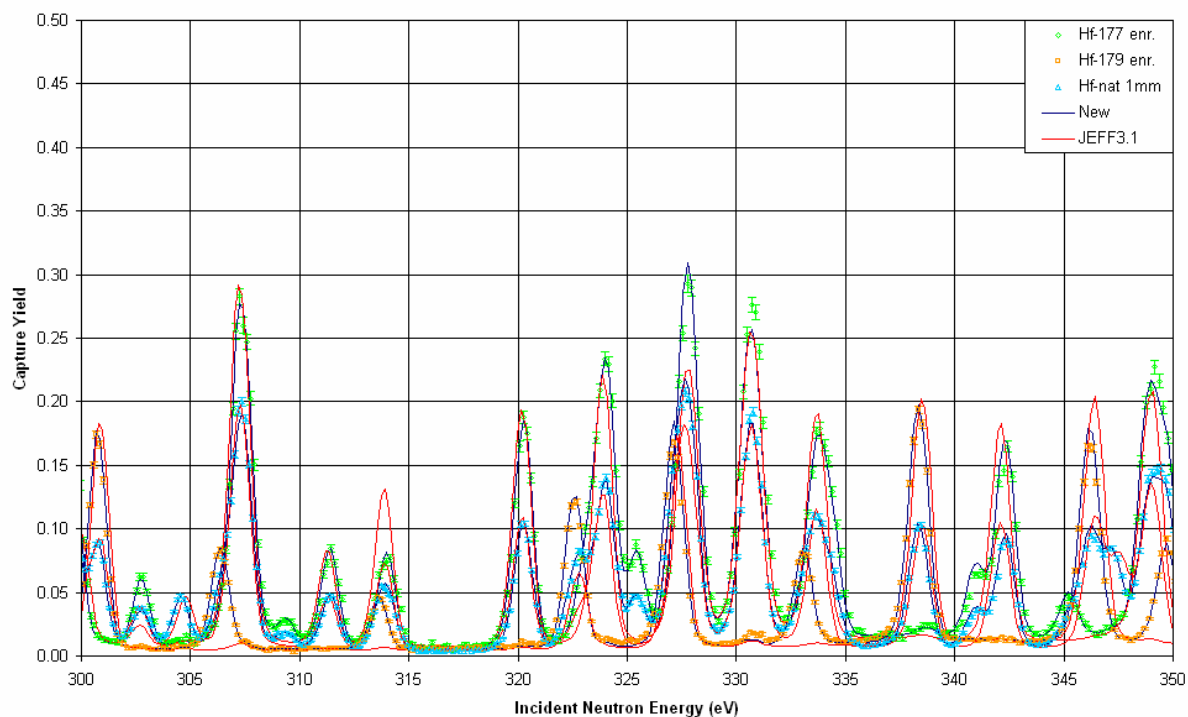


Figure A.17 – Hafnium Transmission Data and Calculations (350 – 400 eV)

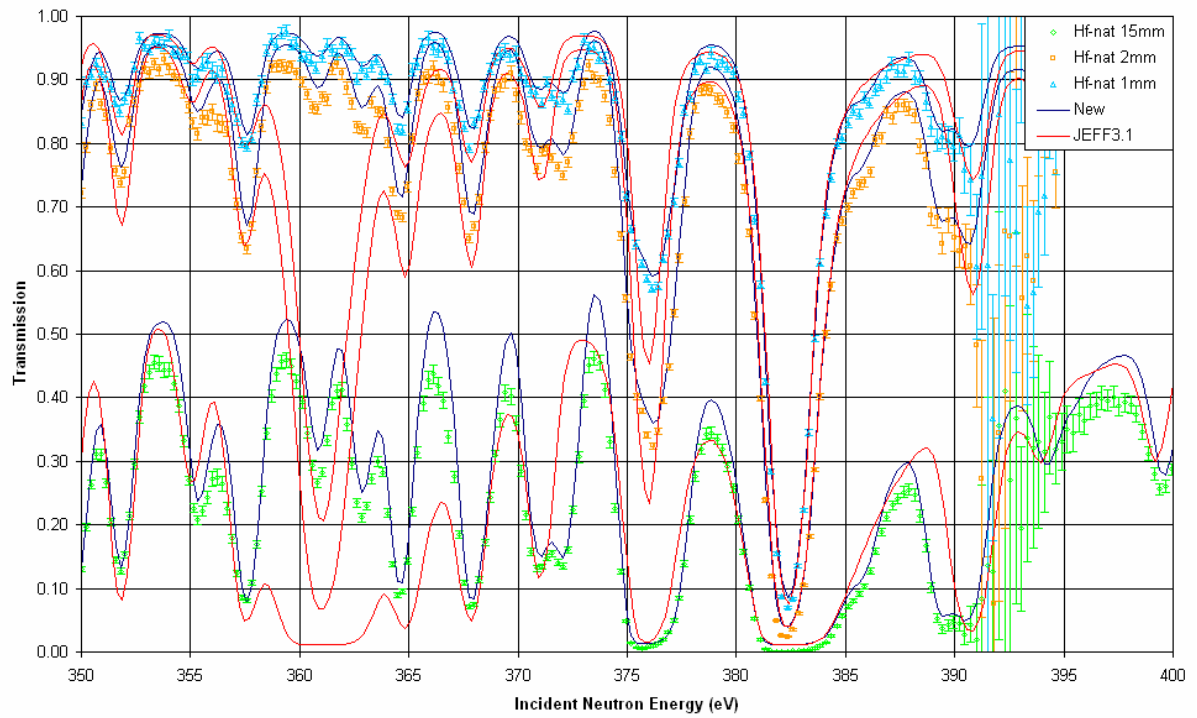


Figure A.18 – Hafnium Capture Data and Calculations (350 – 400 eV)

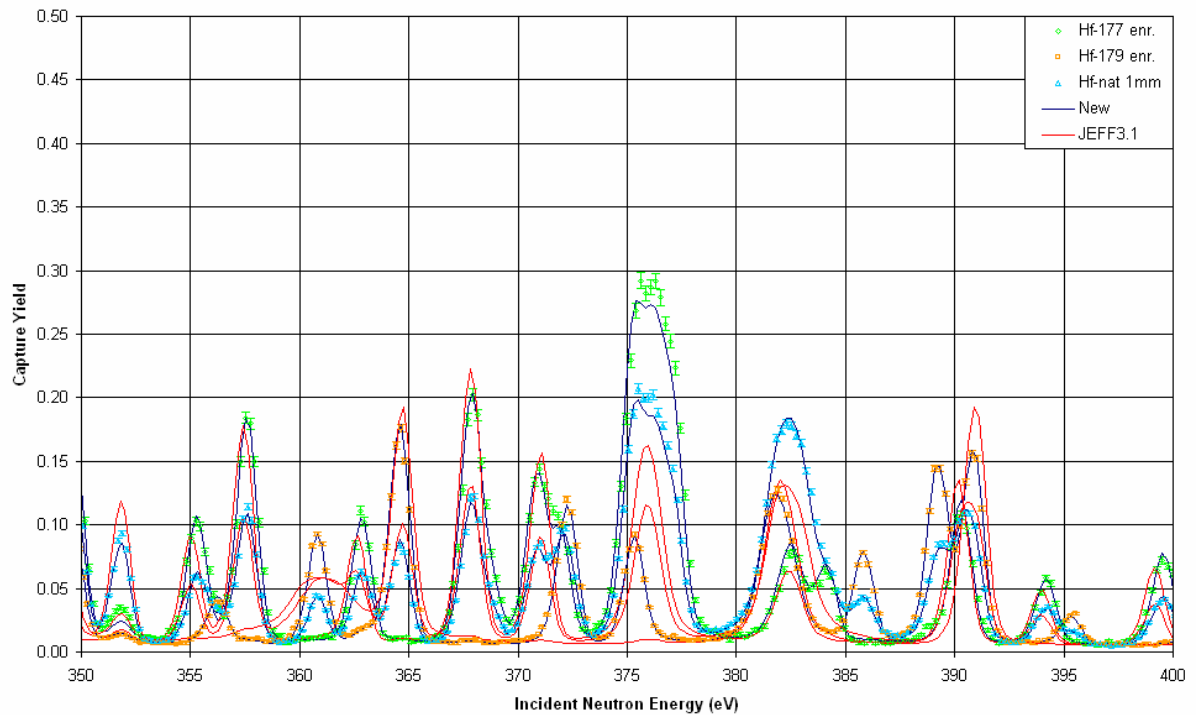


Figure A.19 – Hafnium Transmission Data and Calculations (400 – 500 eV)

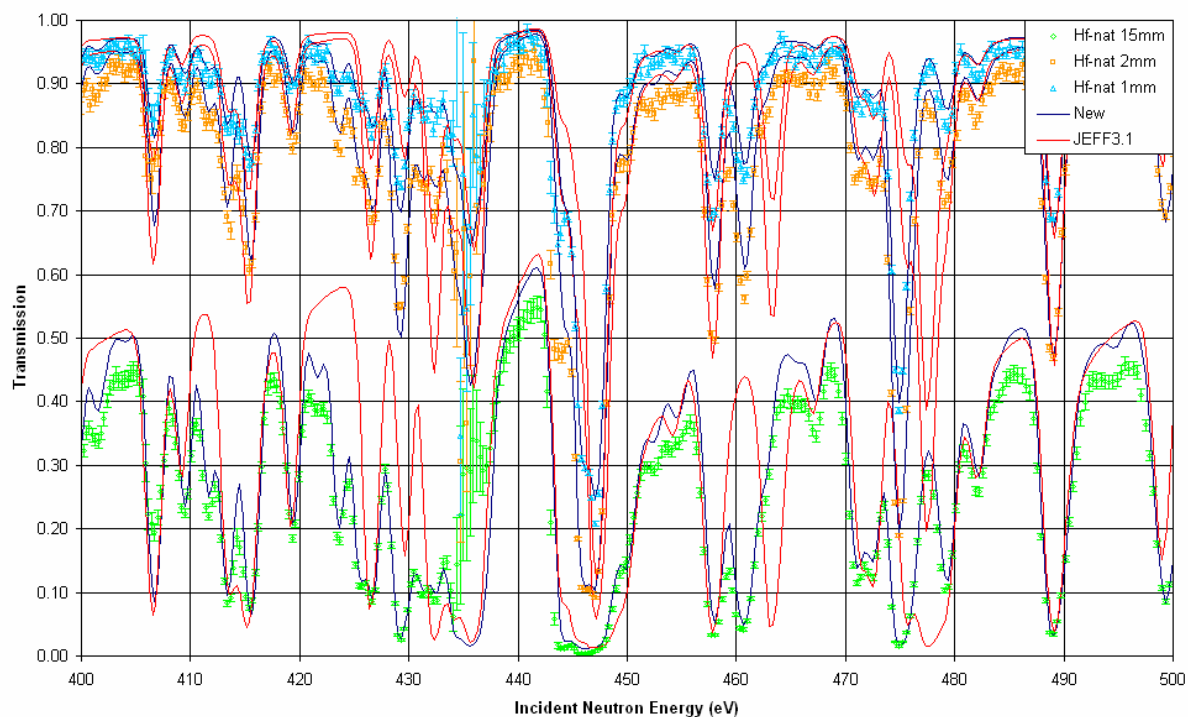


Figure A.20 – Hafnium Capture Data and Calculations (400 – 500 eV)

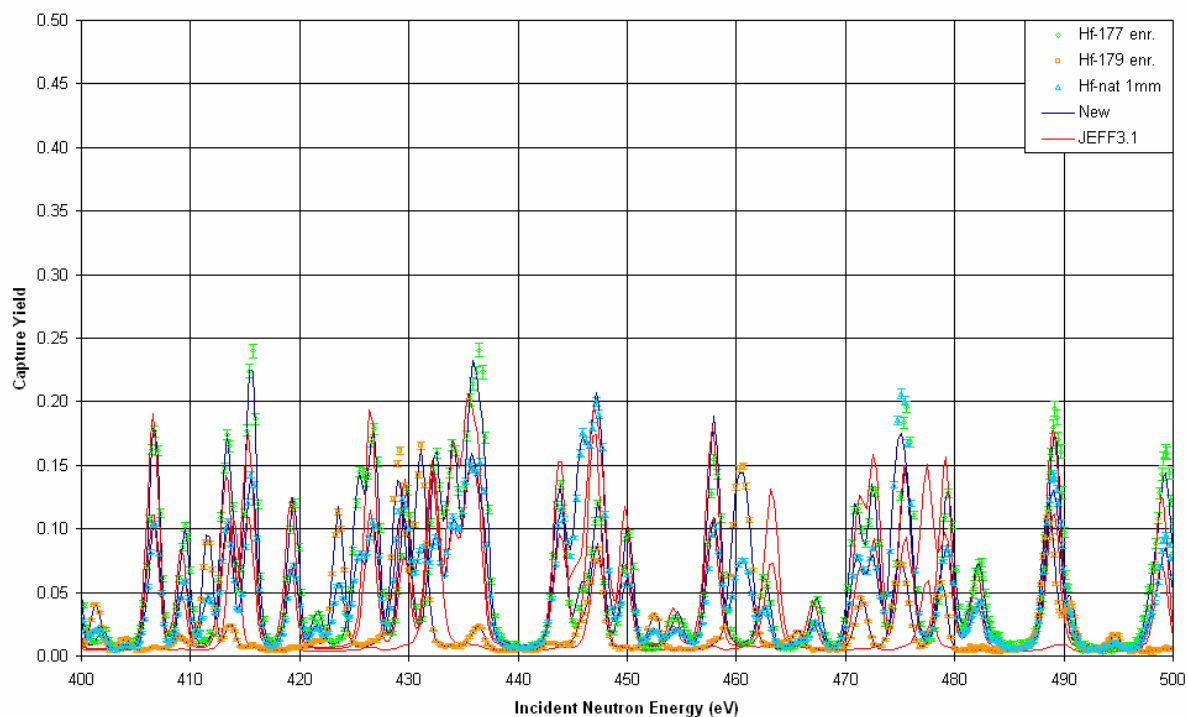


Figure A.21 – Hafnium Transmission Data and Calculations (500 – 600 eV)

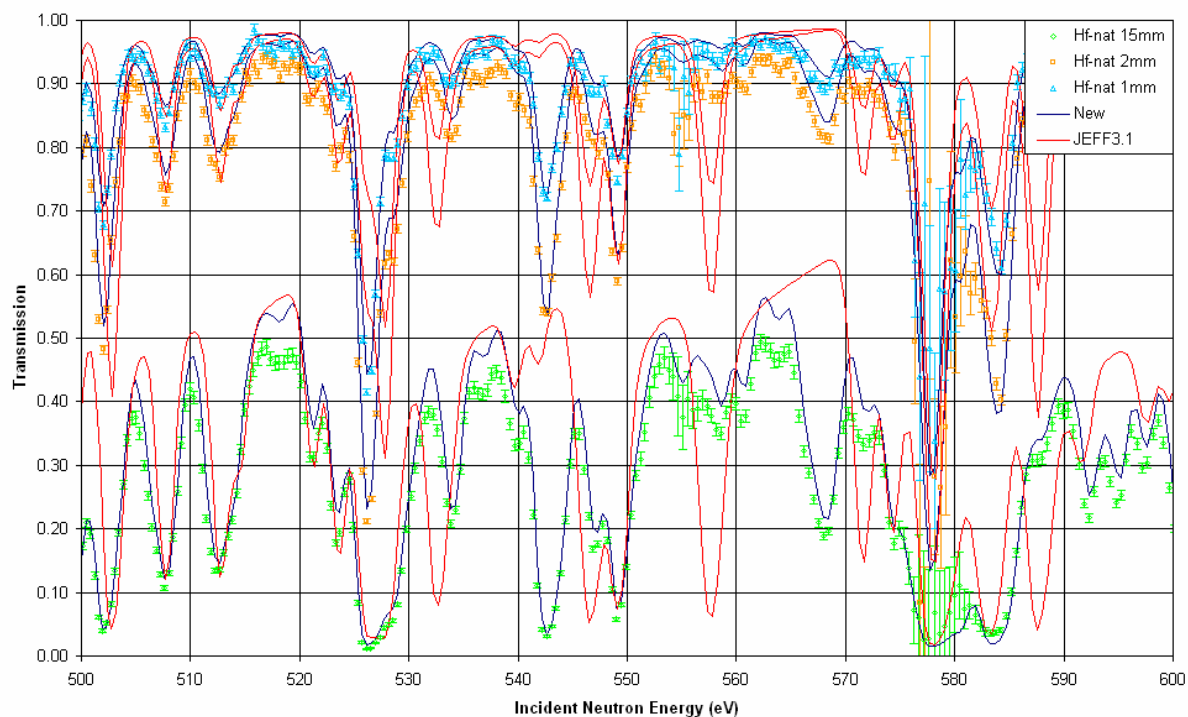


Figure A.22 – Hafnium Capture Data and Calculations (500 – 600 eV)

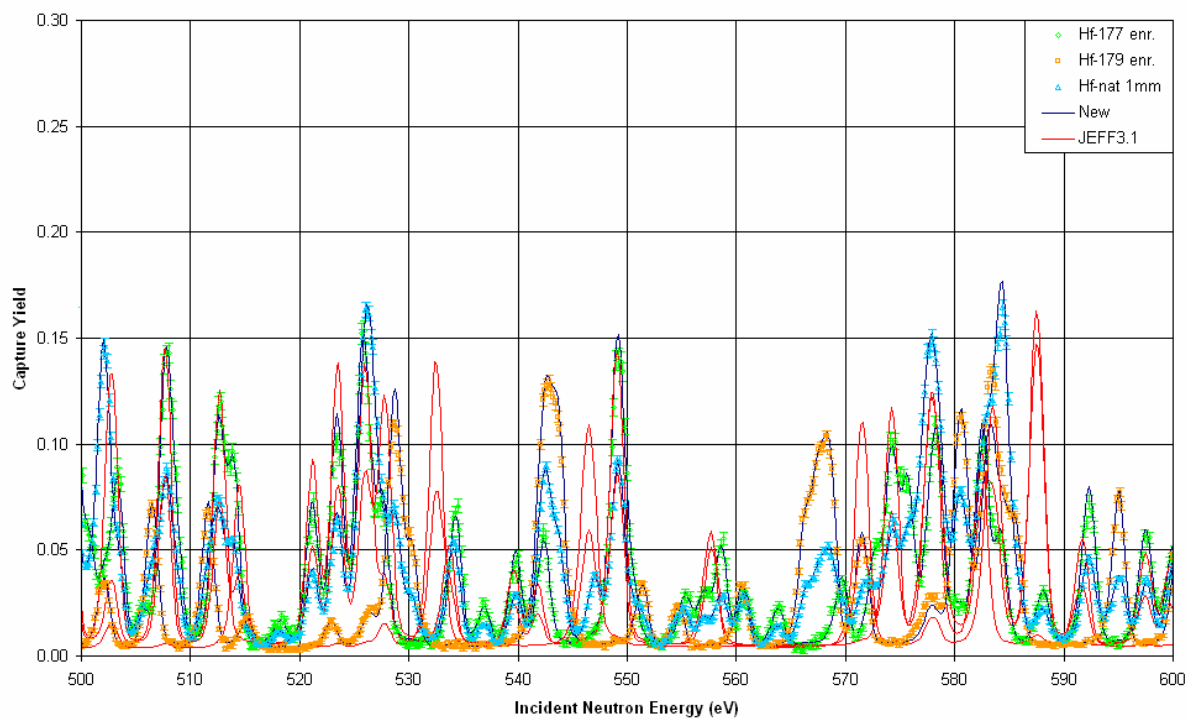


Figure A.23 – Hafnium Transmission Data and Calculations (600 – 700 eV)

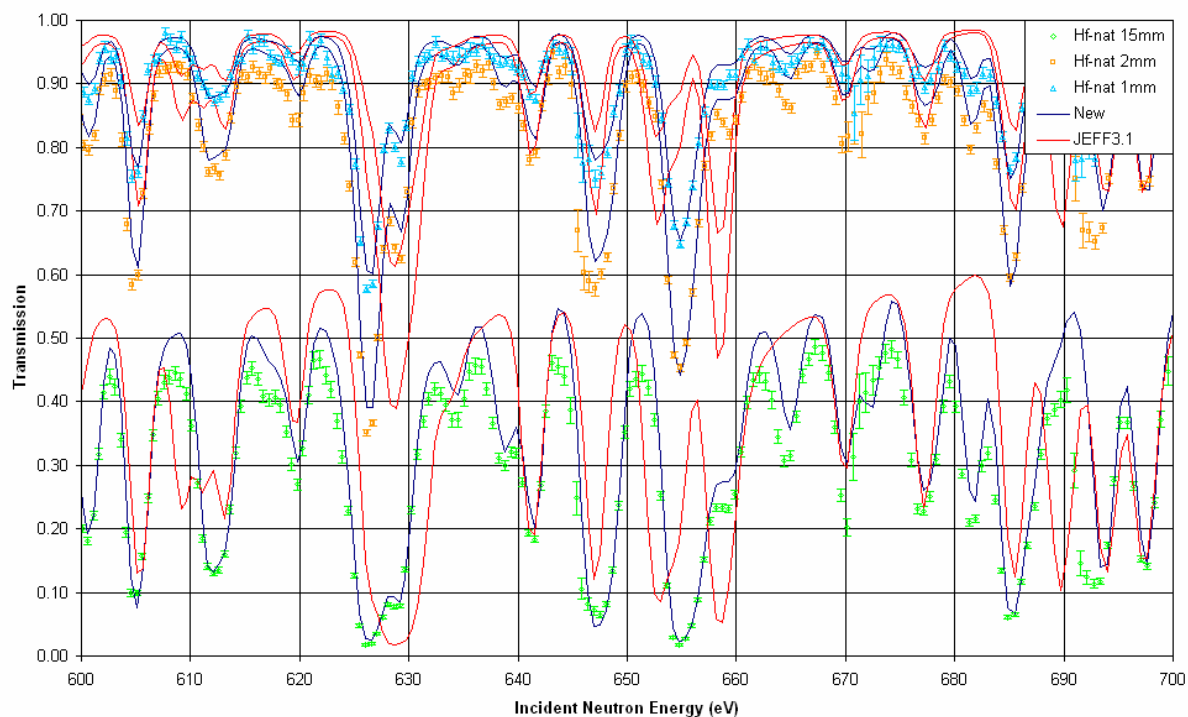


Figure A.24 – Hafnium Capture Data and Calculations (600 – 700 eV)

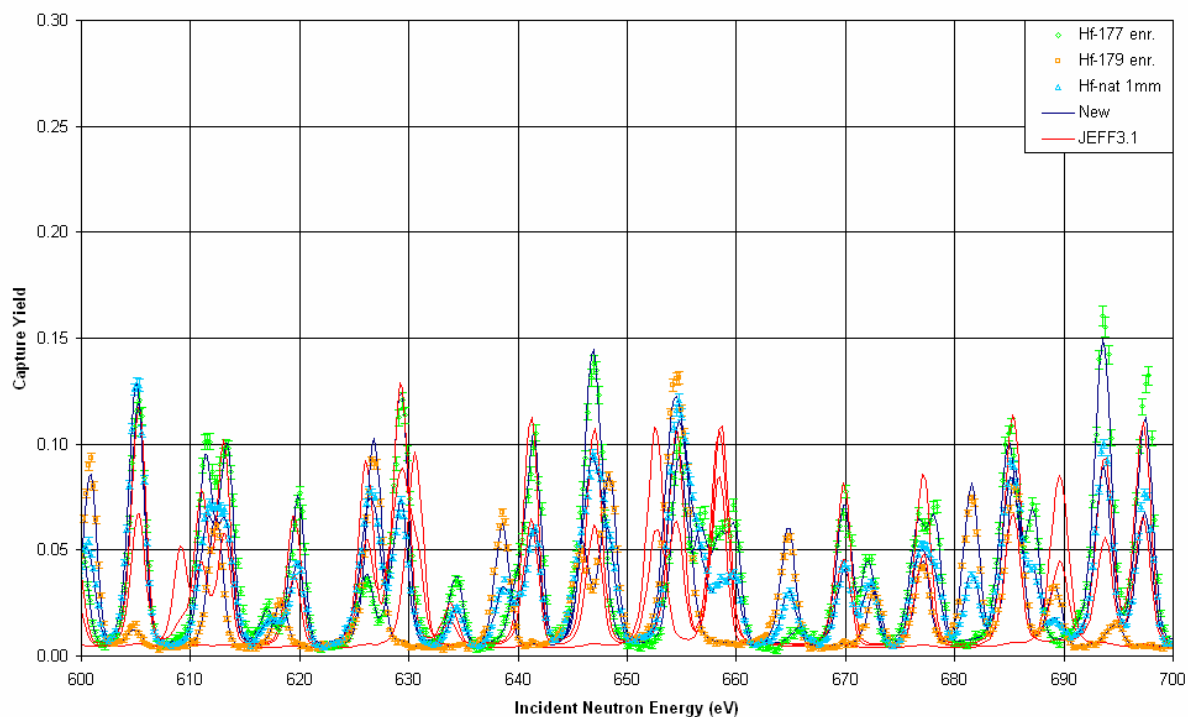


Figure A.25 – Hafnium Transmission Data and Calculations (700 – 800 eV)

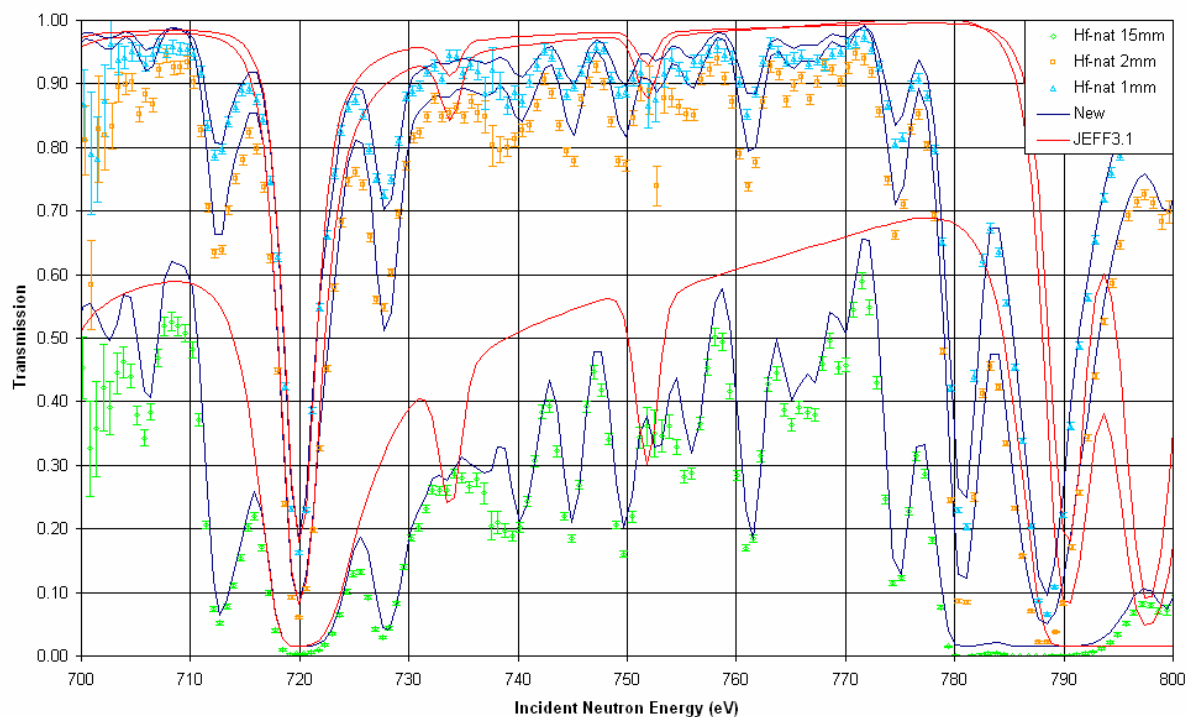


Figure A.26 – Hafnium Capture Data and Calculations (700 – 800 eV)

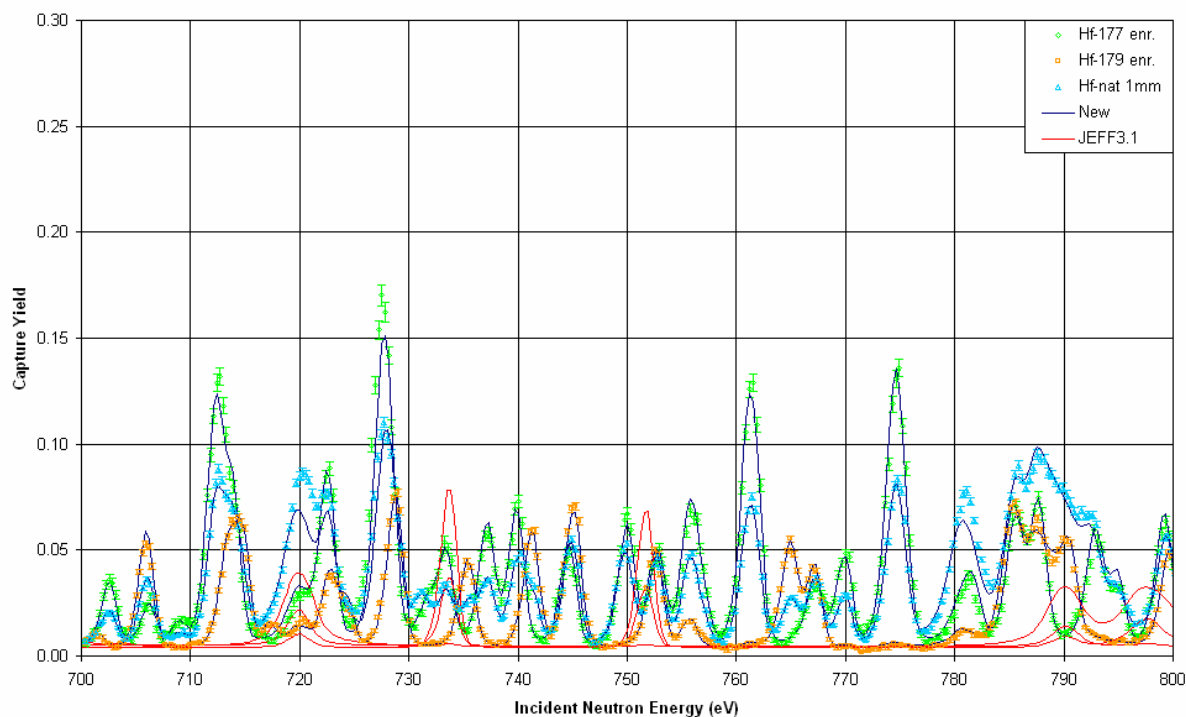


Figure A.27 – Hafnium Transmission Data and Calculations (800 – 900 eV)

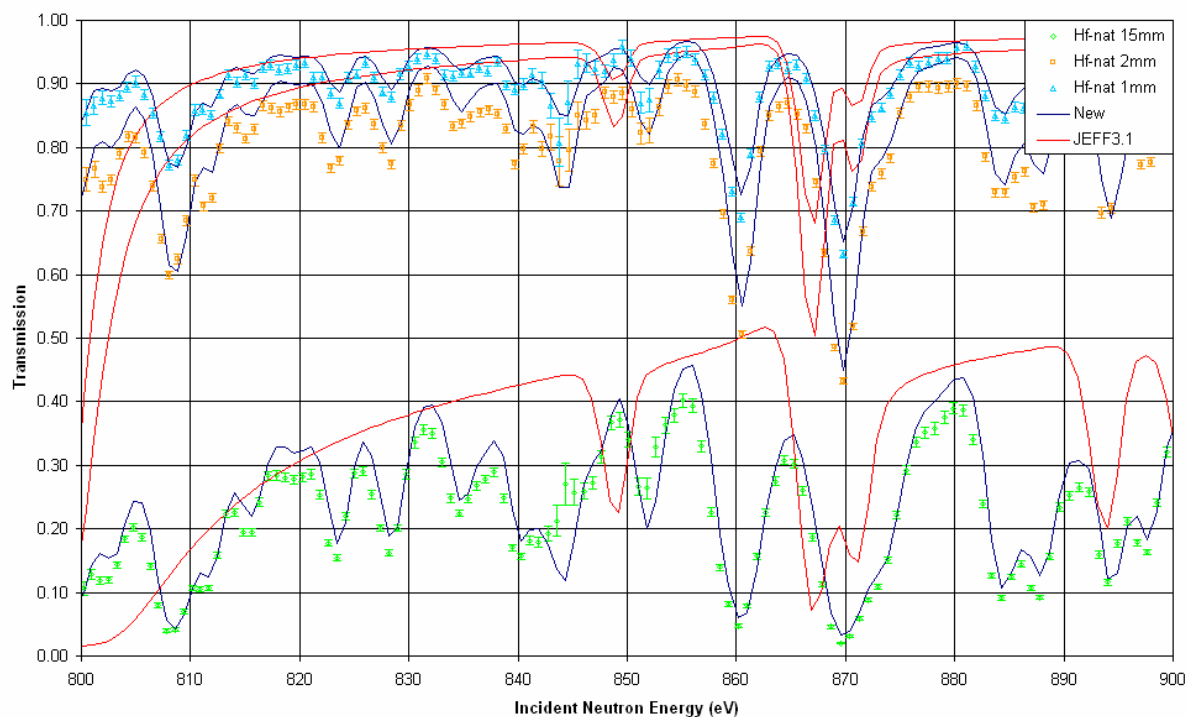


Figure A.28 – Hafnium Capture Data and Calculations (800 – 900 eV)

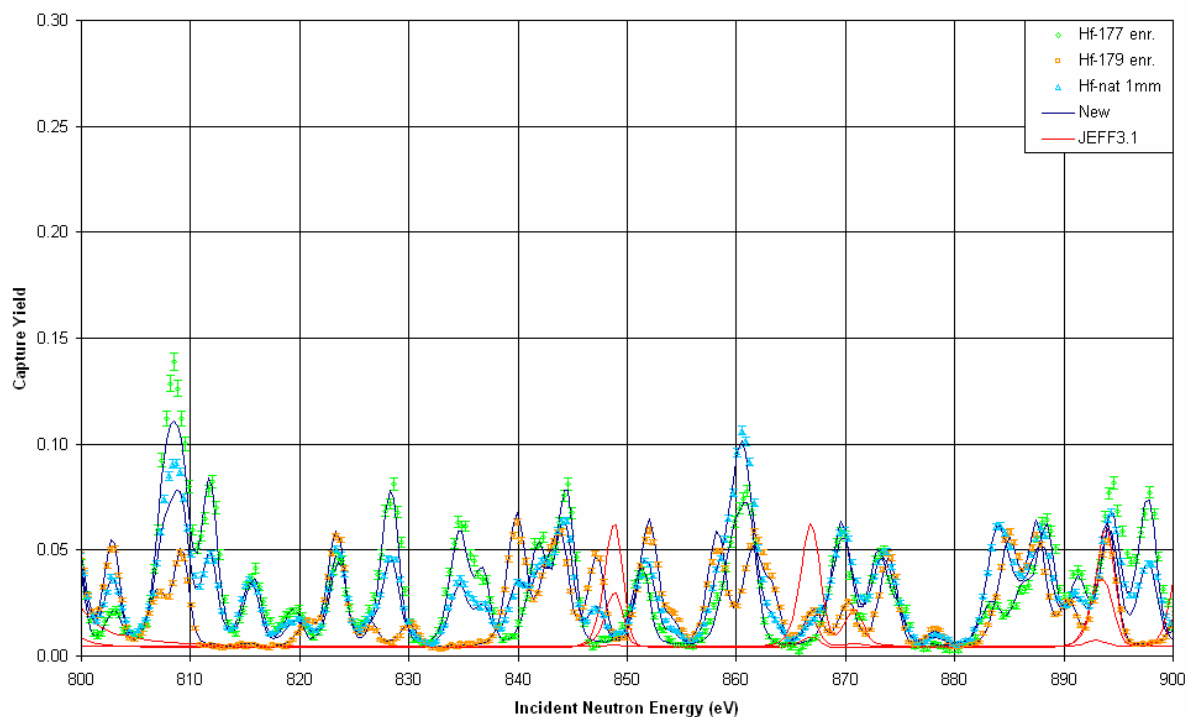


Figure A.29 – Hafnium Transmission Data and Calculations (900 – 1000 eV)

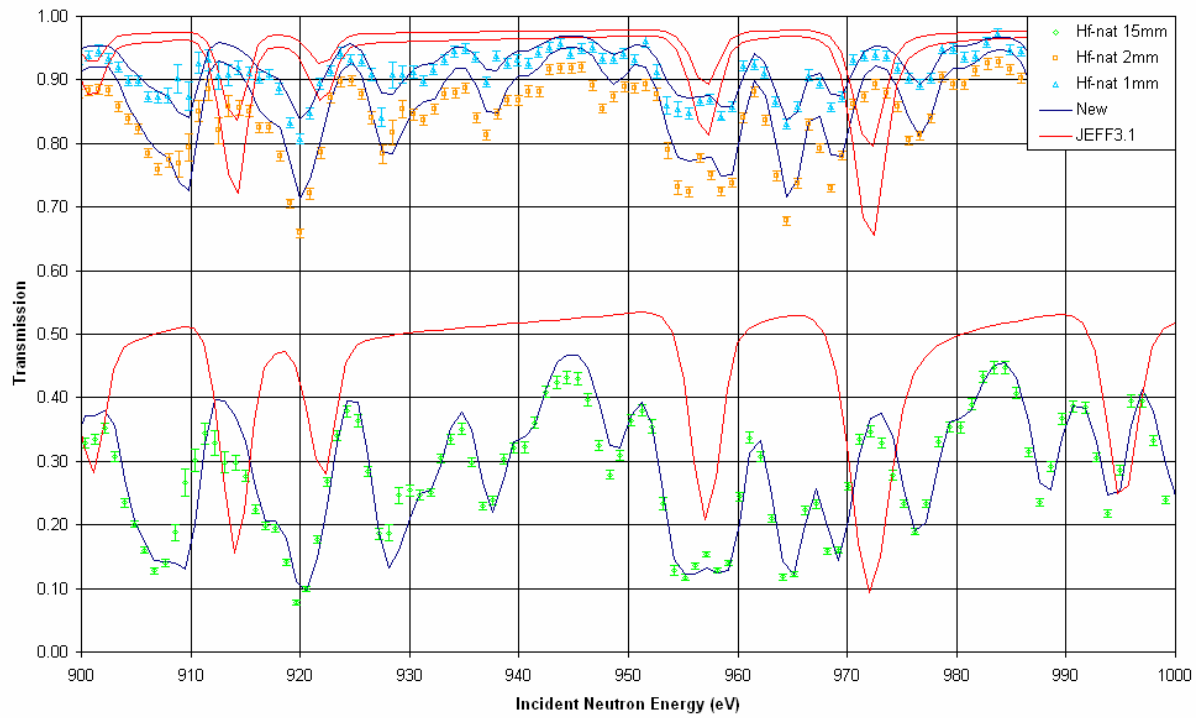
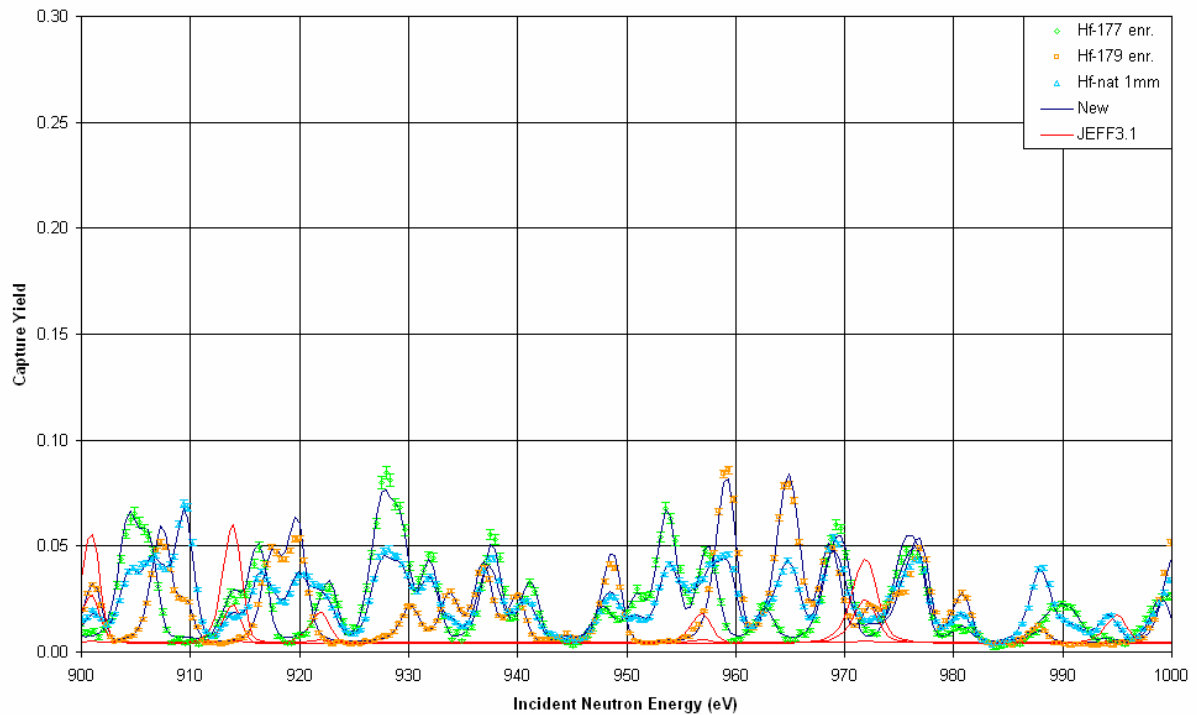


Figure A.30 – Hafnium Capture Data and Calculations (900 – 1000 eV)



APPENDIX B – SUPPORTING DOCUMENTATION

This appendix presents documentation that supports the new hafnium cross section measurements:

- the High Priority Request List [19] entry for hafnium, which underpins the need for improved hafnium cross section data
- the (successful) applications for NUDAME [35] and EUFRAT [38] support to conduct hafnium capture measurements, with associated justification
- a paper summarising progress on the analysis of the NUDAME-supported measurements, as a contribution to the IRMM Neutron Physics Unit Scientific Report 2008 (unpublished).

Author's notes on presentation of the documents in this appendix:

- The documents have been slightly reformatted to allow for the page layout of this thesis being different to that of the original document.
- The source referencing within these documents refers to the “References” list within the individual document and not the References section in the main body of this thesis.
- The tables and figures presented within these documents are not listed at the start of the main body of the thesis. The pertinent information contained within these tables and figures has been amalgamated into the main body.

B.1 High Priority Request List Entry for Hafnium Measurements

Request ID:	5	Status of the request:		High Priority request	
Target:	Reaction and process:	Incident Energy:	Secondary energy or angle:	Target uncertainty:	Covariance:
72-HF-0	(n,g) SIG	0.5-5.0 keV		4	Y
Field:	Subfield:	Date Request created:	Date Request accepted:	Ongoing action:	
Fission	LWR	28-APR-06	16-APR-07		

Requester: Mr. Gilles NOGUERE at CADARACHE, FR

Email: [REDACTED]

Project (context): JEFF

Impact:

In nuclear industry hafnium is used as neutron absorbing material to regulate the fission process. Interpretations of critical experiments with UO_x fuel conducted by CEA in the AZUR zero-power reactors has shown systematic underestimation of the reactivity worth that may be attributed to an overestimated natural hafnium capture cross section in the epi-thermal energy range [1,2].

Accuracy:

Requested accuracy can be found in the CEA Report “Corrélations entre données nucléaires et expériences intégrales a plaques, le cas du hafnium”, Jean-Marc Palau, CEA-R-5843 (1997). The target accuracy on the effective capture integral has to be lower than 4%.

Justification document:

[1] David Bernard, “Détermination des incertitudes liés aux grandeurs neutroniques d’intérêt des réacteurs a eau pressurisée a plaques combustibles et application aux études de conformité”, University Blaise Pascal, Clermont-Ferrand II, France (2001)

[2] G. Noguère, A. Courcelle, J.M. Palau, O.Litaize, “Low neutron energy cross sections of the hafnium isotopes”, JEFDOC-1077, OECD-NEA, Issy-les-Moulineaux, France (2005)

[3] G. Noguère, A. Courcelle, P. Siegler, J.M. Palau, O. Litaize, “Revision of the resolved resonance range of the hafnium isotopes for JEFF-3.1”, Technical note CEA Cadarache NT-SPRC/LEPH-05/2001 (2005)

Comment from requester:

Neither the JENDL3.3 nor the JEFF3.1 libraries, that were recently issued, solve the problem. In fact, this was observed for JENDL3.3 before the JEFF3.1 file was constructed. As a result the JEFF3.1 file has been produced with this problem in mind taken into consideration the recent data from Trbovich et al. obtained at RPI [3]. Finally, a 400 pcm underestimation remains that is likely due to interfering isotopic contributions in the resolved energy region. New high resolution measurements appear needed, and would be particularly valuable if they can distinguish the contributions of different isotopes.

Comments from evaluator/experimentalist:

Measurements on natural Hf were carried out by CEA at IRMM in the frame of the NUDAME (<http://www.irmm.jrc.be/html/nudame/>) transnational access scheme. Further work is planned at IRMM in collaboration with CEA, INRNE, U. Birmingham and Serco.

Comments for achieved accuracy:

Calculations on the AZUR configuration using the JEFF3.1 library give a Hf reactivity worth of about -300 pcm [2].

Review comment:

Additional file attached: JEFDOC-1077.ppt

Additional file attached: NT_Hafnium.pdf

B.2 Application for Support from NUDAME Project



EUROPEAN COMMISSION
DIRECTORATE GENERAL
JOINT RESEARCH CENTRE
Institute for Reference Materials and Measurements

EURATOM: Transnational Access to Large Infrastructure

APPLICATION FORM for funding of access to the NUDAME facilities of EC-DG JRC-IRMM	
Title of the proposed experiment Capture cross section measurements of isotopic enriched Hf samples	
Spokesperson (name, address, phone, fax, e-mail) Christopher John Dean Serco Assurance [Redacted] [Redacted] [Redacted] Phone (from international) [Redacted] Fax (from international) [Redacted]	
Facility GELINA	Type of experiment Capture measurements
Contact person at IRMM P. Schillebeeckx	
Requested beam characteristics 800 Hz, 70 μ A, moderated spectrum, 1 ns time resolution	IRMM experimental set-up of interest Capture measurements at FP5_12 m and FP15_30m using C6D6 detectors
Requested beam time (hours) 200 h	Preferred measurement period
Number of set-up preparation days 0.5 days, mounting of samples	
Potential safety problems (radioactive targets and sources, gases, high activation...) Not applicable	

Participant's List and access period requested

Researcher	Institution	Total number of days	Total number of visits
C. Dean	Serco Ltd.	-	-
T. Ware	Serco Ltd.	14 days	1
M. Moxon	Serco Ltd.	7 days	1
G. Noguère	CEA Cadarache	7 days	1

Special comments

This proposal is a continuation of the activities of a previous proposal which concentrated on measurements with natHf. The results of the activities covered in the previous proposal have indicated the necessity of additional measurements with isotopic enriched Hf samples.

A detailed description of the proposal (max. 3 pages) must be added. This description must contain:

- the context and the goals of the measurements,
- the contribution of the different researchers to the experiment,
- the schedule of the work,
- quantitative estimates of fluxes and beam times,
- special support services that are needed,
- a description of IRMM equipment that is needed and/or equipment that you will bring with you.

Date

.....

Signature of Spokesperson

.....

Signed applications must be sent by mail to the following address:

European Commission
Directorate-General Joint Research Centre
Institute for Reference Materials and Measurements
Retieseweg 111, B-2440 Geel, Belgium

Contact:

Capture cross section measurements with isotopic enriched Hf samples

1) THE CONTEXT AND THE GOALS OF THE MEASUREMENTS

Natural hafnium can be used as a reactor control rod to regulate the fission process because of its high absorption cross section in the thermal and epi-thermal region. In the previous proposal, the interpretation of integral benchmark experiments, in both critical and zero-power reactors, identified the poor quality of the nuclear data files for hafnium in the thermal and epi-thermal region.

Few studies have focussed on the neutron-induced total, capture and scattering cross-sections in hafnium. Experimental data, which can be used for an evaluation of the $^{nat}\text{Hf}(n,\gamma)$ and $^{nat}\text{Hf}(n,\text{tot})$ reactions in the thermal and resolved resonance region (RRR), is rather scarce and the evaluated data files are primarily based on the results of Ref [1-7]. Recently, capture and transmission measurements have been performed at RPI [8,9]. The results of these measurements have been included for the evaluation in JEFF 3.1 [10,11]. However, the resonance parameters file has only been improved for neutron energies below 200 eV.

In 2006 capture measurements on natural hafnium samples were performed at GELINA as part of a NUDAME project proposed by CEA Cadarache (see PAC 2006). The resulting capture data has been analysed together with the results of transmission measurements performed at GELINA by Siegler et al. [12]. From resonance shape analysis of this capture and transmission data, using REFIT, the shortcomings of the evaluated data files have been identified. Figure 1 and 2 compare the experimental transmission factor and capture yield with the theoretical values deduced from the resonance parameters in JEFF 3.1 in the upper energy region. Discrepancies are observed. The quality of the evaluated data can be significantly improved by new measurements. These measurements should be focussed on identification of resonances associated with each major isotope and the determination of the scattering radii. Therefore, these measurements require isotopic enriched samples which will be obtained from Sofia (BG). The request for the samples has been submitted and the samples are expected to arrive in Spring 2007.

2) RESEARCHERS CONTRIBUTING TO THE EXPERIMENT

The project is a joint proposal of Serco Ltd. (UK) and CEA Cadarache (F) The following researchers are involved in the project:

- C. Dean, Serco Ltd., will act as project leader and will be responsible for the final evaluation and verification of integral benchmark data;
- T. Ware, PhD student, will perform the measurements, data reduction and resonance analysis;
- M. Moxon, guest researcher of Serco Ltd., will assist in the measurements and resonance analysis;
- G. Noguère, CEA Cadarache, will assist in the evaluation of the data and the interpretation of the integral benchmark data.
- P. Schillebeeckx, Neutron Physics Unit of the IRMM, will act as local contact and measurement advisor.

3) WORK PROGRAMME

The measurements will be performed at a capture and transmission measurement station of GELINA using the equipment that is routinely used for capture cross section measurements. A total of two weeks of beam time is required. This measurement time is based on an energy differential neutron flux of $d\phi/dE = 10^4 \text{ s}^{-1} \text{ eV}^{-1}$ at 1 eV and 10 m distance with GELINA operating at 800 Hz and an average current of 70 μA . The measurements will cover the resolved resonance region.

Capture measurements will be performed in the thermal and the resolved resonance region on two different flight paths, i.e. FP5_12m and FP15_30m, applying the total energy detection principle using conventional NIM electronics, the IRMM fast time coder and the DAC2000 data acquisition system. For these measurements C_6D_6 scintillators will be used in combination with the Pulse Height Weighting Technique. The transmission measurements will be performed at FP2_28m and FP4_50m using a lithium glass scintillator, together with conventional NIM electronics, the IRMM fast time coder and the DAC2000 data acquisition system.

The isotopic enriched samples are used for an isotope identification of the resonances and to deduce the scattering radii. The data reduction will be performed with the AGS code. The REFIT code will be used for the resonance shape analysis. Improved resonance parameters will be obtained from a simultaneous analysis of the transmission data and capture yields obtained with the natural hafnium (previous proposal) and isotopic enriched hafnium samples.

4) ESTIMATION OF THE REQUESTED TRAVEL AND SUBSISTENCE COSTS

A total of about [REDACTED] will be required to cover the travel and subsistence costs for the participation of T. Ware, M. Moxon and G. Noguère.

Collaborator		Travel costs	Subsistence costs
T. Ware	Birmingham (UK)	[REDACTED]	[REDACTED]
M. Moxon	Oxford (UK)	[REDACTED]	[REDACTED]
G. Noguère	CEA Cadarache (F)	[REDACTED]	[REDACTED]

Table 2. Estimation of the requested travel and subsistence costs

5) REFERENCES

- [1] T. Fuketa and J.A. Harvey, Level spacings and s-wave neutron strength functions of the isotopes of Hafnium, ORNL report, ORNL-3778 (1965).
- [2] T. Fuketa et al., Analysis of total neutron cross section data for the hafnium isotopes, RPI report, RPI-328-68 (1966).
- [3] M.C. Moxon et al., Differential neutron cross-sections of natural hafnium and its isotopes for neutron energies up to 30 eV, Harwell report, AERE-R7864 (1974).
- [4] H.I. Liou et al., Neutron resonance spectroscopy: 177-Hf, Phys. Rev. C 11(1975)2022.
- [5] G. Rohr and H. Weigmann, Short range energy dependence of the neutron widths of 177-Hf resonances, Nucl. Phys. A264(1976)93.
- [6] H. Beer and R.L. Macklin, 178,179,180-Hf and 180-Ta(n, γ) cross sections and their contribution to stellar nucleosynthesis, Phys. Rev. C 26(1982)1404.
- [7] H. Beer et al., Neutron capture cross sections and solar abundances of 160,161-Dy, 170,171-Yb, 175,176-Lu and 176,177-Hf for the s-process analysis of the radionuclide 176-Lu, Phys. Rev. C 30(1984)464.
- [8] M.J. Trbovich, Hafnium Neutron Cross-Sections and Resonance Analysis, RPI Thesis (2003)
- [9] M.J. Trbovich et al., Hafnium resonance parameter analysis using neutron capture and transmission experiments, Int. Conf. on Nuclear Data for Science and Technology, Sept. 26 - Oct. 1, Santa Fe, New Mexico (2004), in press.
- [10] G. Noguère et al., Revision of the resolved resonance range of the hafnium isotopes for JEFF-3.1, CEA/Cadarache Technical Note, NT-SPRC/LEPh-05/201 (2005).
- [11] G. Noguère et al., Low neutron energy cross sections of the hafnium isotopes, OECD/NEA JEF/DOC-1077 (2005).
- [12] P. Siegler et al., Testing of neutron data by comparison of measured and calculated average transmissions, Int. Conf. on Nuclear Data for science and technology, Tsukuba, Japan, 2001.

6) FIGURES

Figure 1 – Comparison of experimental capture yield with the theoretical values from JEFF 3.1 from 250-300eV. (Known resonance energies as marked)

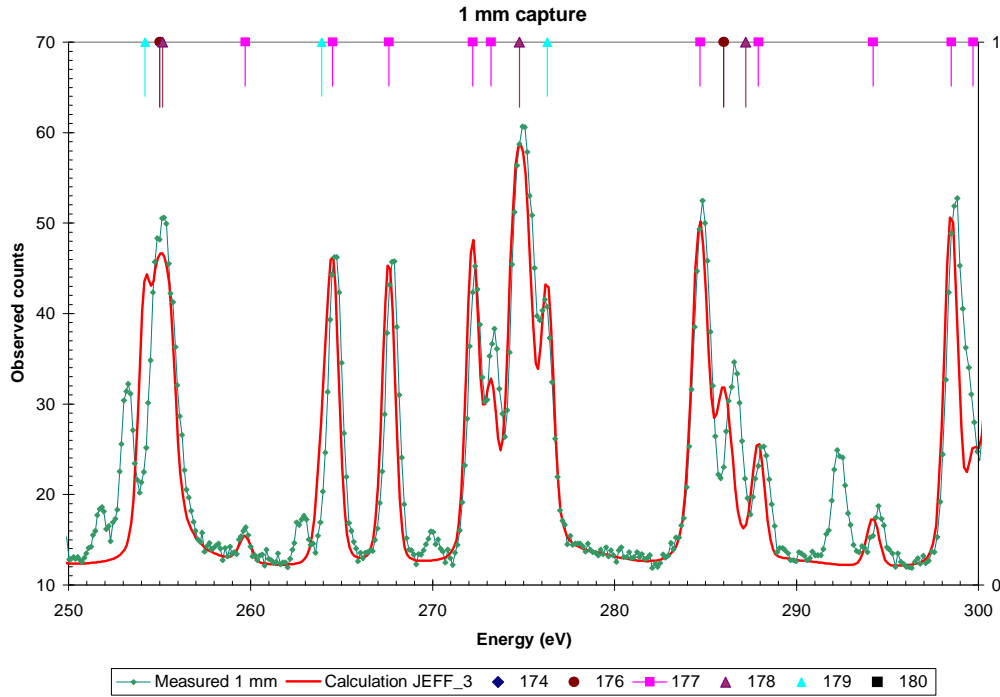
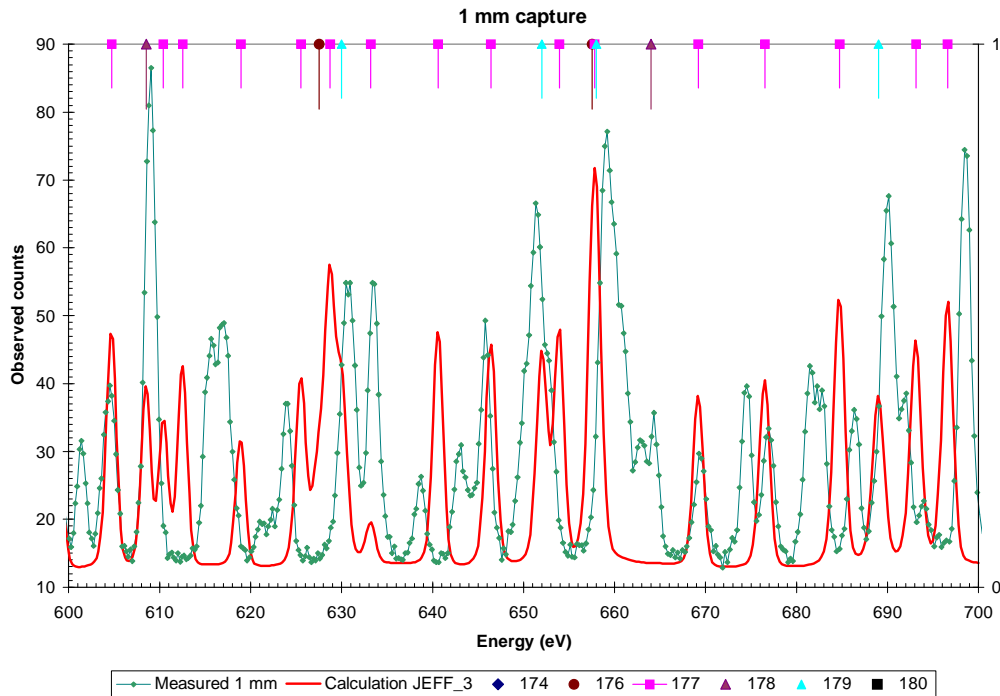


Figure 2 – Comparison of experimental capture yield with the theoretical values from JEFF 3.1 from 600-700eV. (Known resonance energies as marked)




B.3 Application for Support from EUFRAT Project



EUROPEAN COMMISSION
JOINT RESEARCH CENTRE
Institute for Reference Materials and Measurements

APPLICATION FORM for funding of EURATOM transnational access to IRMM facilities

		(Reserved for EUFRAT use) PAC meeting: Experiment ID:
Title of the proposed experiment Total cross-section measurements of natural hafnium samples		
Proposer (name, address, phone, fax, email) Mr Tim Ware (University of Birmingham) [Redacted] [Redacted] [Redacted] [Redacted]		
Facility GELINA	Type of experiment Transmission measurement	
Contact person at IRMM S. Kopecky P. Schillebeeckx		
Requested beam characteristics 800 Hz, 70 μ A, moderated spectrum, 1 ns time resolution	Preferred measurement period March 2009	
Requested beam time (hours) 200 hours	Experimental set-up or flight path of interest Transmission measurement at FP4_50m using lithium glass scintillator	
No. of set-up preparation days 0.5 days		
Transport cost estimation (2 users typically supported) 500 euro x2 = 1000 euro		
Potential safety problems (radioactive targets and sources, gases, high activation, etc.) Not applicable		

Participant list and requested access period

Please put on top the names of the users that you would like to be supported. Typically, support for travel, subsistence and accommodation can be provided for two researchers per experiment, during two experimental weeks at GELINA or one experimental week at the Van de Graaff. The PAC would like to give preference to first-time users of the facilities.

Researcher	Institution	E-mail address	Total no. of days
T. Ware	Uni. of Birmingham		10
M. Moxon	Uni. of Birmingham		10

Objectives and expected deliverables of the experiment

To determine the nuclear scattering radii and scattering cross-sections of the natural hafnium isotopes. Values will be presented with resolved resonance parameters derived from measurements under the NUDAME scheme to the JEFF project.

A detailed description of the proposal (max. 3 pages) must be added, containing:

- the context and the goals of the measurements
- the contribution of the different researchers to the experiment
- the schedule of the work
- quantitative estimates of fluxes and beam times
- special support services that are needed
- a description of equipment that is needed and/or equipment that you will bring with you.

The submission of this proposal implies that you certify that the information given is true and complete, and that you accept the following terms and conditions:

At IRMM you must follow the rules of conduct applicable for all Commission personnel

Access to a controlled area may only be granted when IRMM has received a copy of a valid medical certificate. Access to controlled areas will not be granted to individuals from particular countries (e.g. countries which are not members of the Non Proliferation Treaty or countries for which the Commission has security reservations)

The text of your proposal will be put on the non-public PAC section of the EUFRAT website. This password-protected section of the website will be accessible by the PAC members and all group leaders that have submitted a proposal

You must include the following sentence in your publications of the results obtained at the IRMM infrastructures: "This work was supported by the European Commission within the Seventh Framework Programme through EUFRAT (EURATOM contract no. FP7-211499)". You should also acknowledge the persons who contributed to the success of this experiment.

Date

Signature of Proposer

9th December 2009



Signed applications must be sent by e-mail to



Total cross-section measurements of natural hafnium samples

1) THE CONTEXT AND THE GOALS OF THE MEASUREMENTS

Hafnium can be used in reactor systems to regulate the fission process because of its high absorption cross section in the thermal and epi-thermal region. In previous proposals [1,2], the interpretation of integral benchmark experiments, in both critical and zero-power reactors, identified the poor quality of the nuclear data files for hafnium in the thermal and epi-thermal region.

The natural metal is currently used in some light water reactor (LWR) systems as part of the control rod system [3]. Additionally, there have been studies of the potential use of hafnium-based materials in future reactor design including;

- use of hafnium hydrides (HfH_x) in the control rods of fast reactors [4], where the hydrogen in the compound moderates fast neutrons down to the resonance energy region of hafnium.
- use of hafnium nitride (HfN) as an inert fuel matrix for waste transmutation, in particular that of transuranic nuclides in accelerator-driven systems (ADS) [5]. The HfN provides a physically stable, high-temperature fuel matrix whilst the high hafnium cross-section results in higher burn-up as well as neutronic stability, leading to improved reactor safety and lower radiation damage to the system.
- use of carbides such as $(\text{U,Zr,Hf})\text{C}$ as fuel materials in advanced innovative nuclear energy systems. These have high melting points ($>3500\text{K}$) and are considered in the Generation IV roadmap [6].

As part of a NUDAME project, capture and transmission measurements on natural and isotopically-enriched hafnium samples have been performed at GELINA (proposed by CEA, Cadarache [1] and Serco, Winfrith [2]). Initial analysis of the resulting capture data suggests that the JEFF3.1 resolved resonance region for hafnium can be extended from $\sim 250\text{eV}$ to 1 - 2 keV. However, this analysis lacks a good description of the scattering radius. It is intended that this new evaluation will be combined with an evaluation of the unresolved resonance range conducted by G. Noguère (CEA), which utilises measured data down to $\sim 10\text{keV}$ [7]. There are no measured data between 1 and 10 keV. The new measurement will help validate the models applied in this region.

We propose transmission measurements of natural hafnium metallic samples from which, we will extract the scattering radii. A set of $\sim 1\text{mm}$ natural hafnium metallic discs are available for measurement at GELINA and we propose that these are stacked to give overall thickness of 10-20mm. We may add further Hf discs to obtain $\sim 50\text{mm}$ samples; noting the thicker samples will optimise the results.

At thermal and low resonance energies, the capture cross-section of Hf isotopes tends to dominate the scattering cross-section as a contribution to the total cross-section. Above $\sim 200\text{eV}$ the scattering becomes dominant. In order to predict the scattering cross-section reasonably accurately, the nuclear radius must be estimated from a thick sample ($>20\text{mm}$) transmission measurement. Knowledge of this radius will enhance the accuracy of the data over all energy ranges.

2) CONTRIBUTION OF THE DIFFERENT RESEARCHERS TO THE EXPERIMENT

- T. Ware, Uni. Birm., will perform the data reduction and resonance analysis;
- M. Moxon, Uni. Birm., will assist in the measurements and resonance analysis;
- S. Kopecky, IRMM, will act as local contact and perform the measurements

3) THE SCHEDULE OF THE WORK

The measurements will be performed at a transmission measurement station of GELINA using the equipment that is routinely used for such measurements. The data reduction will be performed with the AGS code. The resonance shape analysis will then be performed with the REFIT code [8].

4) QUANTITATIVE ESTIMATES OF FLUXES AND BEAM TIMES

A total of 200 hours of beam time is required. This measurement time is based on an energy dependent neutron flux of $0.25 \times 10^4 \text{ s}^{-1} \text{ eV}^{-1}$ at 1eV and 50m distance with GELINA operating at 800Hz and an average current of 70 μA .

5) SPECIAL SUPPORT SERVICES REQUIRED

There is no need for special support services anticipated.

6) DESCRIPTION OF EQUIPMENT REQUIRED

Transmission measurement equipment as routinely used for such measurements at GELINA at the FP4_50m measurement station; Li-glass scintillator, with conventional NIM electronics, the IRMM fast time coder and the DAC2000 data acquisition system.

7) REFERENCES

- [1] G. Noguère, “High-Resolution Capture and Transmission Measurements of the Natural Hafnium”, NUDAME proposal PAC1/1 (2005)
- [2] C. Dean, “Capture Cross-Section Measurements of Isotopic Enriched Hf Samples”, NUDAME proposal PAC3/1 (2006)
- [3] www.westinghousenuclear.com Retrieved 09/12/08.
- [4] K. Kenji et al., “Development of Advanced Control Rod of Hafnium Hydride for Fast Reactors”, Proc. ICAPP’06 (2006).
- [5] K. Tuček et al., “Studies of an Accelerator-Driven Transuranium Burner with Hafnium-Based Inert Matrix Fuel”, J. Nucl. Tech. 157, p277-298 (2007).
- [6] http://gif.inel.gov/roadmap/pdfs/018_description_of_candidate_nonclassical_reactor_systems_report.pdf Retrieved 05/12/08.
- [7] G. Noguère and E. Rich URR, “Evaluation of the Unresolved Resonance Range with TALYS” JEF/DOC-1249 (2008).
- [8] M.C. Moxon, T.C. Ware, C.J. Dean, “REFIT-2007: Users’ Guide” UKNSF Report UKNSF(2007)P216 (2007).

B.4 Contribution to IRMM Neutron Physics Unit Scientific Report 2008

Capture cross section measurements of isotopic enriched hafnium samples

T.C. Ware^{1,3}, A. Borella², C.J. Dean³, N. Janeva⁴, S. Kopecky², A. Moens²,
M.C. Moxon⁵, G. Noguère⁶, P. Schillebeeckx²

¹ School of Physics, University of Birmingham, Birmingham, B15 2TT, UK

² EC-JRC-IRMM, B-2440 Geel, Belgium

³ Serco, Building A32, Winfrith Technology Centre, Dorchester, DT2 8DH, UK

⁴ INRNE, BG-1784 Sofia, Bulgaria

⁵ 3 Hyde Copse, Marcham, Oxfordshire, OX13 6PT, UK

⁶ CEA-Cadarache, F-13108 Saint Paul Les Durances, France

The large absorption cross-section of natural hafnium makes it a candidate for use in reactor control rods to regulate the fission process. As it is a resonance absorber it is particularly favoured for use in thermal fission reactors with harder neutron spectra, such as those using MOX fuel. Hence it is important to understand the hafnium cross-section in the resolved resonance energy range.

Calculations on the AZUR criticality experiments conducted by CEA, using the latest JEFF3.1 isotopic hafnium evaluations based on recent RPI measurements [1], indicate a measured rod worth of 7000pcm being underestimated by ~300pcm [2]. This may be due to an overestimate of the natural hafnium capture cross section. Resonances below ~180eV are reasonably defined by recent measurements at RPI [2]. Above ~250eV unresolved resonances are present in JEFF3.1. The Hf isotope files can be improved by extending the resolved resonance range to higher energies, thereby negating uncertainties from the treatment of the unresolved resonance range. Ideally, this objective can be achieved through capture cross-section measurements on hafnium identified on the NEA Nuclear Data High Priority Request List [3].

Table 1. Details of Isotopically Enriched Hafnium Oxide (HfO₂) Samples

Enriched Isotope	Abundance* (%)						Sample thickness (mm)
	¹⁷⁴ Hf	¹⁷⁶ Hf	¹⁷⁷ Hf	¹⁷⁸ Hf	¹⁷⁹ Hf	¹⁸⁰ Hf	
¹⁷⁶ Hf	<0.05	65.0	22.9	6.3	1.8	4.0	2.062 ± 0.0379
¹⁷⁷ Hf	<0.05	1.0	85.4	11.3	0.9	1.4	3.223 ± 0.0498
¹⁷⁸ Hf (#1)	<0.05	0.8	1.9	92.4	3.3	1.6	2.502 ± 0.1125
¹⁷⁸ Hf (#2)				± 0.2			1.052 ± 0.0097
¹⁷⁹ Hf	<0.05	0.2	1.3	4.1	72.1 ± 0.4	22.3	2.452 ± 0.0558
cf. natural	0.16 ± 0.01	5.26 ± 0.07	18.60 ± 0.09	27.28 ± 0.07	13.62 ± 0.02	35.08 ± 0.16	-

* uncertainties on sample compositions are being requested

Through NUDAME proposal PAC3/1 [4], isotopically enriched hafnium oxide samples were sourced from INRNE (BG) and arrived at IRMM in November 2007. A composition analysis of each sample was performed and the samples sealed in aluminium cans for measurement. Table 1 presents the details of each sample.

Capture measurements on these samples were performed on Flight Paths 5 (10m) and 15 (30m) of the GELINA facility. A measurement of a 1mm metallic natural Hf sample was also made on both flight paths during the same period.

These capture measurements used C_6D_6 scintillator detectors [5] in conjunction with conventional NIM electronics, the IRMM fast time coder and the DAC2000 data acquisition system. Data reduction of the measurements was performed with the AGL [6] and AGS [7] codes to produce capture yield data to be used in the resonance analysis.

In the analysis, we intend to include the NUDAME supported natural and enriched Hf sample measurements, natural Hf transmission measurements by Siegler [8] and previous enriched Hf sample measurements at lower resolution made at Harwell [9] and ORNL [10]. In addition, we have identified the need for further transmission measurements on thick natural Hf samples to improve understanding of the scattering radii. These measurements have been proposed and endorsed by the EUFRAT Project Advisory Committee [11].

It is necessary to allocate each resonance of natural hafnium to one of its constituent isotopes in order for the resonance theory to be applied correctly in resonance shape analysis codes such as REFIT [12]. This was achieved by overlaying the capture yields from the 30m measurements of the enriched and 1mm natural Hf samples. The change in the structure of each yield curve relative to the others enabled resonances to be allocated to the five major

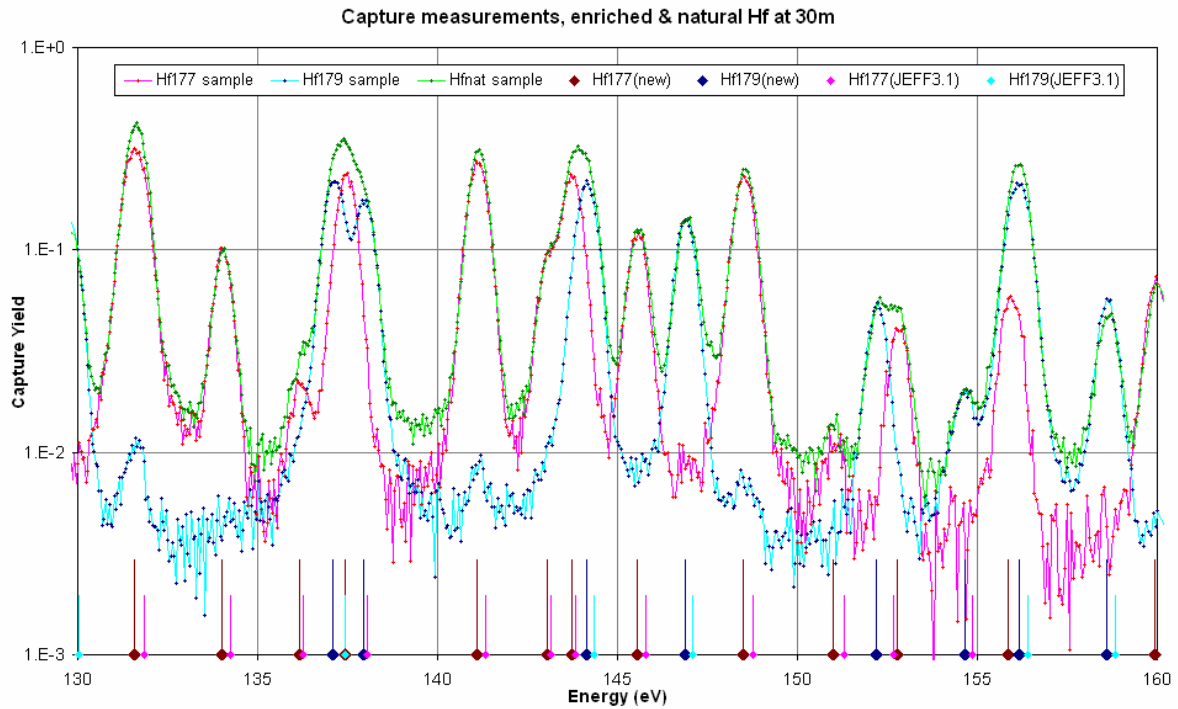


Figure 1 - Comparison of capture yield curves of Hf sample measurements with resonance allocation from JEFF3.1 and new evaluations

isotopes up to ~1 keV for $^{177,179}\text{Hf}$ and several keV for $^{176,178,180}\text{Hf}$. This included the reallocation of some ‘known’ resonances to different isotopes and the identification of resonances missing from the resolved resonance range of previous evaluations. Figure 1 demonstrates this comparison for the $^{177,179}\text{HfO}_2$ and $^{\text{nat}}\text{Hf}$ samples. Some use was made of the Harwell and ORNL enriched sample measurements in verifying the resonance allocation, particularly for ^{180}Hf , as there is no sample available for measurement under this work.

Following resonance allocation, resonance shape analysis was conducted using the REFIT code. To date, this analysis has focused on the 50 eV to 1 keV energy range and has utilised the new 30m enriched and natural Hf sample capture measurements, together with some of the transmission measurements of Siegler. These data, with corresponding experimental parameters supplied by GELINA, have been used simultaneously in REFIT calculations to derive resonance energies, neutron and gamma widths for ‘new’ and existing resonances for the five most abundant Hf isotopes. Capture yields calculated from the preliminary values of the new resonance parameters have been compared with those from the JEF2.2 and JEFF3.1 parameters in Figure 2.

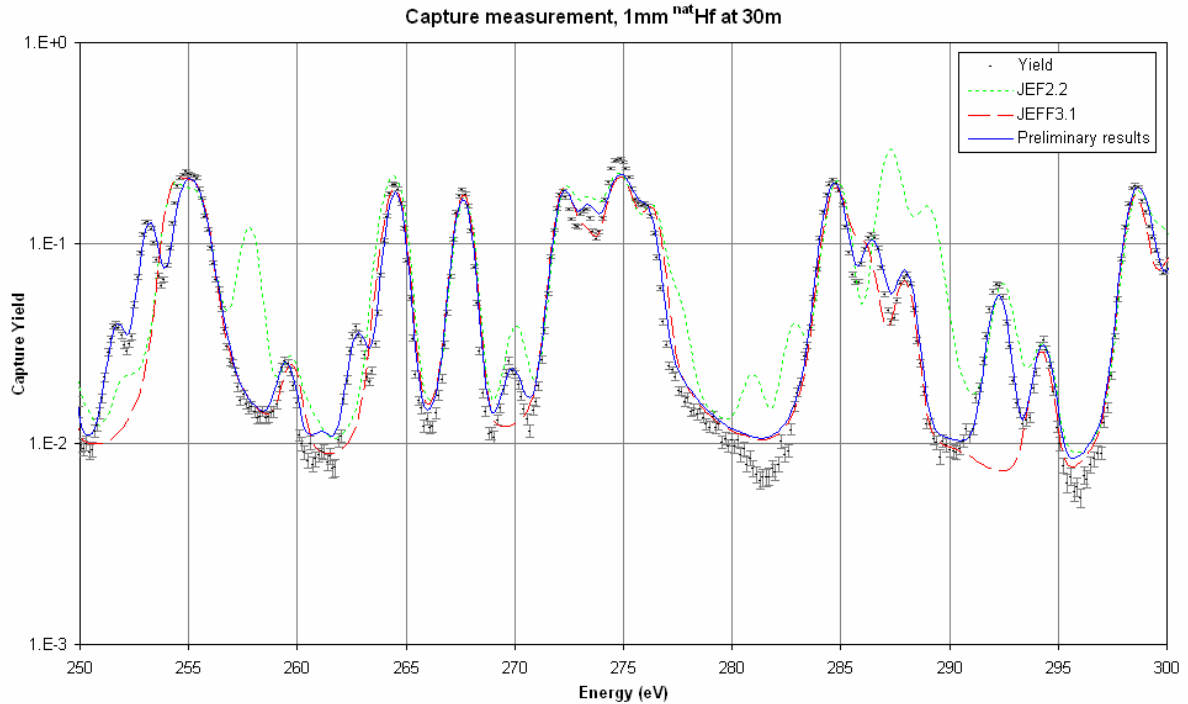


Figure 2 - Measured capture yield compared with those calculated from current evaluations

The preliminary evaluated files were processed into ECCO and BINGO data libraries for use in reactor physics codes. The deterministic WIMS/ECCO [13] and Monte-Carlo MONK [14] codes were used to compute k-effective values for a 17 region slab model, containing hafnium, ^{235}U , ^{238}U , water and zirconium. The difference in treatment of the unresolved resonance region in the two codes results in different values of k-effective [15]. Using JEFF3.1 data this difference is ~230 pcm. By increasing the limit of the resolved resonance region of $^{177,179}\text{Hf}$ to 1 keV and inserting the preliminary resonance parameters derived from the new measurements, this difference decreases to ~100 pcm.

The resonance shape analysis of the enriched hafnium sample capture measurements is continuing. It is hoped that this will be enhanced by the transmission measurements of the enriched hafnium samples scheduled to begin at GELINA shortly. We intend the analysis of these measurements to cover the range from thermal neutron energies to ~1.2 keV for $^{177,179}\text{Hf}$ and ~10 keV for $^{176,178,180}\text{Hf}$, so extending the resolved resonance range in the evaluated files to these energies.

Analysis is expected to be completed in late 2009, when the new evaluated files will be tested with the reactor physics codes and models. The new parameters will be presented in the PhD thesis of T. Ware in November 2009. These data will be joined to unresolved resonance parameters from work by G. Noguère. It is hoped the resultant evaluations will be included in the JEFF3.2 evaluated data library. Measurements will be submitted to EXFOR.

- [1] M.J. Trbovich, "Hafnium neutron cross-sections and resonance analysis", PhD Thesis (2003)
- [2] G. Noguère et al., "Low neutron energy cross sections of the hafnium isotopes", JEFDOC-1077, OECD-NEA, Issy-les-Moulineaux, France (2005)
- [3] NEA High Priority Request List: <http://www.nea.fr/html/dbdata/hprl/index.html>
- [4] C. Dean, "Capture cross-section measurements of isotopic enriched Hf samples", NUDAME proposal PAC3/1 (2006)
- [5] A. Borella, et al., "The used of C6D6 detectors for neutron induced capture cross-section measurements in the resonance region", Nuc. Inst. & Methods A 577(2007)626
- [6] A. Borella, "AGL2 – User manual", IRMM internal report, (2007)
- [7] C. Bastian, "AGS, a set of UNIX commands for neutron data reduction", SPIE - The International Society for Optical Engineering, Vol. 2867, 611 (1997)
- [8] P. Siegler et al., "Testing of neutron data by comparison of measured and calculated average transmissions", Int. Conf. on Nuclear Data for science and technology, Tsukuba, Japan, 2001
- [9] M.C. Moxon et al., "Differential neutron cross-sections of natural hafnium and its isotopes for neutron energies up to 30 eV", Harwell report, AERE-R7864 (1974)
- [10] T. Fuketa and J.A. Harvey, "Level spacings and s-wave neutron strength functions of the isotopes of Hafnium", ORNL report, ORNL-3778 (1965)
- [11] 'Total cross-section measurements of natural hafnium samples' (PAC 1/1)
- [12] M.C. Moxon, T.C. Ware, C.J. Dean, "REFIT-2007: Users' Guide" UKNSF Report UKNSF(2007)P216 (2007)
- [13] T. Newton et al., "Developments within WIMS10", International Conference on the Physics of Reactors, Interlaken, Switzerland (2008)
- [14] M.J. Armishaw and A.J. Cooper., "Current Status and Future Direction of the MONK Software Package", Proceedings of International Conference on Nuclear Criticality Safety, ICNC'07, St. Petersburg (2007)
- [15] S. Wilson, "Investigation of Hafnium Nuclear Data in the MONK and ECCO Criticality Codes", MSc Thesis, University of Birmingham (2008)